frontiers | Research Topics

New compounds, novel targets and mechanism study in inflammation-associated liver diseases

Edited by
Baoming Wu, Lei Zhang, Tatsunori Miyata, Yang Yang and Xiude Fan

Published in
Frontiers in Pharmacology

ISSN 1664-8714
ISBN 978-2-83251-134-3
DOI 10.3389/978-2-83251-134-3

About Frontiers

Frontiers is more than just an open access publisher of scholarly articles: it is a pioneering approach to the world of academia, radically improving the way scholarly research is managed. The grand vision of Frontiers is a world where all people have an equal opportunity to seek, share and generate knowledge. Frontiers provides immediate and permanent online open access to all its publications, but this alone is not enough to realize our grand goals.

Frontiers journal series

The Frontiers journal series is a multi-tier and interdisciplinary set of open-access, online journals, promising a paradigm shift from the current review, selection and dissemination processes in academic publishing. All Frontiers journals are driven by researchers for researchers; therefore, they constitute a service to the scholarly community. At the same time, the *Frontiers journal series* operates on a revolutionary invention, the tiered publishing system, initially addressing specific communities of scholars, and gradually climbing up to broader public understanding, thus serving the interests of the lay society, too.

Dedication to quality

Each Frontiers article is a landmark of the highest quality, thanks to genuinely collaborative interactions between authors and review editors, who include some of the world's best academicians. Research must be certified by peers before entering a stream of knowledge that may eventually reach the public - and shape society; therefore, Frontiers only applies the most rigorous and unbiased reviews. Frontiers revolutionizes research publishing by freely delivering the most outstanding research, evaluated with no bias from both the academic and social point of view. By applying the most advanced information technologies, Frontiers is catapulting scholarly publishing into a new generation.

What are Frontiers Research Topics?

Frontiers Research Topics are very popular trademarks of the *Frontiers journals series*: they are collections of at least ten articles, all centered on a particular subject. With their unique mix of varied contributions from Original Research to Review Articles, Frontiers Research Topics unify the most influential researchers, the latest key findings and historical advances in a hot research area.

Find out more on how to host your own Frontiers Research Topic or contribute to one as an author by contacting the Frontiers editorial office: frontiersin.org/about/contact

New compounds, novel targets and mechanism study in inflammation-associated liver diseases

Topic editors

Baoming Wu — Anhui Medical University, China
Lei Zhang — Anhui Medical University, China
Tatsunori Miyata — Cleveland Clinic, United States
Yang Yang — University of Texas Health Science Center at Houston, United States
Xiude Fan — Shandong Provincial Hospital, China

Citation

Wu, B., Zhang, L., Miyata, T., Yang, Y., Fan, X., eds. (2023). *New compounds, novel targets and mechanism study in inflammation-associated liver diseases*. Lausanne: Frontiers Media SA. doi: 10.3389/978-2-83251-134-3

Table of contents

frontiers | Frontiers in Pharmacology

TYPE Editorial
PUBLISHED 09 December 2022
DOI 10.3389/fphar.2022.1090504

OPEN ACCESS

EDITED AND REVIEWED BY
Angelo A. Izzo,
University of Naples Federico II, Italy

*CORRESPONDENCE
Baoming Wu,
wubaoming@ahmu.edu.cn

SPECIALTY SECTION
This article was submitted to Gastrointestinal and Hepatic Pharmacology, a section of the journal Frontiers in Pharmacology

RECEIVED 05 November 2022
ACCEPTED 15 November 2022
PUBLISHED 09 December 2022

CITATION
Wu B (2022), Editorial: New compounds, novel targets and mechanism study in inflammation-associated liver diseases.
Front. Pharmacol. 13:1090504.
doi: 10.3389/fphar.2022.1090504

Editorial: New compounds, novel targets and mechanism study in inflammation-associated liver diseases

Baoming Wu*

School of Pharmacy, Anhui Medical University, Hefei, China

KEYWORDS

liver diseases, immune cells, immunoregulation, novel targets, drug discovery

Editorial on the Research Topic
New compounds, novel targets and mechanism study in inflammation-associated liver diseases

This Research Topic was initiated to investigate the pathogenesis and pathophysiological processes of inflammation-associated liver diseases, with particular focus on targets research, drug conversion, and druggability research, based on the informatics approach and further discovery of novel therapeutic targets and strategies for treatment.

Total of 18 manuscripts were submitted and reviewed, with 9 manuscripts accepted and others rejected. Scopes of accepted manuscripts involved liver injury, autoimmune hepatitis, liver ischemia/reperfusion injury and liver fibrosis. There were 3 manuscripts that discussed effects of Chinese traditional medicine on liver diseases: paeoniflorin alleviates liver injury in hypercholesterolemic rats through the ROCK/AMPK pathway (Liu et al.), mechanism of Hydroxysafflor yellow A on acute liver injury based on transcriptomics (Hou et al.), and saikosaponin d alleviates liver fibrosis by negatively regulating the ROS/NLRP3 inflammasome through activating the ERβ pathway (Zhang et al.). There were 2 manuscripts that studied the effects and mechanism of chemical medicine on liver diseases: hydroxychloroquine attenuates autoimmune hepatitis by suppressing the interaction of GRK2 with PI3K in T lymphocytes (Jiu et al.), and roxadustat, a hypoxia-inducible factor 1α activator, attenuates both long-and short-term alcohol induced alcoholic liver disease (Gao et al.). There were 3 manuscripts that revealed the effects and mechanism of cytokines on liver diseases: inhibition of macrophage migration inhibitory factor (MIF) suppresses apoptosis signal-regulating kinase 1 to protect against liver ischemia/reperfusion injury (Chen et al.), human umbilical cord blood mononuclear cells ameliorate CCl4 induced acute liver injury in mice via inhibiting inflammatory responses and up-regulating interleukin-22 (Zhang et al.), and interleukin-6 receptor blockade can increase the risk of nonalcoholic fatty liver disease: indications from Mendelian randomization (Li et al.). There was 1 review

manuscript in this Research Topic, which summarized the current literature regarding FAT10 role in developing liver diseases and potential therapeutic targets for nonalcoholic/alcoholic fatty liver disease and hepatocellular carcinoma (Wimalarathne et al.).

Author contributions

The author confirms being the sole contributor of this work and has approved it for publication.

Acknowledgments

In the end, I would like to first thank our guest editors (Dr. Lei Zhang, Dr. Yang Yang, Dr. Xiude Fan, and Dr. Tatsunori Miyata), because they worked very hard to organize the Research Topic and review manuscripts assigned to them. Second, I would like to thank all the contributors who submitted their great work to this topic. Last but not the least, we would like to thank Frontier in Pharmacology for giving us this opportunity to learn a great deal from this special issue.

Conflict of interest

The author declares that the research was conducted in the absence of any commercial or financial relationships that could be construed as a potential conflict of interest.

Publisher's note

References

Madushika, M., Wilkerson-Vidal, Q. C., Hunt, E. C., and Love-Rutledge, S. T. (2022). The case for FAT10 as a novel target in fatty liver diseases. *Front. Pharmacol.* 13, 972320. doi:10.3389/fphar.2022.972320

Tong, L., Zhang, N., Kong, L., Chu, S., Zhang, T., Yan, G., et al. (2022). Paeoniflorin alleviates liver injury in hypercholesterolemic rats through the ROCK/AMPK pathway. *Front. Pharmacol.* 13, 968717. doi:10.3389/fphar.2022.968717

frontiers | Frontiers in Pharmacology

ORIGINAL RESEARCH
published: 10 May 2022
doi: 10.3389/fphar.2022.895710

Roxadustat, a Hypoxia-Inducible Factor 1α Activator, Attenuates Both Long- and Short-Term Alcohol-Induced Alcoholic Liver Disease

*Yongyao Gao[1†], Xiaomeng Jiang[2], Daigang Yang[1†], Wentong Guo[1], Dandan Wang[3], Ke Gong[1], Ying Peng[1], Hong Jiang[2], Cunyuan Shi[2], Yajun Duan[1], Yuanli Chen[1], Jihong Han[1,4] and Xiaoxiao Yang[1]**

[1]Key Laboratory of Metabolism and Regulation for Major Diseases of Anhui Higher Education Institutes, College of Food and Biological Engineering, Hefei University of Technology, Hefei, China, [2]Zhejiang Jianfeng Pharmaceutical Co., Ltd., Jinhua, China, [3]School of Pharmacy, Anhui University of Chinese Medicine, Hefei, China, [4]College of Life Sciences, Key Laboratory of Medicinal Chemical Biology, Key Laboratory of Bioactive Materials of Ministry of Education, Nankai University, Tianjin, China

OPEN ACCESS

Edited by:
Xiude Fan,
Shandong Provincial Hospital, China

Reviewed by:
Wei Zhong,
University of North Carolina at Greensboro, United States
Evgeny Shutov,
City Clinical Hospital named after S.P.Botkin, Russia

***Correspondence:**
Xiaoxiao Yang
yangxiaoxiao@hfut.edu.cn

[†]These authors have contributed equally to this work

Specialty section:
This article was submitted to Gastrointestinal and Hepatic Pharmacology, a section of the journal Frontiers in Pharmacology

Received: 14 March 2022
Accepted: 11 April 2022
Published: 10 May 2022

Citation:
Gao Y, Jiang X, Yang D, Guo W, Wang D, Gong K, Peng Y, Jiang H, Shi C, Duan Y, Chen Y, Han J and Yang X (2022) Roxadustat, a Hypoxia-Inducible Factor 1α Activator, Attenuates Both Long- and Short-Term Alcohol-Induced Alcoholic Liver Disease. Front. Pharmacol. 13:895710. doi: 10.3389/fphar.2022.895710

Alcoholic liver disease (ALD) is a worldwide healthcare problem featured by inflammation, reactive oxygen species (ROS), and lipid dysregulation. Roxadustat is used for chronic kidney disease anemia treatment. As a specific inhibitor of prolyl hydroxylase, it can maintain high levels of hypoxia-inducible factor 1α (HIF-1α), through which it can further influence many important pathways, including the three featured in ALD. However, its effects on ALD remain to be elucidated. In this study, we used chronic and acute ALD mouse models to investigate the protective effects of roxadustat *in vivo*. Our results showed that long- and short-term alcohol exposure caused rising activities of serum transaminases, liver lipid accumulation, and morphology changes, which were reversed by roxadustat. Roxadustat-reduced fatty liver was mainly contributed by the reducing sterol-responsive element-binding protein 1c (SREBP1c) pathway, and enhancing β-oxidation through inducing peroxisome proliferator-activated receptor α (PPARα) and carnitine palmitoyltransferase 1A (CPT1A) expression. Long-term alcohol treatment induced the infiltration of monocytes/macrophages to hepatocytes, as well as inflammatory cytokine expression, which were also blocked by roxadustat. Moreover, roxadustat attenuated alcohol caused ROS generation in the liver of those two mouse models mainly by reducing cytochrome P450 2E1 (CYP2E1) and enhancing superoxidase dismutase 1 (SOD1) expression. *In vitro*, we found roxadustat reduced inflammation and lipid accumulation mainly *via* HIF-1α regulation. Taken together, our study demonstrates that activation of HIF-1α can ameliorate ALD, which is contributed by reduced hepatic lipid synthesis,

Abbreviations: ACC1, acetyl-CoA carboxylase 1; ALD, alcoholic liver disease; ALP, alkaline phosphatase; ALT, alanine aminotransferase; AST, aspartate aminotransferase; ChREBPα, carbohydrate response element-binding protein α; CPT1A, carnitine palmitoyltransferase 1A; CYP2E1, cytochrome P450 2E1; DGAT, diacylglycerol acyltransferase; FASN, fatty acid synthase; GAPDH, glyceraldehyde-3-phosphate dehydrogenase; HFD, high-fat diet; HIF-1α, hypoxia-inducible factor-1α; IL-1β/6, interleukin-1β or 6; PPARα, peroxisome proliferator-activated receptor α; ROS, reactive oxygen species; SOD1/2, superoxidase dismutase 1 or 2; SREBP1c, sterol-responsive element-binding protein 1c; TNF-α, tumor necrosis factor α.

inflammation, and oxidative stress. This study suggested that roxadustat could be a potential drug for ALD treatment.

Keywords: ALD, roxadustat, fatty liver, HIF-1α, inflammation, oxidative stress

INTRODUCTION

The alcohol intake-associated disease, that is, alcoholic liver disease (ALD), remains a serious global human health problem. ALD usually starts with hepatic steatosis, and then develops into alcoholic steatohepatitis, cirrhosis, and even hepatocellular carcinoma (Ceni et al., 2014; Kong et al., 2021). Once ALD progresses to steatohepatitis, abstinence from alcohol cannot totally reverse liver damage. Therefore, it is necessary to treat ALD in the stage of hepatic steatosis. The molecular mechanisms of ALD are not well studied, but there is growing evidence that multiple factors are involved in the pathogenesis of ALD, such as oxidative stress, which can promote lipid peroxidation and accelerate fat deposition in the liver, inflammation, as well as dysregulation of gut microbiota (Xu et al., 2017; Meng et al., 2018). The current treatment of ALD is limited to alcohol withdrawal and a few medications, such as polyene phosphatidylcholine, glucocorticoids, and metadoxine. However, the usage of these drugs has some limitations and side effects. Polyene phosphatidylcholine cannot reverse the pathology of ALD (Wang et al., 2019). Glucocorticoids increase the risk of obesity, hypertension, and cardiovascular diseases (Dixon and Bansback, 2012). Metadoxine has the potential to cause diarrhea (Addolorato et al., 2003). Therefore, the development of new drugs for ALD is urgently needed.

Hypoxia-inducible factor (HIF)-1 is a heterodimeric transcription factor consisting of α- and β-subunits that acts as a master regulator of adaptation to hypoxia. Under conditions of oxygen sufficiency, the α-subunit is hydroxylated at its specific proline residues, resulting in rapid degradation. When exposed to hypoxia, the α-subunit is stabilized and translocated to the nucleus to dimerize with HIF-1β, and then to activate its target genes, such as glucose transporters, glycolysis enzymes, and lipid synthases (Kaelin and Ratcliffe, 2008; Rahtu-Korpela et al., 2014). Alcohol exposure increases liver oxygen consumption and subsequently causes hypoxia in the region surrounding the liver lobules (Tsukamoto and Xi, 1989; Arteel et al., 1997). Chronic hypoxia impairs mitochondrial-mediated fatty acid oxidation through the production of reactive oxygen species (ROS), causing mitochondrial dysfunction, which further affects liver lipid synthesis (Lieber, 2004). Reduced oxygen availability initiates the hypoxic response and is a survival mechanism that evolves to enable organisms to cope with low oxygen levels (Kaelin and Ratcliffe, 2008; Koivunen et al., 2016; Gunton, 2020). Roxadustat (FG-4592) can enhance the stabilization of HIF-1α, and is the first small molecule approved for the treatment of renal anemia by promoting the production of erythropoietin and iron utilization (Huang et al., 2020). Some studies have shown that HIF-1 activation can protect against metabolic disorders by reducing serum cholesterol and glucose levels, and improving insulin sensitivity in type 2 diabetic mice (Rahtu-Korpela et al., 2014; Chen et al., 2015). In addition, the development of atherosclerosis can also be attenuated by FG-4592, which is related to the elimination of hepatocyte cholesterol, and thermogenesis (Zhang et al., 2019; Sugahara et al., 2020). However, little has been reported that HIF-1α controls the lipid metabolism in ALD.

Chronic alcohol consumption is a leading cause of ALD. Accumulating evidence indicated that consuming excess alcohol and being overweight synergistically promoted the development of ALD (Lu et al., 2004). Mice fed with the Lieber–DeCarli liquid diet containing ethanol for 8 weeks plus a single binge ethanol feeding (the NIAAA model) could develop ALD, with the characteristics of inflammation and fatty liver, which were wildly used for ALD research (Bertola et al., 2013). Research study has shown that short-term high-fat diet (HFD) feeding could impair glucose tolerance and insulin sensitivity, along with hepatic inflammatory response and liver damage (Chang et al., 2015). Feeding mice with an HFD for 3 days or 8 weeks plus a single gavage of ethanol can induce liver injury by elevating fatty acid accumulation and hepatic neutrophil infiltration. To explore the role of HIF-1α activation on ALD, we used the NIAAA model and HFD plus ethanol mouse model in this study. Along with the construction of ALD mouse models, mice received roxadustat treatment, followed by the determination of ALD development, as well as involved mechanisms.

MATERIALS AND METHODS

Reagents

Roxadustat was provided by Zhejiang Jianfeng Pharmaceutical Co., Ltd. (Jinhua, China). Bovine serum albumin (BSA) was purchased from Sigma Aldrich (Missouri, United States). Hematoxylin and eosin (H&E) staining solution, 4% polyformaldehyde, phosphate buffer saline (PBS), and BCA Protein Assay Kit were purchased from Biosharp (Hefei, China). Total RNApure reagent (Trizol) was purchased from Beijing Zomen Biotechnology Co., Ltd. (Beijing, China). HiScript II Q Select RT SuperMix and AceQ SYBR qPCR Master Mix were purchased from Vazyme (Nanjing, China). The dihydroethidium (DHE) staining kit was purchased from Beyotime (Shanghai, China). A cocktail of protease inhibitors, PMSF, and enhanced chemiluminescence (ECL) kit were purchased from Millipore (Darmstadt, Germany). Bromphenol blue, triton X-100, and sodium dodecyl sulfate (SDS) were purchased from Solarbio (Beijing, China). Mouse anti-fatty acid synthase (FASN) and CD68 monoclonal antibodies were purchased from Santa Cruz Biotechnology (CA, United States). Mouse anti-glyceraldehyde-3-phosphate dehydrogenase (GAPDH), rabbit anti-superoxidase dismutase 1 (SOD1), SOD2, α-Tubulin, peroxisome proliferator-

TABLE 1 | q-RT-PCR primer sequences.

Gene	Forward	Backward
Mus ACC1	GCCATTGGTATTGGGGCTTAC	CCCGACCAAGGACTTTGTTG
Mus β-actin	ATGGAGGGGAATACAGCCC	TTCTTTGCAGCTCCTTCGTT
Mus ChREBPα	GTCCCCGCAGGATACAGTTT	TTGTTGTCTACACGACCCCG
Mus DGAT1	GGTGCCCTGACAGAGCAGAT	CAGTAAGGCCACAGCTGCTG
Mus FASN	CTGCGATGAAGAGCATGGTTT	CCATAGGCGATTTCTGGGAC
Mus IL-1β	GACCTTCCAGGATGAGGACA	AGCTCATATGGGTCCGACAG
Mus IL-6	GAGGATACCACTCCCAACAGACC	AAGTGCATCATCGTTGTTCATACA
Mus PPARα	AGTTCGGGAACAAGACGTTG	CAGTGGGGAGAGAGGACAGA

ACC1, acetyl-CoA carboxylase 1; ChREBPα, carbohydrate response element-binding protein α; DGAT, acyl-CoA: diacylglycerol acyltransferase; FASN, fatty acid synthase; IL-1β/6, interleukin-1β or 6; PPARα, peroxisome proliferator-activated receptor α.

activated receptor α (PPARα), and interleukin-1β (IL-1β) polyclonal antibodies were purchased from Abclonal (Wuhan, China). Rabbit anti-HIF-1α, carnitine palmitoyltransferase 1A (CPT1A), and cytochrome P450 2E1 (CYP2E1) polyclonal antibodies were purchased from Affinity Biosciences (OH, United States). Mouse anti-tumor necrosis factor α (TNF-α), rabbit anti-sterol-responsive element-binding protein 1c (SREBP1c), carbohydrate response element-binding protein α (ChREBPα) polyclonal antibodies, HRP-conjugated goat anti-rabbit IgG (H + L), and mouse IgG (H + L) were purchased from Proteintech Group Inc. (IL, United States). All other chemical reagents were analytical grade.

Cell Culture

HepG2 and RAW264.7 cells were purchased from ATCC (VA, United States), and cultured in complete MEM or 1640 medium containing 10% fetal bovine serum (FBS, AusGeneX, Australia) and 50 μg/ml streptomycin/penicillin (UT, United States), in a humidified incubator with 5% CO_2 at 37°C. Before treatment, cells were incubated in a serum-free medium.

siRNA Transfection

Homo HIF-1α siRNA and the corresponding scrambled siRNA were purchased from RiboBio Biotechnology (Guangzhou, China). HepG2 cells were cultured in a 6-well plate at a density of 5×10^5 cells/well in a serum-free Opti-MEM. HIF-1α or control siRNA (40 nM/well) were transfected into cells using Lipofectamine RNAiMAX Transfection Reagent (Invitrogen, CA, United States). After 24 h transfection, HepG2 cells received indicated treatment (Wang et al., 2020).

In Vivo Studies

The eight-week-old male C57BL/6J mice were purchased from GemPharmatech (Nanjing, China). Mice were maintained in a chamber with constant temperature (22 ± 2°C) and humidity (55 ± 2%) for a 12-h light/dark cycle.

The chronic ALD mouse model was constructed as described (Bertola et al., 2013). In brief, mice were divided into four groups (8 mice/group); all mice were fed with the Lieber–DeCarli control diet for the first 5 days. Then, mice in control groups were fed with the Lieber–DeCarli control diet (ethanol free) for 8 weeks plus intragastric (i.g.) administration of a single maltose dextrin solution (9 g/kg body weight, equal calorie to ethanol); mice in ALD groups were fed with the Lieber–DeCarli diet (contain 5% ethanol) for 8 weeks plus i.g. administration of single binge ethanol (5 g/kg body weight). Mice were euthanized after 9 h of the single binge ethanol or maltose solution administration.

The acute ALD mouse model was constructed as follows (Chang et al., 2015): mice in the control groups were fed normal chow for 3 days, and then received i.g. administration of maltose dextrin solution (9 g/kg body weight). In model groups, mice were fed an HFD (60% kcal; CAT#D12492) for 3 days and received i.g. administration of 31.25% (vol/vol) ethanol solution (5 g/kg body weight) on the last day. All mice were euthanized after 9 h of ethanol or maltose dextrin solution administration, followed by a collection of blood and tissue samples.

To determine the role of roxadustat in ALD, mice in the vehicle group received intraperitoneal (i.p.) injection of PBS every day; mice in roxadustat groups received i.p. injection of roxadustat solution (10 mg/kg body weight or 25 mg/kg body weight for chronic or acute ALD mouse model, respectively) every day. The selection for doses of roxadustat is described as follows: previous studies used a serious range of roxadustat for *in vivo* experiments, mainly from 10 to 60 mg/kg body weight (Beck et al., 2017; Deguchi et al., 2020; Kabei et al., 2020). To verify if different doses of roxadustat have protective effects in acute and chronic ALD mouse models, we chose a low dose of roxadustat for the chronic model, while a middle dose for the acute model, which is based on the standard of animal ethics that use as fewer animals as possible in *in vivo* experiment.

Western Blot and Immunohistochemical Staining

After treatment, cells or 30 mg liver tissues were lysed or grated with lysis buffer. The BCA Protein Assay Kit was used to determine protein concentration. The same amount of protein (60 μg) from each sample was used to determine the protein expression of ACC1, SREBP1c, FASN, IL-1β, PPARα, CPT1A, CYP2E1, TNF-α, ChREBPα, HIF-1α, GAPDH, and α-Tubulin using Western blot (Yin et al., 2020). The signals were detected by ChemiScope 3000 mini (Qinxiang, Shanghai, China), and the band density was quantified using Photoshop software.

Liver CD68 expression was determined using immunohistochemical staining. Images were obtained using a ZEISS Scope A1 fluorescence microscope, and quantity analysis of CD68 positive cells was determined by Photoshop software.

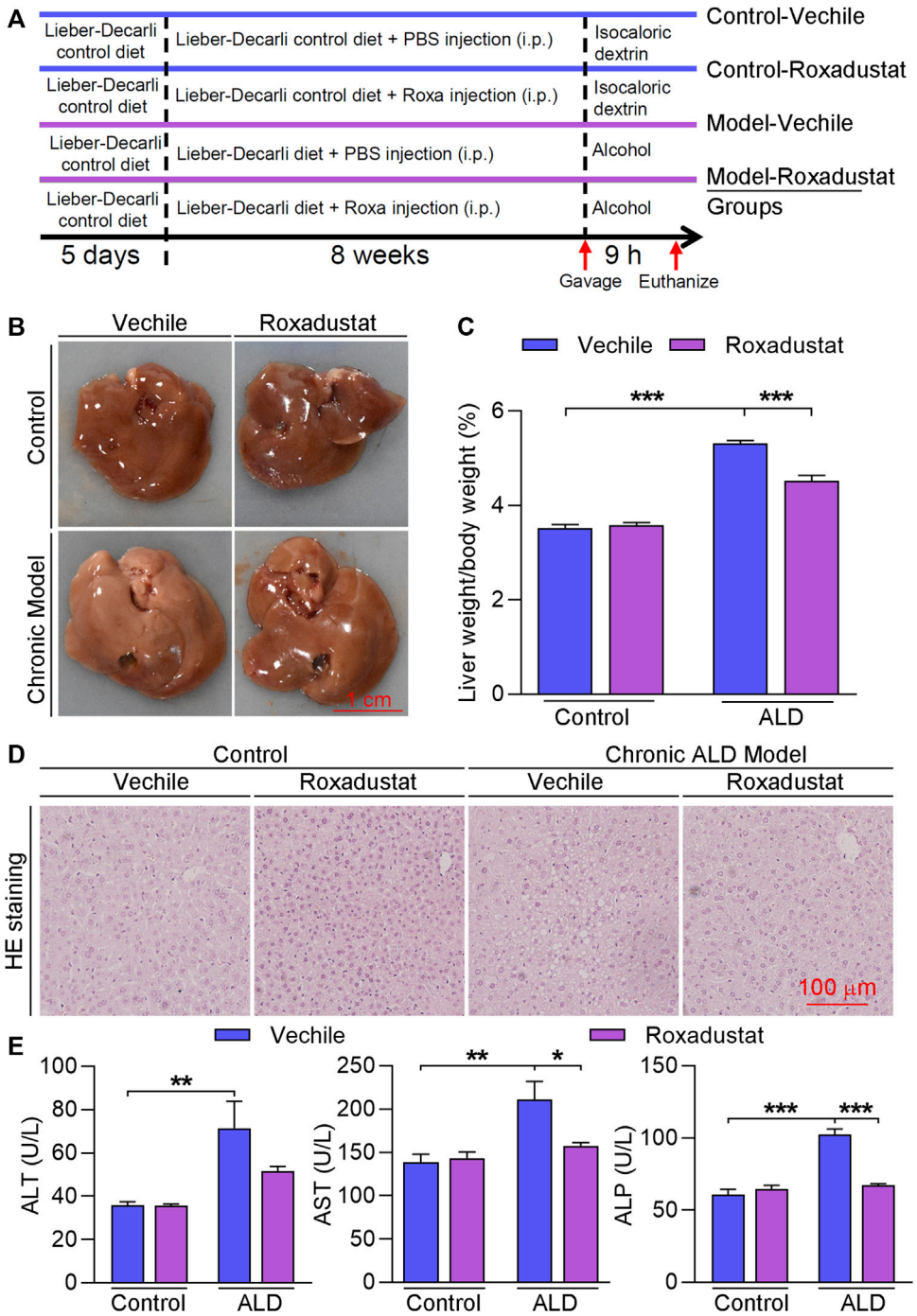

FIGURE 1 | Roxadustat inhibits the development of chronic ALD. **(A)** (experimental design): C57BL/6J mice in four groups (8 mice/group) received the following treatment: control groups: fed with the Lieber–DeCarli control diet plus a single gavage of maltose dextrin solution; model groups: fed with Lieber–DeCarli control diet for 5 days, and then with the Lieber–DeCarli diet for 8 weeks plus a single gavage of ethanol (5 g/kg body weight). Mice in vehicle groups received i.p. injection of PBS; mice in roxadustat groups received i.p. injection of roxadustat solution (10 mg/kg body weight) for 8 weeks daily. Mice were sacrificed after 9 h of maltose dextrin or ethanol gavage, blood, and liver tissues were collected; **(B)** liver from each mouse was photographed, and the representative photographs are presented; **(C)** ratio of liver weight to body weight was calculated; **(D)** liver paraffin sections were conducted with H&E staining; **(E)** serum was used to determine ALT, AST, and ALP activities using an automatic biochemical analyzer. *, $p < 0.05$; **, $p < 0.01$; ***, $p < 0.001$ ($n \geq 5$).

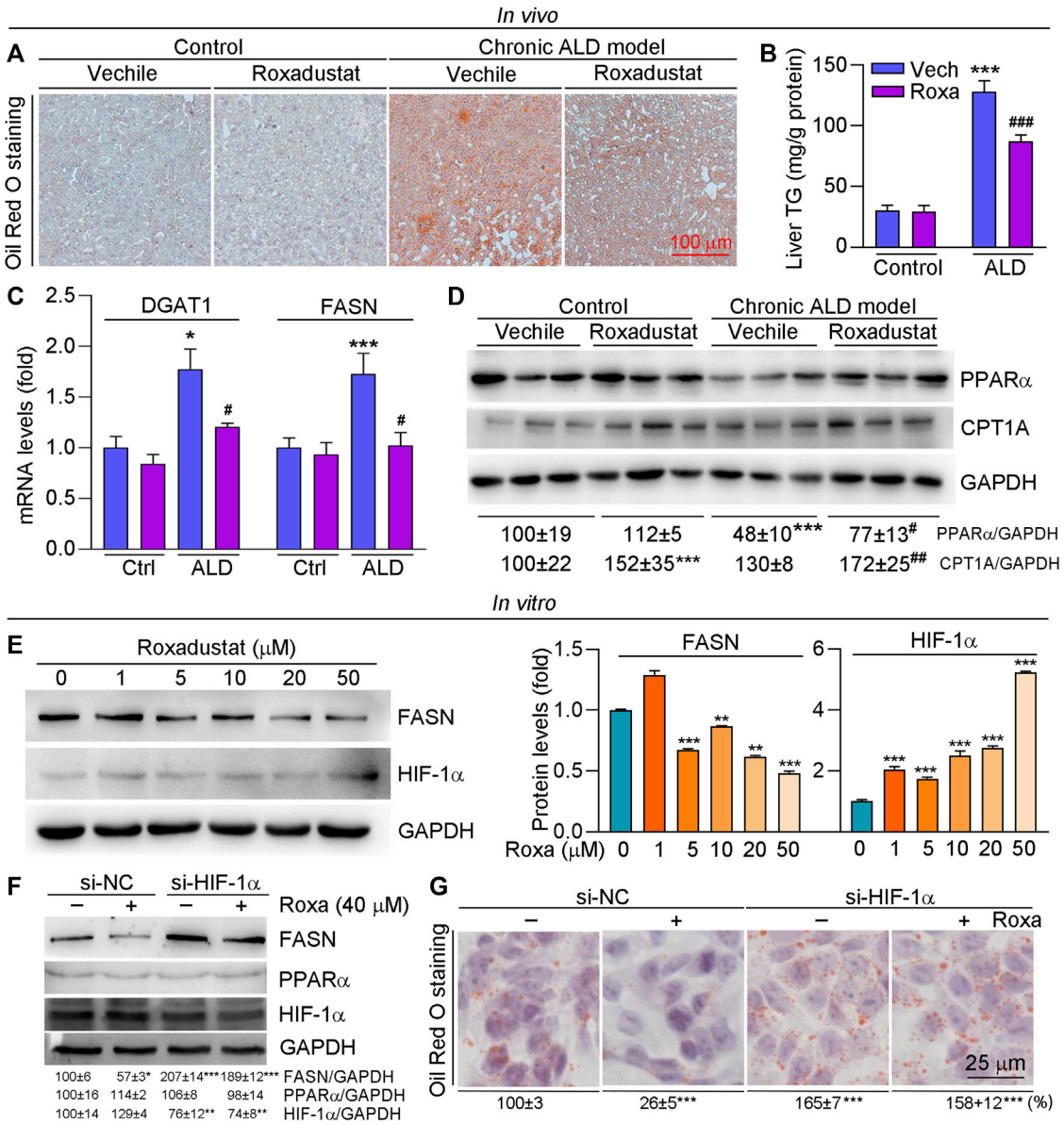

FIGURE 2 | Roxadustat attenuates lipid accumulation by increasing PPARα protein expression in the liver and reducing FASN levels in HepG2 cells. **(A–D)** Liver samples were collected from mice in **Figure 1** and used for the following experiments. Liver frozen sections were stained with Oil Red O staining **(A)**; triglyceride content was determined using an assay kit **(B)**; mRNA expression of DGAT1 and FASN was determined by qRT-PCR **(C)**; protein expression of PPARα and CPT1A was determined by Western blot with quantitative analysis of band density **(D)**; **(E)** HepG2 cells were treated with roxadustat at indicated concentrations for 24 h. Protein expression of FASN and HIF-1α was determined by Western blot with quantitative analysis of band density (right panels); **(F,G)** HepG2 cells were transfected with scrambled siRNA (si-NC) or HIF-1α siRNA (si-HIF-1α) for 24 h, and then treated with roxadustat for 24 h. Protein expression of FASN, PPARα, and HIF-1α was determined by Western blot with quantitative analysis of band density (F); lipid accumulation was determined by Oil Red O staining with quantitative analysis (G). *, $p < 0.05$; **, $p < 0.01$; ***, $p < 0.001$ vs ctrl; #$p < 0.05$, ###, $p < 0.001$ vs ALD group (n ≥ 5); Roxa: roxadustat.

Quantitative Real-Time PCR (qRT-PCR)

After treatment, Trizol was used to extract total RNA from 20 mg liver tissues or RAW264.7 cells. cDNA was synthesized with 1 μg RNA from each sample with HiScript II Q Select RT SuperMix (gDNA wiper). RT-PCR was applied with the primers listed in **Table 1**. mRNA expression was normalized by β-actin mRNA in the corresponding samples.

H&E, Oil Red O, and DHE Staining

A piece of the liver was fixed in 4% paraformaldehyde overnight, and then dehydrated with an auto dehydrator (Leica, Wetzlar, Germany). After being embedded in paraffin, the tissue samples were cut into 5 μm sections, and then conducted with H&E staining. Frozen liver tissues embedded in OCT were cut into 5 μm sections for

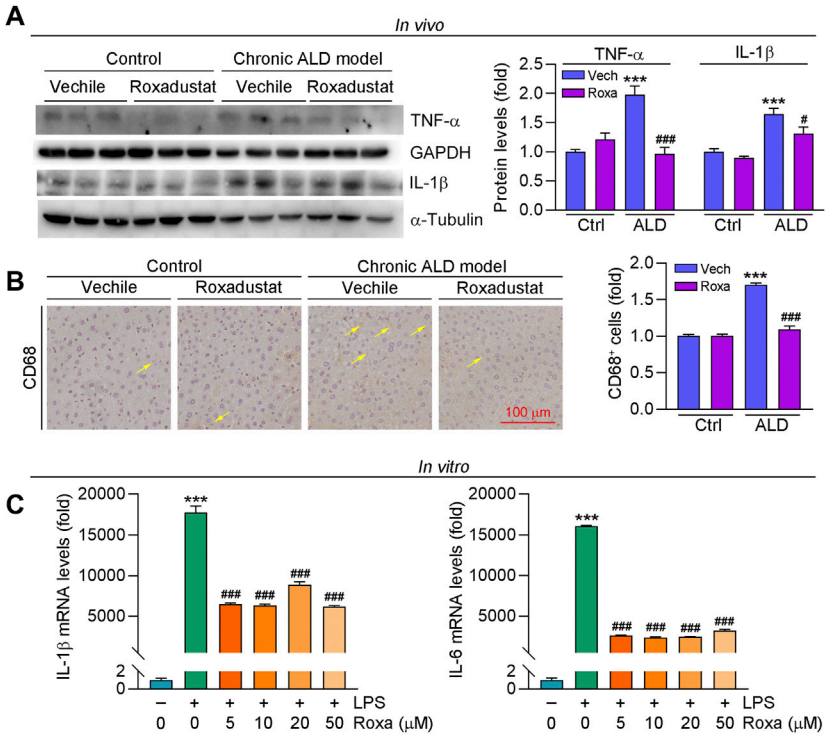

FIGURE 3 | Roxadustat reduces inflammation by reducing inflammatory cytokines both *in vivo* and *in vitro*. **(A,B)** Liver samples were collected from mice in **Figure 1**, protein expression of TNF-α and IL-1β were determined using Western blot with quantitative analysis of band density **(A)**, CD68 protein expression was determined using immunohistochemical staining with quantitative analysis **(B)**. **(C)** RAW264.7 cells were pretreated with indicated concentrations of roxadustat for 2 h, and then co-treated with LPS (1 μg/ml) for 24 h. mRNA levels of IL-1β and IL-6 were determined by qRT-PCR. ***, $p < 0.001$ vs ctrl; #, $p < 0.05$, ###, $p < 0.001$ vs ALD group or LPS-treated group (n ≥ 3); Roxa: roxadustat.

the determination of lipid accumulation or ROS levels by Oil Red O or DHE staining, respectively (Wang et al., 2021). Images were obtained using a ZEISS Scope A1 fluorescence microscope. DHE fluorescence intensity was quantified using ImageJ software.

Statistical Analysis

All data were generated from at least three independent experiments. GraphPad Prism 8.0 was used for data statistical analysis. All data were shown as means ± SEM. Data were analyzed by one-way ANOVA followed by Bartlett's test, and the difference was considered significant at $p < 0.05$.

RESULTS

Roxadustat Inhibits the Development of Chronic Alcoholic Liver Disease

To investigate the role of roxadustat on ALD, we first constructed a chronic ALD mouse model by feeding the Lieber–DeCarli liquid diet plus a single alcohol gavage, and mice received roxadustat treatment for 8 weeks (**Figure 1A**). During the experiment, we monitored the pathology changes in the liver with an ultrasound scanner (Mathiesen et al., 2002; Pandit et al., 2019). The B-mode ultrasound images indicated the Lieber–DeCarli liquid diet caused hepatic steatosis after 2 weeks of feeding, evidenced by enhanced brightness. In contrast, lipid accumulation was attenuated along with roxadustat treatment (**Supplementary Figure S1**). In addition, we found long-term exposure to alcohol resulted in an overall larger and whiter liver, as well as an elevated ratio of liver weight to body weight, which was improved by roxadustat treatment (**Figures 1B,C**). Consistent with morphological changes in the liver, H&E staining revealed significant pathological morphological changes in chronic ALD mouse liver (**Figure 1D**). However, roxadustat improved the damage on liver tissues. Serum transaminase activities are indicators of liver damage, which can be produced by injured hepatocytes (Marin et al., 2017). Our results showed that serum ALT, AST, and ALP activities were enhanced in chronic ALD mouse serum while being attenuated by roxadustat, especially the

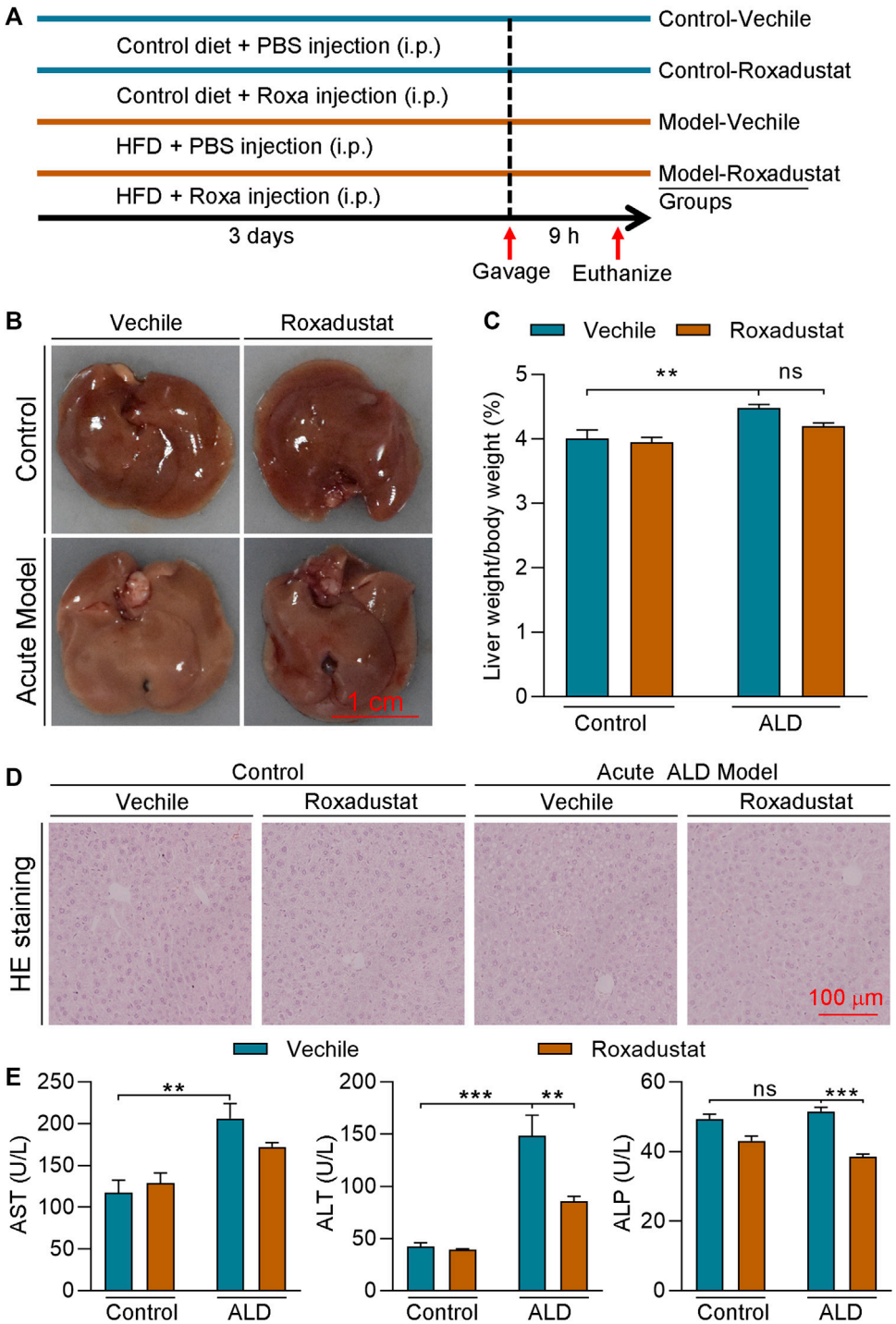

FIGURE 4 | Roxadustat inhibits the development of acute ALD **(A)** (experimental design): C57BL/6J mice in four groups (6 mice/group) received the following treatment: control groups: fed with normal chow for 3 days plus a single gavage of maltose dextrin solution; model groups: fed with HFD for 3 days plus i.g. administration of 31.25% (vol/vol) ethanol solution (5 g/kg body weight) on the last day. Mice in the vehicle groups received i.p. injection of PBS; mice in roxadustat groups received i.p. injection of roxadustat solution (25 mg/kg body weight) daily. Mice were sacrificed after 9 h of maltose dextrin or ethanol gavage, blood, and liver tissues were collected; **(B)** liver from each mouse was photographed, and the representative photographs were presented; **(C)** and the ratio of liver weight to body weight was calculated; **(D)** liver paraffin sections were stained with H&E staining; and **(E)** serum was used to determine ALT, AST, and ALP activities by an automatic biochemical analyzer. **, $p < 0.01$; ***, $p < 0.001$; ns: not significantly different ($n \geq 5$).

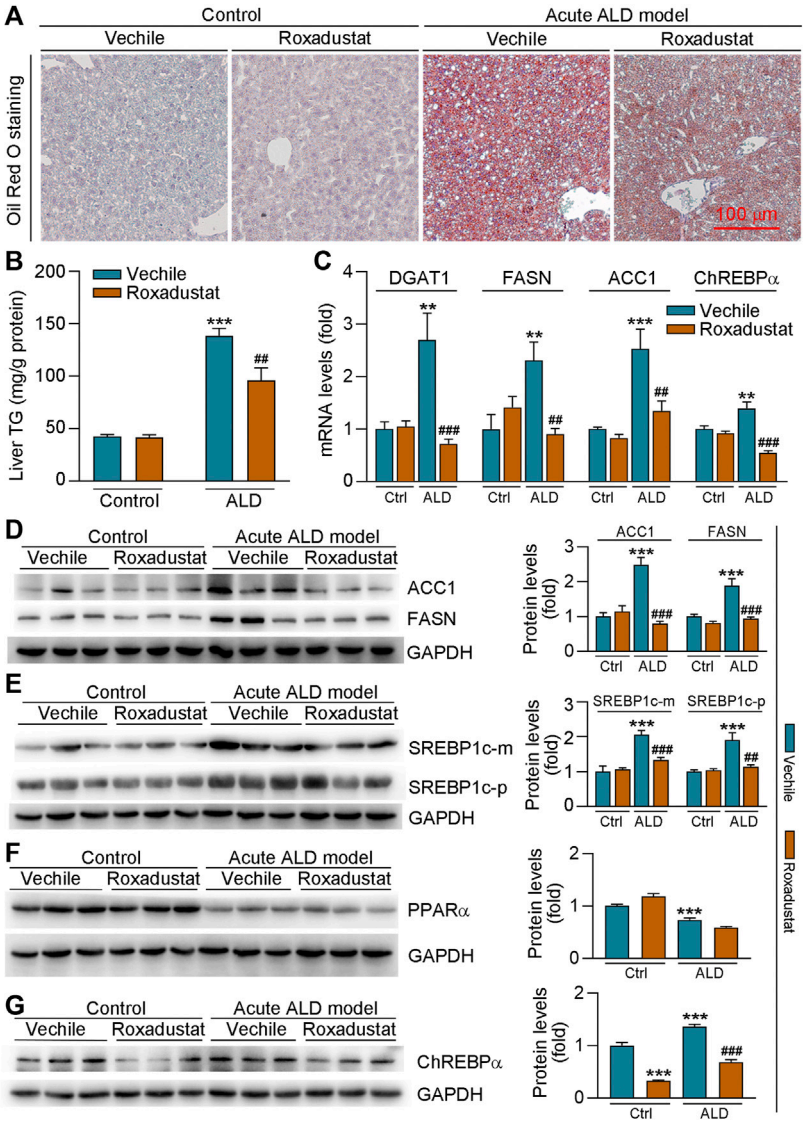

FIGURE 5 | Roxadustat reduces lipid accumulation in acute ALD mouse liver by decreasing fatty acid synthesis-related gene expression. Liver samples were collected from mice in **Figure 4**, and liver frozen sections were conducted with Oil Red O staining **(A)**; mouse liver triglyceride content was measured with an assay kit **(B)**; mRNA levels of DGAT1, FASN, ACC1, and ChREBPα were determined by qRT-PCR **(C)**; **(D-G)** protein expression of ACC1, FASN **(D)**, precursor (p), or mature (m) form of SREBP1c **(E)**, PPARα **(F)**, and ChREBPα **(G)** was determined by Western blot with quantitative analysis of band density (right panels). **, $p < 0.01$; ***, $p < 0.001$ vs ctrl group; ##, $p < 0.01$, ###, $p < 0.001$ vs ALD group ($n \geq 3$).

AST and ALP activities (**Figure 1E**). The aforementioned results indicated that roxadustat inhibits the development of chronic ALD.

Roxadustat Improves Liver Lipid Accumulation by Inhibiting Triglyceride Synthesis-Related Gene Expression and Inducing PPARα Levels in Chronic Alcoholic Liver Disease Mice

The results of B-mode ultrasound and H&E staining indicated that roxadustat can improve Lieber–DeCarli liquid diet-induced hepatic steatosis. We further conducted Oil Red O staining and found that lipid accumulation was enhanced in the chronic ALD group while being alleviated by roxadustat (**Figure 2A**). Compared to the model group, liver triglyceride levels were also attenuated by roxadustat treatment (**Figure 2B**). DGAT and FASN are key enzymes that catalyze the final reaction of triglyceride synthesis (Chitraju et al., 2017). Our results showed that DGAT and FASN mRNA levels were increased under the mediation of alcohol (**Figure 2C**). However, roxadustat treatment reduced alcohol-enhanced DGAT1 and FASN expression. PPARα is a nuclear receptor that regulates the expression of various

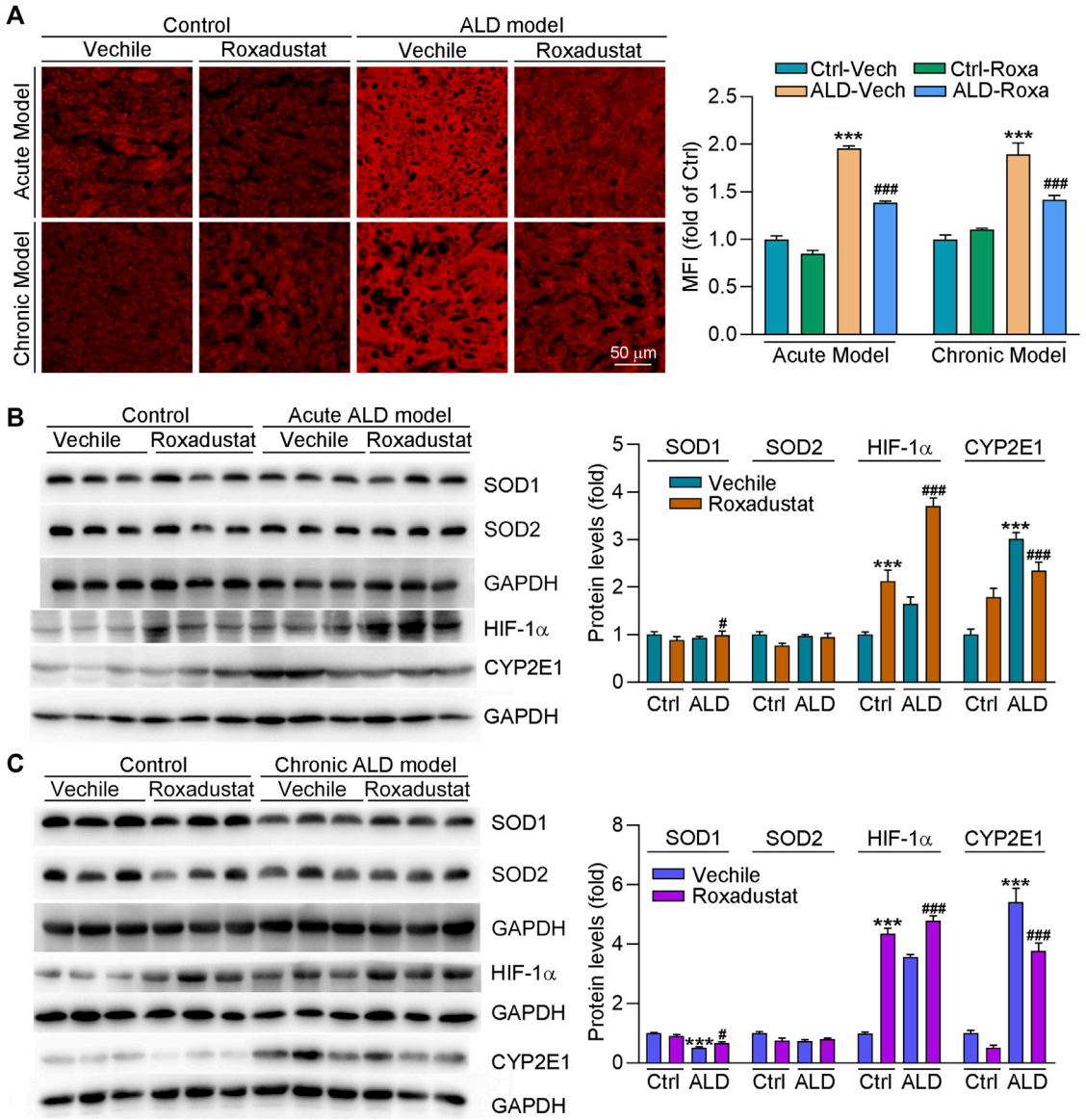

FIGURE 6 | Roxadustat reduces oxidative stress in mouse liver by enhancing SOD1 and decreasing CYP2E1 expression. **(A)** Superoxide in the liver was determined by DHE staining; **(B,C)** total protein extracted from the liver of acute ALD mouse **(B)** and chronic ALD mouse **(C)** was used to determine the protein expression of SOD1, SOD2, HIF-1α, and CYP2E1 using Western blot with quantitative analysis of band density (right panels). ***, $p < 0.001$ vs ctrl group; #, $p < 0.05$, ###, $p < 0.001$ vs ALD group ($n \geq 3$).

genes involved in mitochondrial β-oxidation (You and Arteel, 2019). Alcohol intake affects mitochondrial oxidation and inhibits PPARα signaling. As shown in **Figure 2D**, PPARα protein expression was reduced in ALD mouse liver, which was enhanced in the roxadustat treatment group. CPT1A is a classical target gene of PPARα, a key regulator for fatty acid β-oxidation (Rakhshandehroo et al., 2010). Consistent with the results of PPARα, we also found that roxadustat treatment enhanced CPT1A protein levels (**Figure 2D**).

To further investigate the mechanism of roxadustat on lipid accumulation, we treated HepG2 cells with roxadustat and found that roxadustat reduced FASN protein expression in a dose-dependent manner (**Figure 2E**). Furthermore, we transfected cells with HIF-1α siRNA to knockdown HIF-1α levels. As shown in **Figure 2F**, roxadustat inhibited FASN expression in siNC HepG2 cells while having little effect on siHIF-1α HepG2 cells, indicating roxadustat regulates FASN levels depending on HIF-1α expression. In addition, Oil Red

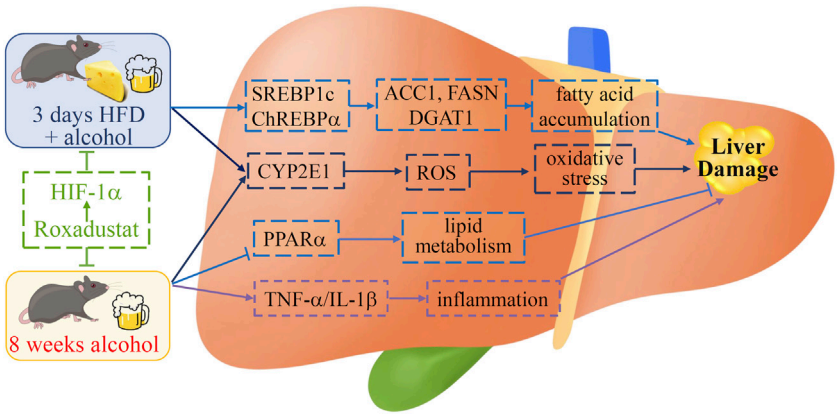

FIGURE 7 | Schematic diagram of the role of roxadustat in ALD. Roxadustat reduces long- and short-term alcohol-induced liver damage. Activation of HIF-1α ameliorates fatty acid accumulation by regulating SERBP1c and ChREBPα in acute ALD mice while improving the lipid metabolism through the PPARα pathway in chronic ALD mice. Roxadustat blocks the expression of long-term alcohol treatment-induced inflammatory cytokines TNF-α and IL-1β. Meanwhile, roxadustat reduces oxidative stress by reducing hepatic CYP2E1 to keep ROS at a low level in those two mouse models. We indicate that roxadustat may be a potential drug for ALD.

O staining results showed that roxadustat inhibited lipid accumulation in control cells, but not in HIF-1α knockdown cells (**Figure 2G**). In contrast to the *in vivo* results, we found roxadustat had little effect on PPARα protein levels neither in control cells nor in HIF-1α knockdown cells (**Figure 2F**). Taken together, the abovementioned results demonstrated that roxadustat inhibits lipid accumulation both *in vivo* and *in vitro*.

Roxadustat Inhibits Inflammatory Response in Chronic Alcoholic Liver Disease Mice

Alcohol and its metabolic derivatives can act as harmful stimuli to the body, leading to an inflammatory response. Inflammation maintains the homeostasis of the body, but can also cause collateral damage to normal tissues (Xu et al., 2017). Alcohol impairs intestinal barrier function and increases LPS flux to the portal vein. Excess LPS binds to toll-like receptor four to activate macrophages, causing inflammatory cytokine secretion (Xu et al., 2017). In this study, we found pro-inflammatory cytokines expression, such as IL-1β and TNF-α, was increased in liver tissues of ALD mice, which was significantly inhibited by roxadustat (**Figure 3A**). In addition, we conducted immunohistochemical staining with CD68 antibody (a marker for monocyte) and found that levels of $CD68^+$ cells were enhanced in ALD mouse liver. Consistent with the results of inflammatory cytokines, roxadustat reduced the infiltration of monocytes (**Figure 3B**). Furthermore, we treated RAW264.7 cells with LPS to induce inflammation in the presence or absence of roxadustat. As shown in **Figure 3C**, LPS-induced IL-1β and IL-6 mRNA levels were largely attenuated by roxadustat treatment. The above results suggest that roxadustat inhibits inflammatory response both *in vivo* and *in vitro*.

Roxadustat Inhibits the Development of Acute Alcoholic Liver Disease

To further investigate if roxadustat has protective effect on HFD plus acute alcohol-caused liver injury, we conducted an acute ALD mouse model by feeding mice an HFD for 3 days plus a single gavage of ethanol (**Figure 4A**). After 9 h of ethanol treatment, the mice were sacrificed. Mouse liver of the model group showed a tendency to be much whiter and larger, with an enhanced ratio of liver weight to body weight (**Figures 4B,C**). In contrast, roxadustat attenuated acute alcohol-caused changes in the liver and slightly decreased liver weight/body weight. Moreover, fat vacuoles were found in acute ALD mouse liver, which were improved by roxadustat (**Figure 4D**). Consistent with the results of the chronic ALD mouse model, we showed acute alcohol also enhanced serum ALT, AST, and ALP activities (**Figure 4E**). However, AST and ALP activities were greatly inhibited by roxadustat treatment, indicating the hepatoprotective function of roxadustat.

Roxadustat Attenuates Lipid Accumulation in Acute Alcoholic Liver Disease Mouse Liver by Regulating Hepatic Lipid Synthesis

The results of H&E staining in **Figure 4D** showed that roxadustat can also inhibit acute alcohol-induced lipid accumulation in the liver. We further conducted Oil Red O staining of liver frozen sections and found that roxadustat treatment significantly reduced lipid accumulation in acute ALD model mouse liver (**Figure 5A**). The results of liver triglyceride levels further confirmed that lipid levels were attenuated by roxadustat (**Figure 5B**). The abovementioned results indicated that roxadustat can inhibit acute alcohol-induced hepatic lipid accumulation. The liver generates fatty acids from non-lipid precursors *via de novo* lipogenesis. Multiple enzymes participate in this process; ACC-1 converts acetyl coenzyme A to malonyl coenzyme A and FASN synthesizes saturated fatty acids from malonyl coenzyme A (Huang et al., 2010). Compared to the

control group, we found mRNA levels of DGAT1, FASN, and ACC1, and protein levels of ACC1 and FASN were induced in acute ALD mouse liver. However, the expression of the aforementioned lipogenesis-related genes was inhibited by roxadustat (**Figures 5C,D**). SREBP1c, a key transcription factor, is a master regulator of lipogenesis by activating genes related to fatty acid and triglyceride synthesis (Li et al., 2011). Our results showed that acute alcohol-induced both precursor and mature forms of SREBP1c protein expression were reduced by roxadustat treatment (**Figure 5E**). However, we found that roxadustat had little effect on acute alcohol-reduced PPARα protein expression (**Figure 5F**), which is consistent with the results of **Figure 2D**. ChREBPα is emerging as a critical driver of the lipid metabolism (Wang et al., 2015; Sanchez-Gurmaches et al., 2018). Our results indicated that ChREBPα mRNA and protein expression were enhanced in acute ALD mouse liver, which was reduced by roxadustat treatment (**Figures 5C,G**). Taken together, the above results suggested that roxadustat can attenuate the development of acute ALD through downregulation of lipid synthesis-related genes expression.

Roxadustat Improves Oxidative Stress in Both Chronic and Acute Alcoholic Liver Disease Mouse Models by Reducing Cytochrome P450 2E1 Expression and Enhancing Superoxidase Dismutase 1 Levels

The alcohol metabolism generates large amounts of free radicals and ROS, which can cause oxidative stress and mitochondrial damage to lead further damage and apoptosis of hepatocytes. To determine if roxadustat can regulate oxidative stress in ALD mouse models, we conducted DHE staining of liver sections. As shown in **Figure 6A**, we found that ROS levels were enhanced in both chronic and acute ALD mouse liver. However, roxadustat decreased ROS accumulation in liver tissues, evidenced by reduced density of red fluorescence. CYP2E1 is an alcohol-inducible enzyme that contributes to ethanol metabolism. It can cause oxidative stress, depletion of the antioxidant system, and liver damage due to massive rupture of hepatocyte mitochondrial membranes (Albano, 2008). We found protein expression of CYP2E1 was largely enhanced in ALD mouse liver. Conversely, roxadustat reduced alcohol-enhanced CYP2E1 levels in those two mouse models with HIF-1α activation (**Figures 6B,C**). SOD1 and SOD2 are critical antioxidant enzymes. Our results showed that roxadustat had little effect on SOD2 protein expression. However, inhibited SOD1 levels were enhanced by roxadustat in both acute and chronic ALD mouse liver tissues (**Figures 6B,C**). The aforementioned results showed that roxadustat ameliorates alcohol-induced ROS accumulation by decreasing CYP2E1 and enhancing SOD1 expression.

DISCUSSION

Roxadustat is a clinical drug used for treating anemia in chronic kidney disease patients. In this study, we used chronic and acute ALD mouse models to explore the protective role of roxadustat in liver diseases. Our study demonstrates that roxadustat inhibits the development of ALD, which was evidenced by reducing serum aminotransferase activities, fatty liver, inflammation, and ROS levels. Mechanistically, roxadustat reduced the expression of fatty acid synthesis-related genes expression, including SREBP1c, ChREBPα, FASN, and ACC1, and enhanced the β-oxidation pathway by promoting the expression of PPARα and CPT1A (**Figures 2**, **5**). At the same time, roxadustat decreased the expression of inflammatory factors IL-6, IL-1β, and TNF-α in the liver, and inhibited macrophage/monocyte migration to ameliorate long-term alcohol-induced inflammation (**Figure 3**). Moreover, we indicated that roxadustat ameliorated oxidative stress by inhibiting CYP2E1 and promoting SOD1 expression in the liver (**Figure 6**).

Chronic alcohol abuse can not only induce liver damage but also impair renal tubular function (Labib et al., 1989). A nationwide database analysis indicated that the incidence of chronic kidney disease is positively related to alcohol use disorder (Pan et al., 2018). Previous studies have shown that alcohol can reduce renal function and interstitial edema in rat kidneys (Van Thiel et al., 1977; Sönmez et al., 2012; Varga et al., 2017). The liver is the dominant organ for the alcohol metabolism and the target organ of toxicity. Alcohol consumption enhances ROS levels in the liver, as well as other tissues, thereby causing serious damage, such as fibrosis, ferroptosis, and DNA damage. Anemia can be caused by both chronic kidney and liver diseases with the feature of decreased hemoglobin and circulating erythrocytes, which is related to inadequate production of erythropoietin in the kidney, accumulation of inflammation, and deficiency of iron (Gonzalez-Casas et al., 2009; Koury and Haase, 2015). HIF activation promotes erythropoietin transcription in both the kidney and liver to alleviate anemia (Gonzalez-Casas et al., 2009; Koury and Haase, 2015). Moreover, anemia is a frequent complication of advanced liver disease (Gkamprela et al., 2017). Therefore, amelioration of anemia benefits chronic kidney and liver diseases.

The early accumulation of triglycerides in hepatocytes can be regulated by several pathways. In the process of ALD, alcohol reduces mitochondrial fatty acid β-oxidation by increasing the level of NADH/NAD^+ in hepatocytes, which leads to steatosis (Baraona and Lieber, 1979). Alcohol consumption can also upregulate hepatic SREBP1c expression, as well as target lipogenic-related genes, to enhance fatty acid synthesis (Galli et al., 2001). Both short- and long-term treatment of HFD promote hepatic steatosis (Wiedemann et al., 2013), indicating alcohol plus HFD may cause severe liver damage. PPARα is inhibited by long-term treatment of alcohol (Fischer et al., 2003). Previous studies have proven fenofibrate (a PPARα agonist) treatment reverses ethanol-induced liver steatosis by stimulating the β-oxidation pathway (Xu et al., 2021). Some evidence has shown that alcohol increases fatty acid synthesis by increasing the ChREBP activity (Dentin et al., 2005). Our results showed that roxadustat reduced lipid accumulation by increasing PPARα and CPT1A expression and reducing DGAT1 and FASN levels in chronic ALD mouse livers (**Figures 2C,D**). In contrast to chronic ALD mouse, roxadustat had little effect on PPARα expression in acute ALD mouse liver or HepG2 cells (**Figures 2F**, **5F**), indicating PPARα is not a direct target gene of

HIF-1α. On the other hand, we found that roxadustat inhibited fatty acid accumulation by reducing SREBP1c, ChREBPα, DGAT1, ACC1, and FASN expression in the acute ALD mouse liver (**Figure 5**).

Inflammation plays an important role in the pathogenesis of ALD. Immune cells are the main sources of pro-inflammatory cytokines and chemokines, which lead to the deterioration of ALD. Hepatocytes and liver non-parenchymal cells can also produce pro-inflammatory cytokines. It has been demonstrated that high level of TNF-α in serum is associated with the pathophysiology of alcoholic hepatitis patients (Tilg et al., 2003). Short- or long-term HFD feeding plus acute alcohol binge synergistically induce acute liver injury by enhancing the expression of hepatic chemokine (C-X-C motif) ligand 1 and promoting the infiltration of hepatic neutrophil (Chang et al., 2015). Previous research has proven that stabilization of HIF-1α exerts an anti-inflammatory effect by inhibiting the expression of pro-inflammatory cytokines in murine colitis (Keely et al., 2014). Our results confirmed that alcohol-induced monocyte/macrophage recruitment in mouse liver was reduced by roxadustat (**Figure 3B**). In addition, roxadustat inhibited alcohol or LPS-enhanced inflammatory cytokines in mouse liver or RAW264.7 cells (**Figures 3A,C**). Our results showed that roxadustat can also inhibit inflammation in ALD.

Alcohol is oxidized in hepatocytes by ethanol dehydrogenase to acetaldehyde, and then metabolized to acetic acid by acetaldehyde dehydrogenase. Alcohol and its metabolites have toxic, neurodegenerative, or cancerogenic properties (Correa et al., 2003; Quertemont and Didone, 2006; Nieminen and Salaspuro, 2018). ROS elevation is closely associated with the pathology of ALD, and high levels of ROS damage cell structure and lead to cell death by oxidizing nucleic acids, proteins, and lipids (Mittler, 2002). CYP2E1 is an enzyme for metabolizing alcohol to acetaldehyde, and can be induced by the alcohol metabolism, which leads to liver injury and ROS production (Lieber et al., 1970). Ethanol induced the accumulation of macrovesicular fat, and liver triglyceride was blocked in CYP2E1 knockout mice. Compared to wild-type mice, oxidative stress and lipid peroxidation were also reduced in CYP2E1 knockout mice. In contrast, restored CYP2E1 expression by adenovirus in CYP2E1 knockout mice induced fat accumulation in the liver (Lu et al., 2008). In addition to alcohol, HFD can also induce oxidative stress (Matsuzawa-Nagata et al., 2008). Studies have shown that mitochondrial HIF-1α can protect against hypoxia or H_2O_2 caused cell apoptosis by reducing oxidative stress (Li et al., 2019). In diabetic rats, a carbohydrate energy-restricted diet attenuates renal damage by upregulating HIF-1α levels to reduce oxidative stress. In addition, HIF-1α activation can protect against doxorubicin-induced cardiotoxicity by inhibiting inflammation and oxidative stress (Long et al., 2020). In this study, we showed that liver ROS generation was attenuated by roxadustat both in acute and chronic ALD mouse models. Our results indicated that roxadustat enhanced SOD1 expression while having little effects on SOD2 levels. However, CYP2E1 expression was largely reduced by roxadustat, indicating roxadustat regulates alcohol-induced liver ROS levels mainly by inhibiting CYP2E1 and enhancing SOD1 expression (**Figure 6**).

In this study, we used two ALD mouse models to explore the protective role of roxadustat on liver injury. In the chronic model, enhanced inflammatory cytokines and infiltration of monocytes/macrophages were almost blocked by roxadustat, indicating the anti-inflammatory properties of roxadustat. Ethanol or ethanol plus HFD caused fatty liver was largely attenuated by roxadustat. Regarding molecular mechanisms, the anti-ALD effects of roxadustat are contributed by decreased fatty acid accumulation, enhanced β-oxidation, reduced inflammation, and oxidative stress (**Figure 7**). In conclusion, our results demonstrate that HIF-1α activation provides protection against ALD in both chronic and acute mouse models, and reveal the potential of roxadustat for ALD treatment.

DATA AVAILABILITY STATEMENT

The original contributions presented in the study are included in the article/**Supplementary Material**, further inquiries can be directed to the corresponding author.

ETHICS STATEMENT

The animal study was reviewed and approved by the Institution Animal Ethics Committee of Hefei University of Technology.

AUTHOR CONTRIBUTIONS

XY and JH conceived and designed the study. YG, DY, WG, DW, KG, and YP performed, analyzed, and interpreted studies. YG and XY wrote the article. XY, JH, XJ, HJ, CS, YD, and YC contributed reagents/materials/analysis tools and revised the article. All authors discussed the data and commented on the manuscript.

FUNDING

This work was supported by the National Natural Science Foundation of China (NSFC) Grant 81973316 to JH, 82173807 to YD, and the China Postdoctoral Science Foundation Grant 2020M681914 to XY.

SUPPLEMENTARY MATERIAL

The Supplementary Material for this article can be found online at: https://www.frontiersin.org/articles/10.3389/fphar.2022.895710/full#supplementary-material

REFERENCES

Addolorato, G., Ancona, C., Capristo, E., and Gasbarrini, G. (2003). Metadoxine in the Treatment of Acute and Chronic Alcoholism: a Review. *Int. J. Immunopathol. Pharmacol.* 16 (3), 207–214. doi:10.1177/039463200301600304

Albano, E. (2008). Oxidative Mechanisms in the Pathogenesis of Alcoholic Liver Disease. *Mol. Aspects Med.* 29, 9–16. doi:10.1016/j.mam.2007.09.004

Arteel, G. E., Iimuro, Y., Yin, M., Raleigh, J. A., and Thurman, R. G. (1997). Chronic Enteral Ethanol Treatment Causes Hypoxia in Rat Liver Tissue *In Vivo*. *Hepatology* 25 (4), 920–926. doi:10.1002/hep.510250422

Baraona, E., and Lieber, C. S. (1979). Effects of Ethanol on Lipid Metabolism. *J. Lipid Res.* 20 (3), 289–315. doi:10.1016/s0022-2275(20)40613-3

Beck, J., Henschel, C., Chou, J., Lin, A., and Del Balzo, U. (2017). Evaluation of the Carcinogenic Potential of Roxadustat (FG-4592), a Small Molecule Inhibitor of Hypoxia-Inducible Factor Prolyl Hydroxylase in CD-1 Mice and sprague Dawley Rats. *Int. J. Toxicol.* 36 (6), 427–439. doi:10.1177/1091581817737232

Bertola, A., Mathews, S., Ki, S. H., Wang, H., and Gao, B. (2013). Mouse Model of Chronic and Binge Ethanol Feeding (The NIAAA Model). *Nat. Protoc.* 8 (3), 627–637. doi:10.1038/nprot.2013.032

Ceni, E., Mello, T., and Galli, A. (2014). Pathogenesis of Alcoholic Liver Disease: Role of Oxidative Metabolism. *World J. Gastroenterol.* 20 (47), 17756–17772. doi:10.3748/wjg.v20.i47.17756

Chang, B., Xu, M. J., Zhou, Z., Cai, Y., Li, M., Wang, W., et al. (2015). Short- or Long-Term High-Fat Diet Feeding Plus Acute Ethanol Binge Synergistically Induce Acute Liver Injury in Mice: an Important Role for CXCL1. *Hepatology* 62 (4), 1070–1085. doi:10.1002/hep.27921

Chen, R., Wang, Y., Ning, R., Hu, J., Liu, W., Xiong, J., et al. (2015). Decreased Carboxylesterases Expression and Hydrolytic Activity in Type 2 Diabetic Mice through Akt/mTOR/HIF-1α/Stra13 Pathway. *Xenobiotica* 45 (9), 782–793. doi:10.3109/00498254.2015.1020353

Chitraju, C., Mejhert, N., Haas, J. T., Diaz-Ramirez, L. G., Grueter, C. A., Imbriglio, J. E., et al. (2017). Triglyceride Synthesis by DGAT1 Protects Adipocytes from Lipid-Induced ER Stress during Lipolysis. *Cell Metab* 26 (2), 407–418.e3. doi:10.1016/j.cmet.2017.07.012

Correa, M., Arizzi, M. N., Betz, A., Mingote, S., and Salamone, J. D. (2003). Open Field Locomotor Effects in Rats after Intraventricular Injections of Ethanol and the Ethanol Metabolites Acetaldehyde and Acetate. *Brain Res. Bull.* 62 (3), 197–202. doi:10.1016/j.brainresbull.2003.09.013

Deguchi, H., Ikeda, M., Ide, T., Tadokoro, T., Ikeda, S., Okabe, K., et al. (2020). Roxadustat Markedly Reduces Myocardial Ischemia Reperfusion Injury in Mice. *Circ. J.* 84 (6), 1028–1033. doi:10.1253/circj.CJ-19-1039

Dentin, R., Benhamed, F., Pégorier, J. P., Foufelle, F., Viollet, B., Vaulont, S., et al. (2005). Polyunsaturated Fatty Acids Suppress Glycolytic and Lipogenic Genes through the Inhibition of ChREBP Nuclear Protein Translocation. *J. Clin. Invest.* 115 (10), 2843–2854. doi:10.1172/jci25256

Dixon, W. G., and Bansback, N. (2012). Understanding the Side Effects of Glucocorticoid Therapy: Shining a Light on a Drug Everyone Thinks They Know. *Ann. Rheum. Dis.* 71 (11), 1761–1764. doi:10.1136/annrheumdis-2012-202021

Fischer, M., You, M., Matsumoto, M., and Crabb, D. W. (2003). Peroxisome Proliferator-Activated Receptor Alpha (PPARalpha) Agonist Treatment Reverses PPARalpha Dysfunction and Abnormalities in Hepatic Lipid Metabolism in Ethanol-Fed Mice. *J. Biol. Chem.* 278 (30), 27997–28004. doi:10.1074/jbc.M302140200

Galli, A., Pinaire, J., Fischer, M., Dorris, R., and Crabb, D. W. (2001). The Transcriptional and DNA Binding Activity of Peroxisome Proliferator-Activated Receptor Alpha Is Inhibited by Ethanol Metabolism. A Novel Mechanism for the Development of Ethanol-Induced Fatty Liver. *J. Biol. Chem.* 276 (1), 68–75. doi:10.1074/jbc.M008791200

Gkamprela, E., Deutsch, M., and Pectasides, D. (2017). Iron Deficiency Anemia in Chronic Liver Disease: Etiopathogenesis, Diagnosis and Treatment. *Ann. Gastroenterol.* 30 (4), 405–413. doi:10.20524/aog.2017.0152

Gonzalez-Casas, R., Jones, E. A., and Moreno-Otero, R. (2009). Spectrum of Anemia Associated with Chronic Liver Disease. *World J. Gastroenterol.* 15 (37), 4653–4658. doi:10.3748/wjg.15.4653

Gunton, J. E. (2020). Hypoxia-inducible Factors and Diabetes. *J. Clin. Invest.* 130 (10), 5063–5073. doi:10.1172/jci137556

Huang, J., Borensztajn, J., and Reddy, J. K. (2010). "Hepatic Lipid Metabolism," in *Molecular Pathology of Liver Diseases. Molecular Pathology Library*. Editor S. Monga, 5, 133–146. doi:10.1007/978-1-4419-7107-4_10

Huang, H., Wang, X., Zhang, X., Wang, H., and Jiang, W. (2020). Roxadustat Attenuates Experimental Pulmonary Fibrosis *In Vitro* and *In Vivo*. *Toxicol. Lett.* 331, 112–121. doi:10.1016/j.toxlet.2020.06.009

Kabei, K., Tateishi, Y., Shiota, M., Osada-Oka, M., Nishide, S., Uchida, J., et al. (2020). Effects of Orally Active Hypoxia Inducible Factor Alpha Prolyl Hydroxylase Inhibitor, FG4592 on Renal Fibrogenic Potential in Mouse Unilateral Ureteral Obstruction Model. *J. Pharmacol. Sci.* 142 (3), 93–100. doi:10.1016/j.jphs.2019.12.002

Kaelin, W. G., and Ratcliffe, P. J. (2008). Oxygen Sensing by Metazoans: the central Role of the HIF Hydroxylase Pathway. *Mol. Cel.* 30 (4), 393–402. doi:10.1016/j.molcel.2008.04.009

Keely, S., Campbell, E. L., Baird, A. W., Hansbro, P. M., Shalwitz, R. A., Kotsakis, A., et al. (2014). Contribution of Epithelial Innate Immunity to Systemic protection Afforded by Prolyl Hydroxylase Inhibition in Murine Colitis. *Mucosal Immunol.* 7 (1), 114–123. doi:10.1038/mi.2013.29

Koivunen, P., Serpi, R., and Dimova, E. Y. (2016). Hypoxia-Inducible Factor Prolyl 4-hydroxylase Inhibition in Cardiometabolic Diseases. *Pharmacol. Res.* 114, 265–273. doi:10.1016/j.phrs.2016.11.003

Kong, L., Chen, J., Ji, X., Qin, Q., Yang, H., Liu, D., et al. (2021). Alcoholic Fatty Liver Disease Inhibited the Co-expression of Fmo5 and PPARα to Activate the NF-κB Signaling Pathway, Thereby Reducing Liver Injury via Inducing Gut Microbiota Disturbance. *J. Exp. Clin. Cancer Res.* 40 (1), 18. doi:10.1186/s13046-020-01782-w

Koury, M. J., and Haase, V. H. (2015). Anaemia in Kidney Disease: Harnessing Hypoxia Responses for Therapy. *Nat. Rev. Nephrol.* 11 (7), 394–410. doi:10.1038/nrneph.2015.82

Labib, M., Abdel-Kader, M., Ranganath, L., Martin, S., and Marks, V. (1989). Impaired Renal Tubular Function in Chronic Alcoholics. *J. R. Soc. Med.* 82 (3), 139–141. doi:10.1177/014107688908200307

Li, Y., Xu, S., Mihaylova, M. M., Zheng, B., Hou, X., Jiang, B., et al. (2011). AMPK Phosphorylates and Inhibits SREBP Activity to Attenuate Hepatic Steatosis and Atherosclerosis in Diet-Induced Insulin-Resistant Mice. *Cel Metab* 13 (4), 376–388. doi:10.1016/j.cmet.2011.03.009

Li, H. S., Zhou, Y. N., Li, L., Li, S. F., Long, D., Chen, X. L., et al. (2019). HIF-1α Protects against Oxidative Stress by Directly Targeting Mitochondria. *Redox Biol.* 25, 101109. doi:10.1016/j.redox.2019.101109

Lieber, C. S., Rubin, E., and DeCarli, L. M. (1970). Hepatic Microsomal Ethanol Oxidizing System (MEOS): Differentiation from Alcohol Dehydrogenase and NADPH Oxidase. *Biochem. Biophys. Res. Commun.* 40 (4), 858–865. doi:10.1016/0006-291x(70)90982-4

Lieber, C. S. (2004). Alcoholic Fatty Liver: its Pathogenesis and Mechanism of Progression to Inflammation and Fibrosis. *Alcohol* 34 (1), 9–19. doi:10.1016/j.alcohol.2004.07.008

Long, G., Chen, H., Wu, M., Li, Y., Gao, L., Huang, S., et al. (2020). Antianemia Drug Roxadustat (FG-4592) Protects against Doxorubicin-Induced Cardiotoxicity by Targeting Antiapoptotic and Antioxidative Pathways. *Front. Pharmacol.* 11, 1191. doi:10.3389/fphar.2020.01191

Lu, X. L., Luo, J. Y., Tao, M., Gen, Y., Zhao, P., Zhao, H. L., et al. (2004). Risk Factors for Alcoholic Liver Disease in China. *World J. Gastroenterol.* 10 (16), 2423–2426. doi:10.3748/wjg.v10.i16.2423

Lu, Y., Zhuge, J., Wang, X., Bai, J., and Cederbaum, A. I. (2008). Cytochrome P450 2E1 Contributes to Ethanol-Induced Fatty Liver in Mice. *Hepatology* 47 (5), 1483–1494. doi:10.1002/hep.22222

Marin, V., Poulsen, K., Odena, G., McMullen, M. R., Altamirano, J., Sancho-Bru, P., et al. (2017). Hepatocyte-derived Macrophage Migration Inhibitory Factor Mediates Alcohol-Induced Liver Injury in Mice and Patients. *J. Hepatol.* 67 (5), 1018–1025. doi:10.1016/j.jhep.2017.06.014

Mathiesen, U. L., Franzén, L. E., Aselius, H., Resjö, M., Jacobsson, L., Foberg, U., et al. (2002). Increased Liver Echogenicity at Ultrasound Examination Reflects Degree of Steatosis but Not of Fibrosis in Asymptomatic Patients with Mild/moderate Abnormalities of Liver Transaminases. *Dig. Liver Dis.* 34 (7), 516–522. doi:10.1016/s1590-8658(02)80111-6

Matsuzawa-Nagata, N., Takamura, T., Ando, H., Nakamura, S., Kurita, S., Misu, H., et al. (2008). Increased Oxidative Stress Precedes the Onset of High-Fat

Diet-Induced Insulin Resistance and Obesity. *Metabolism* 57 (8), 1071–1077. doi:10.1016/j.metabol.2008.03.010

Meng, X., Li, S., Li, Y., Gan, R. Y., and Li, H. B. (2018). Gut Microbiota's Relationship with Liver Disease and Role in Hepatoprotection by Dietary Natural Products and Probiotics. *Nutrients* 10 (10), 1457. doi:10.3390/nu10101457

Mittler, R. (2002). Oxidative Stress, Antioxidants and Stress Tolerance. *Trends Plant Sci.* 7 (9), 405–410. doi:10.1016/s1360-1385(02)02312-9

Nieminen, M. T., and Salaspuro, M. (2018). Local Acetaldehyde-An Essential Role in Alcohol-Related Upper Gastrointestinal Tract Carcinogenesis. *Cancers (Basel)* 10 (1), 11. doi:10.3390/cancers10010011

Pan, C. S., Ju, T. R., Lee, C. C., Chen, Y. P., Hsu, C. Y., Hung, D. Z., et al. (2018). Alcohol Use Disorder Tied to Development of Chronic Kidney Disease: A Nationwide Database Analysis. *PLoS One* 13 (9), e0203410. doi:10.1371/journal.pone.0203410

Pandit, H., Tinney, J. P., Li, Y., Cui, G., Li, S., Keller, B. B., et al. (2019). Utilizing Contrast-Enhanced Ultrasound Imaging for Evaluating Fatty Liver Disease Progression in Pre-clinical Mouse Models. *Ultrasound Med. Biol.* 45 (2), 549–557. doi:10.1016/j.ultrasmedbio.2018.10.011

Quertemont, E., and Didone, V. (2006). Role of Acetaldehyde in Mediating the Pharmacological and Behavioral Effects of Alcohol. *Alcohol. Res. Health* 29 (4), 258–265.

Rahtu-Korpela, L., Karsikas, S., Hörkkö, S., Blanco Sequeiros, R., Lammentausta, E., Mäkelä, K. A., et al. (2014). HIF Prolyl 4-hydroxylase-2 Inhibition Improves Glucose and Lipid Metabolism and Protects against Obesity and Metabolic Dysfunction. *Diabetes* 63 (10), 3324–3333. doi:10.2337/db14-0472

Rakhshandehroo, M., Knoch, B., Müller, M., and Kersten, S. (2010). Peroxisome Proliferator-Activated Receptor Alpha Target Genes. *PPAR Res.* 2010, 1–20. doi:10.1155/2010/612089

Sanchez-Gurmaches, J., Tang, Y., Jespersen, N. Z., Wallace, M., Martinez Calejman, C., Gujja, S., et al. (2018). Brown Fat AKT2 Is a Cold-Induced Kinase that Stimulates ChREBP-Mediated De Novo Lipogenesis to Optimize Fuel Storage and Thermogenesis. *Cel Metab* 27 (1), 195–209.e6. doi:10.1016/j.cmet.2017.10.008

Sönmez, M. F., Narin, F., Akkuş, D., and Türkmen, A. B. (2012). Melatonin and Vitamin C Ameliorate Alcohol-Induced Oxidative Stress and eNOS Expression in Rat Kidney. *Ren. Fail.* 34 (4), 480–486. doi:10.3109/0886022x.2011.649678

Sugahara, M., Tanaka, S., Tanaka, T., Saito, H., Ishimoto, Y., Wakashima, T., et al. (2020). Prolyl Hydroxylase Domain Inhibitor Protects against Metabolic Disorders and Associated Kidney Disease in Obese Type 2 Diabetic Mice. *J. Am. Soc. Nephrol.* 31 (3), 560–577. doi:10.1681/asn.2019060582

Tilg, H., Jalan, R., Kaser, A., Davies, N. A., Offner, F. A., Hodges, S. J., et al. (2003). Anti-tumor Necrosis Factor-Alpha Monoclonal Antibody Therapy in Severe Alcoholic Hepatitis. *J. Hepatol.* 38 (4), 419–425. doi:10.1016/s0168-8278(02)00442-7

Tsukamoto, H., and Xi, X. P. (1989). Incomplete Compensation of Enhanced Hepatic Oxygen Consumption in Rats with Alcoholic Centrilobular Liver Necrosis. *Hepatology* 9 (2), 302–306. doi:10.1002/hep.1840090223

Van Thiel, D. H., Gavaler, J. S., Little, J. M., and Lester, R. (1977). Alcohol: its Effect on the Kidney. *Adv. Exp. Med. Biol.* 85a, 449–457. doi:10.1007/978-1-4899-5181-6_27

Varga, Z. V., Matyas, C., Paloczi, J., and Pacher, P. (2017). Alcohol Misuse and Kidney Injury: Epidemiological Evidence and Potential Mechanisms. *Alcohol. Res.* 38 (2), 283–288.

Wang, Y., Viscarra, J., Kim, S. J., and Sul, H. S. (2015). Transcriptional Regulation of Hepatic Lipogenesis. *Nat. Rev. Mol. Cel. Biol.* 16 (11), 678–689. doi:10.1038/nrm4074

Wang, W. J., Xiao, P., Xu, H. Q., Niu, J. Q., and Gao, Y. H. (2019). Growing burden of Alcoholic Liver Disease in China: A Review. *World J. Gastroenterol.* 25 (12), 1445–1456. doi:10.3748/wjg.v25.i12.1445

Wang, D., Yang, X., Chen, Y., Gong, K., Yu, M., Gao, Y., et al. (2020). Ascorbic Acid Enhances Low-Density Lipoprotein Receptor Expression by Suppressing Proprotein Convertase Subtilisin/kexin 9 Expression. *J. Biol. Chem.* 295 (47), 15870–15882. doi:10.1074/jbc.RA120.015623

Wang, D., Yin, Z., Ma, L., Han, L., Chen, Y., Pan, W., et al. (2021). Polysaccharide MCP Extracted from Morchella Esculenta Reduces Atherosclerosis in LDLR-Deficient Mice. *Food Funct.* 12 (11), 4842–4854. doi:10.1039/d0fo03475d

Wiedemann, M. S., Wueest, S., Item, F., Schoenle, E. J., and Konrad, D. (2013). Adipose Tissue Inflammation Contributes to Short-Term High-Fat Diet-Induced Hepatic Insulin Resistance. *Am. J. Physiol. Endocrinol. Metabendocrinol. Metab.* 305 (3), E388–E395. doi:10.1152/ajpendo.00179.2013

Xu, M. J., Zhou, Z., Parker, R., and Gao, B. (2017). Targeting Inflammation for the Treatment of Alcoholic Liver Disease. *Pharmacol. Ther.* 180, 77–89. doi:10.1016/j.pharmthera.2017.06.007

Xu, L., Zhang, X., Xin, Y., Ma, J., Yang, C., Zhang, X., et al. (2021). Depdc5 Deficiency Exacerbates Alcohol-Induced Hepatic Steatosis via Suppression of PPARα Pathway. *Cell Death Dis.* 12 (7), 710. doi:10.1038/s41419-021-03980-6

Yin, Z., Wang, X., Zheng, S., Cao, P., Chen, Y., Yu, M., et al. (2020). LongShengZhi Capsule Attenuates Alzheimer-like Pathology in APP/PS1 Double Transgenic Mice by Reducing Neuronal Oxidative Stress and Inflammation. *Front. Aging Neurosci.* 12, 582455. doi:10.3389/fnagi.2020.582455

You, M., and Arteel, G. E. (2019). Effect of Ethanol on Lipid Metabolism. *J. Hepatol.* 70 (2), 237–248. doi:10.1016/j.jhep.2018.10.037

Zhang, X., Zhang, Y., Wang, P., Zhang, S. Y., Dong, Y., Zeng, G., et al. (2019). Adipocyte Hypoxia-Inducible Factor 2α Suppresses Atherosclerosis by Promoting Adipose Ceramide Catabolism. *Cel Metab* 30 (5), 937–951.e5. doi:10.1016/j.cmet.2019.09.016

Conflict of Interest: XJ, HJ, and CS are employed by Zhejiang Jianfeng Pharmaceutical Co., Ltd.

The remaining authors declare that the research was conducted in the absence of any commercial or financial relationships that could be construed as a potential conflict of interest.

Publisher's Note: All claims expressed in this article are solely those of the authors and do not necessarily represent those of their affiliated organizations, or those of the publisher, the editors, and the reviewers. Any product that may be evaluated in this article, or claim that may be made by its manufacturer, is not guaranteed or endorsed by the publisher.

frontiers | Frontiers in Pharmacology

ORIGINAL RESEARCH
published: 25 May 2022
doi: 10.3389/fphar.2022.894981

Saikosaponin d Alleviates Liver Fibrosis by Negatively Regulating the ROS/NLRP3 Inflammasome Through Activating the ERβ Pathway

Kehui Zhang[†‡], *Liubing Lin*[‡], *Yingying Zhu*[‡], *Na Zhang*, *Meng'en Zhou* and *Yong Li*[*]

Department of Gastroenterology, Shanghai Municipal Hospital of Traditional Chinese Medicine, Shanghai University of Traditional Chinese Medicine, Shanghai, China

Background and aims: Saikosaponin d (SSd) has a steroidal structure and significant anti-inflammatory effects. The purpose of this study was to explore the mechanism underlying SSd's inhibitory effects on liver fibrosis.

Methods: Wild-type and estrogen receptor knockout (ERKO) mice were treated with CCl_4 to establish liver fibrosis mouse models. The effects of SSd on hepatic fibrogenesis were studied in these mouse models. Hepatic stellate cells (HSCs) were activated by H_2O_2 to investigate the potential molecular mechanisms. The establishment of the models and the degrees of inflammation and liver tissue fibrosis were evaluated by detecting changes in serum liver enzymes and liver histopathology. The expression of α-SMA and TGF-β1 was determined by immunohistochemistry. The expression and significance of NLRP3 inflammasome proteins were explored by RT-PCR and Western blotting analyses. The mitochondrial ROS-related indexes were evaluated by MitoSOX Red.

Results: In wild-type and ERKO mice treated with CCl_4, the fluorescence expression of mitochondrial ROS was up-regulated, while the mitochondrial membrane potential and ATP content were decreased, suggesting that the mitochondria were damaged. In addition, the expression of NLRP3 inflammatory bodies and fibrosis markers (α-SMA, TGF-β, TIMP-1, MMP-2, and Vimentin) in liver tissue increased. Furthermore, the above indexes showed the same expression trend in activated HSCs. In addition, the peripheral serum ALT and AST levels increased in CCl_4-induced liver injury model mice. And HE staining showed a large number of inflammatory cell infiltration in the liver of model mice. Picric acid-Sirius staining and Masson staining showed that there was significant collagen fibrous tissue deposition in mice liver sections. IHC and WB detection confirmed that the expression of α-SMA and TGF-β1 increased. Liver fibrosis scores were also elevated. Then, after SSd intervention, the expression of ROS in wild-type mice and αERKO mice decreased, mitochondrial membrane potential recovered, ATP level increased, NLRP3 inflammasome and fibrosis indexes decreased, liver enzyme levels decreased, and liver

OPEN ACCESS

Edited by:
Lei Zhang,
Anhui Medical University, China

Reviewed by:
Amany Mohammed Gad,
Sinai University, Egypt
Barbara Ruaro,
University of Trieste, Italy

****Correspondence:***
Yong Li
liyong@shutcm.edu.cn

[†]ORCID:
Kehui Zhang
orcid.org/0000-0002-3603-6553

[‡]These authors have contributed equally to this work

Specialty section:
This article was submitted to Gastrointestinal and Hepatic Pharmacology, a section of the journal Frontiers in Pharmacology

Received: *12 March 2022*
Accepted: *09 May 2022*
Published: *25 May 2022*

Citation:
Zhang K, Lin L, Zhu Y, Zhang N, Zhou M and Li Y (2022) Saikosaponin d Alleviates Liver Fibrosis by Negatively Regulating the ROS/NLRP3 Inflammasome Through Activating the ERβ Pathway. Front. Pharmacol. 13:894981. doi: 10.3389/fphar.2022.894981

Abbreviations: CCl4, carbon tetrachloride; ER-β, estrogen receptor β; ERKO, estrogen receptors knockout; HSCs, hepatic stellate cells; mtROS, mitochondrial reactive oxygen species; MitoSOX Red, MitoSOX Red mitochondrial superoxide indication; NLRP3, NLR family, domain containing protein 3; SSd, saikosaponind d.

pathology showed liver inflammation. The damage and collagen deposition were significantly relieved, the expression of α-SMA and TGF-β1 was decreased, and the fibrosis score was also decreased. More importantly, the effect of SSd in alleviating liver injury and liver fibrosis had no effect on βERKO mice.

Conclusion: SSd alleviated liver fibrosis by negatively regulating the ROS/NLRP3 inflammasome through activating the ERβ pathway. By establishing liver fibrosis models using wild-type and ERKO mice, we demonstrated that SSd could alleviate liver fibrosis by inhibiting the ROS/NLRP3 inflammasome axis through activating the ERβ pathway.

Keywords: saikosaponin d, estrogen receptors, mitochondrial reactive oxygen species, nodlike receptor protein 3 inflammasome, liver fibrosis

INTRODUCTION

Liver fibrosis is a pathological process through which various chronic liver diseases develop into liver cirrhosis (Pinzani, 2015). Epidemiological studies have shown that various pathogenic factors can trigger liver inflammation, leading to liver cell damage, abnormal proliferation of connective tissue, reduced liver elasticity, and ultimately deteriorated liver tissue structure and functions (Fattovich et al., 2004; Pinzani, 2015; Parola and Pinzani, 2019). Liver fibrosis is reversible. However, once liver cirrhosis develops, liver fibrosis becomes irreversible. Therefore, blocking or reversing liver fibrosis is essential for the treatment of chronic liver diseases (Friedman, 2007; Böttcher and Pinzani, 2017; Parola and Pinzani, 2019). At present, the treatments for liver fibrosis mainly include anti-inflammation, anti-fibrosis, liver protection and other therapies. Although considerable effort has been spent on further understanding the mechanisms of current treatments and exploring effective novel treatments, satisfactory results have not been obtained (Chen et al., 2015; Böttcher and Pinzani, 2017). None of the new methods developed so far is perfect and all of them are far from ready for clinical practice. Therefore, there is still an urgent need to develop novel methods to block or reverse liver fibrosis.

The activation of hepatic stellate cells (HSCs) is a key step during liver fibrosis, which can lead to the production of a large amount of ROS from mitochondria. Overproduction of ROS can in turn promote the activation of HSCs and the NLPR3 inflammasome (Mederacke et al., 2013). According to previous studies, the NLRP3 inflammasome is expressed in many types of liver cells, including HSCs and damaged hepatocytes (Ning et al., 2017; Kim et al., 2018; Mohamed et al., 2018). Anomalous NLRP3 inflammasome activation is associated with the development of many diseases (Zahid et al., 2019). Oxidative stress injury of Mitochondria and activation of NLRP3 inflammatory body play an important role in the development of liver fibrosis. Key components of a functional NLRP3 inflammasome are NLRP3, the adaptor protein ASC and caspase-1. When oxidative stress occurs, NLRP3 recruits ASC and Pro-caspase-1, resulting in activation of Caspase-1 and prohibiting cytokines IL-1β and IL-18 (Martinon et al., 2002; Zahid et al., 2019). It has been widely documented that ROS play an important role in upstream signaling pathways that activate NLRP3 inflammasome (Mederacke et al., 2013; Abais et al., 2015). Recent literature found that NLRP3 inflammasome activation induced by mitochondrial oxidative stress plays an important role in the development of liver fibrosis (Zhao et al., 2019). Physiologically, quiescent HSCs are required for extracellular matrix (ECM) remodeling. Once activated, quiescent HSCs turn into myofibroblasts, accompanied by the overexpression and deposition of ECM. MMP and TIMP proteins play an important role in the process of liver fibrosis and activation of HSCs by regulating the homeostasis and remodeling of ECM. The levels of MMP-2 and TIMP-1 increase during those processes. Studies have confirmed that a reduction in E-Cadherin expression can promote the development of liver fibrosis, renal interstitial fibrosis, peritoneal fibrosis, and pulmonary fibrosis in experiments (Lu et al., 2018). Vimentin, which is mainly expressed in mesenchymal cells, is an intermediate filament protein and an important biomarker of epithelial–mesenchymal transition (EMT) (Cheng et al., 2016). EMT sustains the generation of pathologically "activated" ATII cells that, by secreting pro-fibrotic factors, further amplifies the fibrotic response (Ruaro et al., 2021). When HSCs were activated by lipopolysaccharide (LPS) and H_2O_2, the expression of NLRP3 inflammatory bodies in HSCs increased (Lin et al., 2018; Zahid et al., 2019).

Bupleurum is a traditional Chinese medicine that has been used for the treatment of liver disorders and other common diseases in China for centuries. As an active component of Bupleurum, saikosaponin d (SSd) plays a significant role in anti-inflammation, anti-liver fibrosis, anti-lipid peroxidation, inhibiting the activation of HSCs, and reducing matrix production (Dang et al., 2007; Fan et al., 2007). SSd is a potential treatment for liver fibrosis. Our previous research proved that SSd has estrogenic effects *in vivo* and *in vitro* and is an estrogen receptor (ER) modulator (Que et al., 2018). In addition, no obvious hepatotoxicity was observed for SSd at an effective drug dose (Wang et al., 2010). Research on the anti-fibrosis effects of estrogen confirmed that ERs are expressed in hepatocytes, sinusoidal endothelial cells, Kupffer cells and stellate cells, and that estrogen can improve the microcirculation of damaged liver, inhibit the proliferation of activated HSCs and the synthesis of collagen, promote the activity of antioxidant enzyme GPx in hepatocytes, prevent lipid peroxidation, regulate the expression of cytokines such as transforming growth factor, and inhibit the occurrence and development of liver fibrosis (Zhang et al., 2016; Lee et al., 2019).

Studies have shown that the inhibition of NLRP3 inflammasome depends on the blockade of ERα in colitis (Gao et al., 2020). Zhang et al. demonstrated that estrogen exerted its anti-fibrosis effects via ERβ rather than ERα or GPER (Zhang et al., 2018). However, it is unclear whether SSd or estrogen alleviates liver fibrosis by inhibiting the expression of NLRP3 inflammasome proteins via activating the ERβ pathway.

In this study, we established models of CCl_4-induced liver injure and fibrosis in wild-type and ERKO mice to investigate the molecular mechanism underlying SSd's anti-fibrosis effects. Specifically, we focused on the expression of protein components of the NLRP3 inflammasome and the role of ERs.

MATERIALS AND METHODS

Animal Experiments

Male specific-pathogen-free (SPF) C57BL/6 mice (6–8 weeks, 20 ± 2 g) were purchased from Shanghai SLAC Laboratory Animal Co., Ltd (Shanghai, China). After purchase, the mice were raised in the animal room without specific pathogens (SPF) in Shanghai Municipal Hospital of Traditional Chinese Medicine. With 5 mice in each cage, they were allowed free access to foods and drinks. Throughout 1 week when the mice were fed adaptively, the temperature was maintained at 20–25°C and the humidity was restricted to the range of 40–70%. All the animal experiments were performed in compliance with local and national guidelines. These experiments approved by the animal experimental ethics and welfare committee of Shanghai Municipal Hospital of Traditional Chinese Medicine (No. 2015032).

For establishment of liver fibrosis mouse models, we injected male wild-type and ER-α and -β knockout mice (αERKO and βERKO mice, respectively, TOS160106CC1, Cyagen Biosciences) subcutaneously twice weekly for 6 weeks with 5 ml/kg body weight carbon tetrachloride (CCl_4) diluted 1:4 in vegetable oil. Mice injected with only vegetable oil served as a vehicle control group. To investigate the effect of SSd and the relationship between mitochondrial ROS level and the expression of NLRP3 inflammasome proteins, C57BL/6 male mice were injected subcutaneously with SSd (China National Institute for the Control of Pharmaceutical and Biological Products, China) at a dosage of 2 mg/kg body weight twice a week for 6 weeks. Thus, the following groups (10 mice per group) were established in this study (Pinzani, 2015): vehicle control group (Fattovich et al., 2004); CCl_4-induced hepatic fibrosis model group (Parola and Pinzani, 2019); CCl_4+SSd group: hepatic fibrosis mice treated with SSd.

Serum Biochemical Analyses

Pre-treatment of samples for determination of serum ALT and AST levels: About 500 μl blood was collected from eyeballs of mice and placed in a 1.5 ml apical centrifuge tube at room temperature for 1–2 h, then centrifuged at 4°C at 3,000 rpm for 10 min. The upper serum was collected and placed in a new centrifuge tube for analysis, or stored in a −80°C freezer. ALT and AST analysis kits (Nanjing Jiancheng Biology Research Institute Co., Ltd.) were used to determine their serum levels.

Histological Staining and Determination of the Non-Alcoholic Fatty Liver Disease Fibrosis Score

Liver tissue sections were prepared, fixed in 4% paraformaldehyde at room temperature overnight, and subjected to hematoxylin-eosin (H&E) staining, Masson's trichrome staining and picric acid-Sirius red staining. The stage of liver fibrosis was assessed according to the Ishak score.

Immunohistochemical (IHC) Analysis of the Expression of α-SMA and TGF-β1

Paraffin-embedded sections were baked in a thermostat for 2 h, dewaxed and rehydrated with xylene and ethanol, incubated in 3% H_2O_2 solution at room temperature for 10 min to block endogenous peroxidase activity, antigen-retrieved with citric acid buffer, incubated for 30 min with 2% goat serum, incubated with primary antibodies against α-SMA and TGF-β1 overnight at 4°C, washed with PBS, incubated with polymer auxiliaries 20 min at 37°C, and incubated with a biotinylated secondary antibody for 2 h at room temperature. The sections were visualized with DBA and the nuclei were stained with hematoxylin. Sectioning, dehydration and mounting were performed according to routine protocols and the sections were observed under a microscope (AE41, McAudi Industrial Group Co., Ltd.).

Cell Culturing and Treatment

HSCs-LX2 (Shanghai Fanling Biotechnology Co., Ltd., Shanghai, China) were cultured in DMEM at 37°C with 5% CO_2. After seeding in 6 well plates, HSCs were treated with H_2O_2 at a concentration of 200 μmol/L for 4 h. To investigate the role of ERs in SSd's anti-fibrotic effects, HSCs-LX2 were treated with MPP (1 μM) (Tocris Bioscience Co., Ltd. UK) or THC (1 μM) (Tocris Bioscience Co., Ltd. UK) for 30 min, subsequently with SSd (5 μM) for 24 h, and finally incubated with H_2O_2 (200 μM) for 4 h in complete DMEM.

Protein Extraction and Western Blotting Analysis

After being extracted from liver tissues and cells, protein samples were separated with SDS-PAGE, and electroblotted onto polyvinylidene difluoride membranes. After blocking with 5% skimmed milk, the membranes were incubated with primary antibodies, then with an appropriate horseradish peroxidase-labeled secondary antibody (1:2000; CST signaling, United States). Specific bands were detected by an enhanced chemiluminescence assay. Primary antibodies and their working concentrations are listed in **Supplementary Table S1**.

RNA Isolation and Real-Time Polymerase Chain Reaction (RT-PCR)

The TRIzol (Invitrogen,United States) reagent was applied for total RNA extraction. Reverse transcription and quantitative RT-PCR were performed with the PrimeScript® RT reagent kit (TaKaRa, Japan) and SYBR Premix Ex Taq (TaKaRa, Japan). The primers were synthesized by Shanghai Shenggong Biology Co., Ltd. Expression levels of genes relative to β-actin mRNA levels in each sample were calculated according to the $2^{-\Delta\Delta Ct}$ method. The primer sequences are shown in **Supplementary Table S2, S3**.

Determination of Mitochondrial ROS Level Using MitoSOX Red

To determine the level of mitochondrial ROS, a working solution of the probe (5 μM, Beyotime Institute of Biotechnology) was added into cells and incubated in the dark. The cells were washed with preheated PBS, re-stained with a working solution of Hoechst33342 (10 μg/ml, Beyotime Institute of Biotechnology), washed with PBS again, and observed under a fluorescence microscope (DMI3000B, Leica Corp.).

The mitochondria isolation solution was added to liver tissues for grinding. The liquid phase was centrifuged, and the precipitate, which contained mitochondria from liver tissues, was retained. The precipitate was resuspended with mitochondria storage solution, mixed with MitoSOX Red (5 μM, Beyotime Institute of Biotechnology), and incubated at 37°C for 30 min. The fluorescence intensity was determined by a fluorescence microplate reader (DMI3000B, Leica Corp.).

Evaluation of HSCs-LX2 Viability and Lipid Peroxidation

HSCs-LX2 were seeded into 96-well plates at a density of 1×10^4 cells per well and cultured in an incubator at 37°C with 5% CO_2. H_2O_2 (at a concentration of 200 μM) was added into the cells for a 4-h incubation. The viability of HSCs-LX2 was determined by CCK-8 assays (Shanghai Yisheng Bio, China). MDA is an important product of lipid peroxidation, the level of which reflects the degree of lipid peroxidation. Therefore, we evaluated the degree of lipid peroxidation using an MDA assay kit (Beyotime Institute of Biotechnology) according to the manufacturer's instructions.

Measurement of Mitochondrial Membrane Potential

The JC-1 probe (Beyotime Institute of Biotechnology) was used for mitochondrial membrane potential measurement. Briefly, cells were treated with JC-1 probe monomers according to the manufacturer's instructions. Then, nuclei were visualized by DAPI staining (Beyotime Institute of Biotechnology) in the dark. The ratio of red and green fluorescence signal intensities of JC-1 probe monomers was calculated.

Intracellular Adenosine Triphosphate (ATP) Level Assay

Intracellular ATP levels were measured with an assay kit (Beyotime Institute of Biotechnology) in accordance with the manufacturer's instructions.

Data Presentation and Statistical Analyses

All data are expressed as means ± SEM. Student's t-test was used to compare the differences between the means of two groups. One-way analysis of variance (ANOVA) with post hoc Fisher's least significant difference tests was performed for comparisons among multiple groups using SPSS 22.0 (SPSS Inc., Chicago, United States). A p value of less than 0.05 was considered statistically significant.

RESULTS

SSd Alleviated CCL_4-Induced Liver Injury and Liver Fibrosis in Mice

To investigate the effect of SSd on liver injury, we established a mouse model of CCL_4-induced liver injury and liver fibrosis. Unlike to the control group, the AST and ALT levels of the model group increased significantly (**Figures 1A,B**). The liver fibrosis score of the model group was also meaningfully higher than that of the control group (**Figure 1C**). Liver injury and fibrosis was occurred as shown by H&E staining (inflammatory cell infiltration and lobular disorder), Masson's trichrome staining (blue color was indicative of collagen deposition), Picrosirius red staining (red color was indicative of collagen deposition) and the IHC of α-SMA and TNF-β1 (**Figures 1D–F**). On the contrary, the intervention of SSd significantly promoted the recovery of liver function and the normal liver structure. First of all, we also observed that the activities of liver enzymes AST and ALT were lower in the SSd group than in the control group, indicating an improved liver function (**Figures 1A,B**). Furthermore, the liver fibrosis score also decreased in the treatment group compared with the model group (**Figure 1C**). H&E staining displayed significantly reduced proliferation of fibrous tissues, significantly decreased inflammatory cell infiltration, and not obvious fat infiltration in the liver of model mice treated with SSd (**Figure 1E**). Masson staining revealed that the deposition of collagen fibers was reduced in the SSd intervention group (**Figure 1E**). Picric acid-Sirius red staining exhibited only a few collagen fibers in the vascular wall of the portal area after SSd intervention (**Figure 1E**). Correspondingly, the expression levels of α-SMA and TGF-β1 in the portal area and liver tissues of the SSd intervention group were significantly decreased compared with the model group (**Figures 1D,E**), suggesting that SSd treatment reduced hepatic inflammation and damages in the model mice.

SSd Inhibited Mitochondrial Dysfunctions and NLRP3 Inflammasome Activation in Mice

Compared with untreated mice, the intensity of MitoSOX Red fluorescence in the SSd intervention group was decreased (**Figure 2A**). Determination of mitochondrial membrane potential showed that the ratio of JC-1 monomers with red fluorescence was higher in the SSd group than in the model group, and a similar trend was observed for intracellular ATP content (**Figures 2B,C**). As illustrated in **Figures 2D,E**, the expression levels of NLRP3 inflammasome, pro-IL-1β, IL-1β,

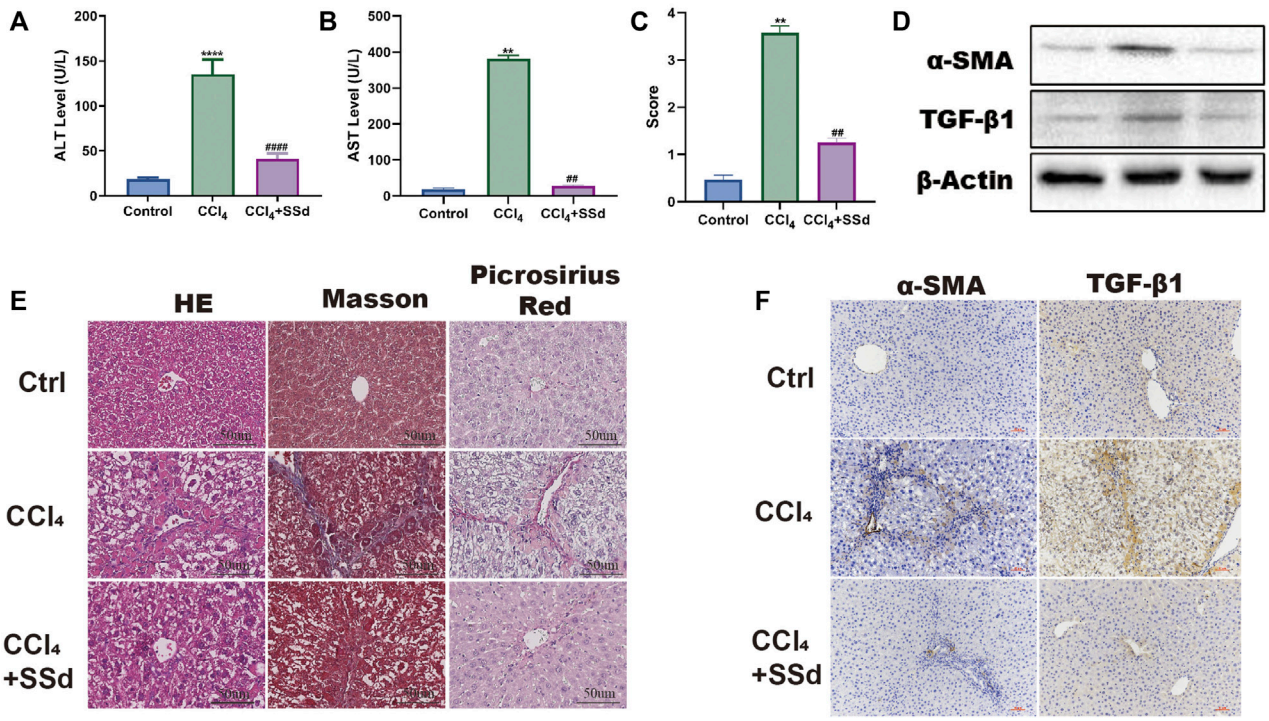

FIGURE 1 | SSd alleviated CCL_4-induced liver injury and liver fibrosis. **(A,B)** the changes of serological ALT and AST concentration, $n = 6$. **(C)** Liver Fibrosis Score, $n = 6$. **(D–F)** liver histological determination (H&E) and IHC of α-SMA and TNF-β (×200; scale bar: 50 μm). Data are expressed in mean ± SEM; $^{**}p < 0.01$, $^{****}p < 0.0001$, versus control group; $\#\#p < 0.01$, $\#\#\#\#p < 0.0001$, AND versus CCL_4 treated group.

and IL-18 in model mice were decreased significantly after treatment with SSd. Altogether, these data suggested that the effect of SSd on NLRP3 inflammasome activation in liver fibrosis was likely mediated through the regulation of mitochondrial ROS level. Taken together, these data suggested that SSd had inhibitory effects on the activation of the NLRP3 inflammatory proteins and mitochondrial oxidative stress damage in a model of liver fibrosis.

SSd Alleviated H_2O_2-Induced Mitochondrial Dysfunctions and NLRP3 Inflammasome Activation in HSCs

To investigate whether SSd can protect the mitochondrial functions of activated HSCs *in vitro*, activated HSCs were treated with SSd. It was found that both MDA content and mitochondrial ROS level in HSCs were significantly decreased after SSd treatment (**Figures 3A,B**). Conversely, both intracellular ATP content and the mitochondrial proportion of JC-1 monomers with red fluorescence were increased after SSd treatment (**Figures 3C,D**). The effects of SSd treatment on the expression of NLRP3 inflammatory and fibro-genic proteins in activated HSCs were also examined. The results showed that SSd inhibited the expression of α-SMA, NLRP3 inflammasome, pro-IL-1β, IL-1β, and IL-18 (**Figures 3E–H**). Collectively, these results indicated that SSd alleviated H_2O_2-induced mitochondrial dysfunctions, as well as in reducing the expression of inflammatory factors in HSCs.

Deficiency of ERβ, But Not ERα, Blocked the Inhibitory Effects of SSd Against CCL_4-Induced Mitochondrial Dysfunctions and NLRP3 Inflammasome Activation

Mitochondrial damages were also present in the CCL_4-induced ERKO mice model. Compared with wild-type mice, mitochondrial ROS production was significantly upregulated, while the proportion of JC-1 monomers with red fluorescence and ATP content in the mitochondria were decreased in wild-type and ERKO mice treated by CCL_4 (**Figures 4A–C**). After intervention with SSd, the above changes were reversed in wild-type and αERKO mice, but not in βERKO mice (**Figures 4A–C**). NLRP3 related mRNA and proteins were further examined in the liver of wild-type and ERKO mice treated with CCL_4 alone or in combination with SSd. The results indicated that SSd effectively prevented CCl_4-induced increase in NLRP3 inflammasome, pro-IL-1β, IL-1β, and IL-18 levels in wild-type mice and αERKO mice, but not in βERKO mice (**Figures 4D,E**).

Deficiency of ERβ, But Not ERα, Blocked the Inhibitory Effect of SSd Against CCL_4-Induced Liver Injury

SSd has estrogen-like effects *in vivo* and *in vitro*, and is an estrogen receptor modulator (Wang et al., 2010). It was

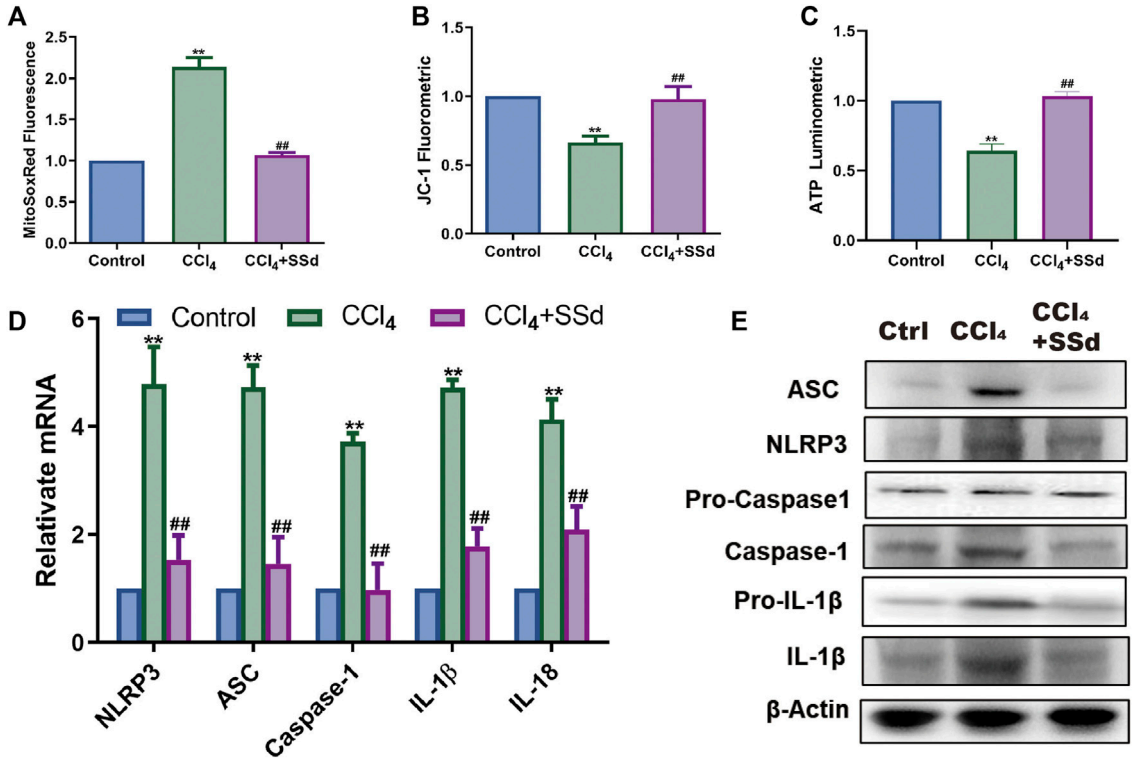

FIGURE 2 | SSd inhibited mitochondrial dysfunctions and NLRP3 inflammasome activation. **(A)** MitoSOX Red Mitochondrial Superoxide Indicator detection, $n = 6$. **(B)** mitochondrial JC-1 fluorescence expression, $n = 6$. **(C)** ATP content, $n = 6$. **(D,E)** relative mRNA and proteins expression of inflammasome, $n = 3$. Data are expressed in mean ± SEM; $^{**}p < 0.01$, CCL_4 group versus control group; $\#\#p < 0.01$, CCl_4+SSd versus CCL_4 treated group.

hypothesized that SSd would have a therapeutic effect on liver injure and fibrosis. After CCl_4 administration, increased ALT and AST activities were observed in both wild-type and ERKO mice, which could be significantly inhibited by SSd intervention in both wild-type and αERKO mice, but not in βERKO model mice (**Figures 5A,B**). Additionally, the H&E staining results revealed that SSd significantly reduced the necrotic area and the number of inflammatory cells in the liver of wild-type and αERKO liver fibrosis mice compared with the control group (**Figure 5C**). However, these changes were not observed in βERKO liver injure mice, suggesting that SSd blocked the inhibitory effects of SSd against CCL_4-induced liver injury through the ERβ pathway.

Deficiency of ERβ, But Not ERα, Blocked the Inhibitory Effect of SSd Against CCL_4-Induced Liver Fibrosis

Consistent with the blood biochemistry results, SSd treatment failed to prevent liver fibrosis induced by CCl_4 in βERKO mice. RT-PCR and WB analyses indicated that liver fibrosis-related factors (including α-SMA, TGF-β1, TIMP-1, MMP-2, and Vimentin) were significantly downregulated, while E-cadherin was significantly upregulated in wild-type and αERKO mice after SSd treatment (**Figures 6A,B**). Liver fibrosis scores of wild type mice and αERKO mice were also significantly lower than that of the control mice after SSd treatment (**Figure 6C**). Furthermore, liver sections from CCl_4-induced wild-type and ERKO mice with or without SSd treatment were analyzed by Masson's trichrome staining, Picric acid-Sirius red staining and IHC. It was observed that SSd effectively decreased collagen accumulation and the expression of α-SMA and TGF-β1 as compared with controls group in wild-type and αERKO mice (**Figures 6D–G**). No significant changes were observed in βERKO mice after SSd treatment, suggesting that SSd inhibited CCl_4-induced liver fibrosis via the ERβ pathway.

Specifically Antagonizing ERβ, But Not ERα, Blocked the Inhibitory Effects of SSd Against H_2O_2-Induced Mitochondrial Dysfunctions and NLRP3 Inflammasome Activation in HSCs

To better understand the molecular mechanism underlying SSd's effects on liver fibrosis, we attempted to link the ER pathway with the impaired activation of HSCs. First, ER blockers alone or in combination with SSd were used to treat HSCs (normal or activated). It was found that ER inhibitors alone had no significant effect on HSCs compared with the control group. Interestingly, when combined with SSd, ERα inhibitor MPP decreased ROS

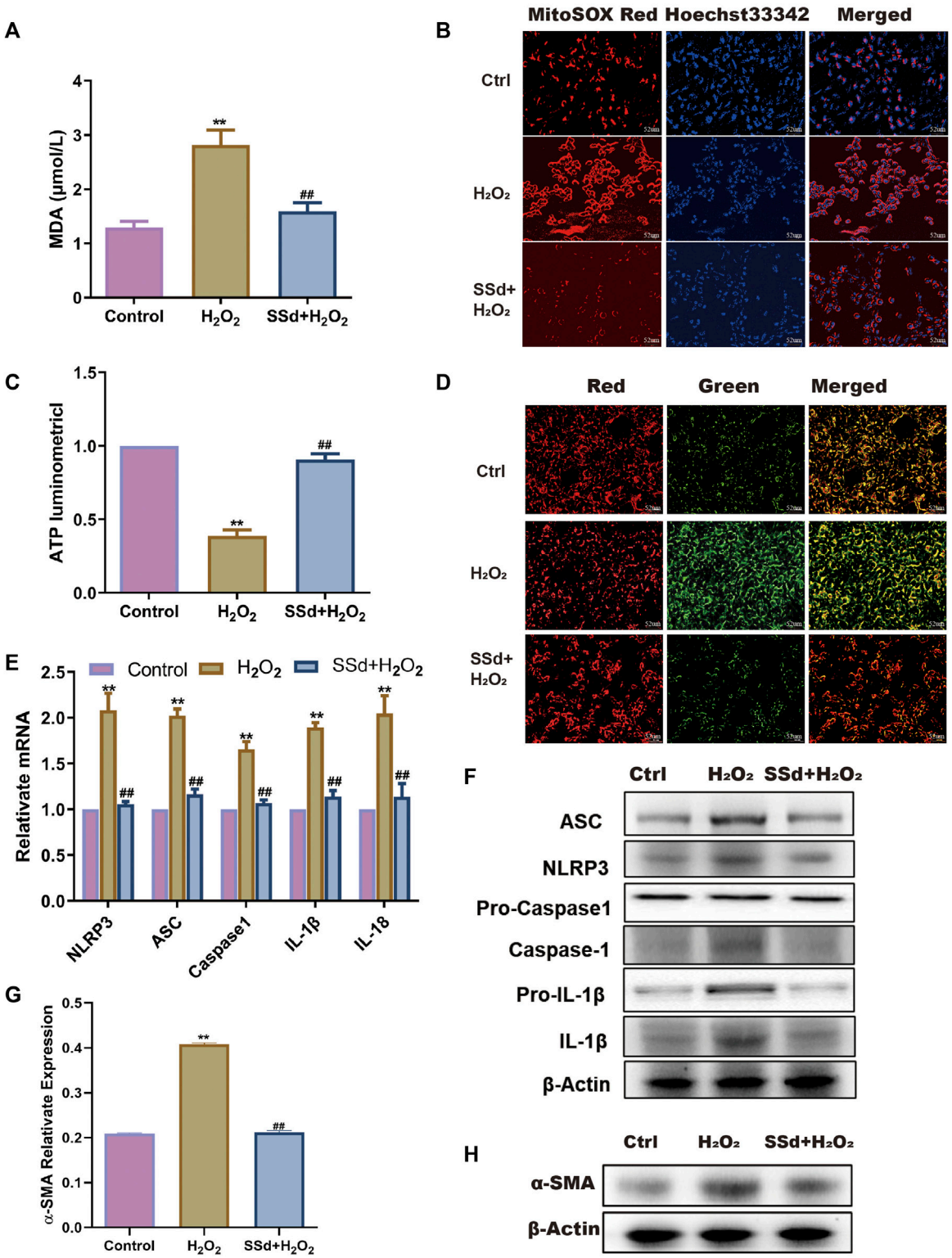

FIGURE 3 | SSd alleviated H_2O_2-induced mitochondrial dysfunction and NLRP3 activation in HSCs **(A)** the content of MDA in HSCs after SSd intervention combination with H_2O_2 or not, $n = 6$. **(B)** MitoSOX Red fluorescence images (the heavier the red, the more damage, scale bar, 52 μm). **(C)** ATP content, shows the degree of damage to mitochondria in HSCs, $n = 6$. **(D)** JC-1 fluorescence images (the more JC-1 monomers with green, the more damage to mitochondria, scale bar, 52 μm). **(E,F)** RT-PCR and WB was employed to examine the expression of inflammasome, $n = 3$. **(G,H)** α-SMA protein expression, $n = 3$. Data are expressed in mean ± SEM; $^{**}p < 0.01$, H_2O_2 treated group versus control group; $^{\#\#}p < 0.01$, H_2O_2+SSd group versus H_2O_2 treated group.

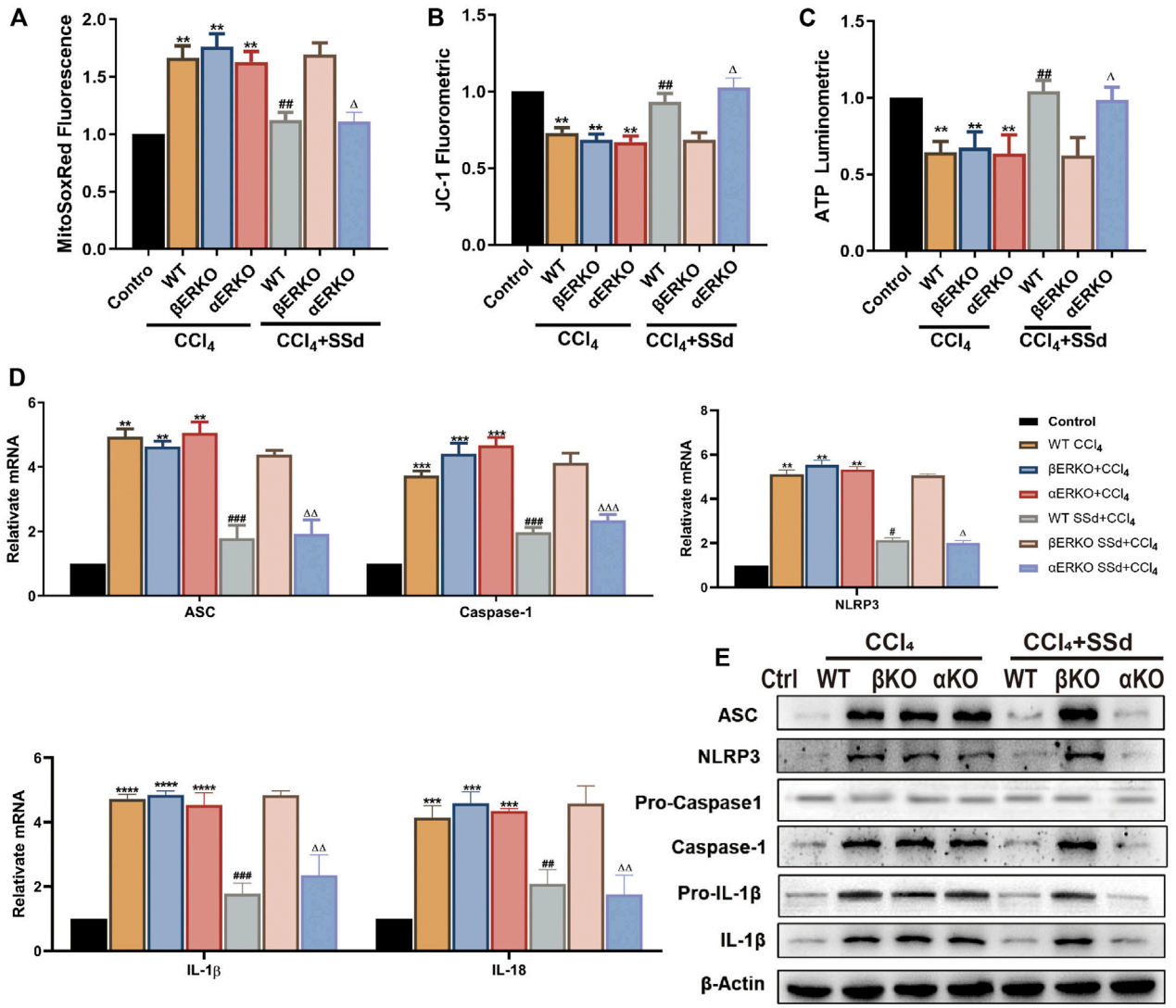

FIGURE 4 | Deficiency of ERβ, but not ERα, blocked the inhibitory effect of SSd against CCl_4-induced mitochondrial dysfunction and NLRP3 activation in the liver **(A)**. ROS fluorescence expression in the CCl_4-induced ERKO mouse model combine with SSd or not, $n = 6$. **(B)** the mitochondrial JC-1 fluorescence expression in liver tissue, $n = 6$. **(C)** ATP content, $n = 6$. **(D,E)** inflammasome complex expression was tested by western blot experiment and PT-PCR in each group, $n = 3$. Data are expressed in mean ± SEM; $^{**}p < 0.01$, $^{***}p < 0.001$, $^{****}p < 0.0001$, CCl_4 treated versus control in WT and ERKO mice; $^{\#\#}p < 0.01$, $^{\#\#\#}p < 0.001$, $^{\#\#\#\#}p < 0.0001$, SSd + CCl_4 group versus CCl_4 group in WT mice; $^{\Delta}P < 0.05$, $^{\Delta\Delta}P < 0.01$, $^{\Delta\Delta\Delta}P < 0.001$, $^{\Delta\Delta\Delta\Delta}P < 0.0001$, SSd + CCl_4 group versus CCl_4 group in αERKO mice.

production, increased the proportion of JC-1 monomers with red fluorescence and intracellular ATP content, which were similar to the therapeutic effects of SSd alone (**Figures 7A–C**). However, treatment with the combination of SSd and ERβ inhibitor THC showed no significant effect (**Figures 7A–C**). Furthermore, the levels of NLRP3 related proteins were assessed, which shown that treatment with the combination of SSd and ERα blocker notably decreased the levels of NLRP3, pro-IL-1β and IL-1β proteins, the degrees of which were comparable to those caused by SSd treatment alone (**Figure 7D**). Consistent with these results, RT-PCR analysis revealed that the combination of ERα inhibitor and SSd inhibited the expression of inflammasome genes in HSCs (**Figure 7E**).

Specifically Antagonizing of ERβ, But Not ERα, Blocked the Inhibitory Effects of SSd Against H_2O_2-Induced ECM Deposition and EMT in HSCs

To explore the biomechanism underlying SSd's inhibitory effects on ECM deposition and EMT in activated HSCs, we tested the expression levels of relative indicators. The results showed that the combination of SSd and MPP significantly impaired the expression of α-SMA, TGF-β, TIMP-1, MMP-2, and vimentin, and improved the expression of E-cadherin in HSCs exposed to H_2O_2, while no therapeutic effect was observed in the SSd + THC intervention group (**Figures 8A,B**). Our results indicated that SSd-induced changes in expression of

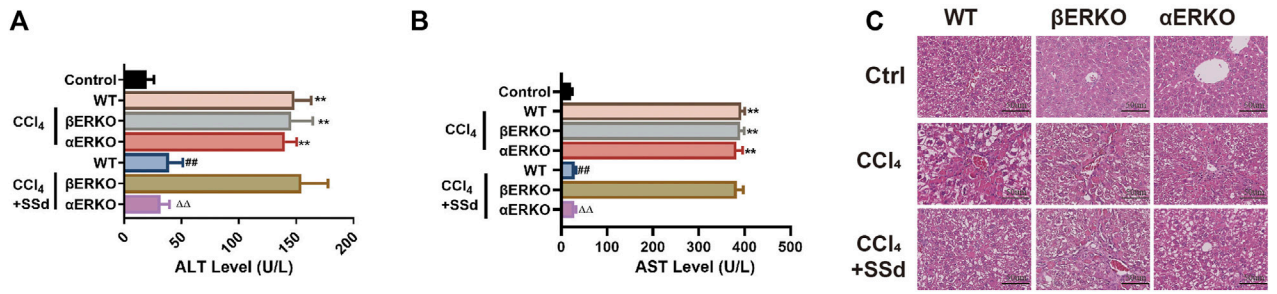

FIGURE 5 | Deficiency of ERβ, but not ERα, blocked the inhibitory effect of SSd against CCL_4-induced liver injury **(A,B)** plasma ALT and AST levels were tested after CCl_4 treatment in WT and ERKO mice treated with SSd or without SSd, $n = 6$. **(C)** liver injury was detected by HE (×200; scale bar: 50 μm). Data are expressed in mean ± SEM; $^{**}p < 0.01$, CCl_4 treated versus control in WT and ERKO mice; $^{\#\#}p < 0.01$, SSd + CCl_4 group versus CCl_4 group in WT mice; $^{\Delta\Delta}P < 0.01$, SSd + CCl_4 group versus CCl_4 group in αERKO mice.

fibrosis-related factors depended on the activation of the ERβ pathway.

DISCUSSION

Our research confirmed the important role of SSd in the treatment of liver fibrosis. First, the application of SSd reduced mitochondria damage, activation of the NLRP3 inflammasome and inhibited HSCs activation and proliferation and liver injure and fibrosis. Second, the ERβ pathway played an important role in anti-liver fibrosis effects about SSd.

Subcutaneous CCl_4 administration has been successfully applied to induce liver injury and cirrhosis, with histological changes and serum ALT levels being similar to those of human hepatic diseases. Persistent hepatocyte damages, excessive ECM deposition, and abnormal proliferation of connective tissue in the liver can lead to liver fibrosis (Hernandez-Gea and Friedman, 2011). HSCs activation, a key event in the occurrence of liver fibrosis, is the source of myofibroblasts and the final target of various fibrosis-inducing factors (Mederacke et al., 2013; Ray, 2014). Fortunately, EMT can be reversed into mesenchymal-epithelial transformation (MET), promoting the repair and reversal of hepatic fibrosis (Cicchini et al., 2015; Yang et al., 2020). Our experimental results showed that SSd intervention accelerated the degradation of deposited ECM, inhibited and reversed the process of EMT, and had anti-fibrosis effects. Early interventions can effectively alleviate liver fibrosis. Radix Bupleuri, the dry root of *Bupleurum Chinense* DC, has been characterized as a hepatoprotective herbal medicine that can treat various liver diseases, such as chronic hepatic inflammation, liver cirrhosis, hepatocellular carcinoma, and viral hepatitis (Li et al., 2018; Tian et al., 2019). SSd is one of the pharmacologically active compounds of Bupleurum. Recently, the anti-inflammatory, anti-fibrotic, anti-tumor, and hepatoprotective effects of SSd observed both *in vivo* and *in vitro* have attracted widespread attention (Xie et al., 2012; Yuan et al., 2017; Cui et al., 2019). A previous study showed that SSd could prevent hepatic inflammation and liver injury in acetaminophen-induced mice (Liu et al., 2014). The study showed that SSd reduced the infiltration and proliferation of $CD8^+$ T cells, increased the expression of anti-inflammatory cytokines, inhibited the expression of TGF-β1, and ultimately alleviated inflammation and fibrosis in a mouse model of glomerulonephritis (Li et al., 2005). Furthermore, studies have shown that SSd can inhibit the activation of HSCs by regulating intracellular inflammatory responses, thereby eventually inhibiting liver fibrosis (Chen et al., 2013). Our previous studies also confirmed that SSd had a protective effect on CCl_4-induced acute liver injury (Chen et al., 2020). CCl_4-induced chronic liver injury and liver fibrosis model mice were treated with SSd, and found that liver injury and liver fibrosis were significantly alleviated by SSd treatment compared with the control group.

Activation of the NLRP3 inflammasome has been shown to cause liver injury and hepatic fibrosis in various acute and chronic liver diseases (Wree et al., 2014). Key components of a functional NLRP3 inflammasome are NLRP3, the adaptor protein ASC and caspase-1. NLRP3 recruits ASC and procaspase-1, which results in caspase-1 activation and processing of cytoplasmic targets, including the pro-inflammatory cytokines IL-1β and IL-18, whose purpose being to drive the inflammatory process and restore homeostasis. Mostly, priming is provided by signals of tissue damage activation downstream of pattern recognition receptors and is thought to be required both for NLRP3 and pro-IL-1β induction (Haneklaus and O'Neill, 2015). Active caspase-1 cleaves the cytokines pro-IL-1β and pro-IL-18 into their mature and biologically active forms (Martinon et al., 2002). Maria et al. introduced an $NLRP3^{-/-}$ mouse model and confirmed that the NLRP3 inflammasome could directly activate HSCs and trigger liver fibrosis (Inzaugarat et al., 2019). Our experimental results confirmed that the NLRP3 inflammasome was overexpressed and activated during the process of liver fibrosis, suggesting that the increased levels of NLRP3 inflammasome proteins were associated with liver injury, liver fibrosis and HSCs activation. According to a previous study, mitochondrial ROS is the main activator of the NLRP3 inflammasome (Scambler et al., 2019). ROS can induce chronic inflammation and fibrous hyperplasia, leading to the activation of HSCs and finally promoting fibrosis (Dickie et al., 2012; Chen et al., 2019). In addition, oxidative stress significantly

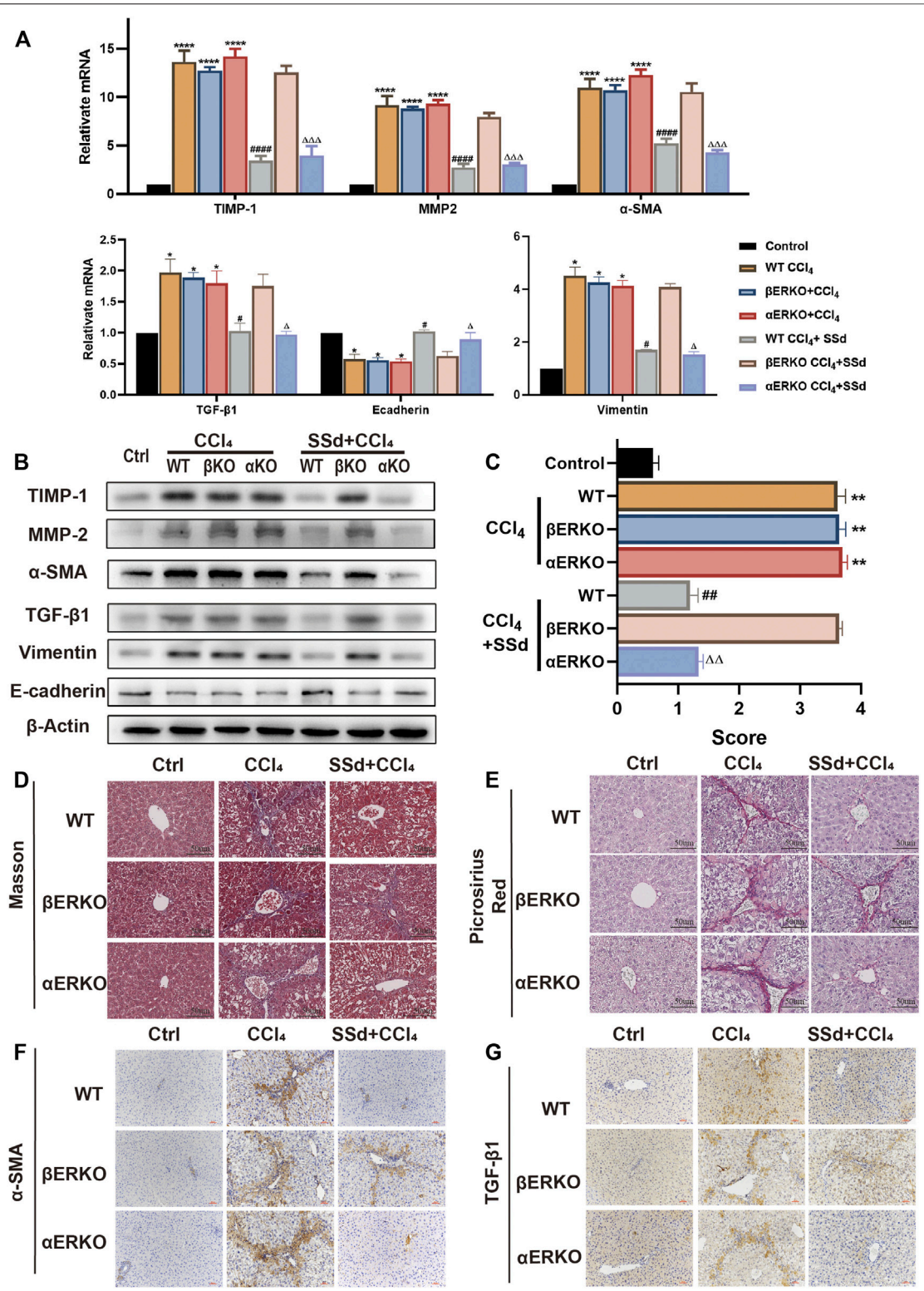

FIGURE 6 | Deficiency of ERβ, but not ERα, blocks the inhibitory effect of SSd against CCl_4-induced liver fibrosis **(A,B)**. α-SMA, TGF-β1, TIMP-1, MMP-2, E-cadherin, and Vimentin mRNA and protein expression were tested by RT-PCR and WB in liver tissues, $n = 3$. **(C)** liver fibrosis scores in each group, n = 6. **(D,E)** Liver fibrosis was detected by Masson staining, picric acid-Sirius staining (×200; scale bar: 50 μm). **(F,G)** IHC detection of the expression of α-SMA, TGF-β1 (×200; scale bar: 100 μm). Data are expressed in mean ± SEM; $^{*}p < 0.05$, $^{**}p < 0.001$, $^{****}p < 0.0001$, CCl_4 treated versus control in WT and ERKO mice; $^{\#}p < 0.05$, $^{\#\#}p < 0.01$, $^{\#\#\#\#}p < 0.0001$, SSd + CCl_4 group versus CCl_4 group in WT mice; $^{\Delta}P < 0.05$, $^{\Delta\Delta}P < 0.01$, $^{\Delta\Delta\Delta\Delta}P < 0.0001$, SSd + CCl_4 group versus CCl_4 group in αERKO mice.

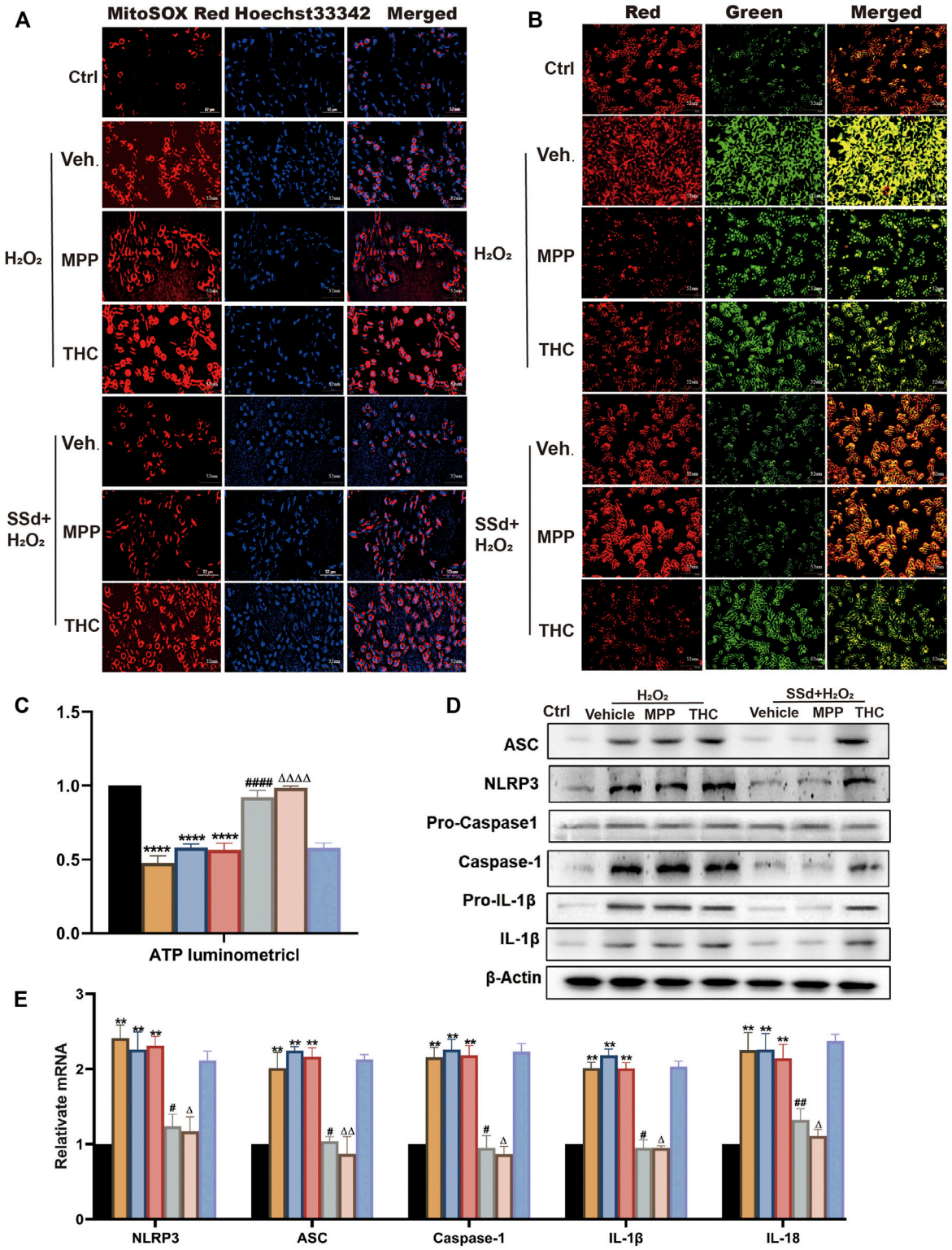

FIGURE 7 | Specific antagonist of ERβ, but not ERα, blocked the inhibitory effect of SSd against H_2O_2-induced mitochondrial dysfunction and NLRP3 activation in HSCs **(A)**. ROS production in HSCs in each group in estrogen receptor blockers alone or in combination with SSd treated group in HSCs (normal or activated state) (Scale bar, 52 μm). **(B)** JC-1 membrane potential (Scale bar, 52 μm). **(C)** ATP content, $n = 6$. **(D,E)** inflammasome complex expression was tested by PT-PCR and western blot experiment. in each group, n = 3. Data are expressed in mean ± SEM; $^{**}p < 0.01$, $^{****}p < 0.0001$, H_2O_2, H_2O_2 +MPP, and H_2O_2 +THC group versus control group; $^{\#}p < 0.05$, $^{\#\#}p < 0.01$, $^{\#\#\#\#}p < 0.0001$, SSd + H_2O_2 group versus H_2O_2 group; $^{\Delta}P < 0.05$, $^{\Delta\Delta}P < 0.01$, $^{\Delta\Delta\Delta\Delta}P < 0.0001$, MPP + SSd + H_2O_2 group versus MPP + H_2O_2 group.

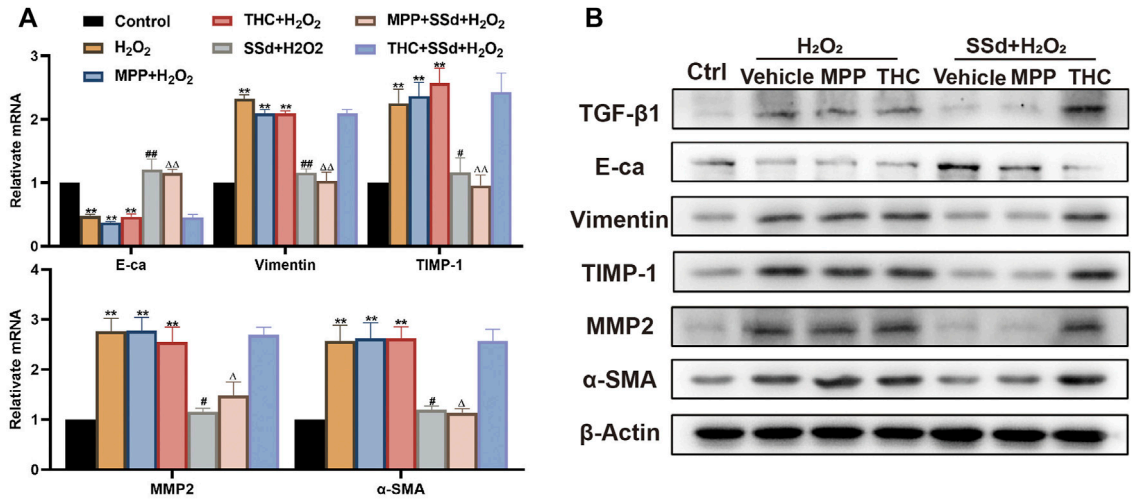

FIGURE 8 | Specific antagonist of ERβ, but not ERα, blocked the inhibitory effect of SSd against H_2O_2-induced extracellular matrix deposition and EMT in HSCs **(A,B)** the indicators of extracellular matrix deposition and EMT (α-SMA, TGF-β1, TIMP-1, MMP-2, Vimentin, and Ecadherin) expression in HSCs were detected by RT-PCR and WB, $n = 3$. Data are expressed in mean ± SEM; $^{**}p < 0.01$, H_2O_2, H_2O_2 +MPP, and H_2O_2 +THC group versus control group; $^{\#}p < 0.05$, $^{\#\#}p < 0.01$, SSd + H_2O_2 group versus H_2O_2 group; $^{\Delta}P < 0.05$, $^{\Delta\Delta}P < 0.01$, MPP + SSd + H_2O_2 group versus MPP + H_2O_2 group.

contributes to HSCs activation and fibrosis (Lin et al., 2020). Consistent with the findings in literature, our analyses of mitochondrial functions *in vivo* and *in vitro* confirmed that the production of mitochondrial ROS increased in CCl_4-induced liver fibrosis mice and H_2O_2-induced activated HSCs. Therefore, reducing oxidative stress and eliminating ROS have been promising treatment strategies for liver fibrosis. SSd possesses anti-oxidative stress effects. According to a previous study, SSd could prevent oxidative damage, oxidative stress, and cytotoxicity in neural cells (Lin et al., 2016). SSd can reverse the impaired hepatic activity of superoxide dismutase, improve liver antioxidant capacity, inhibit lipid peroxidation, eliminate ROS, and ultimately prevent oxidative stress and liver injury (Fan et al., 2007). It was found that SSd significantly protected HL-7702 cells against CCl_4-mediated oxidative stress and inhibited NLRP3 inflammasome-induced inflammation (Lin et al., 2018). Consistent with these findings, our study also confirmed that mitochondrial oxidative stress could activate HSCs and the NLRP3 inflammasome, which played an important role in the development of liver fibrosis. In this study, it was also focused on the correlation between SSd treatment and activation of the ROS/NLRP3 inflammasome axis. It was found that SSd treatment inhibited mitochondrial oxidative stress, reduced the production of mitochondrial ROS, downregulated the expression of NLRP3 inflammasome proteins and pro-IL-1β, IL-1β, and IL-18 induction, and eventually protected liver from injury and fibrosis.

Estradiol acts by binding to and activating different subtypes of estrogen receptors, including the two classical receptors ERα and ERβ, and the G protein-coupled estrogen receptor on the plasma membrane (Revankar et al., 2005; Dahlman-Wright et al., 2006). ERα and ERβ receptors can be detected in many tissues, but their distributions and expression levels are different. In liver cells, ERα is the predominant ER subtype, while ERβ is expressed in a variety of tissues during human fetal development; HSCs have been demonstrated to possess functional ERβ but not ERα; these findings suggest different organ-specific roles for the ERs (Brandenberger et al., 1997; Zhou et al., 2001; Gao et al., 2008). Some studies have shown that the function of E2 in preventing liver inflammation is mediated by ERα (Evans et al., 2002). Preclinical findings in rodents demonstrate that endogenous estradiol can prevent steatosis, insulin resistance, and fibrosis in liver diseases by activating the ER signal pathways (Grossmann et al., 2019). ERβ2 can lead to suppression of the ERα signaling (Zhao et al., 2007). ERβ may inhibit EMT (Mak et al., 2010) and effectively improve cirrhosis with portal hypertension in ovariectomized rats (Zhang et al., 2016). Zhang et al. found that selective agonists for ERβ exert antifibrogenic effects by inhibiting the activation and proliferation of HSCs (Zhang et al., 2018). These effects were obviously mediated by ERβ, but not ERα or GPER. SSd has estrogen-like effects *in vivo* and *in vitro*, and is an ER modulator (Wang et al., 2010). Liu et al. demonstrated that SSd improved memory in rats by modulating ERα activation, but not E2 level or ERβ activity, in the hippocampus (Liu et al., 2019). Que et al. found that SSd could inhibit oxidative stress-induced activation of HSCs, an effect that depended on the regulation of ERβ (21). Therefore, it can be seen that SSd activates estrogen ligands in difference organs and tissues with different functions. To this end, we introduced ERKO mice to verify that the anti-fibrosis effects of SSd were mediated by the ERβ pathway.

Studies have shown that E2 is a strong endogenous antioxidant that inhibits oxidative stress-induced lipid peroxidation and ROS production in rat liver mitochondria (Yagi, 1997; Omoya et al., 2001). Simvastatin could activate the expression of ERα and ERβ, thereby inhibiting the activation of the NLRP3 inflammasome and decreasing the levels of pro-inflammatory mediators (Menze et al., 2021). 17β-estradiol can reduce NLRP3 inflammasome activation to abrogate

airway inflammation (Cheng et al., 2019). However, it has also been reported that E2 significantly inhibited the malignant behaviors of hepatocellular carcinoma cells through E2/ERβ pathway-mediated upregulation of the NLRP3 inflammasome (Wei et al., 2015). So far, a variety of estrogen receptor modulators have been found, such as soybean isoflavones, lignans, stilbenes, resveratrol, ginsenosides and SSd (Chan et al., 2002; Dixon, 2004). However, studies have shown that phytoestrogens have different affinities and transactivating activities for ERα and ERβ. For example, genistein and coumestrol preferentially interact with and activate ERβ rather than ERα to mediate estrogenic effects (Gutendorf and Westendorf, 2001). In addition, a previous study showed that SSd could upregulate the expression of ERα in the hippocampus of ovariectomized rats, but had no significant effect on the expression of ERβ (Liu et al., 2019). Moreover, they can inhibit the expression of NLRP3, HSCs activation, and liver fibrosis by acting on different estrogen ligands. Soybean isoflavones can alleviate DSS-induced colitis by inhibiting the ERα pathway and downregulating the subsequent activation of the NLRP3 inflammasome (Gao et al., 2020). Phytoestrogen calycosin inhibits the activation, proliferation, and migration of HSCs induced by TGF-β1 via downregulating ERβ (Deng et al., 2018). Comprehensive studies have shown that the mechanism of interaction between estrogen regulators and ligands is complex, and a specific regulator may even have opposite effects under different circumstances. Therefore, we used ER knockout mice to carry out experiments, and obtained strong evidence to support that SSd has ERβ pathway-dependent anti-liver fibrosis effects, such as inhibiting the expression of NLRP3 inflammasome proteins. By treating HSCs with ERα and ERβ blockers and establishing αERKO and βERKO knockout liver fibrosis mouse models, we found that the experimental results obtained from mouse and cellular model groups were not significantly different from those obtained from the THC intervention group and the βERKO mouse group, while there were significant differences between the MPP intervention group, the αERKO mouse group and the control group. These findings suggested that SSd inhibited HSCs activation through the ERβ pathway, and alleviated liver injury and liver fibrosis by negatively regulating the ROS/NLRP3 inflammasome. Thus, we confirmed a new molecular mechanism underlying SSd's anti-fibrosis effects—by negatively regulating the ROS/NLRP3 inflammasome through activating the ERβ pathway.

CONCLUSION

Collectively, the results of our study demonstrate SSd suppresses hepatic injure and fibrosis by exerting inhibiting mitochondrial injury effect that inhibit the activation of NLRP3 inflammasome, which in turn leads to inhibition of HSCs activation and proliferation. This suggests SSd may be an effective therapeutic agent for the treatment of hepatic fibrosis.

DATA AVAILABILITY STATEMENT

The original contributions presented in the study are included in the article/**Supplementary Material**, further inquiries can be directed to the corresponding author.

ETHICS STATEMENT

The animal study was reviewed and approved by Shanghai Municipal Hospital of Traditional Chinese Medicine Ethics Committee.

AUTHOR CONTRIBUTIONS

KZ conducted experimental operation, performed data acquisition and analysis and wrote the manuscript. LL made contributions in the revision stage of the article. YZ contributed to the correction of article writing. NZ and MEZ performed part of the experimental operations and data collection. Others had great help to the author in terms of articles logic and writing. YL conceived the study design and is the guarantor of the article.

FUNDING

This work was supported by the National Natural Science Foundation of China (NO. 81573775; NO. 81873157); Shanghai Natural Science Foundation (NO. 22ZR1459400); Future Plan for Traditional Chinese Medicine development of Science and Technology of Shanghai Municipal Hospital of Traditional Chinese Medicine (WL-HBQN-2021005K). The afore-mentioned support agents provided financial support only and had no role in study design, data collection, data analysis, data interpretation, decision to publish, or preparation of the manuscript.

SUPPLEMENTARY MATERIAL

The Supplementary Material for this article can be found online at: https://www.frontiersin.org/articles/10.3389/fphar.2022.894981/full#supplementary-material

REFERENCES

Abais, J. M., Xia, M., Zhang, Y., Boini, K. M., and Li, P. L. (2015). Redox Regulation of NLRP3 Inflammasomes: ROS as Trigger or Effector? *Antioxid. Redox Signal* 22 (13), 1111–1129. doi:10.1089/ars.2014.5994

Böttcher, K., and Pinzani, M. (2017). Pathophysiology of Liver Fibrosis and the Methodological Barriers to the Development of Anti-fibrogenic Agents. *Adv. drug Deliv. Rev.* 121, 3–8. doi:10.1016/j.addr.2017.05.016

Brandenberger, A. W., Tee, M. K., Lee, J. Y., Chao, V., and Jaffe, R. B. (1997). Tissue Distribution of Estrogen Receptors Alpha (ER-Alpha) and Beta (ER-Beta) mRNA in the Midgestational Human Fetus. *J. Clin. Endocrinol. Metab.* 82 (10), 3509–3512. doi:10.1210/jcem.82.10.4400

Chan, R. Y., Chen, W. F., Dong, A., Guo, D., and Wong, M. S. (2002). Estrogen-like Activity of Ginsenoside Rg1 Derived from Panax Notoginseng. *J. Clin. Endocrinol. Metab.* 87 (8), 3691–3695. doi:10.1210/jcem.87.8.8717

Chen, M. F., Huang, C. C., Liu, P. S., Chen, C. H., and Shiu, L. Y. (2013). Saikosaponin a and Saikosaponin D Inhibit Proliferation and Migratory Activity of Rat HSC-T6 Cells. *J. Med. Food* 16 (9), 793–800. doi:10.1089/jmf.2013.2762

Chen, R. J., Wu, H. H., and Wang, Y. J. (2015). Strategies to Prevent and Reverse Liver Fibrosis in Humans and Laboratory Animals. *Arch. Toxicol.* 89 (10), 1727–1750. doi:10.1007/s00204-015-1525-6

Chen, Y., Que, R., Lin, L., Shen, Y., Liu, J., and Li, Y. (2020). Inhibition of Oxidative Stress and NLRP3 Inflammasome by Saikosaponin-D Alleviates Acute Liver Injury in Carbon Tetrachloride-Induced Hepatitis in Mice. *Int. J. Immunopathol. Pharmacol.* 34, 2058738420950593. doi:10.1177/2058738420950593

Chen, Y., Zhao, C., Liu, X., Wu, G., Zhong, J., Zhao, T., et al. (2019). Plumbagin Ameliorates Liver Fibrosis via a ROS-Mediated NF-Kb Signaling Pathway *In Vitro* and *In Vivo*. *Biomed. Pharmacother.* 116, 108923. doi:10.1016/j.biopha.2019.108923

Cheng, C., Wu, H., Wang, M., Wang, L., Zou, H., Li, S., et al. (2019). Estrogen Ameliorates Allergic Airway Inflammation by Regulating Activation of NLRP3 in Mice. *Biosci. Rep.* 39 (1). doi:10.1042/bsr20181117

Cheng, F., Shen, Y., Mohanasundaram, P., Lindström, M., Ivaska, J., Ny, T., et al. (2016). Vimentin Coordinates Fibroblast Proliferation and Keratinocyte Differentiation in Wound Healing via TGF-β-Slug Signaling. *Proc. Natl. Acad. Sci. U. S. A.* 113 (30), E4320–E4327. doi:10.1073/pnas.1519197113

Cicchini, C., Amicone, L., Alonzi, T., Marchetti, A., Mancone, C., and Tripodi, M. (2015). Molecular Mechanisms Controlling the Phenotype and the EMT/MET Dynamics of Hepatocyte. *Liver Int.* 35 (2), 302–310. doi:10.1111/liv.12577

Cui, L. H., Li, C. X., Zhuo, Y. Z., Yang, L., Cui, N. Q., and Zhang, S. K. (2019). Saikosaponin D Ameliorates Pancreatic Fibrosis by Inhibiting Autophagy of Pancreatic Stellate Cells via PI3K/Akt/mTOR Pathway. *Chem. Biol. Interact.* 300, 18–26. doi:10.1016/j.cbi.2019.01.005

Dahlman-Wright, K., Cavailles, V., Fuqua, S. A., Jordan, V. C., Katzenellenbogen, J. A., Korach, K. S., et al. (2006). International Union of Pharmacology. LXIV. Estrogen Receptors. *Pharmacol. Rev.* 58 (4), 773–781. doi:10.1124/pr.58.4.8

Dang, S. S., Wang, B. F., Cheng, Y. A., Song, P., Liu, Z. G., and Li, Z. F. (2007). Inhibitory Effects of Saikosaponin-D on CCl4-Induced Hepatic Fibrogenesis in Rats. *World J. Gastroenterol.* 13 (4), 557–563. doi:10.3748/wjg.v13.i4.557

Deng, T., Liu, J., Zhang, M., Wang, Y., Zhu, G., and Wang, J. (2018). Inhibition Effect of Phytoestrogen Calycosin on TGF-B1-Induced Hepatic Stellate Cell Activation, Proliferation, and Migration via Estrogen Receptor β. *Can. J. Physiol. Pharmacol.* 96 (12), 1268–1275. doi:10.1139/cjpp-2018-0474

Dickie, L. J., Aziz, A. M., Savic, S., Lucherini, O. M., Cantarini, L., Geiler, J., et al. (2012). Involvement of X-Box Binding Protein 1 and Reactive Oxygen Species Pathways in the Pathogenesis of Tumour Necrosis Factor Receptor-Associated Periodic Syndrome. *Ann. Rheum. Dis.* 71 (12), 2035–2043. doi:10.1136/annrheumdis-2011-201197

Dixon, R. A. (2004). Phytoestrogens. *Annu. Rev. Plant Biol.* 55, 225–261. doi:10.1146/annurev.arplant.55.031903.141729

Evans, M. J., Lai, K., Shaw, L. J., Harnish, D. C., and Chadwick, C. C. (2002). Estrogen Receptor Alpha Inhibits IL-1beta Induction of Gene Expression in the Mouse Liver. *Endocrinology* 143 (7), 2559–2570. doi:10.1210/endo.143.7.8919

Fan, J., Li, X., Li, P., Li, N., Wang, T., Shen, H., et al. (2007). Saikosaponin-d Attenuates the Development of Liver Fibrosis by Preventing Hepatocyte Injury. *Biochem. Cell Biol.* 85 (2), 189–195. doi:10.1139/o07-010

Fattovich, G., Stroffolini, T., Zagni, I., and Donato, F. (2004). Hepatocellular Carcinoma in Cirrhosis: Incidence and Risk Factors. *Gastroenterology* 127 (5 Suppl. 1), S35–S50. doi:10.1053/j.gastro.2004.09.014

Friedman, S. L. (2007). Reversibility of Hepatic Fibrosis and Cirrhosis-Iis it All Hype? *Nat. Clin. Pract. Gastroenterol. Hepatol.* 4 (5), 236–237. doi:10.1038/ncpgasthep0813

Gao, H., Fält, S., Sandelin, A., Gustafsson, J. A., and Dahlman-Wright, K. (2008). Genome-wide Identification of Estrogen Receptor Alpha-Binding Sites in Mouse Liver. *Mol. Endocrinol.* 22 (1), 10–22. doi:10.1210/me.2007-0121

Gao, X., Fan, W., Tan, L., Shi, Y., Ding, C., Liu, S., et al. (2020). Soy Isoflavones Ameliorate Experimental Colitis by Targeting ERα/NLRP3 Inflammasome Pathways. *J. Nutr. Biochem.* 83, 108438. doi:10.1016/j.jnutbio.2020.108438

Grossmann, M., Wierman, M. E., Angus, P., and Handelsman, D. J. (2019). Reproductive Endocrinology of Nonalcoholic Fatty Liver Disease. *Endocr. Rev.* 40 (2), 417–446. doi:10.1210/er.2018-00158

Gutendorf, B., and Westendorf, J. (2001). Comparison of an Array of *In Vitro* Assays for the Assessment of the Estrogenic Potential of Natural and Synthetic Estrogens, Phytoestrogens and Xenoestrogens. *Toxicology* 166, 79–89. doi:10.1016/s0300-483x(01)00437-1

Haneklaus, M., and O'Neill, L. A. (2015). NLRP3 at the Interface of Metabolism and Inflammation. *Immunol. Rev.* 265 (1), 53–62. doi:10.1111/imr.12285

Hernandez-Gea, V., and Friedman, S. L. (2011). Pathogenesis of Liver Fibrosis. *Annu. Rev. Pathol.* 6, 425–456. doi:10.1146/annurev-pathol-011110-130246

Inzaugarat, M. E., Johnson, C. D., Holtmann, T. M., McGeough, M. D., Trautwein, C., Papouchado, B. G., et al. (2019). NLR Family Pyrin Domain-Containing 3 Inflammasome Activation in Hepatic Stellate Cells Induces Liver Fibrosis in Mice. *Hepatology* 69 (2), 845–859. doi:10.1002/hep.30252

Kim, J. W., Roh, Y. S., Jeong, H., Yi, H. K., Lee, M. H., Lim, C. W., et al. (2018). Spliceosome-Associated Protein 130 Exacerbates Alcohol-Induced Liver Injury by Inducing NLRP3 Inflammasome-Mediated IL-1β in Mice. *Am. J. Pathol.* 188 (4), 967–980. doi:10.1016/j.ajpath.2017.12.010

Lee, Y. H., Son, J. Y., Kim, K. S., Park, Y. J., Kim, H. R., Park, J. H., et al. (2019). Estrogen Deficiency Potentiates Thioacetamide-Induced Hepatic Fibrosis in Sprague-Dawley Rats. *Int. J. Mol. Sci.* 20 (15). doi:10.3390/ijms20153709

Li, P., Gong, Y., Zu, N., Li, Y., Wang, B., and Shimizu, F. (2005). Therapeutic Mechanism of Saikosaponin-D in Anti-thy1 mAb 1-22-3-induced Rat Model of Glomerulonephritis. *Nephron Exp. Nephrol.* 101 (4), e111–8. doi:10.1159/000087437

Li, X., Li, X., Huang, N., Liu, R., and Sun, R. (2018). A Comprehensive Review and Perspectives on Pharmacology and Toxicology of Saikosaponins. *Phytomedicine* 50, 73–87. doi:10.1016/j.phymed.2018.09.174

Lin, L., Gong, H., Li, R., Huang, J., Cai, M., Lan, T., et al. (2020). Nanodrug with ROS and pH Dual-Sensitivity Ameliorates Liver Fibrosis via Multicellular Regulation. *Adv. Sci. (Weinh)* 7 (7), 1903138. doi:10.1002/advs.201903138

Lin, L., Que, R., Shen, Y., Chen, Y., Yan, N., and Li, Y. (2018). Saikosaponin-d A-lleviates C-arbon-tetrachloride I-nduced A-cute H-epatocellular I-njury by I-nhibiting O-xidative S-tress and NLRP3 I-nflammasome A-ctivation in the HL-7702 C-ell L-ine. *Mol. Med. Rep.* 17 (6), 7939–7946. doi:10.3892/mmr.2018.8849

Lin, X., Wu, S., Wang, Q., Shi, Y., Liu, G., Zhi, J., et al. (2016). Saikosaponin-D Reduces H2O2-Induced PC12 Cell Apoptosis by Removing ROS and Blocking MAPK-dependent Oxidative Damage. *Cell Mol. Neurobiol.* 36 (8), 1365–1375. doi:10.1007/s10571-016-0336-5

Liu, A., Tanaka, N., Sun, L., Guo, B., Kim, J. H., Krausz, K. W., et al. (2014). Saikosaponin D Protects against Acetaminophen-Induced Hepatotoxicity by Inhibiting NF-Kb and STAT3 Signaling. *Chem. Biol. Interact.* 223, 80–86. doi:10.1016/j.cbi.2014.09.012

Liu, L., Yan, J., Ge, F., Xu, X., Lu, J., Shi, H., et al. (2019). Saikosaponin-D I-mproves F-ear M-emory D-eficits in O-variectomized R-ats via the A-ction of E-strogen R-eceptor-α in the hippocampus. *Mol. Med. Rep.* 20 (1), 332–340. doi:10.3892/mmr.2019.10232

Lu, M., Wu, J., Hao, Z. W., Shang, Y. K., Xu, J., Nan, G., et al. (2018). Basolateral CD147 Induces Hepatocyte Polarity Loss by E-Cadherin ubiquitination and Degradation in Hepatocellular Carcinoma Progress. *Hepatology* 68 (1), 317–332. doi:10.1002/hep.29798

Mak, P., Leav, I., Pursell, B., Bae, D., Yang, X., Taglienti, C. A., et al. (2010). ERbeta Impedes Prostate Cancer EMT by Destabilizing HIF-1alpha and Inhibiting VEGF-Mediated Snail Nuclear Localization: Implications for Gleason Grading. *Cancer Cell* 17 (4), 319–332. doi:10.1016/j.ccr.2010.02.030

Martinon, F., Burns, K., and Tschopp, J. (2002). The Inflammasome: a Molecular Platform Triggering Activation of Inflammatory Caspases and Processing of proIL-Beta. *Mol. Cell* 10 (2), 417–426. doi:10.1016/s1097-2765(02)00599-3

Mederacke, I., Hsu, C. C., Troeger, J. S., Huebener, P., Mu, X., Dapito, D. H., et al. (2013). Fate Tracing Reveals Hepatic Stellate Cells as Dominant Contributors to Liver Fibrosis Independent of its Aetiology. *Nat. Commun.* 4, 2823. doi:10.1038/ncomms3823

Menze, E. T., Ezzat, H., Shawky, S., Sami, M., Selim, E. H., Ahmed, S., et al. (2021). Simvastatin Mitigates Depressive-like Behavior in Ovariectomized Rats:

Possible Role of NLRP3 Inflammasome and Estrogen Receptors' Modulation. *Int. Immunopharmacol.* 95, 107582. doi:10.1016/j.intimp.2021.107582

Mohamed, I. N., Sarhan, N. R., Eladl, M. A., El-Remessy, A. B., and El-Sherbiny, M. (2018). Deletion of Thioredoxin-Interacting Protein Ameliorates High Fat Diet-Induced Non-alcoholic Steatohepatitis through Modulation of Toll-like Receptor 2-NLRP3-Inflammasome axis: Histological and Immunohistochemical Study. *Acta histochem.* 120 (3), 242–254. doi:10.1016/j.acthis.2018.02.006

Ning, Z. W., Luo, X. Y., Wang, G. Z., Li, Y., Pan, M. X., Yang, R. Q., et al. (2017). MicroRNA-21 Mediates Angiotensin II-Induced Liver Fibrosis by Activating NLRP3 Inflammasome/IL-1β Axis via Targeting Smad7 and Spry1. *Antioxid. Redox Signal* 27 (1), 1–20. doi:10.1089/ars.2016.6669

Omoya, T., Shimizu, I., Zhou, Y., Okamura, Y., Inoue, H., Lu, G., et al. (2001). Effects of Idoxifene and Estradiol on NF-kappaB Activation in Cultured Rat Hepatocytes Undergoing Oxidative Stress. *Liver* 21 (3), 183–191. doi:10.1034/j.1600-0676.2001.021003183.x

Parola, M., and Pinzani, M. (2019). Liver Fibrosis: Pathophysiology, Pathogenetic Targets and Clinical Issues. *Mol. Asp. Med.* 65, 37–55. doi:10.1016/j.mam.2018.09.002

Pinzani, M. (2015). Pathophysiology of Liver Fibrosis. *Dig. Dis.* 33 (4), 492–497. doi:10.1159/000374096

Que, R., Shen, Y., Ren, J., Tao, Z., Zhu, X., and Li, Y. (2018). Estrogen Receptor-β-dependent E-ffects of S-aikosaponin-d on the S-uppression of O-xidative S-tress-induced R-at H-epatic S-tellate C-ell A-ctivation. *Int. J. Mol. Med.* 41 (3), 1357–1364. doi:10.3892/ijmm.2017.3349

Ray, K. (2014). Liver: Hepatic Stellate Cells Hold the Key to Liver Fibrosis. *Nat. Rev. Gastroenterol. Hepatol.* 11 (2), 74. doi:10.1038/nrgastro.2013.244

Revankar, C. M., Cimino, D. F., Sklar, L. A., Arterburn, J. B., and Prossnitz, E. R. (2005). A Transmembrane Intracellular Estrogen Receptor Mediates Rapid Cell Signaling. *Science* 307 (5715), 1625–1630. doi:10.1126/science.1106943

Ruaro, B., Salton, F., Braga, L., Wade, B., Confalonieri, P., Volpe, M. C., et al. (2021). The History and Mystery of Alveolar Epithelial Type II Cells: Focus on Their Physiologic and Pathologic Role in Lung. *Int. J. Mol. Sci.* 22 (5). doi:10.3390/ijms22052566

Scambler, T., Jarosz-Griffiths, H. H., Lara-Reyna, S., Pathak, S., Wong, C., Holbrook, J., et al. (2019). ENaC-mediated Sodium Influx Exacerbates NLRP3-dependent Inflammation in Cystic Fibrosis. *eLife* 8, e49248. doi:10.7554/eLife.49248

Tian, Y. D., Lin, S., Yang, P. T., Bai, M. H., Jin, Y. Y., Min, W. L., et al. (2019). Saikosaponin-d Increases the Radiosensitivity of Hepatoma Cells by Adjusting Cell Autophagy. *J. Cancer* 10 (20), 4947–4953. doi:10.7150/jca.30286

Wang, P., Ren, J., Tang, J., Zhang, D., Li, B., and Li, Y. (2010). Estrogen-like Activities of Saikosaponin-D *In Vitro*: a Pilot Study. *Eur. J. Pharmacol.* 626 (2-3), 159–165. doi:10.1016/j.ejphar.2009.09.047

Wei, Q., Guo, P., Mu, K., Zhang, Y., Zhao, W., Huai, W., et al. (2015). Estrogen Suppresses Hepatocellular Carcinoma Cells through ERβ-Mediated Upregulation of the NLRP3 Inflammasome. *Lab. Invest.* 95 (7), 804–816. doi:10.1038/labinvest.2015.63

Wree, A., Eguchi, A., McGeough, M. D., Pena, C. A., Johnson, C. D., Canbay, A., et al. (2014). NLRP3 Inflammasome Activation Results in Hepatocyte Pyroptosis, Liver Inflammation, and Fibrosis in Mice. *Hepatology* 59 (3), 898–910. doi:10.1002/hep.26592

Xie, J. Y., Di, H. Y., Li, H., Cheng, X. Q., Zhang, Y. Y., and Chen, D. F. (2012). Bupleurum Chinense DC Polysaccharides Attenuates Lipopolysaccharide-Induced Acute Lung Injury in Mice. *Phytomedicine* 19 (2), 130–137. doi:10.1016/j.phymed.2011.08.057

Yagi, K. (1997). Female Hormones Act as Natural Antioxidants-Aa Survey of Our Research. *Acta Biochim. Pol.* 44 (4), 701–709. doi:10.18388/abp.1997_4372

Yang, J., Antin, P., Berx, G., Blanpain, C., Brabletz, T., Bronner, M., et al. (2020). Guidelines and Definitions for Research on Epithelial-Mesenchymal Transition. *Nat. Rev. Mol. Cell Biol.* 21 (6), 341–352. doi:10.1038/s41580-020-0237-9

Yuan, B., Yang, R., Ma, Y., Zhou, S., Zhang, X., and Liu, Y. (2017). A Systematic Review of the Active Saikosaponins and Extracts Isolated from Radix Bupleuri and Their Applications. *Pharm. Biol.* 55 (1), 620–635. doi:10.1080/13880209.2016.1262433

Zahid, A., Li, B., Kombe, A. J. K., Jin, T., and Tao, J. (2019). Pharmacological Inhibitors of the NLRP3 Inflammasome. *Front. Immunol.* 10, 2538. doi:10.3389/fimmu.2019.02538

Zhang, B., Zhang, C. G., Ji, L. H., Zhao, G., and Wu, Z. Y. (2018). Estrogen Receptor β Selective Agonist Ameliorates Liver Cirrhosis in Rats by Inhibiting the Activation and Proliferation of Hepatic Stellate Cells. *J. Gastroenterol. Hepatol.* 33 (3), 747–755. doi:10.1111/jgh.13976

Zhang, C. G., Zhang, B., Deng, W. S., Duan, M., Chen, W., and Wu, Z. Y. (2016). Role of Estrogen Receptor β Selective Agonist in Ameliorating Portal Hypertension in Rats with CCl4-Induced Liver Cirrhosis. *World J. Gastroenterol.* 22 (18), 4484–4500. doi:10.3748/wjg.v22.i18.4484

Zhao, C., Matthews, J., Tujague, M., Wan, J., Ström, A., Toresson, G., et al. (2007). Estrogen Receptor Beta2 Negatively Regulates the Transactivation of Estrogen Receptor Alpha in Human Breast Cancer Cells. *Cancer Res.* 67 (8), 3955–3962. doi:10.1158/0008-5472.Can-06-3505

Zhao, Y., Wang, Z., Feng, D., Zhao, H., Lin, M., Hu, Y., et al. (2019). p66Shc Contributes to Liver Fibrosis through the Regulation of Mitochondrial Reactive Oxygen Species. *Theranostics* 9 (5), 1510–1522. doi:10.7150/thno.29620

Zhou, Y., Shimizu, I., Lu, G., Itonaga, M., Okamura, Y., Shono, M., et al. (2001). Hepatic Stellate Cells Contain the Functional Estrogen Receptor Beta but Not the Estrogen Receptor Alpha in Male and Female Rats. *Biochem. Biophys. Res. Commun.* 286 (5), 1059–1065. doi:10.1006/bbrc.2001.5479

Conflict of Interest: The authors declare that the research was conducted in the absence of any commercial or financial relationships that could be construed as a potential conflict of interest.

Publisher's Note: All claims expressed in this article are solely those of the authors and do not necessarily represent those of their affiliated organizations, or those of the publisher, the editors and the reviewers. Any product that may be evaluated in this article, or claim that may be made by its manufacturer, is not guaranteed or endorsed by the publisher.

frontiers | Frontiers in Pharmacology

ORIGINAL RESEARCH
published: 07 June 2022
doi: 10.3389/fphar.2022.905936

Interleukin-6 Receptor Blockade can Increase the Risk of Nonalcoholic Fatty Liver Disease: Indications From Mendelian Randomization

*Shuxuan Li, Lanlan Chen and Guoyue Lv**

Department of Hepatobiliary and Pancreatic Surgery, First Affiliated Hospital of Jilin University, Changchun, China

Background: Interleukin-6 receptor (IL-6R) blockade has been approved for inflammation-associated diseases and whether it is effective in treating non-alcoholic fatty liver disease (NAFLD) is still unknown.

Methods: A target-based Mendelian randomization was performed to appraise whether inhibiting the IL-6 signaling pathway *via* IL-6R blockade can reduce the risk of NAFLD. The previously established genetic proxy SNP rs2228145 was mainly used to appraise the therapeutic effects and the genetic-predicted circulating IL-6 level was treated as the exposure with ~30,000 samples. The genetic association between SNP rs2228145 (A > C) and NAFLD was obtained from non-FinnGen GWAS (1,483 cases and 17,781controls) and FinnGen GWAS (894 cases and 217,898 controls). The causal effects were estimated using a Wald ratio method and were combined using a fixed-effects meta-analysis. Furthermore, the SNP rs12048091 was employed as another proxy in the sensitivity analysis.

Results: The positive control analysis suggested the SNP rs2228145 can mimic the effects of IL-6R blockade where inhibiting IL-6 signaling can reduce the risk of rheumatoid arthritis [OR = 0.68 (0.58, 0.80)] and coronary heart disease [OR = 0.75 (0.68, 0.84)]. This Mendelian randomization analysis suggested that IL-6R blockade can adversely increase the risk of NAFLD in the non-FinnGen GWAS [OR = 1.99 (1.27, 3.13)] while not significant in the FinnGen consortium. The fixed-effects meta-analysis indicated inhibiting the IL-6 signaling pathway can reduce the risk of NAFLD [OR = 1.80 (1.26, 2.57)]. When including SNP rs12048091 as the genetic instrument, the meta-analysis using two genetic variants also indicated a similar effect on NAFLD [OR = 1.83 (1.32, 2.53)]. There was no heterogeneity in the whole analysis.

Conclusion: Our Mendelian randomization suggested inhibiting the IL-6 signaling pathway *via* IL-6R blockade might increase the risk of NAFLD, suggesting IL-6R should play a protective role in NAFLD.

Keywords: interleukin-6 receptor blockade, interleukin-6 signaling pathway, nonalcoholic fatty liver disease, mendelian randomization, causal inference

OPEN ACCESS

Edited by:
Xiude Fan,
Shandong Provincial Hospital, China

Reviewed by:
Jie Ding,
Nanjing Medical University, China
Ruilian You,
Peking Union Medical College Hospital (CAMS), China
Aihui Yan,
China Medical University, China

****Correspondence:***
Guoyue Lv
lvgy@jlu.edu.cn

Specialty section:
This article was submitted to Gastrointestinal and Hepatic Pharmacology, a section of the journal Frontiers in Pharmacology

Received: *28 March 2022*
Accepted: *02 May 2022*
Published: *07 June 2022*

Citation:
Li S, Chen L and Lv G (2022) Interleukin-6 Receptor Blockade can Increase the Risk of Nonalcoholic Fatty Liver Disease: Indications From Mendelian Randomization. Front. Pharmacol. 13:905936. doi: 10.3389/fphar.2022.905936

INTRODUCTION

The prevalence of non-alcoholic fatty liver disease (NAFLD), also termed metabolic associated fatty liver disease (MAFLD), is increasing worldwide and almost 1 billion people are harassed by it (Eslam et al., 2020). Currently, no effective therapeutics have been approved for it though the pan-PPAR agonist lanifibranor displayed the efficacy in phase 2b trial (Francque et al., 2021). Thus, it is of necessity to find therapeutic targets and potential drugs to help ameliorate NAFLD. Interleukin-6 (IL-6) is a pivotal cytokine in inflammation-associated liver disease, and the current evidence suggested it has both pro-inflammation and anti-inflammation effects where IL-6 released from adiposity can promote inflammation and muscle-derived IL-6 can ameliorate inflammation (Giraldez et al., 2021). Furthermore, chronic exposure to high IL-6 levels can increase hepatic gluconeogenesis and result in impaired lipid metabolism (Perry et al., 2015), however, the IL-6 has hepatoprotective effects in acute liver injury (Gao et al., 2020). Also, a recent study suggested IL-6 receptor (IL-6R) can reduce NAFLD-associated inflammation (Skuratovskaia et al., 2021).

It is still unknown whether targeting the IL-6 signaling pathway would have a causal effect on NAFLD through several drugs targeting this pathway that have been approved or displayed clinical potency for metabolic diseases, inflammatory bowel disease (IBD), and liver and gastrointestinal cancer (Giraldez et al., 2021). The rapid developments in Mendelian randomization (MR) have provided strategies to evaluate the causal effect of specific targets with the integration of results derived from genome-wide association studies (GWAS). Several target-based MR investigations have been performed to appraise the therapeutic effects of specific targets and signaling pathways, including the IL-6 signaling pathway (Swerdlow et al., 2012). The target-based MR study used germline genetic variants located in the target gene region as the instruments and it is a quasi-randomized clinical trial (quasi-RCT) since germline genetic variants were usually randomly allocated at conception (Smith and Ebrahim, 2003). Considering the MR estimates often represent a life-long causal effect of exposure on the outcome, this target-based design can evaluate the effect of chronic exposure to a biomarker (Davies et al., 2018).

It should be noted that the inhibiting IL-6 signaling pathway can increase the serum IL-6 level *via* a negative feedback mechanism (Peters et al., 1996). Therefore, we cannot determine whether the hazardous effect of chronic exposure to high IL-6 levels might rise from a loss function of IL-6R. In this target-based MR study, we attempted to explore the causal effect of the IL-6 signaling pathway on NAFLD and furthermore appraise the effect of chronic exposure to high IL-6 levels on NAFLD.

METHODS

Data Source Description

The genetic associations with circulating IL-6 levels were obtained from the largest GWAS meta-analysis with more than 30,000 European individuals (Folkersen et al., 2020). The IL-6 level was normalized or standardized and this meta-analysis adjusted for population structure and study-specific parameters. The genetic associations with NAFLD were extracted from two independent GWAS summary statistics where one is composed of 1,483 European cases and 17,781 European controls (Anstee et al., 2020), and the other consists of 894 European cases and 217,898 European controls (https://www.finngen.fi/en). The former NAFLD was diagnosed by histopathology and associated laboratory examinations while the latter NAFLD was determined by electronic medical records. In addition, the former was analyzed by a multiple logistic regression by adjusting for the top 5 principal components and the latter was performed under the protocols of FinnGen GWAS round 5 (https://finngen.gitbook.io/documentation/v/r5/). There was no sample overlapping between the data sources of exposure and outcome.

Selection of Genetic Variants Mimicking IL-6R Blockade

The genetic variants mimicking IL-6R blockade were determined *via* two ways, one is from previous literature and the other was directly from the GWAS summary statistics. Previously, two SNPs located in the gene region coding IL-6R were reported to imitate the effect of inhibiting the IL-6 signaling pathway, namely SNP rs7529229 (Swerdlow et al., 2012) and rs2228145 (Parisinos et al., 2018). The two SNPs are in high linkage disequilibrium among Europeans (LD R^2 = 0.94). They can increase the proteolysis of IL-6R and result in a reduction in classic signaling, and have a similar effect to tocilizumab, an approved anti-IL6R monoclonal antibody (Swerdlow et al., 2012).

From the GWAS summary statistics of IL-6 level, only three SNP retained based on three criteria (p-value $< 5 \times 10^{-8}$, minor allele frequency >0.01 and LD R2 < 0.3), including SNP rs2228145, rs12048091 and rs10752641. The SNP rs10752641 was removed further as it is a palindromic one. The LD R^2 between SNP rs2228145 and rs12048091 was 0.11. To furthermore demonstrate that the selected genetic variants can mimic the effect of inhibiting the IL-6 signaling pathway by IL-6R blockade, we examined their genetic associations with C-reactive protein and fibrinogen, two downstream biomarkers of the IL-6 signaling pathway, in the UK Biobank with 361,194 Europeans. The F statistic was calculated to appraise the weak instrument bias.

Mendelian Randomization Design and Meta-analysis

The MR study should be carried out following three basic criteria: 1) relevance: genetic variants, usually single nucleotide polymorphism (SNP), should be close to the exposure; 2) independence: genetic variants should not be associated with any potential confounders; 3) exclusion-restriction: genetic variants should not be associated with the outcome except *via* the way of exposure (Emdin et al., 2017) (**Figure 1**). In addition, other assumptions should be satisfied such as linearity and no interaction (Bowden and Holmes, 2019).

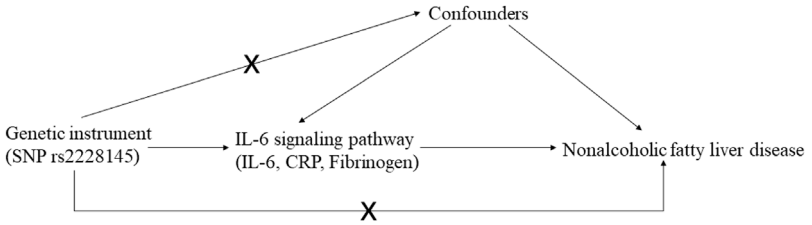

FIGURE 1 | The basic assumptions and main design of this Mendelian randomization.

TABLE 1 | Genetic associations with serum interleukin-6 level and F statistics.

SNP	A1	A2	EAF	BETA	SE	P	F
rs2228145	C	A	0.38	0.17	0.012	3.34×10^{-45}	198.49
rs12048091	A	G	0.82	0.09	0.016	3.95×10^{-08}	30.01

Note: A1 is the effect allele.

Preliminarily, we extracted genetic association with NAFLD from two GWASs for SNP rs2228145 and estimated the effect of IL-6 level on NAFLD using the Wald ratio method. Then, two MR estimates based on the ratio method were combined using a meta-analysis. The fixed-effects model was adopted if there was no heterogeneity. Otherwise, we would use a random-effects model.

Positive Control Analysis and Sensitivity Analysis

To further guarantee the validity and rigorousness of this MR study, we selected two well-established outcomes as the positive controls such as rheumatoid arthritis (RA) (Okada et al., 2014) and coronary heart disease (CHD) (Nikpay et al., 2015). The causal effect of IL-6R blockade on them was estimated using SNP rs2228145.

As there might be a lack of statistical power with only one SNP, we further included SNP rs12048091 in the sensitivity analysis. The inverse-variance weighted (IVW) method was employed to estimate the causal effect of IL-6 blockade using two SNPs.

Statistical Analysis and Data Visualization

All statistical analyses and data visualization were performed using the R programming software (R 3.6.0, https://www.r-project.org/). The Wald ratio and IVW methods were provided by the R package "TwoSampleMR" (https://github.com/MRCIEU/TwoSampleMR) (Hemani et al., 2018). The statistical power was assessed by the mRnd (https://cnsgenomics.shinyapps.io/mRnd/) (Brion et al., 2013).

RESULTS

Description of Selected Genetic Variants

The SNP rs2228145 (A > C), a missense variant (IL-6R Asp358Ala), was used in the primary analysis, and this variant was associated with increased soluble IL-6R (sIL-6R) and IL-6 levels (Ferreira et al., 2013). In the light of its association with the IL-6 level, its F statistic was 198, much greater than the empirical threshold of 10. The SNP rs12048091 (A > G) was an intron variant located in the IL-6R gene region, however, its biological function is still unknown. Its F statistic was 30, respectively. All genetic associations were aligned to the allele that raises the IL-6 level (**Table 1**).

Genetic Associations With CRP and Fibrinogen

The genetic associations with CRP and fibrinogen confirmed the validity of selected genetic variants (**Table 2**). As displayed in **Table 2**, the allele increasing IL-6 level was inversely associated with CRP and fibrinogen for each SNP, suggesting that the SNPs can mimic the inhibition of the classical IL-6 signaling pathway.

When estimating the change of CRP and fibrinogen scaled by the IL-6 level change, we obtained that the CRP level would decrease 0.54 standard deviation (SD) (95% confidence interval (CI): (−0.56, −0.51), p-value < 0.001) with per SD increase in IL-6 level and the fibrinogen level would decrease 0.06 [95% CI: (−0.09, −0.02), p-value = 0.001) for SNP rs2228145. There were similar results for SNP rs12048091 where the CRP level was reduced 0.62 SD [95% CI: (−0.69, −0.55), p-value < 0.001], together with fibrinogen [beta = −0.11 [−0.20, −0.02), p-value = 0.013).

Results of Positive Control Analysis

The genetic association with positive controls suggested SNP rs2228145 were inversely associated with the risk of RA and CHD. However, the SNP rs12048091 was not associated with CHD. The MR results of the positive control analysis were all statistically significant and concordant with the expectations. Initially, inhibiting IL-6 signaling pathway could reduce the risk of RA [OR = 0.68 (0.58, 0.80), p-value < 0.001]. Like RA, the risk of CHD would decrease as well [OR = 0.75 (0.68, 0.84), p-value < 0.001]. In the fixed-effects model using two SNPs, we obtained similar results (**Figure 2**).

Main Mendelian Randomization Results and Meta-Analysis

In the largest NAFLD GWAS, we observed that the odds of NAFLD would increase if inhibiting IL-6 signaling pathway [OR

TABLE 2 | Genetic associations with serum CRP and fibrinogen levels and two positive controls (rheumatoid arthritis and coronary heart disease).

SNP	A1	A2	CRP			Fibrinogen			Rheumatoid arthritis			Coronary heart disease		
			BETA	SE	P	BETA	SE	P	BETA	SE	P	BETA	SE	P
rs2228145	C	A	−0.09	0.002	1.00×10^{-200}	−0.01	0.003	0.001	−0.07	0.015	4.50×10^{-6}	−0.05	0.010	1.86×10^{-7}
rs12048091	A	G	−0.06	0.003	4.36×10^{-65}	−0.01	0.004	0.013	−0.09	0.021	1.30×10^{-5}	0.02	0.013	0.243

Note: A1 is the effect allele.

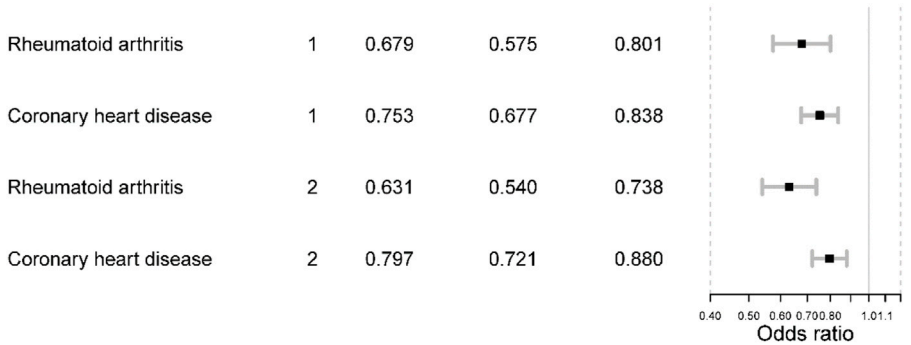

FIGURE 2 | The positive control analysis results. NSNP is the number of SNPs used in analysis and the SNP rs2228145 was used if NSNP = 1. The SNP rs2228145 and rs12048091 were used if NSNP = 2. OR is the odds ratio. 95% LCI is the lower limit of 95% confidence interval while 97%UCI is the upper limit of 95% confidence interval.

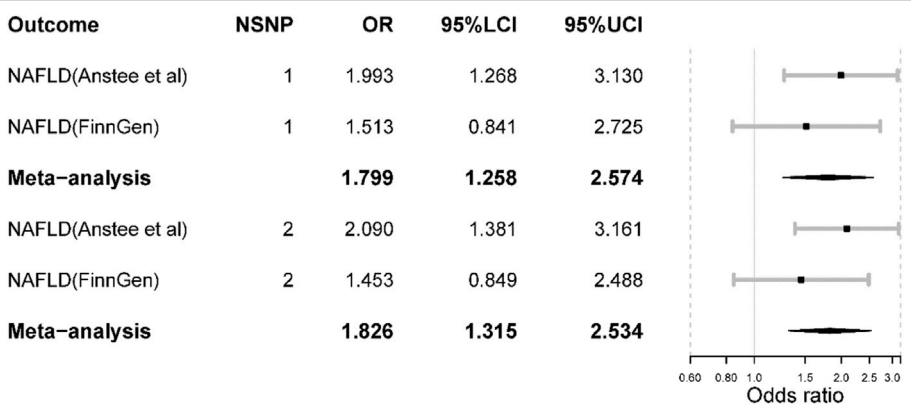

FIGURE 3 | The main Mendelian randomization results. NSNP is the number of SNPs used in analysis and the SNP rs2228145 was used if NSNP = 1. The SNP rs2228145 and rs12048091 were used if NSNP = 2. OR is the odds ratio. 95% LCI is the lower limit of 95% confidence interval while 97%UCI is the upper limit of 95% confidence interval.

= 1.99 (1.27, 3.13), *p*-value = 0.003] where the inhibitive effect was measured by IL-6 level and proxied by SNP rs2228145. However, such causal effect was not detected in the FinnGen NAFLD GWAS [OR = 1.51 (0.84, 2.72), *p*-value = 0.167]. In the meta-analysis, the odds of NAFLD would increase [OR = 1.80 (1.26, 2.57), *p*-value = 0.001] (**Figure 3**). There was no heterogeneity in the meta-analysis (I square = 0; Q *p*-value > 0.05).

When including SNP rs12048091 in the MR analysis, the odds of NAFLD would increase in the largest NAFLD GWAS [OR = 2.09 (1.38, 3.16), *p*-value < 0.001]. Also, the result was not significant in the FinnGen NAFLD GWAS (**Figure 3**). The meta-analysis yielded a significant result [OR = 1.83 (1.32, 2.53), *p*-value < 0.001]. Compared to the results from the main analysis using only one SNP, the results derived from two SNPs displayed larger effect sizes and statistical power. Furthermore, both MR and meta-analysis results suggested that inhibiting the IL-6 signaling pathway *via* IL-6R blockade could increase the risk of NAFLD.

The statistical powers of the non-FinnGen dataset were 98 and 84% for the FinnGen dataset. In addition, all the other results were above 80%.

DISCUSSION

This target-based MR analysis gave novel insights into the increased risk of NAFLD when inhibiting the IL-6 signaling pathway *via* IL-6R blockade, especially inhibiting the classic IL-6 signaling pathway.

Currently, there was no direct clinical trial reporting the incidence rate of NAFLD among patients receiving anti-IL6R therapy. Thus, we would concentrate on the effect of anti-IL6R drugs on metabolism, especially on lipid and glucose metabolism. The available evidence indicated that anti-IL6R drugs seemed to be associated with a marginal reduction in glycated hemoglobin (HbA1c) levels ($p = 0.047$) (Lurati et al., 2021) while another trial ruled out this association (Chen et al., 2020). Overall, the anti-IL6R drugs appear not to reduce the risk of diabetes mellitus. The ASCERTAIN trial suggested application of subcutaneous sarilumab and intravenous tocilizumab could increase alanine transaminase (ALT) and lipids, including low-density lipoprotein cholesterol (LDL-C), high-density lipoprotein cholesterol (HDL-C) and triglycerides (TG) (Emery et al., 2019). In addition, other clinical trials also corroborated that tocilizumab treatment could increase the levels of serum lipids, especially LDL-C and HDL-C (Gabay et al., 2016; Hoffman et al., 2019).

However, all these trials correlated the lipid elevation with the increased risk of cardiovascular events and neglected the potential risk of NAFLD. Our study indicated that IL-6R blockade could increase the risk of NAFLD. These trials lent support to our findings since NAFLD is characterized by lipid accumulation and genetically-elevated LDL-C could increase the risk of NAFLD (Liu et al., 2020). Nonetheless, it should be noted that we used CHD as the positive control where IL-6R blockade could reduce the risk of it. Thus, the association between IL-6R blockade, lipid elevation, and NAFLD should be independent of the common IL-6 signaling pathway and might be liver-specific.

The IL-6 signaling can be classified into two categories: 1) classical signaling: IL-6 binds to the signal transducing subunit gp130 in complex with the membrane-bound IL-6R; 2) trans-signaling: IL-6 binds to the gp130 *via* the soluble IL-6R (Schmidt-Arras and Rose-John, 2016). The classical signaling has anti-inflammatory and regenerative properties while the trans-signaling can promote inflammation (Skuratovskaia et al., 2021). Skuratovskaia et al. reported that higher plasma IL-6 level was correlated with a decreased CRP level and IL-6R could reduce chronic inflammation in NAFLD (Skuratovskaia et al., 2021). These findings were consistent with our results as the IL-6 signaling inhibition was scaled by the IL-6 level and this level was inversely associated with CRP and fibrinogen. In this MR study, the SNP rs2228145 promotes the proteolysis of membrane-bound IL-6R and increases the serum level of soluble IL-6R (Ferreira et al., 2013), suggesting this SNP has an inhibitive effect on classical signaling while amplifying the trans-signaling. Thus, it is plausible that we observed an increased risk of NAFLD.

However, the evidence that the impaired lipid metabolism often concurs with high IL-6 levels suggested chronic exposure to high IL-6 levels should promote liver inflammation (Giraldez et al., 2021). In our study, we observed that high IL-6 level caused by IL-6R blockade was associated with the elevated risk of NAFLD. Therefore, we postulated that the chronic exposure to high IL-6 caused by a loss function of IL-6R could promote the chronic inflammation process. A recent study corroborated our findings from another aspect where myeloid-specific IL-6 signaling inhibits liver fibrosis *via* exosomal transfer of antifibrotic miR-223 into hepatocytes, suggesting the protective role of IL-6 signaling in NAFLD (Hou et al., 2021). Although an early study suggested the blockade of interleukin 6 signalings could ameliorate hepatic steatosis *via* modulating insulin resistance, it should be noted that this experiment was performed on mice instead of on human beings and the higher IL-6 level was caused by a high-fat diet (Yamaguchi et al., 2015). Thus, it should be emphasized that the cause of high IL-6 levels should induce different effects and IL-6 signaling effects might vary between mice and people. In addition, the muscle-derived IL-6 could ameliorate inflammation (Pedersen and Febbraio, 2008) while adiposity-derived IL-6 was pro-inflammatory (Coppack, 2001), suggesting the IL-6 effects might vary between tissues. However, the tissue-specificity was not taken into consideration in our study due to data limitations.

Anyhow, this target-based Mendelian randomization suggested the potential risk of NAFLD caused by inhibiting the classic IL-6 signaling, which should be paid attention to in patients receiving anti-IL6R treatments. This study has several strengths as follows: 1) the relatively large sample size of NAFLD; 2) this population-based study added much more robust evidence than animal models or observational studies with small sample sizes. However, several limitations should be pointed out as well. Currently, most of the anti-IL6R monoclonal antibodies usually inhibit both classical signaling and trans-signaling such as tocilizumab (Tanaka et al., 2014). As mentioned above, classical IL-6 signaling is anti-inflammatory while trans-signaling is pro-inflammatory in the liver. Thus, IL-6R monoclonal antibodies should have both anti-/pro-inflammatory effects in the liver and SNP rs2228145 has a single pro-inflammatory effect in the liver, and we cannot equal the MR results to that derived for RCTs. Only two IVs were used in estimating the causal effect, guaranteeing the power and validity of this MR study. In addition, the function of included SNP rs12048091 is unknown and it adds some uncertainty to our results. The causal effects were estimated in European ancestry individuals and the generalizability of our conclusion might not be suitable for other ethnicities.

Last but not least, this target-based MR study assessed the effect of IL-6R blockade proxied by SNP rs2228145 on NAFLD though IL-6R blockade was measured by serum IL-6 level. We cannot obtain the conclusion that the genetically-elevated IL-6 level could increase the risk of NAFLD despite it might be reasonable. Our study implicated that clinical trials focused on anti-IL6R drugs should not neglect the incidence rate of NAFLD. However, clinical trials should be carried out to further corroborate these findings and further investigations should be performed to clarify the tissue-specific effects of IL-6 signaling.

CONCLUSION

Our target-based suggested IL-6R blockade might increase the risk of NAFLD and it should be corroborated and paid attention to in further clinical trials.

DATA AVAILABILITY STATEMENT

Publicly available datasets were analyzed in this study. This data can be found here: https://www.ebi.ac.uk/gwas/.

ETHICS STATEMENT

Each GWAS was approved by its corresponding Ethical Review Committee and each participant has provided consent to the study or the study is exempt from patient's consent. The patients/participants provided their written informed consent to participate in this study.

AUTHOR CONTRIBUTIONS

GL proposed the idea and designed the research. SL performed the main analysis and wrote the original manuscript. LC provided assistance in statistical analysis and scientific writing.

ACKNOWLEDGMENTS

We would like to thank all investigators for making their GWAS results publicly available. We want to acknowledge the participants and investigators of the FinnGen study.

REFERENCES

Anstee, Q. M., Darlay, R., Cockell, S., Meroni, M., Govaere, O., Tiniakos, D., et al. (2020). Genome-wide Association Study of Non-alcoholic Fatty Liver and Steatohepatitis in a Histologically Characterised Cohort☆. *J. Hepatol.* 73 (3), 505–515. doi:10.1016/j.jhep.2020.04.003

Bowden, J., and Holmes, M. V. (2019). Meta-analysis and Mendelian Randomization: A Review. *Res. Synth. Methods* 10 (4), 486–496. doi:10.1002/jrsm.1346

Brion, M. J., Shakhbazov, K., and Visscher, P. M. (2013). Calculating Statistical Power in Mendelian Randomization Studies. *Int. J. Epidemiol.* 42 (5), 1497–1501. doi:10.1093/ije/dyt179

Chen, S. K., Lee, H., Jin, Y., Liu, J., and Kim, S. C. (2020). Use of Biologic or Targeted-Synthetic Disease-Modifying Anti-rheumatic Drugs and Risk of Diabetes Treatment Intensification in Patients with Rheumatoid Arthritis and Diabetes Mellitus. *Rheumatol. Adv. Pract.* 4 (2), rkaa027. doi:10.1093/rap/rkaa027

Coppack, S. W. (2001). Pro-inflammatory Cytokines and Adipose Tissue. *Proc. Nutr. Soc.* 60 (3), 349–356. doi:10.1079/pns2001110

Davies, N. M., Holmes, M. V., and Davey Smith, G. (2018). Reading Mendelian Randomisation Studies: a Guide, Glossary, and Checklist for Clinicians. *BMJ* 362, k601. doi:10.1136/bmj.k601

Emdin, C. A., Khera, A. V., and Kathiresan, S. (2017). Mendelian Randomization. *Jama* 318 (19), 1925–1926. doi:10.1001/jama.2017.17219

Emery, P., Rondon, J., Parrino, J., Lin, Y., Pena-Rossi, C., van Hoogstraten, H., et al. (2019). Safety and Tolerability of Subcutaneous Sarilumab and Intravenous Tocilizumab in Patients with Rheumatoid Arthritis. *Rheumatol. Oxf.* 58 (5), 849–858. doi:10.1093/rheumatology/key361

Eslam, M., Sanyal, A. J., and George, J. (2020). MAFLD: A Consensus-Driven Proposed Nomenclature for Metabolic Associated Fatty Liver Disease. *Gastroenterology* 158 (7), 1999–e1. doi:10.1053/j.gastro.2019.11.312

Ferreira, R. C., Freitag, D. F., Cutler, A. J., Howson, J. M., Rainbow, D. B., Smyth, D. J., et al. (2013). Functional IL6R 358Ala Allele Impairs Classical IL-6 Receptor Signaling and Influences Risk of Diverse Inflammatory Diseases. *PLoS Genet.* 9 (4), e1003444. doi:10.1371/journal.pgen.1003444

Folkersen, L., Gustafsson, S., Wang, Q., Hansen, D. H., Hedman, Å. K., Schork, A., et al. (2020). Genomic and Drug Target Evaluation of 90 Cardiovascular Proteins in 30,931 Individuals. *Nat. Metab.* 2 (10), 1135–1148. doi:10.1038/s42255-020-00287-2

Francque, S. M., Bedossa, P., Ratziu, V., Anstee, Q. M., Bugianesi, E., Sanyal, A. J., et al. (2021). A Randomized, Controlled Trial of the Pan-PPAR Agonist Lanifibranor in NASH. *N. Engl. J. Med.* 385 (17), 1547–1558. doi:10.1056/NEJMoa2036205

Gabay, C., McInnes, I. B., Kavanaugh, A., Tuckwell, K., Klearman, M., Pulley, J., et al. (2016). Comparison of Lipid and Lipid-Associated Cardiovascular Risk Marker Changes after Treatment with Tocilizumab or Adalimumab in Patients with Rheumatoid Arthritis. *Ann. Rheum. Dis.* 75 (10), 1806–1812. doi:10.1136/annrheumdis-2015-207872

Gao, R. Y., Wang, M., Liu, Q., Feng, D., Wen, Y., Xia, Y., et al. (2020). Hypoxia-Inducible Factor-2α Reprograms Liver Macrophages to Protect against Acute Liver Injury through the Production of Interleukin-6. *Hepatology* 71 (6), 2105–2117. doi:10.1002/hep.30954

Giraldez, M. D., Carneros, D., Garbers, C., Rose-John, S., and Bustos, M. (2021). New Insights into IL-6 Family Cytokines in Metabolism, Hepatology and Gastroenterology. *Nat. Rev. Gastroenterol. Hepatol.* 18 (11), 787–803. doi:10.1038/s41575-021-00473-x

Hemani, G., Zheng, J., Elsworth, B., Wade, K. H., Haberland, V., Baird, D., et al. (2018). The MR-Base Platform Supports Systematic Causal Inference across the Human Phenome. *Elife* 7:e34408. doi:10.7554/eLife.34408

Hoffman, E., Rahat, M. A., Feld, J., Elias, M., Rosner, I., Kaly, L., et al. (2019). Effects of Tocilizumab, an Anti-interleukin-6 Receptor Antibody, on Serum Lipid and Adipokine Levels in Patients with Rheumatoid Arthritis. *Int. J. Mol. Sci.* 20 (18), 4633. doi:10.3390/ijms20184633

Hou, X., Yin, S., Ren, R., Liu, S., Yong, L., Liu, Y., et al. (2021). Myeloid-Cell-Specific IL-6 Signaling Promotes MicroRNA-223-Enriched Exosome Production to Attenuate NAFLD-Associated Fibrosis. *Hepatology* 74 (1), 116–132. doi:10.1002/hep.31658

Liu, Z., Zhang, Y., Graham, S., Wang, X., Cai, D., Huang, M., et al. (2020). Causal Relationships between NAFLD, T2D and Obesity Have Implications for Disease Subphenotyping. *J. Hepatol.* 73 (2), 263–276. doi:10.1016/j.jhep.2020.03.006

Lurati, A., Laria, A., Mazzocchi, D., Re, K. A., Marrazza, M. G., Faggioli, P. M., et al. (2021). Improvement of HbA1c in Patients with Type 2 Diabetes Mellitus and Rheumatoid Arthritis Treated with bDMARDs. *Open Access Rheumatol.* 13, 73–78. doi:10.2147/oarrr.s302679

Nikpay, M., Goel, A., Won, H. H., Hall, L. M., Willenborg, C., Kanoni, S., et al. (2015). A Comprehensive 1,000 Genomes-Based Genome-wide Association Meta-Analysis of Coronary Artery Disease. *Nat. Genet.* 47 (10), 1121–1130. doi:10.1038/ng.3396

Okada, Y., Wu, D., Trynka, G., Raj, T., Terao, C., Ikari, K., et al. (2014). Genetics of Rheumatoid Arthritis Contributes to Biology and Drug Discovery. *Nature* 506 (7488), 376–381. doi:10.1038/nature12873

Parisinos, C. A., Serghiou, S., Katsoulis, M., George, M. J., Patel, R. S., Hemingway, H., et al. (2018). Variation in Interleukin 6 Receptor Gene Associates with Risk of Crohn's Disease and Ulcerative Colitis. *Gastroenterology* 155 (2), 303–e2. doi:10.1053/j.gastro.2018.05.022

Pedersen, B. K., and Febbraio, M. A. (2008). Muscle as an Endocrine Organ: Focus on Muscle-Derived Interleukin-6. *Physiol. Rev.* 88 (4), 1379–1406. doi:10.1152/physrev.90100.2007

Perry, R. J., Camporez, J. G., Kursawe, R., Titchenell, P. M., Zhang, D., Perry, C. J., et al. (2015). Hepatic Acetyl CoA Links Adipose Tissue Inflammation to Hepatic Insulin Resistance and Type 2 Diabetes. *Cell* 160 (4), 745–758. doi:10.1016/j.cell.2015.01.012

Peters, M., Jacobs, S., Ehlers, M., Vollmer, P., Müllberg, J., Wolf, E., et al. (1996). The Function of the Soluble Interleukin 6 (IL-6) Receptor *In Vivo*: Sensitization of Human Soluble IL-6 Receptor Transgenic Mice towards IL-6 and Prolongation of the Plasma Half-Life of IL-6. *J. Exp. Med.* 183 (4), 1399–1406. doi:10.1084/jem.183.4.1399

Schmidt-Arras, D., and Rose-John, S. (2016). IL-6 Pathway in the Liver: From Physiopathology to Therapy. *J. Hepatol.* 64 (6), 1403–1415. doi:10.1016/j.jhep.2016.02.004

Skuratovskaia, D., Komar, A., Vulf, M., Quang, H. V., Shunkin, E., Volkova, L., et al. (2021). IL-6 Reduces Mitochondrial Replication, and IL-6 Receptors Reduce Chronic Inflammation in NAFLD and Type 2 Diabetes. *Int. J. Mol. Sci.* 22 (4). doi:10.3390/ijms22041774

Smith, G. D., and Ebrahim, S. (2003). 'Mendelian Randomization': Can Genetic Epidemiology Contribute to Understanding Environmental Determinants of Disease? *Int. J. Epidemiol.* 32 (1), 1–22. doi:10.1093/ije/dyg070

Swerdlow, D. I., Swerdlow, D. I., Holmes, M. V., Kuchenbaecker, K. B., Engmann, J. E., Shah, T., et al. (2012). The Interleukin-6 Receptor as a Target for Prevention of Coronary Heart Disease: a Mendelian Randomisation Analysis. *Lancet* 379 (9822), 1214–1224. doi:10.1016/S0140-6736(12)60110-X

Tanaka, T., Narazaki, M., and Kishimoto, T. (2014). IL-6 in Inflammation, Immunity, and Disease. *Cold Spring Harb. Perspect. Biol.* 6 (10), a016295. doi:10.1101/cshperspect.a016295

Yamaguchi, K., Nishimura, T., Ishiba, H., Seko, Y., Okajima, A., Fujii, H., et al. (2015). Blockade of Interleukin 6 Signalling Ameliorates Systemic Insulin Resistance through Upregulation of Glucose Uptake in Skeletal Muscle and Improves Hepatic Steatosis in High-Fat Diet Fed Mice. *Liver Int.* 35 (2), 550–561. doi:10.1111/liv.12645

Conflict of Interest: The authors declare that the research was conducted in the absence of any commercial or financial relationships that could be construed as a potential conflict of interest.

Publisher's Note: All claims expressed in this article are solely those of the authors and do not necessarily represent those of their affiliated organizations, or those of the publisher, the editors, and the reviewers. Any product that may be evaluated in this article, or claim that may be made by its manufacturer, is not guaranteed or endorsed by the publisher.

frontiers | Frontiers in Pharmacology

ORIGINAL RESEARCH
published: 22 July 2022
doi: 10.3389/fphar.2022.924464

Human Umbilical Cord Blood Mononuclear Cells Ameliorate CCl_4-Induced Acute Liver Injury in Mice *via* Inhibiting Inflammatory Responses and Upregulating Peripheral Interleukin-22

Jinming Zhang[1,2†], *Hengben Zhai*[1,2†], *Pei Yu*[3†], *Dabao Shang*[1,2], *Ruidong Mo*[1,2], *Ziqiang Li*[1,2], *Xiaolin Wang*[1,2], *Jie Lu*[1,2*], *Qing Xie*[1,2*] *and Xiaogang Xiang*[1,2*]

[1]*Department of Infectious Diseases, Ruijin Hospital, Shanghai Jiao Tong University School of Medicine, Shanghai, China,* [2]*Translational Lab of Liver Diseases, Department of Infectious Diseases, Ruijin Hospital, Shanghai Jiao Tong University School of Medicine, Shanghai, China,* [3]*Department of Orthopedics, Ruijin Hospital, Shanghai Jiao Tong University School of Medicine, Shanghai, China*

Background: Human umbilical cord blood mononuclear cells (hUCBMNCs) show therapeutic effects on many inflammatory diseases. The deterioration of acute liver injury is attributed to excessive inflammatory responses triggered by damage-associated molecular patterns (DAMPs) and pathogen-associated molecular patterns (PAMPs). Whether hUCBMNCs treatment is a promising strategy for acute liver injury/failure needs to be investigated.

Methods: Liver injury mice induced by PAMPs, DAMPs, or DAMPs plus PAMPs were developed. DAMPs included CCl_4 (carbon tetrachloride), APAP (acetaminophen), and ConA (Concanavalin A). PAMPs included *Klebsiella pneumoniae* (*K.P.*) and *Salmonella typhimurium* (*S. Typhimurium*). DAMP plus PAMP-induced liver injury was developed by sequential CCl_4 and *K.P.* administration. hUCBMNCs were injected intravenously.

Results: hUCBMNCs significantly prolonged mice survival time in DAMP plus PAMP-induced liver failure but had no benefit in bacteria-infected mice. hUCBMNCs significantly alleviated hepatic necrosis post CCl_4/ConA insult. In CCl_4-induced acute liver injury, peripheral levels of interleukin (IL)-22 were upregulated and liver regeneration was enhanced after treating with hUCBMNCs at 48h. The levels of p62 and LC3B-II, autophagy markers, were also upregulated in the hUCBMNC-treated group.

Conclusion: hUCBMNCs as a kind of cell therapeutic strategy could attenuate acute liver injury in mice, which is executed by enhancing autophagy and regeneration in the liver via inhibiting inflammatory responses and upregulating peripheral IL-22.

Keywords: cell therapy, liver injury, liver inflammation, liver regeneration, IL-22

OPEN ACCESS

Edited by:
Yang Yang,
University of Texas Health Science Center at Houston, United States

Reviewed by:
Yong He,
Shanghai Institute of Materia Medica (CAS), China
Lingzi Hong,
Cleveland Clinic, United States

***Correspondence:**
Jie Lu
jessielu1978@163.com
Qing Xie
xieqingrjh@163.com
Xiaogang Xiang
shine-xxg@163.com

[†]*These authors have contributed equally to this work*

Specialty section:
This article was submitted to Gastrointestinal and Hepatic Pharmacology, a section of the journal Frontiers in Pharmacology

Received: *20 April 2022*
Accepted: *21 June 2022*
Published: *22 July 2022*

Citation:
Zhang J, Zhai H, Yu P, Shang D, Mo R, Li Z, Wang X, Lu J, Xie Q and Xiang X (2022) Human Umbilical Cord Blood Mononuclear Cells Ameliorate CCl_4-Induced Acute Liver Injury in Mice via Inhibiting Inflammatory Responses and Upregulating Peripheral Interleukin-22. Front. Pharmacol. 13:924464. doi: 10.3389/fphar.2022.924464

INTRODUCTION

The incidence of acute liver failure (ALF) ranges from 1.4/10 000 (Escorsell et al., 2007) to 5.5/10 000 (Bower et al., 2007) worldwide. It is impossible for the liver to compensate in fulminant liver failure. The only feasible treatment option is liver transplantation (Chew et al., 2020). Thus, new therapeutic strategies for ALF in the reversible stage need to be explored. Inflammatory response and immune-mediated damage of hepatocytes play fatal roles during the deterioration from acute liver injury (ALI) to ALF (Wu et al., 2010). Necrosis of cells triggers the release of cellular contents with some of the endogenous compounds (alarmins) including heat shock proteins, DNA, RNA, and others, called damage-associated molecular patterns (DAMPs), which are able to activate innate immune cells (Scaffidi et al., 2002; Bianchi, 2007). The milieu of inflammation and necrosis in ALF is presumed to predispose patients to infection due to complement deficiency, and/or impaired function of polymorphonuclear or Kupffer cell (Chung et al., 2012). Bacteria release a set of pathogen-associated molecular patterns (PAMPs) such as lipopolysaccharide (LPS), which would be recognized by the innate and acquired immunity system (Bianchi, 2007). DAMPs/PAMPs activate the immune system and generate excessive inflammatory responses, which subsequently aggravate tissue damage and eventually result in liver failure or multiorgan failure (Mihm, 2018; Arroyo et al., 2020).

Cells as a direct therapeutic strategy open a new era for the remedy of many diseases (Yamanaka, 2020). Human umbilical cord blood mononuclear cells (hUCBMNCs) contain a variety of stem cells and low immunogenic immune cells, such as hematopoietic stem cells, endothelial stem cells, lymphoblasts, small embryonic stem cells, mesenchymal stem cells, lymphocytes and bone marrow cells, and can be isolated from human umbilical cord blood conveniently and easily (Weiss and Troyer, 2006). hUCBMNCs have been reported for the immunomodulatory effects on other inflammation-related diseases, such as renal tubulointerstitial fibrosis (Li et al., 2020), inflammation-induced preterm brain injury (Dalous et al., 2013), and LPS-induced acute kidney injury (Paton et al., 2019). However, whether hUCBMNCs have therapeutic effects on ALI/ALF remains to be elucidated. Thus, the present study aimed to investigate the application value and mechanisms of hUCBMNCs treatment in several DAMPs-/PAMPs-induced acute liver injury mouse models.

MATERIALS AND METHODS

Isolation and Identification of hUCBMNCs

The hUCBMNCs were provided by Shandong Cord Blood Bank (Shandong Qilu stem cell engineering Co., Ltd, Jinan, Shandong, China). Human umbilical cord blood samples were collected from healthy newborns with mothers' consents as described previously (Rubinstein et al., 1995). The blood samples were negative for antibodies against hepatitis B virus, hepatitis C virus, cytomegalovirus, human immunodeficiency virus, and syphilis. hUCBMNCs were isolated from umbilical cord blood by centrifugation on lymphocyte separation medium (Ficoll, d = 1.077 g/ml; Eurobio) (Dalous et al., 2013) and washed twice in Dulbecco's modified eagle medium (DMEM). hUCBMNCs of 5×10^7 cells were frozen in a sterile 5 ml cryovial with 10% dimethylsulfoxide. hUCBMNCs identified by China National Institutes for Food and Drug Control (NIFDC) showed major expression of CD38, CD4, CD5, and CD3 and expressed no less than 1% of CD34 (Feng et al., 2020). Details for the identification of hUCBMNCs are included in supplementary materials (**Supplementary Table S1** and **Supplementary Attachment S1**) and representative flow cytometry plots of typical cells subsets in hUCBMNCs are shown in **Supplementary Figure S1**. hUCBMNCs from the same donor were used in each experiment. This study was approved by the Ethics Committee of Ruijin Hospital, Shanghai Jiao Tong University School of Medicine.

Mouse Experiments

All animal experiments were performed on adult 8-week-old male C57BL/6J mice purchased from Beijing Vital River Laboratory Animal Technology Co., Ltd. Mice were kept in a cage (up to five mice per cage) and maintained in a light (12–12h light-dark cycle) and temperature (24 ± 1°C) controlled room with water and food freely available unless otherwise stated.

For PAMPs-induced liver injury, *Klebsiella pneumoniae* (*K.P.*) (ATCC, 43816, Manassas, United States) (500 CFU/mouse) (Xiang et al., 2020) or *Salmonella typhimurium* (*S. Typhimurium*) (ATCC, 14028s, Manassas, United States) (8×10^3 CFU/mouse) (Ren et al., 2019) was injected intraperitoneally to simulate bacterial infection in mice at appointed time points. For mouse models of DAMPs-induced liver injury, mice were injected intraperitoneally with CCl_4 (1 μl/g, dissolved in olive oil, v/v 1:4) and APAP [350 mg/kg, dissolved in phosphate-buffered solution (PBS)] (Bird et al., 2018). For ConA-induced acute liver injury model, mice were injected intravenously with ConA (12 mg/kg, dissolved in PBS) (He et al., 2021). For DAMPs plus PAMPs-induced liver injury model, CCl_4 (0.4 μl/g, dissolved in olive oil, v/v 1:4) and *K.P.* (500 CFU/mouse) were administrated sequentially (Xiang et al., 2020). IL-22 neutralizing antibody (R&D system, Minnesota, United States) (PBS as carrier) was administrated intravenously 2 h before CCl_4 injection in hUCBMNCs-treated mice (1μg/mouse/time point) (Ji et al., 2017), as well as 20 and 44 h post CCl_4 injection. Mice administrated with PBS served as a control group. All mouse experiments were approved by the *Institutional Animal Care and Use Committee of Ruijin Hospital, Shanghai Jiao Tong University School of Medicine* (**Supplementary Attachment S2**).

Treatments of hUCBMNCs in Mouse Models

hUCBMNCs (8×10^6 cells/ml) suspended in PBS were prepared in advance. In CCl_4 plus *K.P.*-induced liver injury mouse model, CCl_4 and *K.P.* were administrated intraperitoneally at 0 and 24 h, and hUCBMNCs (1×10^6 cells/mouse) were administrated intravenously at 22 h for pre-treatment or 26 h for treatment. hUCBMNCs were also used to treat the bacterial infection-induced liver injury with *K.P.* or *S. Typhimurium*. In CCl_4- or APAP-induced acute liver injury mouse models, mice were

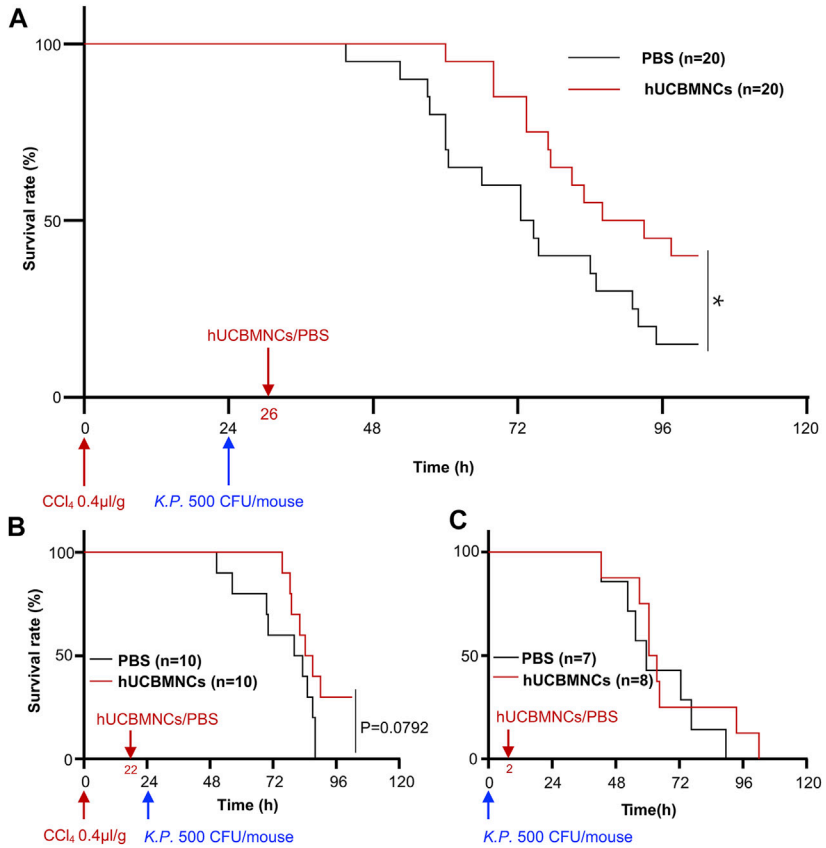

FIGURE 1 | hUCBMNCs treatment prolonged mice survival time in DAMPs plus PAMPs-induced liver injury. **(A)** hUCBMNCs showed a therapeutic effect on CCl_4 plus *Klebsiella pneumoniae* (*K.P.*) -induced liver injury. CCl_4 (0.4 μl/g) plus *K.P.* (500 CFU/mouse) were administrated at 0 and 24h, respectively, to induce acute liver injury, and hUCBMNCs ($n = 20$) or PBS ($n = 20$) was applied at 26h for the observation of therapeutic effects. **(B)** Pretreatment of hUCBMNCs on CCl_4 plus *K.P.*-induced liver injury hardly improved the mice survival. CCl_4 (0.4 μl/g) plus *K.P.* (500 CFU/mouse) was administrated at 0 and 24h, respectively, to develop liver injury model, and hUCBMNCs ($n = 10$) or PBS ($n = 10$) was applied at 22h for the verification of preventative effects. **(C)** hUCBMNCs had no therapeutic effects on *K.P.*-induced liver injury. *K.P.* (500 CFU/mouse) was administrated intraperitoneally at 0h, and hUCBMNCs ($n = 7$) or PBS ($n = 8$) was applied at 2h post infection. *, $p < 0.05$.

injected intravenously with hUCBMNCs (1×10^6 cells/mouse) or PBS (as a control treatment) 2 hours (2 h) post insult. Blood and liver tissues were collected at 24, 48, and 72 h post CCl_4 insult and mice were injected intraperitoneally with BrdU (Bromodeoxyuridine/5-bromo-2′-deoxyuridine) 2 h before they were sacrificed. In APAP model, blood and liver tissues were collected at 6, 12, 24, and 48 h post APAP injection. In ConA-induced acute liver injury model, mice were injected intravenously with hUCBMNCs (1×10^6 cells/mouse) or PBS (as control) 1 h post ConA injection and were sacrificed for the collection of blood and liver tissue at 4, 6, 9 h post insult. Intact right lobe of the liver was fixed in 10% formalin overnight for the paraffin section (Xiang et al., 2012) and the rest of liver tissue was frozen in −80°C. Sera diluted 10 times were sent to the *Department of Laboratory Medicine of Ruijin hospital, Shanghai Jiao Tong University School of Medicine* for the test of alanine transaminase (ALT) or aspartate transaminase (AST).

The following methods are described in **Supplementary Material S1**: Western blotting; Real-time quantitative polymerase chain reaction (RT-qPCR); Hematoxylin & eosin (H&E) staining; BrdU staining; Determination of mouse serum interleukin 22 (IL-22); Determination of malondialdehyde (MDA) in mouse liver tissue; Determination of multi-inflammatory cytokines in mouse serum.

Statistical Analysis

Mean ± standard error (SEM) was used to describe the distribution of the data. Means for continuous variables were compared using paired or unpaired Student t-test between the two groups when the data were normally distributed. A *p*-value less than 0.05 was considered statistically significant.

RESULTS

hUCBMNCs Treatment Prolonged Survival Time in the DAMP Plus PAMP-Induced Liver Injury Mouse Model

Intravenous infusion of hUCBMNCs was applied 2 h before or after *K.P.* injection in CCl_4 plus *K.P.*-induced acute liver injury mice. In the group of 2 h after *K.P.* injection, the application of

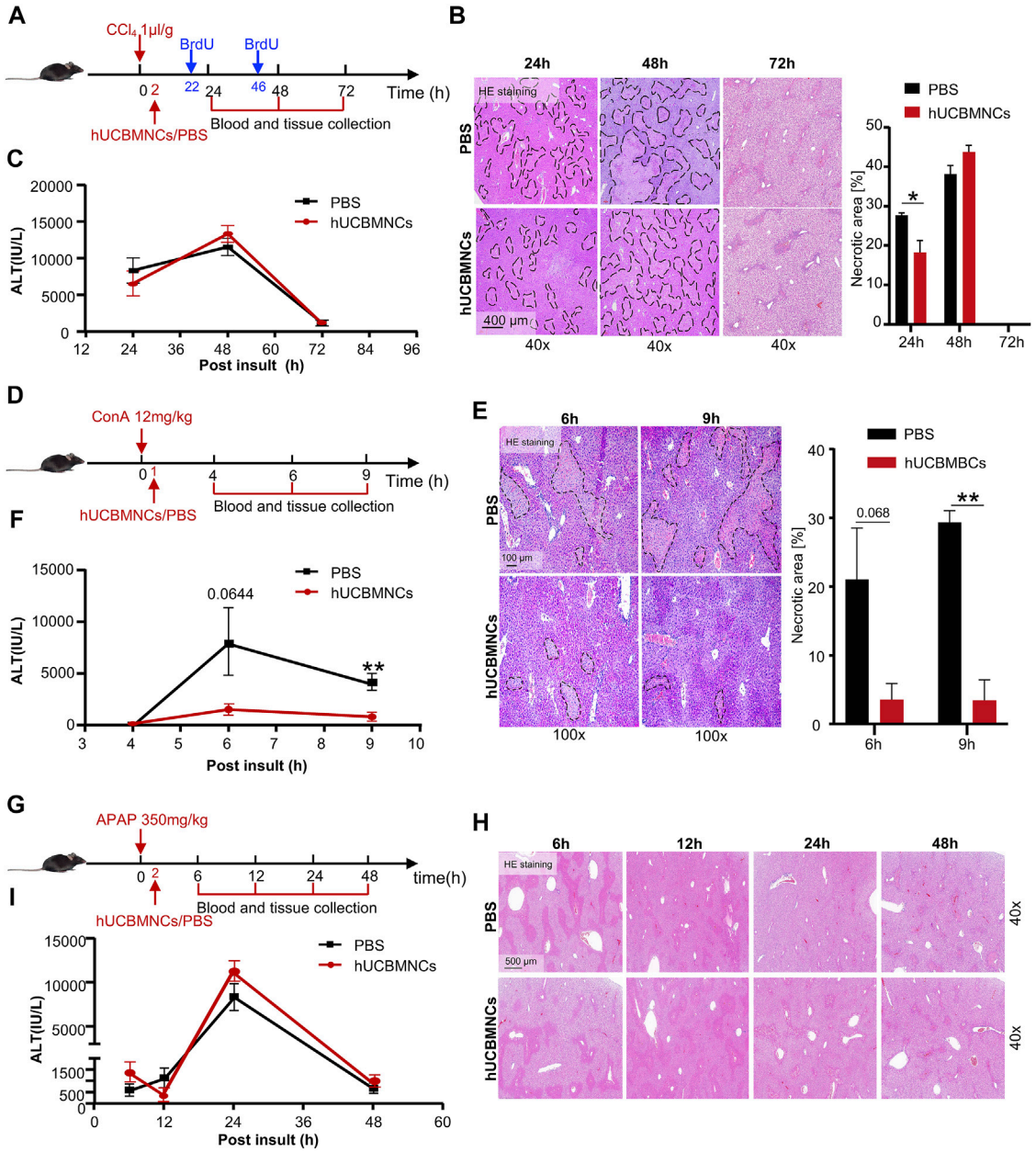

FIGURE 2 | hUCBMNCs treatment improved CCl_4/ConA-induced liver injury but did not improve APAP-induced liver injury. **(A–C)** hUCBMNCs treatment alleviated liver necrosis in CCl_4-induced liver injury (PBS, n = 5/time point; hUCBMNCs, n = 5/time point). **(A)** Schematic experiment timeline of hUCBMNCs in CCl_4-induced acute liver injury. **(B)** H&E staining (40×) and the percentage of necrotic areas of mice liver at 24, 48, and 72 h post CCl_4 injection. Necrotic areas are circled with black dashed lines. **(C)** Serum ALT levels of mice at 24, 48, and 72 h post CCl_4 insult. The bars represent mean ± SEM. **(D–F)** hUCBMNCs treatment alleviated liver necrosis in ConA-induced liver injury (PBS, n = 4/time point; hUCBMNCs, n = 4/time point). **(D)** Schematic experiment timeline of hUCBMNCs in ConA-induced acute liver injury. **(E)** H&E staining (100×) and the percentage of necrotic area of mice liver at 6 h, 9 h post ConA injection. Necrotic areas were circled with black dashed lines. **(F)** Serum ALT levels of mice at 4, 6, and 9 h post ConA injection. **(G–I)** hUCBMNCs treatment did not alleviate liver necrosis in APAP-induced liver injury (PBS, n = 4/time point; hUCBMNCs, n = 4/time point). **(G)** Schematic experiment timeline of hUCBMNCs in APAP-induced liver injury. **(H)** H&E staining (40×) of mice liver at 6, 12, 24, 48 h post APAP injection. **(I)** Serum ALT levels of mice at 6, 12, 24, and 48 h post APAP injection.

hUCBMNCs showed an improved survival rate ($p < 0.05$) compared with the PBS group (**Figure 1A**). However, in the group of 2 h before *K.P.* injection, the survival rate showed no significant difference between the two groups (**Figure 1B**). To observe the exact function of hUCBMNCs in DAMP- or PAMP-induced inflammatory processes, we applied hUCBMNCs or PBS to PAMP-induced liver injury by using *K.P.* infection (**Figure 1C**) and found that there was no significant difference in survival rate between the two groups. hUCBMNCs treatment was also used in *S. Typhimurium* infection mouse model, and no significant

difference was found as well (**Supplementary Figure S2**). These results indicated that hUCBMNCs might improve the damage of hepatocytes in DAMP-induced liver injury.

hUCBMNCs Improved DAMP-Induced Acute Liver Injury in CCl_4/ConA-Treated Mice

To verify the hypothesis that hUCBMNCs played a protective role in DAMP-induced liver injury, three kinds of acute liver injury mouse models induced by DAMPs were developed and hUCBMNCs were infused intravenously (**Figures 2A,D,G**). hUCBMNCs dramatically improved liver damages in CCl_4-induced liver injury mouse model (**Figure 2B**) and ConA-induced liver injury mouse model (**Figures 2E,F**). However, hUCBMNCs did not alleviate liver damage in APAP-induced liver injury mouse model (**Figures 2H,I**). For CCl_4-induced liver injury, although ALT levels showed no significant changes at the appointed time points, there was a significant difference in necrotic areas of liver H&E staining images at 24 h between the two groups post CCl_4 injection (**Figure 2B**). H&E staining demonstrated that necrotic areas and degrees of necrosis were both ameliorated in the hUCBMNCs-treated group compared to the control group at 24h post CCl_4 insult (**Figure 2B**). ALT levels, as a regular marker for assessing the severity of liver damage, were not significantly improved at 24, 48, and 72h post CCl_4 insult (**Figure 2C**).

In ConA-induced acute liver injury, hUCBMNCs treatment significantly downregulated the necrotic areas [%] (**Figure 2E**) and ALT levels at 9h post insult ($p < 0.01$) were decreased correspondingly (**Figure 2F**). However, hUCBMNCs treatment did not improve APAP-induced acute liver injury significantly. The levels of liver necrosis areas (**Figure 2H**) and serum ALT (**Figure 2I**) in the APAP model were not improved after the treatment of hUCBMNCs, as well as mRNA levels of inflammatory cytokines (**Supplementary Figure S3A**). In addition, the phosphorylation levels of regeneration-associated phosphorylation of STAT3 (p-STAT3) protein were not enhanced in the liver but phosphorylation of ERK (p-ERK) was activated at 24h in the hUCBMNCs group after APAP insult (**Supplementary Figure S3B**).

hUCBMNCs Alleviated Liver Inflammation and Oxidative Stress in CCl_4/ConA-Induced Acute Liver Injury

Since inflammatory response and oxidative stress were two main pathological processes contributing to the deterioration of liver injury (Reyes-Gordillo et al., 2017), we assumed that hUCBMNCs treatment would attenuate the levels of inflammation and oxidative stress in both CCl_4- and ConA-induced liver injury.

To confirm this hypothesis, hepatic mRNA levels of inflammatory markers were measured by RT-qPCR. hUCBMNCs treatment significantly suppressed mRNA expression of pro-inflammatory cytokines of *Il6*, *Tnfα*, *Ifng*, *Il17a* except for *Il1b* in CCl_4-induced liver injury at 48 h (**Figure 3A**). Moreover, the expression of *Cxcl1* and *Cxcr1* markedly declined after hUCBMNCs treatment at 48h (**Figure 3A**), but the expression levels of inflammatory markers were not decreased at 24 h (**Supplementary Figure S4**). *F4/80*, a mouse-specific macrophage marker, was also downregulated at the mRNA level compared with the control group at 48 h. Interestingly, mRNA levels of anti-inflammatory cytokines IL-4 and IL-10 were also decreased after the treatment of hUCBMNCs. Although hUCBMNCs treatment did not influence mRNA expression of inflammatory cytokines in ConA-induced liver injury (**Supplementary Figure S5**), protein levels of inflammatory cytokines such as TNF-α, IFN-γ, IL-17A, IL-1α, MCP-1, IL-12p70, and IL-22 were downregulated in our experiment (**Figure 3B**).

Subsequently, we determined the levels of oxidative stress in mice liver. The expression of MDA in liver homogenate supernatants was measured by MDA Assay Kit, and the levels of MDA were significantly decreased in the hUCBMNCs treatment group at 48h post CCl_4 insult ($p < 0.01$) (**Figure 3C**). We further detected the expression of ROS-related oxidant enzymes and found that mRNA expression levels of NADPH oxidase Duox2 and Nox3 were decreased at 48h post CCl_4 insult in the hUCBMNCs treatment group (**Figure 3D**).

hUCBMNCs Played a Protective Role Against CCl_4-Induced Acute Liver Injury via Upregulating IL-22

Improved necrosis of hepatocytes was demonstrated in hUCBMNCs-treated mice with CCl_4-induced liver injury and ConA-induced liver injury. Whether liver regeneration was enhanced in these mice required further confirmation.

In CCl_4-induced mouse liver injury model, BrdU staining was performed on liver slices in mice. The percentage of BrdU-positive (BrdU+) hepatocytes was counted per ×200 field. Notably, hUCBMNCs treatment enhanced liver regeneration at 48 h post CCl_4 injection. BrdU + hepatocytes were increased in the hUCBMNCs group compared to the control group at 48 h ($p < 0.01$) (**Figures 4A,B**). Subsequently, Western blotting results showed that the phosphorylation of STAT3 (p-STAT3) was strongly activated in the hUCBMNCs group at 48 h ($p < 0.05$) (**Figure 4E**), but the expression levels of phosphorylation of STAT1 (p-STAT1) at 24 and 48 h were not significantly different between the PBS treatment group and the hUCBMNCs treatment group (**Supplementary Figure S6**). Marginal activation of p-ERK protein in the hUCBMNCs group was also found compared with the control group at 48 h (**Figure 4E**). In ConA-induced mouse liver injury model, there were no significant differences of p-STAT1 and p-STAT3 at 6 and 9 h between the PBS treatment group and the hUCBMNCs treatment group (**Supplementary Figure S7**). IL-6 and IL-22 are both described as pro-proliferative cytokines in liver regeneration and the two cytokines signal through activation of STAT3 pathway (Schmidt-Arras and Rose-John, 2016; Xiang et al., 2020). The mRNA levels of IL-6 in liver were significantly decreased under the treatment of hUCBMNCs (**Figure 3A**). Thus, serum IL-22 levels were determined by using ELISA. Compared to PBS group, serum IL-22 levels were elevated under the treatment of hUCBMNCs at 48h. Usually, in normal mice, serum IL-22 is

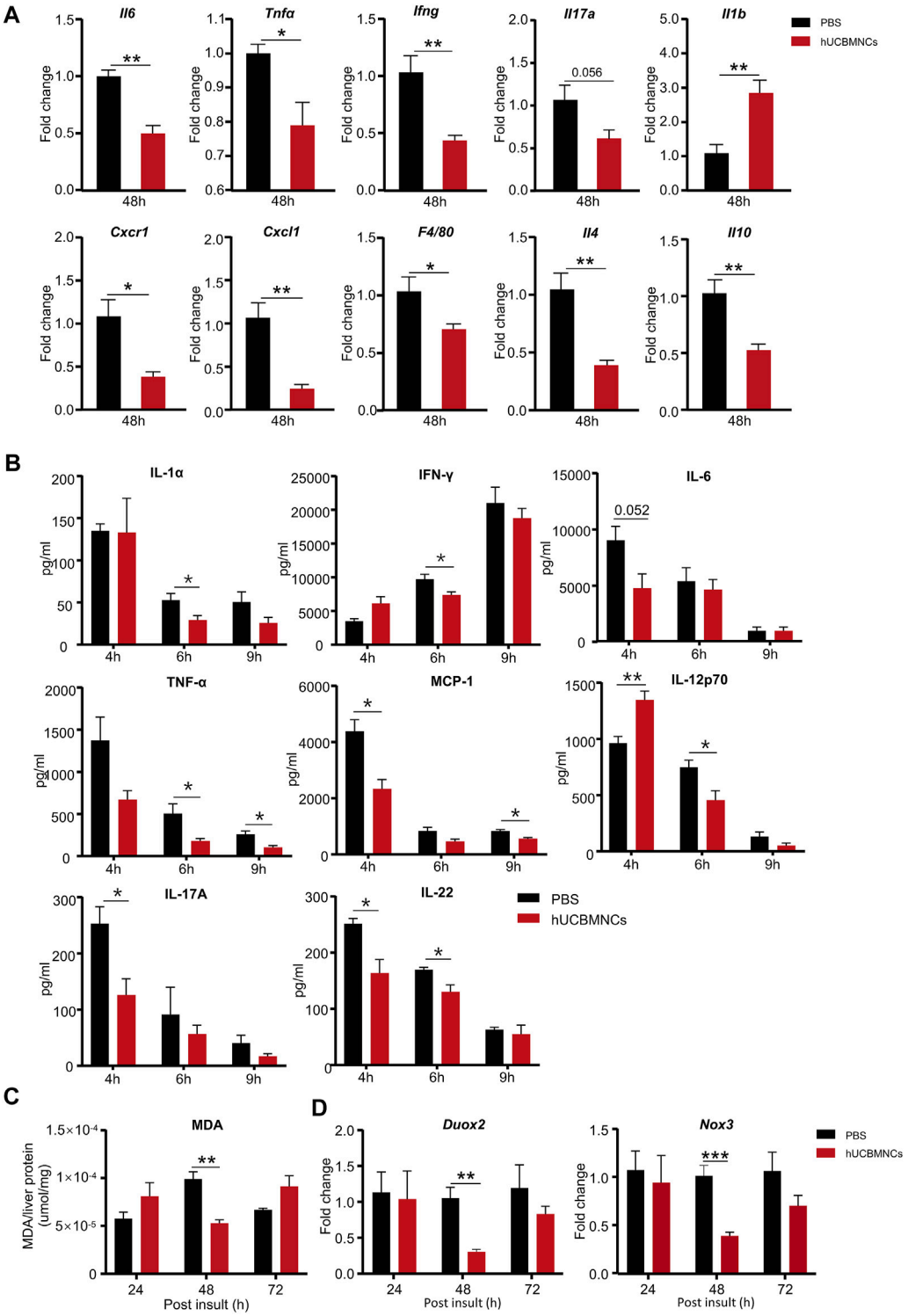

FIGURE 3 | hUCBMNCs treatment suppressed inflammation and oxidative stress in mice liver in CCl_4-induced acute liver injury and ConA-induced liver injury. **(A)** mRNA levels of liver representative inflammatory markers in hUCBMNCs and control groups at 48h post CCl_4 injection (n = 5/time point, experiments were repeated for 3 times). **(B)** Protein levels of serum inflammatory cytokines in ConA-induced liver injury mouse model at 4, 6, and 9h (n = 5/time point). **(C)** Malondialdehyde (MDA) expression in liver tissue at 24, 48,and 72h post CCl_4 insult (n = 5/time point, experiments were repeated for 3 times). **(D)** mRNA expression levels of *Duox2* and *Nox3* in liver at 24, 48, and 72h post CCl_4 injection (n = 5/time point, experiments were repeated for 3 times). The bars represent mean ± SEM.

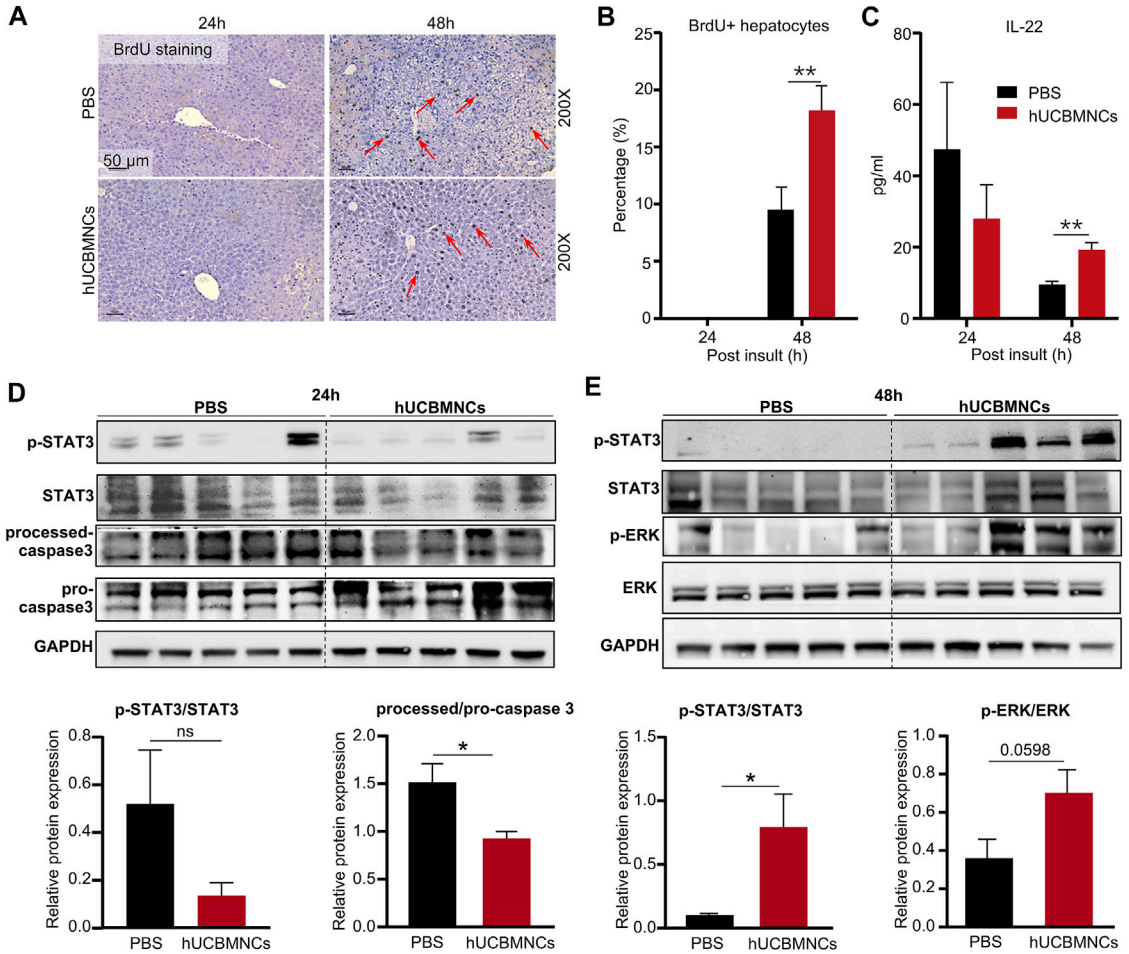

FIGURE 4 | hUCBMNCs treatment promoted liver regeneration at 48h post CCl_4 injection via IL-22. **(A)** BrdU staining of liver slices at 24 h, 48 h post CCl_4 injection (PBS, n = 5/time point; hUCBMNCs, n = 5/time point). **(B)** Percentage of BrdU positive hepatocytes. **(C)** Serum IL-22 levels in the hUCBMNCs group (n = 4/time point) and the control group (n = 4/time point). **(D,E)** Western blotting results of proteins and relative protein expression in liver regeneration and apoptosis pathways, including p-STAT3, STAT3, processed-caspase 3, pro-caspase 3, p-ERK, ERK, and GAPDH at 24 h **(D)** and 48 h **(E)** post CCl_4 injection (n = 5/time point, experiments were repeated for 3 times). The bars represent mean ± SEM.

maintained at a low level (~10 pg/ml) (Xu et al., 2014). After CCl_4 injury, serum IL-22 levels were elevated both in PBS (~40 pg/ml) and hUCBMNCs (~30 pg/ml) groups at 24h. However, IL-22 levels declined to baseline (~10 pg/ml) at 48h in the PBS group (**Figure 4C**). Interestingly, in the hUCBMNCs group, serum IL-22 levels were upregulated and maintained around 20 pg/ml (p < 0.001) at 48h (**Figure 4C**). Activation of caspase-3 protein was attenuated at 24 h under hUCBMNCs treatment (**Figure 4D**). But there was no significant difference in hepatocyte apoptosis at 48 and 72 h between the two groups via TUNEL staining (**Supplementary Figure S8**).

hUCBMNCs Treatment Enhanced Autophagy of Hepatocyte and Promoted Liver Repair

Autophagy is widely involved in many pathophysiological courses, especially in oxidative stress and inflammation (You et al., 2015). We have previously found that IL-22 could protect drug-induced liver injury by enhancing autophagy (Lai et al., 2015; Mo et al., 2018). Therefore, we further explored whether enhanced autophagy would contribute to the protective effects of hUCBMNCs against CCl_4-induced liver injury.

A series of autophagy-related genes (ATG) regulate and participate in the process of autophagy. To confirm the involvement of autophagy in hUCBMNCs treatment in CCl_4-induced liver injury, expression of ATG in the liver was detected by RT-qPCR. mRNA expression levels of *Binp3*, *Pik3c3*, *Ctsb*, *Becn1*, *Bnip3l* were significantly elevated at 24 h in the hUCBMNCs group compared with the control group (p < 0.01) (**Figure 5A**). Additionally, hUCBMNCs treatment induced enhanced expression of hypoxia-inducible factor 1α (Hif1α) (p < 0.05) (**Figure 5B**), which could interact with BINP3 to promote autophagy and exert beneficial effects on liver repair after damage (Zhang et al., 2019). Further assessment of autophagy markers was performed by Western

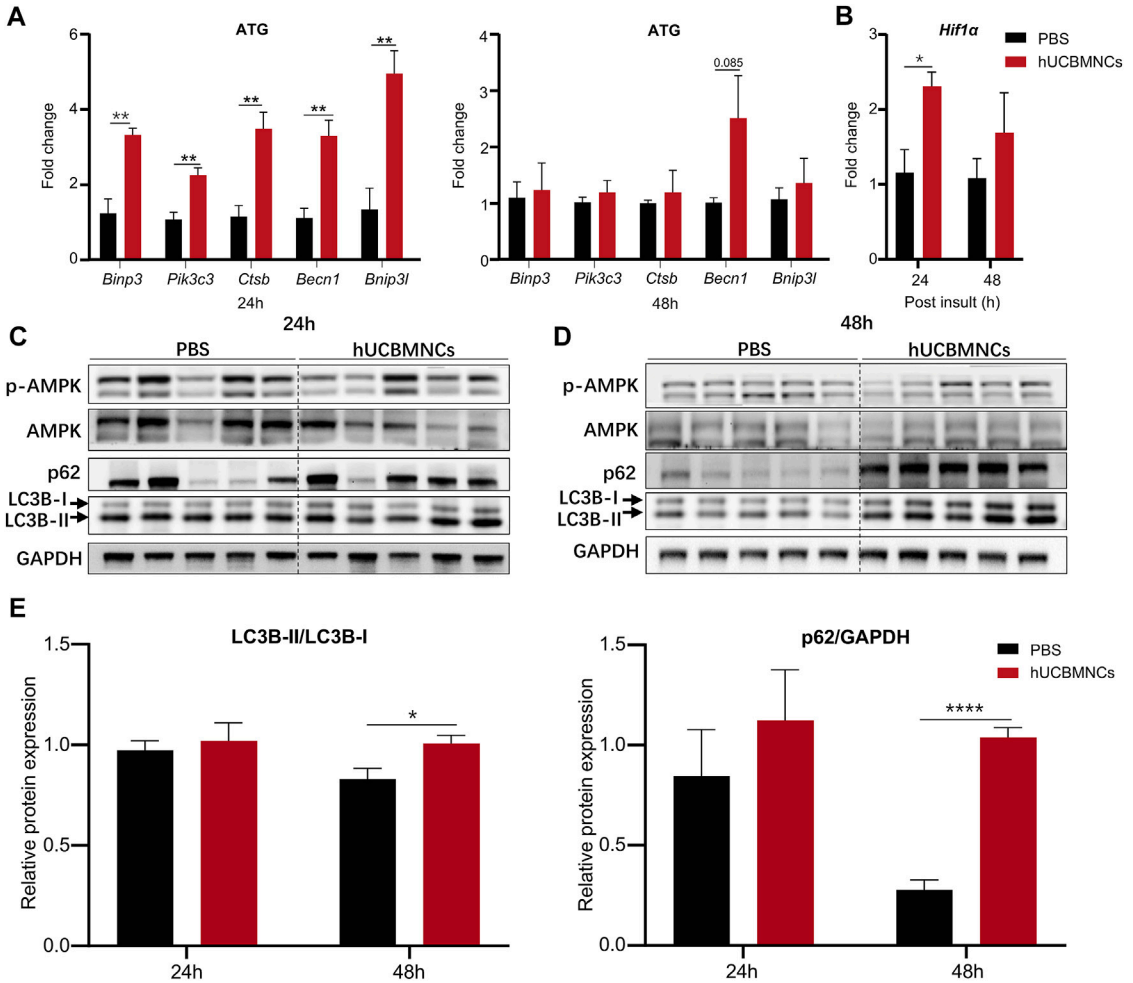

FIGURE 5 | hUCBMNCs treatment enhanced hepatocellular autophagy at mRNA and protein levels. **(A)** mRNA levels of autophagy-related genes (ATG) in liver at 24 and 48h post CCl_4 injection (n = 5/time point, experiments were repeated for 3 times). **(B)** Liver mRNA level of *hypoxia inducible factor 1α* (*Hif1α*) (n = 5/time point, experiments were repeated for 3 times). **(C,D)** Western blotting results of proteins in autophagy pathway in the liver, including p-AMPK, AMPK, p62, LC3B-I and LC3B-II at 24h **(C)** and 48h **(D)** post CCl_4 injection (n = 5/time point, experiments were repeated for 3 times). **(E)** Relative protein expression of LC3B-II/LC3B-I, p62/GAPDH at 24 and 48 h post CCl_4 insult (n = 5/time point, experiments were repeated for 3 times). The bars represent mean ± SEM.

blotting (**Figures 5C,D**), and expression levels of LC3B-II and p62 were significantly increased under hUCBMNCs treatment at 48 h (**Figure 5E**).

Blocking IL-22 Could Partly Impair the Therapeutic Effects of hUCBMNCs

To confirm whether the upregulated peripheral IL-22 would contribute to the promoted liver regeneration and enhanced autophagy after hUCBMNCs treatment, we blocked peripheral IL-22 by administrating neutralizing IL-22 antibody synchronously. Liver H&E staining suggested that IL-22 neutralizing antibody impaired the therapeutic effects of hUCBMNCs (**Figure 6A**).

Serum ALT and AST levels were higher in the anti-IL-22 treatment group than that in the control group at 48h (**Figure 6B**). In addition, the expression levels of regeneration-related protein p-STAT3 were declined at 48h in anti-IL-22 mice (**Figure 6C**). The expression levels of autophagy-related protein p62 were also downregulated at both 24 and 48 hours after treating with anti-IL-22 antibody (**Figure 6C**). There were no significant differences of LC3B-II/LC3B-I (**Figure 6C**).

DISCUSSION

To our knowledge, the present study is the first investigation to utilize hUCBMNCs to treat acute liver injury in mouse models induced by DAMPs or PAMPs. The hepato-protective role of hUCBMNCs was surprisingly found in CCl_4/ConA-induced acute liver injury model. We have provided the first evidence that hUCBMNCs could alleviate DAMPs-induced liver injury including CCl_4-/ConA- except APAP-induced liver injury. The hepatoprotective effects of hUCBMNCs were demonstrated as

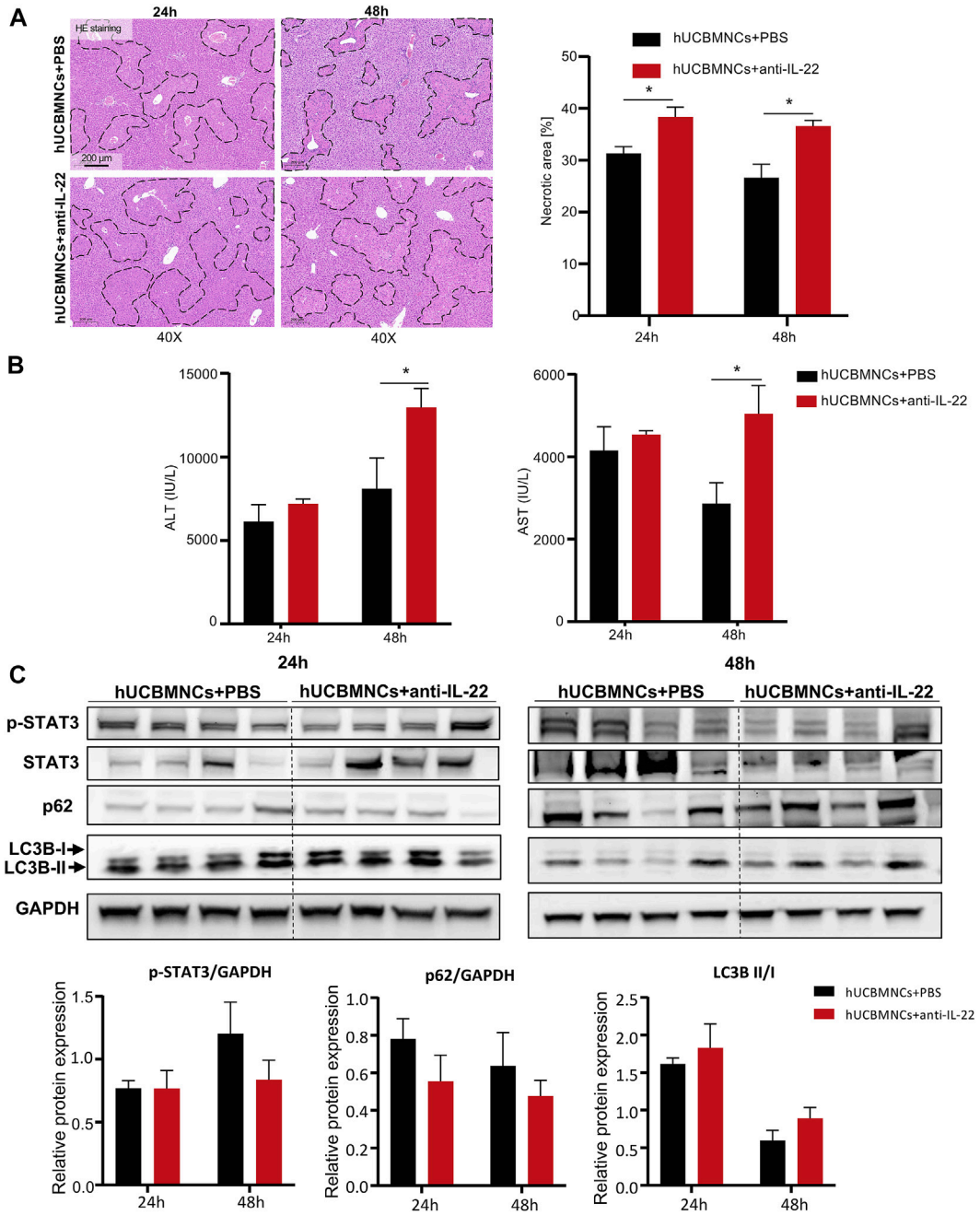

FIGURE 6 | Blocking IL-22 impaired the therapeutic effects of hUCBMNCs. **(A)**. H&E staining (×40) and necrotic areas percentage of mice liver at 24 h, 48 h post CCl_4 injection in the anti-IL-22 group and the control group (4 mice each group). **(B)** Serum ALT and AST levels of mice at 24 h, 48 h post CCl_4 injection in the anti-IL-22 group and the control group (4 mice each group). **(C)** Expression of p-STAT3, p62, LC3B, and GAPDH of mice liver at 24 h, 48 h post CCl_4 injection in the anti-IL-22 group and the control group (4 mice each group, experiments were repeated for 3 times). The bars represent mean ± SEM.

intensified pro-regeneration and enhanced autophagy in the liver, which turned out to be partly via upregulation of peripheral IL-22 level (**Figure 7**).

Cell therapies provide unprecedented opportunities for intractable diseases and injury (Yamanaka, 2020). The combined disciplines of cell and gene therapy and tissue engineering, broadly known as regenerative medicine, have the potential to revolutionize the treatment of diseases (De Luca et al., 2019). Mesenchymal stem cells (MSCs) have been the main subject of clinical trials for the functions of immunoregulation (Tasso and Pennesi, 2009), differentiation potential (Musina et al., 2006), pro-regeneration (Jackson et al., 2010), and anti-infective property (Shaw et al., 2021). Both hUCBMNCs and MSCs can be isolated from cord blood. hUCBMNCs have already

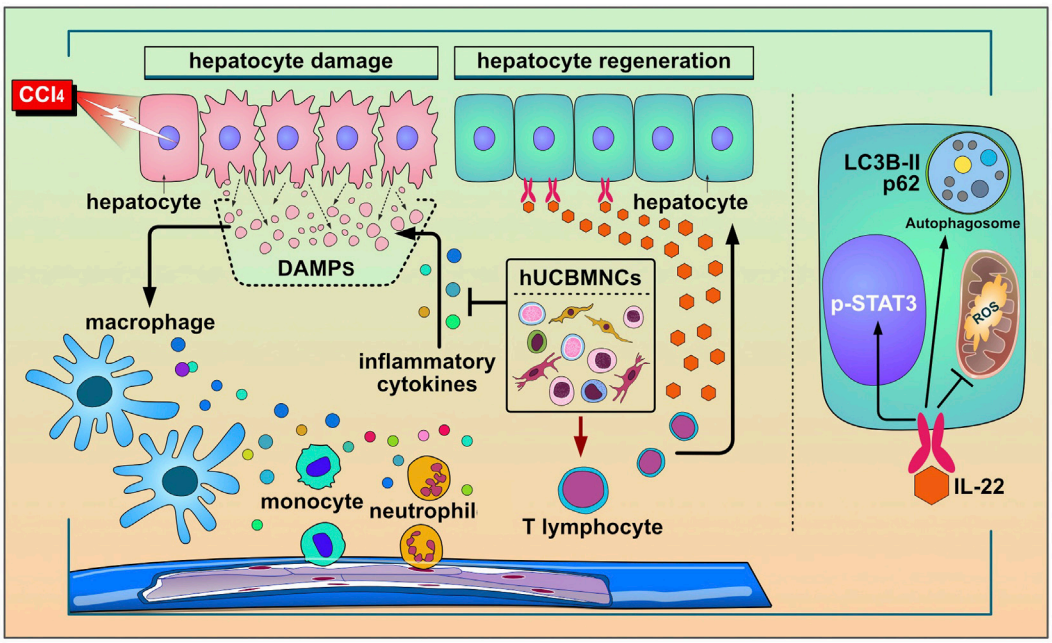

FIGURE 7 | The working model for the protective roles of hUCBMNCs in acute liver injury/failure. hUCBMNCs treatment as a kind of cell therapeutic strategy could attenuate CCl_4-induced acute liver injury/failure in mice with hepatoprotective role, which is executed by enhancing autophagy and regeneration in the liver via inhibiting inflammatory responses and upregulating peripheral IL-22.

presented with immunoregulation function in a variety of diseases (Alvarez-Mercado et al., 2008; Paton et al., 2019; Feng et al., 2020; Li et al., 2020). In the present study, hUCBMNCs treatment was revealed to play a protective role by improving survival rate in DAMPs plus PAMPs-induced liver injury mice. However, in PAMPs-induced liver injury mice, hUCBMNCs showed no protective effects on mouse models with bacterial infection including *K.P.* or *S. Typhimurium*, which indicated that hUCBMNCs treatment might have beneficial effects on DAMP-induced liver injury. Cell therapy as an emerging therapeutic strategy has been applied for many intractable liver diseases, such as acute liver injury, acute-on-chronic liver failure (Dwyer et al., 2021), and diabetic hepatocyte damage in mice (Nagaishi et al., 2014). It is reported that cells could successfully reach the liver after administrating intravenously in mice (Starkey Lewis et al., 2020). Several studies have shown that labeled cells can migrate to the injured liver by APAP and alleviate liver injury (Resaz et al., 2011; Nagaishi et al., 2014; Starkey Lewis et al., 2020). For hUCBMNCs treatment, we have no evidence showing that these cells would surely migrate to the liver in the present study, and we will perform this in the further study with cell labeling and tracking techniques.

CCl_4- or APAP-induced acute liver injury mouse model is the representative animal model of hepatotoxin-mediated acute liver injury (Forbes and Newsome, 2016). The core pathological processes in both models are oxidative stress and inflammatory response (Reyes-Gordillo et al., 2017). In our study, hUCBMNCs treatment exerted hepatoprotective effects on CCl_4-induced acute liver injury mice but could hardly improve the necrosis in APAP-induced mice, which is consistent with the effects of MSCs on APAP mice model (Ryu et al., 2014). Nonetheless, hUCBMNCs treatment indeed reduced the expression of p-ERK activation in the pathogenesis of APAP-induced liver damage. This indicated that hUCBMNCs could alleviate APAP-induced liver injury at the protein level. For ALT levels, though there were no statistically significant differences between the hUCBMNCs treatment group and the control group in CCl_4- or APAP-induced liver injury mouse model, the elevated ALT levels could demonstrate the liver damage in the two models. In CCl_4-induced liver injury model, ALT levels were elevated at 24 h and reached a peak level at 48 h, which indicated that liver damage already occurred at 24 h (Liu et al., 2015). However, in APAP-induced liver injury, ALT levels were elevated at 6h in our experiment. In fact, it was reported that serum ALT levels were elevated at 0.5 h and reached the peak at 24h in APAP-induced liver injury (Yi et al., 2021). Therefore, hepatic necrosis can be found at 6 h in APAP-induced liver injury. However, calculations based on the total amount of ALT in the damaged liver indicate that the increase in the serum ALT activity cannot be explained simply by leakage from necrotic cells (Hauss and Leppelmann, 1958; Freidman and Lapan, 1964). Poor correlation between the degree of necrosis and the magnitude of serum ALT levels has often been reported (Rees and Sinha, 1960). Thus, hepatic histopathologic changes are always needed as the gold standard to confirm liver necrosis (Khalifa and Rockey, 2020). In liver H&E staining, the necrotic areas of mice liver at 24h post CCl_4 injection were significantly decreased in the hUCBMNCs treatment group, though there was no significant difference of ALT levels between the two groups.

ConA-induced T-cell-mediated liver injury is a well-established model for investigating autoimmune or viral fulminant hepatitis with acute immune response playing a pivotal role in mediating liver damage (Wang et al., 2012). Immunosuppression therapy has an obvious effect on autoimmune hepatitis (Mieli-Vergani et al., 2018). In the present study, hUCBMNCs treatment demonstrated a dramatic attenuation of ConA-induced liver injury. Unlike hUCBMNCs in CCl_4-induced liver injury, improved liver function and necrosis were both shown in ConA-induced liver injury. A previous study demonstrated that glucocorticoids, as immunosuppressants, have opposing effects on CCl_4-induced liver injury and ConA-induced liver injury (Kwon et al., 2014). hUCBMNCs, reported for the immunomodulatory functions, showed hepatoprotective effects both on CCl_4- and ConA-induced acute liver injury in the present study. Therefore, hUCBMNCs treatment would provide an alternative therapeutic strategy in clinical practice. The underlying mechanism of hUCBMNCs on ConA-induced liver injury needs to be further explored.

Our study showed that hUCBMNCs alleviated the levels of inflammatory responses and oxidative stress in the liver at 48 h post-CCl_4 injection. The process of oxidative stress induces cells death involved a wide range of DAMPs (Jaeschke, 2011; Yang and Tonnesseen, 2019), and then activates innate immune cells to release abundant of inflammatory cytokines. The aggravation of inflammatory response would contribute to systemic inflammatory response syndrome (SIRS), and eventually lead to multiple organ failures (Rolando et al., 2000). Our study revealed that hUCBMNCs treatment alleviated both inflammatory responses (*Il6*, *Tnfa*, *Ifng*, *Il17a*, *Il1b*, *Cxcl1*, *Cxcr1*, *F4/80*) and oxidative stress in CCl_4-induced liver injury. Further experiments uncovered that NADPH oxidase *Duox2* and *Nox3*, leading to accumulation of peroxides (Babior, 2004), were also downregulated at mRNA levels at 48h in the hUCBMNCs group. These results demonstrated the promising and inspiring therapeutic values for acute liver injury of hUCBMNCs treatment.

Besides, it was exciting that hUCBMNCs enhanced the phosphorylation levels of STAT3 protein, which would promote liver regeneration in CCl_4-induced acute liver injury (Gao, 2005). And BrdU staining also confirmed the effect of pro-regeneration in hUCBMNCs treated mice at 48 h. IL-6 is a critical pro-regenerative factor and acute-phase inducer. IL-6 activates downstream signal through p-STAT3 in the liver, which confers resistance to liver damage (Schmidt-Arras and Rose-John, 2016). However, it was reported that mRNA and protein levels of IL-6 were both inhibited after treatment of hUCBMNCs (Rosenkranz et al., 2012; Yu et al., 2021), which are parallel to our study. The inhibition of IL-6 expression by hUCBMNCs in the early stage of liver injury would theoretically lead to the inhibition of liver regeneration which might be harmful for liver repair. However, the elevated levels of serum IL-22 could partly illustrate the activation of p-STAT3 in the liver. In addition, the attenuated phosphorylation levels of STAT3 (p-STAT3) after blocking peripheral IL-22 could partly demonstrate the pro-regenerative effect of hUCBMNCs. IL-22, a member of the IL-10 family, is mainly produced by innate lymphoid cells, Th17 cells, and Th22 cells (Radaeva et al., 2004; Xiang et al., 2012; Dudakov et al., 2015; Gao and Xiang, 2019). The function of IL-22 is mainly mediated via the activation of the Jak1/Tyk2-STAT3 pathway by binding to the heterodimeric receptors of IL-22R1 and IL-10R2 (Kong et al., 2013). IL-22 was mainly reported for its robust effects of pro-regenerative and hepatoprotective roles (Pan et al., 2004; Radaeva et al., 2004). Interestingly, compared to PBS treatment, hUCBMNCs treatment upregulated serum IL-22 in CCl_4-induced liver injury mouse model, but downregulated serum IL-22 in ConA-induced liver injury mouse model. Considering that serum IL-22 was reduced to ~10 pg/ml in the PBS treatment group, mildly elevated serum IL-22 in CCl_4-induced liver injury mice might possibly be secreted by hUCBMNCs. It was reported that IL-22 was mainly produced by lymphoid cells (Dudakov et al., 2015). Our flow cytometry results of the constituents of hUCBMNCs manifested that there were activated T cells in hUCBMNCs, including NK cells and $CD4^+$ T cells. These cells could secret IL-22, which would contribute to the increased serum level of IL-22 and the promoted liver regeneration at 48 h (Xiang et al., 2020).

Autophagy is a crucial process for maintaining cellular homeostasis (Dunlop et al., 2014), and many genes are involved in autophagy regulation. We further explored the expression of autophagy-related genes (ATG) in mouse liver. The expression levels of *Binp3*, *Pik3c3*, *Ctsb*, *Becn1*, and *Bnip3l* were significantly elevated under the treatment of hUCBMNCs. Among these targets, BECN1 and PIK3C3 are involved in the initiation of autophagy (Feng et al., 2014). BECN1 is reported as a direct transcriptional target of STAT3, and the phosphorylation of STAT3 after IL-6 administration could inhibit BECN1 expression at mRNA and protein levels (Miao et al., 2014). But in the present study, hUCBMNCs treatment promoted the phosphorylation of STAT3 at 48 h and did not suppress mRNA expression of BECN1. Further investigation is still needed. BINP3 and BINP3L proteins are crucial for hypoxia-induced autophagy (Bellot et al., 2009). Elevated HIF-1α has a protective effect on hepatocytes in liver injury (Khan et al., 2017). hUCBMNCs treatment promoted the expression of HIF-1α. BNIP3, a HIF-1α interacting protein, which was known to play a fundamental role in response to hypoxia (Zhang et al., 2019), was also increased at the mRNA level after hUCBMNCs treatment. LC3B-II protein, the cleaved and lapidated form of autophagy protein LC3B, is a widely known marker of autophagy (Dikic and Elazar, 2018). In our study, the expression of LC3B-II and p62 was significantly enhanced. These elevated expression levels of autophagy-related genes and autophagy proteins strongly suggested that autophagy played a role in the hepatoprotective effects after hUCBMNCs treatment.

In the present study, hUCBMNCs showed various effects on CCl_4-induced liver injury. In our opinion, hUCBMNCs treatment might alleviate CCl_4-induced liver injury through the elevation of peripheral IL-22 (**Figure 7**). With low immunogenicity (Kang et al., 2020), hUCBMNCs are more convenient to obtain from

cord blood compared to MSCs, and the functions of hUCBMNCs with anti-inflammation, pro-regeneration and enhancement of autophagy in CCl_4-induced hepatotoxin-mediated liver injury highlight that hUCBMNCs could be an alternative optimal cell therapy strategy for patients with liver injury or liver failure.

DATA AVAILABILITY STATEMENT

The raw data supporting the conclusions of this article will be made available by the authors, without undue reservation.

ETHICS STATEMENT

The studies involving human participants were reviewed and approved by the Ethics Committee of Ruijin Hospital, Shanghai Jiao Tong University School of Medicine. The patients/participants provided their written informed consent to participate in this study. The animal study was reviewed and approved by the Institutional Animal Care and Use Committee of Ruijin Hospital, Shanghai Jiao Tong University School of Medicine. Written informed consent was obtained from the individual(s) for the publication of any potentially identifiable images or data included in this article.

AUTHOR CONTRIBUTIONS

Conceptualization: JL, QX, and XX; data curation: JZ, HZ, and PY; investigation: JZ, HZ, and PY; methodology: JZ; supervision: XX; writing—original draft: JZ and XX; and writing—review and editing: DS, RM, ZL, XW, and JL.

FUNDING

This research was supported by the National Natural Science Foundation of China (No. 82170619, 81970544, 82070604, 81770587, 81770578, and 81900527), the Three-Year Public Health Action Plan (2020–2022) of Shanghai (No. GWV-10.1-XK13), the Shanghai Municipal Key Clinical Specialty (shslczdzk01103), the Shanghai Ruijin Hospital Clinical Skills and Innovations (2018CR005), the Shanghai talent development fund (2020097), the Shanghai "Rising Stars of Medical Talent" Youth Development Program Outstanding Youth Medical Talents [SHWJRS (2021)-99], the Shanghai Outstanding Academic Leader Youth Program (20XD1422600), and the Shanghai Sailing Program (No. 19YF1429200).

ACKNOWLEDGMENTS

The authors want to thank the Shandong Cord Blood Bank (Shandong Qilu stem cell engineering Co., Ltd., Jinan, Shandong, China) for providing hUCBMNCs for the study. The authors also want to thank Guojun Liu, Meng Luo, and Xiaopeng Jia from the Shandong Cord Blood Bank who helped to isolate hUCBMNCs and provided technical support and guidance.

SUPPLEMENTARY MATERIAL

The Supplementary Material for this article can be found online at: https://www.frontiersin.org/articles/10.3389/fphar.2022.924464/full#supplementary-material

REFERENCES

Alvarez-Mercado, A. I., Sáez-Lara, M. J., García-Mediavilla, M. V., Sánchez-Campos, S., Abadía, F., Cabello-Donayre, M., et al. (2008). Xenotransplantation of Human Umbilical Cord Blood Mononuclear Cells to Rats with D-Galactosamine-Induced Hepatitis. *Cell Transpl.* 17 (7), 845–857. doi:10.3727/096368908786516837

Arroyo, V., Moreau, R., and Jalan, R. (2020). Acute-on-Chronic Liver Failure. *N. Engl. J. Med.* 382 (22), 2137–2145. doi:10.1056/NEJMra1914900

Babior, B. M. (2004). NADPH Oxidase. *Curr. Opin. Immunol.* 16 (1), 42–47. doi:10.1016/j.coi.2003.12.001

Bellot, G., Garcia-Medina, R., Gounon, P., Chiche, J., Roux, D., Pouysségur, J., et al. (2009). Hypoxia-Induced Autophagy Is Mediated through Hypoxia-Inducible Factor Induction of BNIP3 and BNIP3L via Their BH3 Domains. *Mol. Cell Biol.* 29 (10), 2570–2581. doi:10.1128/MCB.00166-09

Bianchi, M. E. (2007). DAMPs, PAMPs and Alarmins: All We Need to Know about Danger. *J. Leukoc. Biol.* 81 (1), 1–5. doi:10.1189/jlb.0306164

Bird, T. G., Müller, M., Boulter, L., Vincent, D. F., Ridgway, R. A., Lopez-Guadamillas, E., et al. (2018). TGFβ Inhibition Restores a Regenerative Response in Acute Liver Injury by Suppressing Paracrine Senescence. *Sci. Transl. Med.* 10, eaan1230. doi:10.1126/scitranslmed.aan1230

Bower, W. A., Johns, M., Margolis, H. S., Williams, I. T., and Bell, B. P. (2007). Population-based Surveillance for Acute Liver Failure. *Am. J. Gastroenterol.* 102 (11), 2459–2463. doi:10.1111/j.1572-0241.2007.01388.x

Chew, C. A., Iyer, S. G., Kow, A. W. C., Madhavan, K., Wong, A. S. T., Halazun, K. J., et al. (2020). An International Multicenter Study of Protocols for Liver Transplantation during a Pandemic: A Case for Quadripartite Equipoise. *J. Hepatol.* 73 (4), 873–881. doi:10.1016/j.jhep.2020.05.023

Chung, R. T., Stravitz, R. T., Fontana, R. J., Schiodt, F. V., Mehal, W. Z., Reddy, K. R., et al. (2012). Pathogenesis of Liver Injury in Acute Liver Failure. *Gastroenterology* 143 (3), e1–e7. doi:10.1053/j.gastro.2012.07.011

Dalous, J., Pansiot, J., Pham, H., Chatel, P., Nadaradja, C., D'Agostino, I., et al. (2013). Use of Human Umbilical Cord Blood Mononuclear Cells to Prevent Perinatal Brain Injury: a Preclinical Study. *Stem Cells Dev.* 22 (1), 169–179. doi:10.1089/scd.2012.0183

De Luca, M., Aiuti, A., Cossu, G., Parmar, M., Pellegrini, G., and Robey, P. G. (2019). Advances in Stem Cell Research and Therapeutic Development. *Nat. Cell Biol.* 21 (7), 801–811. doi:10.1038/s41556-019-0344-z

Dikic, I., and Elazar, Z. (2018). Mechanism and Medical Implications of Mammalian Autophagy. *Nat. Rev. Mol. Cell Biol.* 19 (6), 349–364. doi:10.1038/s41580-018-0003-4

Dudakov, J. A., Hanash, A. M., and van den Brink, M. R. (2015). Interleukin-22: Immunobiology and Pathology. *Annu. Rev. Immunol.* 33, 747–785. doi:10.1146/annurev-immunol-032414-112123

Dunlop, E. A., Seifan, S., Claessens, T., Behrends, C., Kamps, M. A., Rozycka, E., et al. (2014). FLCN, a Novel Autophagy Component, Interacts with GABARAP and Is Regulated by ULK1 Phosphorylation. *Autophagy* 10 (10), 1749–1760. doi:10.4161/auto.29640

Dwyer, B. J., Macmillan, M. T., Brennan, P. N., and Forbes, S. J. (2021). Cell Therapy for Advanced Liver Diseases: Repair or Rebuild. *J. Hepatol.* 74 (1), 185–199. doi:10.1016/j.jhep.2020.09.014

Escorsell, A., Mas, A., and de la Mata, M. (2007). Acute Liver Failure in Spain: Analysis of 267 Cases. *Liver Transpl.* 13 (10), 1389–1395. doi:10.1002/lt.21119

Feng, Y., He, D., Yao, Z., and Klionsky, D. J. (2014). The Machinery of Macroautophagy. *Cell Res.* 24 (1), 24–41. doi:10.1038/cr.2013.168

Feng, L. X., Zhao, F., Liu, Q., Peng, J. C., Duan, X. J., Yan, P., et al. (2020). Role of Nrf2 in Lipopolysaccharide-Induced Acute Kidney Injury: Protection by Human Umbilical Cord Blood Mononuclear Cells. *Oxid. Med. Cell Longev.* 2020, 6123459. doi:10.1155/2020/6123459

Forbes, S. J., and Newsome, P. N. (2016). Liver Regeneration - Mechanisms and Models to Clinical Application. *Nat. Rev. Gastroenterol. Hepatol.* 13 (8), 473–485. doi:10.1038/nrgastro.2016.97

Freidman, M. M., and Lapan, B. (1964). Enzyme Activities During Hepatic Injury Caused by Carbon Tetrachloride. *Clin. Chem.* 10, 335–345.

Gao, B., and Xiang, X. (2019). Interleukin-22 from Bench to Bedside: a Promising Drug for Epithelial Repair. *Cell Mol. Immunol.* 16 (7), 666–667. doi:10.1038/s41423-018-0055-6

Gao, B. (2005). Cytokines, STATs and Liver Disease. *Cell Mol. Immunol.* 2 (2), 92–100.

Hauss, W. H., and Leppelmann, H. J. (1958). Reactive Changes of Enzyme Activities in Serum and Liver as Symptoms of Acute Syndrome. *Ann. N. Y. Acad. Sci.* 75 (1), 250–259. doi:10.1111/j.1749-6632.1958.tb36871.x

He, Y., Feng, D., Hwang, S., Mackowiak, B., Wang, X., Xiang, X., et al. (2021). Interleukin-20 Exacerbates Acute Hepatitis and Bacterial Infection by Downregulating IjBf Target Genes in Hepatocytes. *J. Hepatol.* 75, 163–176. doi:10.1016/j.jhep.2021.02.004

Jackson, W. M., Nesti, L. J., and Tuan, R. S. (2010). Potential Therapeutic Applications of Muscle-Derived Mesenchymal Stem and Progenitor Cells. *Expert Opin. Biol. Ther.* 10 (4), 505–517. doi:10.1517/14712591003610606

Jaeschke, H. (2011). Reactive Oxygen and Mechanisms of Inflammatory Liver Injury: Present Concepts. *J. Gastroenterol. Hepatol.* 26 Suppl 1 (Suppl. 1), 173–179. doi:10.1111/j.1440-1746.2010.06592.x

Ji, Y. W., Mittal, S. K., Hwang, H. S., Chang, E. J., Lee, J. H., Seo, Y., et al. (2017). Lacrimal Gland-Derived IL-22 Regulates IL-17-mediated Ocular Mucosal Inflammation. *Mucosal Immunol.* 10 (5), 1202–1210. doi:10.1038/mi.2016.119

Kang, J. Y., Oh, M. K., Joo, H., Park, H. S., Chae, D. H., Kim, J., et al. (2020). Xeno-Free Condition Enhances Therapeutic Functions of Human Wharton's Jelly-Derived Mesenchymal Stem Cells against Experimental Colitis by Upregulated Indoleamine 2,3-Dioxygenase Activity. *J. Clin. Med.* 9 (9), 2913. doi:10.3390/jcm9092913

Khalifa, A., and Rockey, D. C. (2020). The Utility of Liver Biopsy in 2020. *Curr. Opin. Gastroenterol.* 36 (3), 184–191. doi:10.1097/mog.0000000000000621

Khan, H. A., Ahmad, M. Z., Khan, J. A., and Arshad, M. I. (2017). Crosstalk of Liver Immune Cells and Cell Death Mechanisms in Different Murine Models of Liver Injury and its Clinical Relevance. *Hepatobiliary Pancreat. Dis. Int.* 16 (3), 245–256. doi:10.1016/s1499-3872(17)60014-6

Kong, X., Feng, D., Mathews, S., and Gao, B. (2013). Hepatoprotective and Anti-fibrotic Functions of Interleukin-22: Therapeutic Potential for the Treatment of Alcoholic Liver Disease. *J. Gastroenterol. Hepatol.* 28 Suppl 1 (Suppl. 10 1), 56–60. doi:10.1111/jgh.12032

Kwon, H. J., Won, Y. S., Park, O., Feng, D., and Gao, B. (2014). Opposing Effects of Prednisolone Treatment on T/NKT Cell- and Hepatotoxin-Mediated Hepatitis in Mice. *Hepatology* 59 (3), 1094–1106. doi:10.1002/hep.26748

Lai, R., Xiang, X., Mo, R., Bao, R., Wang, P., Guo, S., et al. (2015). Protective Effect of Th22 Cells and Intrahepatic IL-22 in Drug Induced Hepatocellular Injury. *J. Hepatol.* 63 (1), 148–155. doi:10.1016/j.jhep.2015.02.004

Li, X. W., Feng, L. X., Zhu, X. J., Liu, Q., Wang, H. S., Wu, X., et al. (2020). Human Umbilical Cord Blood Mononuclear Cells Protect against Renal Tubulointerstitial Fibrosis in Cisplatin-Treated Rats. *Biomed. Pharmacother.* 121, 109310. doi:10.1016/j.biopha.2019.109310

Liu, J., Zhang, Q. Y., Yu, L. M., Liu, B., Li, M. Y., and Zhu, R. Z. (2015). Phycocyanobilin Accelerates Liver Regeneration and Reduces Mortality Rate in Carbon Tetrachloride-Induced Liver Injury Mice. *World J. Gastroenterol.* 21 (18), 5465–5472. doi:10.3748/wjg.v21.i18.5465

Miao, L. J., Huang, F. X., Sun, Z. T., Zhang, R. X., Huang, S. F., and Wang, J. (2014). Stat3 Inhibits Beclin 1 Expression through Recruitment of HDAC3 in Nonsmall Cell Lung Cancer Cells. *Tumour Biol.* 35 (7), 7097–7103. doi:10.1007/s13277-014-1961-6

Mieli-Vergani, G., Vergani, D., Czaja, A. J., Manns, M. P., Krawitt, E. L., Vierling, J. M., et al. (2018). Autoimmune Hepatitis. *Nat. Rev. Dis. Prim.* 4, 18017. doi:10.1038/nrdp.2018.17

Mihm, S. (2018). Danger-Associated Molecular Patterns (DAMPs): Molecular Triggers for Sterile Inflammation in the Liver. *Int. J. Mol. Sci.* 19 (10). doi:10.3390/ijms19103104

Mo, R., Lai, R., Lu, J., Zhuang, Y., Zhou, T., Jiang, S., et al. (2018). Enhanced Autophagy Contributes to Protective Effects of IL-22 against Acetaminophen-Induced Liver Injury. *Theranostics* 8 (15), 4170–4180. doi:10.7150/thno.25798

Musina, R. A., Bekchanova, E. S., Belyavskii, A. V., and Sukhikh, G. T. (2006). Differentiation Potential of Mesenchymal Stem Cells of Different Origin. *Bull. Exp. Biol. Med.* 141 (1), 147–151. doi:10.1007/s10517-006-0115-2

Nagaishi, K., Ataka, K., Echizen, E., Arimura, Y., and Fujimiya, M. (2014). Mesenchymal Stem Cell Therapy Ameliorates Diabetic Hepatocyte Damage in Mice by Inhibiting Infiltration of Bone Marrow-Derived Cells. *Hepatology* 59 (5), 1816–1829. doi:10.1002/hep.26975

Pan, H., Hong, F., Radaeva, S., and Gao, B. (2004). Hydrodynamic Gene Delivery of Interleukin-22 Protects the Mouse Liver from Concanavalin A-, Carbon Tetrachloride-, and Fas Ligand-Induced Injury via Activation of STAT3. *Cell Mol. Immunol.* 1 (1), 43–49.

Paton, M. C. B., Allison, B. J., Fahey, M. C., Li, J., Sutherland, A. E., Pham, Y., et al. (2019). Umbilical Cord Blood versus Mesenchymal Stem Cells for Inflammation-Induced Preterm Brain Injury in Fetal Sheep. *Pediatr. Res.* 86 (2), 165–173. doi:10.1038/s41390-019-0366-z

Radaeva, S., Sun, R., Pan, H. N., Hong, F., and Gao, B. (2004). Interleukin 22 (IL-22) Plays a Protective Role in T Cell-Mediated Murine Hepatitis: IL-22 Is a Survival Factor for Hepatocytes via STAT3 Activation. *Hepatology* 39 (5), 1332–1342. doi:10.1002/hep.20184

Rees, K. R., and Sinha, K. P. (1960). Blood Enzymes in Liver Injury. *J. Pathol. Bacteriol.* 80, 297–307. doi:10.1002/path.1700800213

Ren, J., Sang, Y., Qin, R., Su, Y., Cui, Z., Mang, Z., et al. (2019). Metabolic Intermediate Acetyl Phosphate Modulates Bacterial Virulence via Acetylation. *Emerg. Microbes Infect.* 8 (1), 55–69. doi:10.1080/22221751.2018.1558963

Resaz, R., Emionite, L., Vanni, C., Astigiano, S., Puppo, M., Lavieri, R., et al. (2011). Treatment of Newborn G6pc(-/-) Mice with Bone Marrow-Derived Myelomonocytes Induces Liver Repair. *J. Hepatol.* 55 (6), 1263–1271. doi:10.1016/j.jhep.2011.02.033

Reyes-Gordillo, K., Shah, R., and Muriel, P. (2017). Oxidative Stress and Inflammation in Hepatic Diseases: Current and Future Therapy. *Oxid. Med. Cell Longev.* 2017, 3140673. doi:10.1155/2017/3140673

Rolando, N., Wade, J., Davalos, M., Wendon, J., Philpott-Howard, J., and Williams, R. (2000). The Systemic Inflammatory Response Syndrome in Acute Liver Failure. *Hepatology* 32 (4 Pt 1), 734–739. doi:10.1053/jhep.2000.17687

Rosenkranz, K., Kumbruch, S., Tenbusch, M., Marcus, K., Marschner, K., Dermietzel, R., et al. (2012). Transplantation of Human Umbilical Cord Blood Cells Mediated Beneficial Effects on Apoptosis, Angiogenesis and Neuronal Survival after Hypoxic-Ischemic Brain Injury in Rats. *Cell Tissue Res.* 348 (3), 429–438. doi:10.1007/s00441-012-1401-0

Rubinstein, P., Dobrila, L., Rosenfield, R. E., Adamson, J. W., Migliaccio, G., Migliaccio, A. R., et al. (1995). Processing and Cryopreservation of Placental/umbilical Cord Blood for Unrelated Bone Marrow Reconstitution. *Proc. Natl. Acad. Sci. U. S. A.* 92 (22), 10119–10122. doi:10.1073/pnas.92.22.10119

Ryu, K. H., Kim, S. Y., Kim, Y. R., Woo, S. Y., Sung, S. H., Kim, H. S., et al. (2014). Tonsil-derived Mesenchymal Stem Cells Alleviate Concanavalin A-Induced Acute Liver Injury. *Exp. Cell Res.* 326 (1), 143–154. doi:10.1016/j.yexcr.2014.06.007

Scaffidi, P., Misteli, T., and Bianchi, M. E. (2002). Release of Chromatin Protein HMGB1 by Necrotic Cells Triggers Inflammation. *Nature* 418 (6894), 191–195. doi:10.1038/nature00858

Schmidt-Arras, D., and Rose-John, S. (2016). IL-6 Pathway in the Liver: From Physiopathology to Therapy. *J. Hepatol.* 64 (6), 1403–1415. doi:10.1016/j.jhep.2016.02.004

Shaw, T. D., Krasnodembskaya, A. D., Schroeder, G. N., Zumla, A., Maeurer, M., and O'Kane, C. M. (2021). Mesenchymal Stromal Cells: an Antimicrobial and Host-Directed Therapy for Complex Infectious Diseases. *Clin. Microbiol. Rev.* 34 (4), e0006421. doi:10.1128/cmr.00064-21

Starkey Lewis, P., Campana, L., Aleksieva, N., Cartwright, J. A., Mackinnon, A., O'Duibhir, E., et al. (2020). Alternatively Activated Macrophages Promote Resolution of Necrosis Following Acute Liver Injury. *J. Hepatol.* 73 (2), 349–360. doi:10.1016/j.jhep.2020.02.031

Tasso, R., and Pennesi, G. (2009). When Stem Cells Meet Immunoregulation. *Int. Immunopharmacol.* 9 (5), 596–598. doi:10.1016/j.intimp.2009.01.014

Wang, H. X., Liu, M., Weng, S. Y., Li, J. J., Xie, C., He, H. L., et al. (2012). Immune Mechanisms of Concanavalin A Model of Autoimmune Hepatitis. *World J. Gastroenterol.* 18 (2), 119–125. doi:10.3748/wjg.v18.i2.119

Weiss, M. L., and Troyer, D. L. (2006). Stem Cells in the Umbilical Cord. *Stem Cell Rev.* 2 (2), 155–162. doi:10.1007/s12015-006-0022-y

Wu, Z., Han, M., Chen, T., Yan, W., and Ning, Q. (2010). Acute Liver Failure: Mechanisms of Immune-Mediated Liver Injury. *Liver Int.* 30 (6), 782–794. doi:10.1111/j.1478-3231.2010.02262.x

Xiang, X., Gui, H., King, N. J., Cole, L., Wang, H., Xie, Q., et al. (2012). IL-22 and Non-ELR-CXC Chemokine Expression in Chronic Hepatitis B Virus-Infected Liver. *Immunol. Cell Biol.* 90 (6), 611–619. doi:10.1038/icb.2011.79

Xiang, X., Feng, D., Hwang, S., Ren, T., Wang, X., Trojnar, E., et al. (2020). Interleukin-22 Ameliorates Acute-On-Chronic Liver Failure by Reprogramming Impaired Regeneration Pathways in Mice. *J. Hepatol.* 72 (4), 736–745. doi:10.1016/j.jhep.2019.11.013

Xu, M. J., Feng, D., Wang, H., Guan, Y., Yan, X., and Gao, B. (2014). IL-22 Ameliorates Renal Ischemia-Reperfusion Injury by Targeting Proximal Tubule Epithelium. *J. Am. Soc. Nephrol.* 25 (5), 967–977. doi:10.1681/ASN.2013060611

Yamanaka, S. (2020). Pluripotent Stem Cell-Based Cell Therapy-Promise and Challenges. *Cell Stem Cell* 27 (4), 523–531. doi:10.1016/j.stem.2020.09.014

Yang, R., and Tonnesseen, T. I. (2019). DAMPs and Sterile Inflammation in Drug Hepatotoxicity. *Hepatol. Int.* 13 (1), 42–50. doi:10.1007/s12072-018-9911-9

Yi, Y., Zhang, W., Tao, L., Shao, Q., Xu, Q., Chen, Y., et al. (2021). RIP1 Kinase Inactivation Protects against Acetaminophen-Induced Acute Liver Injury in Mice. *Free Radic. Biol. Med.* 174, 57–65. doi:10.1016/j.freeradbiomed.2021.07.034

You, L., Wang, Z., Li, H., Shou, J., Jing, Z., Xie, J., et al. (2015). The Role of STAT3 in Autophagy. *Autophagy* 11 (5), 729–739. doi:10.1080/15548627.2015.1017192

Yu, H., Yuan, X., Zhao, M., Wang, W., and Gong, D. (2021). Efficacy of Human Umbilical Cord Blood-Mononuclear Cell Transplantation for MSA Treatment and its Effects on Changes in T-Cell Subsets in Peripheral Blood and Inflammatory Factors. *Dis. Markers* 2021, 5290766. doi:10.1155/2021/5290766

Zhang, Y., Liu, D., Hu, H., Zhang, P., Xie, R., and Cui, W. (2019). HIF-1α/BNIP3 Signaling Pathway-Induced-Autophagy Plays Protective Role during Myocardial Ischemia-Reperfusion Injury. *Biomed. Pharmacother.* 120, 109464. doi:10.1016/j.biopha.2019.109464

Conflict of Interest: The authors declare that the research was conducted in the absence of any commercial or financial relationships that could be construed as a potential conflict of interest.

Publisher's Note: All claims expressed in this article are solely those of the authors and do not necessarily represent those of their affiliated organizations, or those of the publisher, the editors, and the reviewers. Any product that may be evaluated in this article, or claim that may be made by its manufacturer, is not guaranteed or endorsed by the publisher.

frontiers | Frontiers in Pharmacology

TYPE Original Research
PUBLISHED 23 August 2022
DOI 10.3389/fphar.2022.968717

OPEN ACCESS

EDITED BY
Xiude Fan,
Shandong Provincial Hospital, China

REVIEWED BY
Suowen Xu,
University of Science and Technology of China, China
Yifan Bao,
Johnson and Johnson (United States), United States

*CORRESPONDENCE
Zhihong Ma,
mazh1969@163.com
Donglai Ma,
mdl_hebei@aliyun.com
Jun Dai,
calldj@163.com

†These authors have contributed equally to this work

SPECIALTY SECTION
This article was submitted to Gastrointestinal and Hepatic Pharmacology, a section of the journal Frontiers in Pharmacology

RECEIVED 14 June 2022
ACCEPTED 27 July 2022
PUBLISHED 23 August 2022

CITATION
Liu T, Zhang N, Kong L, Chu S, Zhang T, Yan G, Ma D, Dai J and Ma Z (2022), Paeoniflorin alleviates liver injury in hypercholesterolemic rats through the ROCK/AMPK pathway.
Front. Pharmacol. 13:968717.
doi: 10.3389/fphar.2022.968717

Paeoniflorin alleviates liver injury in hypercholesterolemic rats through the ROCK/AMPK pathway

Tong Liu[1†], Ning Zhang[1†], Lingya Kong[2], Sijie Chu[1], Ting Zhang[3], Guangdi Yan[1], Donglai Ma[4]*, Jun Dai[1]* and Zhihong Ma[1,5]*

[1]School of Basic Medicine, Hebei University of Chinese Medicine, Shijiazhuang, Hebei, China, [2]Department of Infectious Disease, The Third Hospital of Hebei Medical University, Shijiazhuang, Hebei, China, [3]Experimental Center, Hebei University of Chinese Medicine, Shijiazhuang, Hebei, China, [4]School of Pharmacy, Hebei University of Chinese Medicine, Shijiazhuang, Hebei, China, [5]Hebei Key Laboratory of Integrative Medicine on Liver-Kidney Patterns, Shijiazhuang, Hebei, China

Paeoniflorin (PF) is the main active component in *Paeonia lactiflora Pall*, and it has multiple effects. However, the precise mechanism of PF in hypercholesterolemia is unclear. In this study, rats were either fed a high-cholesterol diet (HCD) for 4 weeks to establish the hypercholesterolemic model or administered normal saline or PF (20 mg/kg/day). PF significantly reduced liver weight and the liver index. PF reduced hepatic lipid deposition and inflammation, improved serum lipid metabolism, and significantly inhibited serum and hepatic oxidative stress and the inflammatory response. PF treatment caused a marked decrease in the phosphorylated myosin phosphatase target subunit (p-MYPT)-1, nuclear sterol regulatory element-binding protein-1c (SREBP-1c), fatty acid synthase (FAS) levels, and an increase in the low-density lipoprotein receptor (LDLR) and phosphorylated-AMP-activated protein kinase (p-AMPK). Thus, PF could alleviate liver injury in hypercholesterolemic rats, and the specific mechanism may be related to the antioxidant, anti-inflammatory properties, and ROCK/AMPK/SREBP-1c signaling pathway.

KEYWORDS

paeoniflorin, rho kinase (ROCK), AMPK, anti-inflammation, anti-oxidation, hypercholesterolemia

Introduction

Hypercholesterolemia is a lipid metabolic disorder characterized by an increase in blood cholesterol, particularly low-density lipoprotein cholesterol (LDL) (Csonka et al., 2016). Epidemiological studies indicated that dietary habits such as intake of foods containing excessive saturated fats and cholesterol are the risk factors for hypercholesterolemia (AlSaad A. M. et al., 2020). Hypercholesterolemia is an important cause of obesity, atherosclerosis, and nonalcoholic fatty liver disease (NAFLD). In 2015, the World Health Organization reported that approximately 4.5%

of global deaths worldwide were due to hypercholesterolemia. Thus, it is significant to find effective drugs to treat hypercholesterolemia.

The pathogenesis of hypercholesterolemia remains unclear, and oxidative stress and the inflammatory response are often mentioned as key factors (Zhang et al., 2022). Studies have shown that excessive accumulation of cholesterol in the blood leads to increased reactive oxygen species (ROS) production (Li et al., 2020), and these highly reactive species mediate low-grade inflammation (Reyes-Gordillo et al., 2017) (Liao et al., 2021) (Incalza et al., 2018). Systematic oxidative stress and inflammatory response impair lipid metabolism, and thus, lipids accumulate in the liver (Abbasi et al., 2021). Therefore, reducing the oxidative stress and the inflammatory response is an important strategy to reduce hepatic lipid deposition and protect the liver in hypercholesterolemic rats.

An increasing amount of evidence showed that Rho kinase (ROCK) is closely related to oxidative stress and the inflammatory response (Zhang et al., 2019; Matoba et al., 2020). Fasudil, a ROCK inhibitor, inhibits ROCK activation and reduces oxidative stress and the inflammatory response in hypercholesterolemic rats (Ma et al., 2011a; Ma et al., 2011b). A recent study reported that hepatic ROCK suppresses AMP-activated protein kinase (AMPK) activity, and the ROCK/AMPK pathway is required to mediate hepatic lipogenesis during overnutrition (Huang et al., 2018). A large amount of evidence showed that activating the AMPK pathway can improve lipid deposition through the key downstream pathway in NAFLD (Xiao et al., 2019; Huang et al., 2021). Sterol regulatory element-binding protein-1c (SREBP-1c) is downstream of the AMPK pathway and plays an important role in gene expression related to intracellular lipid synthesis such as fatty acid synthase (FAS) (Mohammadi et al., 2020). At the same time, the activation of AMPK can increase the level of low-density lipoprotein receptor (LDLR) protein to regulate cholesterol homeostasis (Li et al., 2021). Taken together, ROCK inhibition and AMPK activation are potential targets to reduce oxidative stress, the inflammatory response, and hepatic lipid deposition in hypercholesterolemia.

Paeoniflorin (PF) has well known for pharmacological effects such as anti-inflammatory, anti-oxidation, reduces lipid deposition (Ma et al., 2020). Our previous studies showed that PF could reduce oxidative stress and the inflammatory response and improve hepatic lipid metabolism in NAFLD rats induced by high-fat diet (HFD) (Ma et al., 2017). However, the beneficial effects of PF on liver damage induced by hypercholesterolemia and the potential molecular mechanism remain unclear. We investigated whether PF reduces oxidative stress and inflammation response and improves lipid metabolism by inhibiting ROCK activation, and in turn, influencing the AMPK/SREBP-1c/FAS pathway. In this study, we established a hypercholesterolemic rat model using a high-cholesterol diet (HCD) to explore the hepatic protection effect and potential mechanism of PF in hypercholesterolemia.

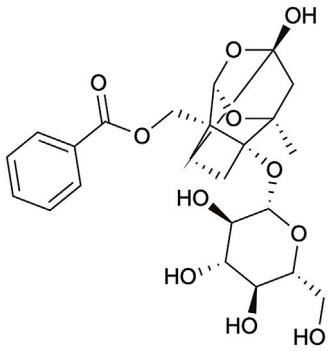

FIGURE 1
The general structure of paeoniflorin.

Materials and methods

Materials

PF (purity 98%) (Figure 1) was purchased from Nanjing Zelang Pharmaceutical Technology Co., Ltd. (Nanjing, China). Cholesterol was purchased from Beijing Solarbio Science and Technology Co., Ltd (Beijing, China). The normal diet and HCD were provided and supervised by Hebei Medical University (Shijiazhuang, China). Myosin phosphatase target subunit (MYPT)-1 and phosphorylated MYPT (p-MYPT)-1 primary antibodies were purchased from Affinity Biosciences Ltd. (Jiangsu, China), AMPK and phosphorylated-AMPK antibodies were purchased from Shanghai Abways Biotechnology Co., Ltd. (Shanghai, China), LDLR, SREBP-1c, and FAS antibodies were purchased from Jiangsu Affinity Biosciences Co., Ltd (Jiangsu, China), glyceraldehyde 3-phosphate (GAPDH) antibodies were purchased from Bioworld Technology, lnc. (Nanjing, China). Secondary horseradish peroxidase (HRP) antibodies were purchased from Shanghai Abways Biotechnology Co., Ltd. (Shanghai, China).

Animals and experimental design

Forty specific pathogen-free male Sprague–Dawley (SD) rats, weighing 180–200g, were provided by Hebei Medical University (Shijiazhuang, China). All rats were housed in cages under standard conditions (e.g., kept at room temperature, 24 ± 2°C) with free access to food and water. All animal handling procedures were performed in accordance with the 1996 National Institutes of Health Guide for the Care and Use of Laboratory Animals and approved by the Ethics Committee for Animal Experiments at the Hebei University of Chinese Medicine (approval number: DWLL2020008).

Forty rats were randomly allocated to four groups (n = 10 per group), as follows: normal control group (NC), PF-treated control group (NPF), model group (MOD), and PF-treated model group (MPF). The NC group and NPF group were fed with normal diet, MOD group and MPF group were fed with HCD (HCD composition: protein 18%, fat 4%, fiber 5%, ash 8%, water 10%, cholesterol 2%, cholic acid 0.5%, total energy 1780 kcal/kg) for 4 weeks. Within 4 weeks of HCD feeding, both NPF group and MPF group were administered PF (20 mg/kg/day) orally (Ma et al., 2017), and the NC and the MOD groups were administered the same volume of normal saline orally. Food intake was monitored daily and body weight was measured weekly during the experiment. After 4 weeks, rats were fasted for 12 h, weighed, and then intraperitoneally injected with pentobarbital (40 mg/kg) for anesthesia. Blood was collected from the femoral artery and the serum was immediately centrifuged for separation. The liver appearance was observed, quickly removed, weighed, and the liver index was calculated (liver weight/body weight × 100%). The same part of the liver was fixed in 4% paraformaldehyde, while the rest of the liver was temporarily stored in liquid nitrogen and stored in a −80 °C freezer until subsequent experimentation.

Preparation of liver homogenate

Liver tissue from each group was accurately weighed and ground in a homogenate medium. After centrifugation at 2,500 rpm for 10 min, the supernatant was removed for analysis.

Detection of biochemical indicators in serum and liver

According to the kit instructions, serum and liver homogenates were used to detect total cholesterol (TC), triglycerides (TG), LDL, and high-density lipoprotein cholesterol (HDL) levels. Serum aspartate aminotransferase (AST) and alanine aminotransferase (ALT) activity were also detected. The above kits were purchased from Nanjing Jiancheng Bioengineering Institute Co., Ltd. (Nanjing, China).

Detection of inflammation indicators in serum and liver

Enzyme-linked immunosorbent assays were used to detect serum and hepatic C-reactive protein (CRP), tumor necrosis factor (TNF)-α, interleukin (IL)-1β, and IL-6 levels in serum and liver according to the kit instructions. The above kits were purchased from Hangzhou Lianke Biotechnology Co., Ltd (Hangzhou, China).

Histological changes in the liver

From each rat, the same part of the liver tissue was fixed in 4% paraformaldehyde for over 48 h. The liver sample was dehydrated in gradient alcohol, embedded in paraffin wax, and then sliced into 4-μm thick sections and stained with hematoxylin-eosin (H and E) for observation. Each section was observed with a microscope at ×200 magnification (Leica DM4000B, Solms, Germany).

The frozen liver tissue was sliced into 8-μm thick sections using a cryomicrotome (Thermo Fisher Scientific Inc, Massachusetts, United States), fixed in fixing solution (Servicebio Technology Co., Ltd, Wuhan, China) for 15 min, and stained with oil red O solution (Servicebio Technology Co., Ltd, Wuhan, China) for 15 min, The liver tissues were washed with 60% isopropanol, and then the nuclei were then stained with hematoxylin staining solution (Servicebio Technology Co., Ltd, Wuhan, China). The slices were observed, and photos were taken using an optical microscope (Olympus, Tokyo, Japan).

Detection of oxidative stress indicators in serum and liver

According to the kit instructions, the prepared serum and liver homogenates were used to detect superoxide dismutase (SOD) and catalase (CAT) activity and the malondialdehyde (MDA) and glutathione (GSH) content. The above kits were purchased from Nanjing Jiancheng Bioengineering Institute Co., Ltd. (Nanjing, China).

We used a dihydroethidium (DHE) probe to measure the ROS fluorescence intensity in the liver tissues in each group. Frozen fresh liver tissue was taken and sliced under freezing conditions for ROS detection. The frozen section was rewarmed at room temperature to control the water content. Spontaneous fluorescence quenching reagent (Servicebio Technology Co. Ltd., Wuhan, China) was added and incubated for 5 min followed by rinsing with running water for 10 min. ROS staining solution (Sigma, St. Louis, MO, United States) was added and incubated in a light-proof incubator at 37°C for 30 min. After the slides were cleaned with PBS, DAPI solution was added and incubated at room temperature without light for 10 min. The liver tissue slices were washed again with PBS, dried, and sealed with an anti-fade mounting medium. The sections were observed under a fluorescence microscope (Nikon eclipse C1, Nikon, Japan), and the images were collected.

Western blot analysis of protein expression in liver

The frozen tissue was removed, and RIPA lysate (Servicebio Technology Co., Ltd, Wuhan, China), protease

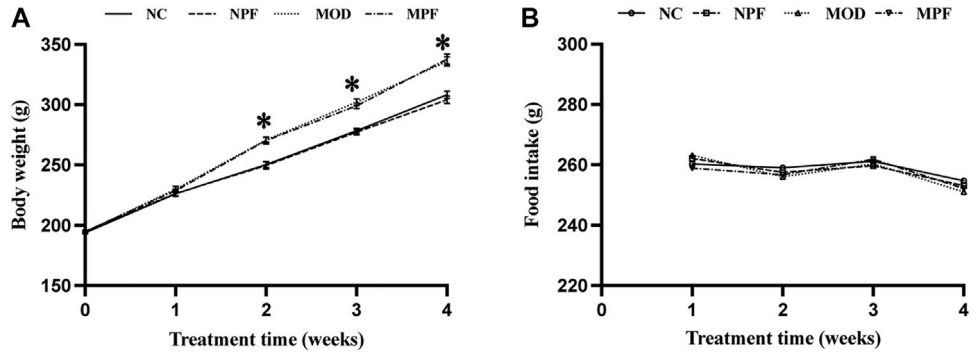

FIGURE 2
Effects of paeoniflorin (PF) on body weight, and food intake. **(A)** Weight changes for rats in the four groups during the treatment with PF. **(B)** Food intake of each rat in the four groups during the treatment with PF. The liver samples were obtained from the normal control group (NC), PF-treated control group (NPF), model group (MOD), and PF-treated model group (MPF). Data are presented as the mean ± S.E.M (n = 10). *$p < 0.05$ vs. NC and #$p < 0.05$ vs. MOD.

inhibitor, and phosphorylated protease inhibitor (Boster Biological Technology Co., Ltd. Wuhan, China) were added, and the tissue was homogenated. After centrifugation, the supernatant was extracted to prepare protein samples. Nuclear protein was extracted according to the instructions of the kit (Beyotime Biotechnology Co., Ltd. Shanghai, China) and used to detect the expression of nuclear SREBP-1c. The equivalent protein sample or nuclear protein sample was added to 8% sodium dodecyl sulfate-polyacrylamide gel to undergo electrophoresis, and the protein was then transferred to the polyvinylidene difluoride (PVDF) membranes. After blocking with 5% skimmed milk powder, the PVDF membrane was incubated overnight with the following antibodies: p-MYPT-1, MYPT-1, p-AMPK, AMPK, LDLR, SREBP-1c, FAS, or GAPDH at 4 °C. After cleaning the primary antibody, the membranes were incubated with the corresponding secondary antibody and then treated with the Super ECL detection reagent (Yeasen Biotechnology Co., Ltd. Shanghai, China). The obtained bands were analyzed using Vision Capt software (Kunming Beijie Technology Co., Ltd. Kunming, China).

Statistical analysis

Results are presented as the mean ± standard error of the mean (S.E.M.). Data analysis was conducted using the GraphPad Prism 8.0.1 software package for Windows (GraphPad Software, America). We first tested the data's normality and homogeneity of variance. The differences among the four groups were then estimated using a one-way analysis of variance followed by Tukey's post-hoc test. $p < 0.05$ was considered to be statistically significant.

Results

Effect of PF on body weight, and food intake

As shown in Figure 2, the weight of rats in the MOD group was significantly higher than that in the NC group ($p < 0.05$). There was no obvious difference in body weight between the MOD and MPF groups or between the NPF and NC groups, indicating that PF had no significant influence on the weight of the rats. Additionally, food intake did not change significantly during the treatment. Therefore, we excluded the anorexia effect of PF on hypercholesterolemia.

Effects of PF on lipids level in serum

Serum lipid levels are presented in Figure 3. In the MOD group, the serum levels of TC, TG, and LDL were markedly higher than those in the NC group, and the HDL level was markedly lower than those in the NC group (all $p < 0.05$). After PF treatment, the serum TC, TG, and LDL levels were markedly decreased, and the serum HDL level was significantly increased (all $p < 0.05$). Among the above indicators, there were no differences between the NC and NPF groups.

Effects of PF on oxidative stress indicators in the serum and liver

Compared with the NC group, SOD and CAT activity and the GSH content in the serum and liver in the MOD group

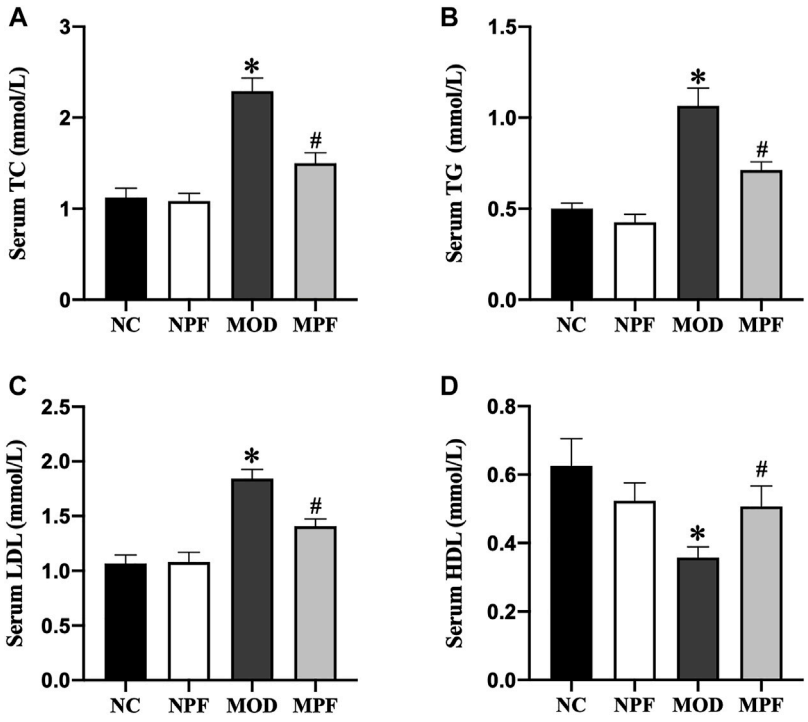

FIGURE 3
Effects of paeoniflorin (PF) on lipids level in serum. Serum levels of **(A)** TC, **(B)** TG, **(C)** LDL, and **(D)** HDL. Serum samples were obtained from the normal control group (NC), PF-treated control group (NPF), model group (MOD), and PF-treated model group (MPF). Data are presented as the mean ± S.E.M (n = 10). *$p < 0.05$ vs. NC and #$p < 0.05$ vs. MOD.

showed an obvious decrease. The serum and liver MDA content also increased significantly (all $p < 0.05$). PF treatment could increase SOD and CAT activity and the GSH content and decrease the MDA content (all $p < 0.05$) (Figures 4A–D). Compared to the NC group and the NPF group, there were no apparent differences.

For liver ROS sections, we used the DHE probe to detect ROS expression in liver tissue. Compared with the CON group, the MOD group had a higher fluorescence intensity. However, after PF treatment, the fluorescence intensity decreased significantly, which showed that PF could reduce ROS production in the liver (Figure 4E).

Effects of PF on inflammatory cytokines in the serum and liver

Serum and liver CRP, IL-1β, IL-6, and TNF-α levels in the MOD group were considerably higher than those of the NC and NPF groups (all $p < 0.05$). After PF treatment, these levels were all distinctly decreased (all $p < 0.05$) (Figure 5). There was no statistically significant difference between the NC and NPF groups.

Effects of PF on liver function and histological changes in the liver

Serum ALT, AST, and the liver index are important indicators reflecting liver injury. As shown in Figure 6A, compared with the NC group, ALT and AST activity showed an obvious increase in the MOD group. Conversely, the MPF group showed lower of ALT and AST activity (both $p < 0.05$). Compared with the NC group, the liver index in the MOD group was significantly higher. PF treatment also significantly reduced the liver index ($p < 0.05$) (Figure 6B).

Macroscopic observation showed that the livers of rats in the NC and NPF groups were chestnut-colored, while livers in MOD group rats were yellowish, butyrous, brittle, and larger than those in the NC and NPF groups. The livers of rats treated with PF had less histological damage than those of the MOD group (Figure 6C).

Microscopically, H&E staining of liver tissue showed that the NC and NPF group liver tissue had a normal structure with hepatocytes showing healthy nuclei and parenchymal structure, but the rats of the MOD group showed obvious fatty changes and inflammatory cell infiltration in liver

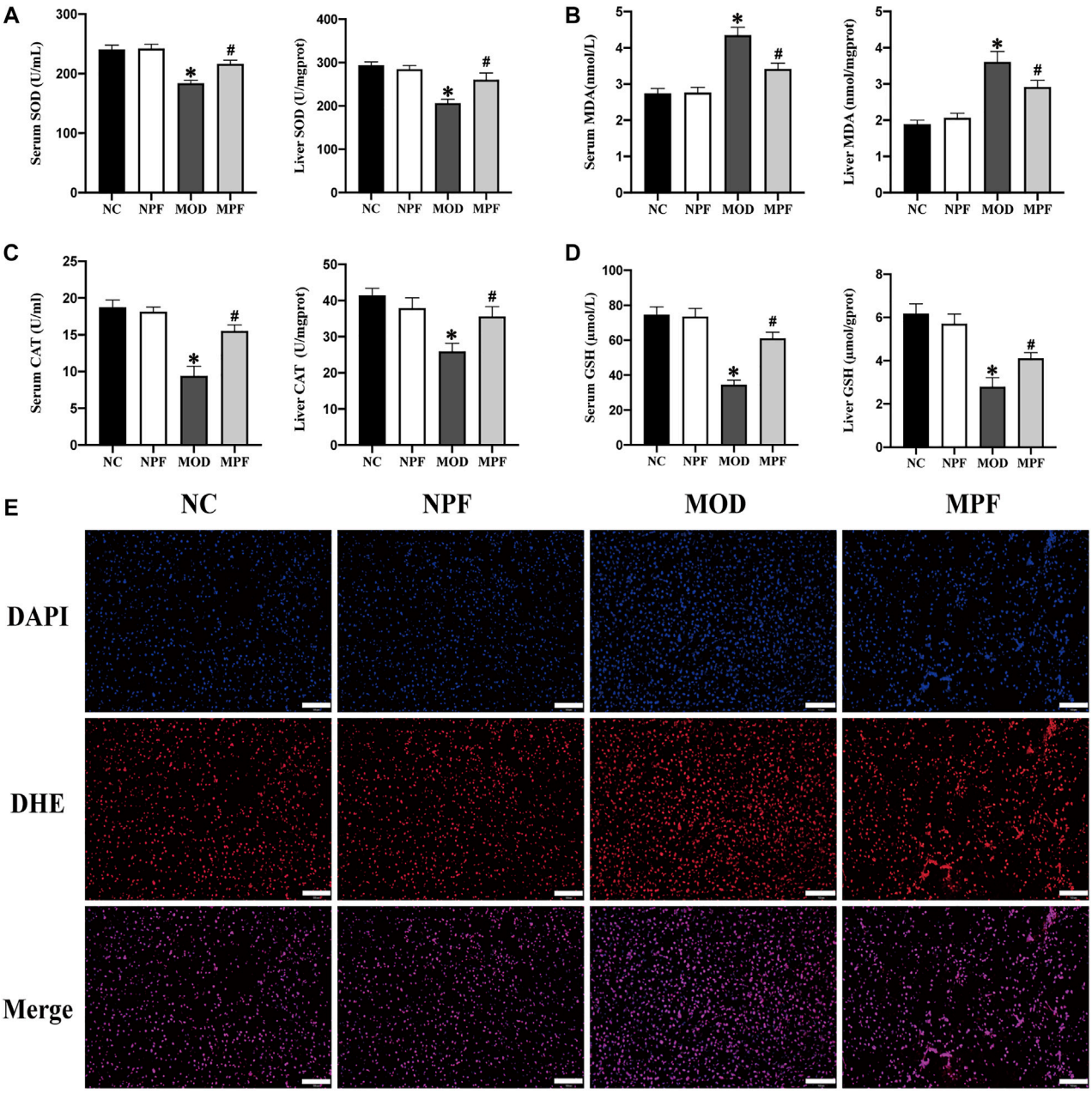

FIGURE 4
Effects of paeoniflorin (PF) on oxidative stress indicators in the serum and liver. **(A)** Serum and liver SOD activity. **(B)** Serum and liver MDA content. **(C)** Serum and liver CAT activity. **(D)** Serum and liver GSH content. **(E)** Representative reactive oxygen species (ROS) histologic slices in four groups, (200×, scale bar = 100 μm). The serum and liver samples were obtained from the normal control group (NC), PF-treated control group (NPF), model group (MOD), and PF-treated model group (MPF). Data are presented as the mean ± S.E.M (n = 10). *p < 0.05 VS. NC and #p < 0.05 VS. MOD.

sections. After PF treatment, liver lipid deposition and inflammatory cell infiltration were significantly reduced (Figure 6D).

To evaluate the effect of PF on liver lipid deposition, we used oil red O staining to detect the lipid deposition in the livers of each group. In Figure 3B, compared to the NC group, lipid deposition was significantly increased in the MOD group. After PF treatment, lipid deposition was significantly reduced in the MPF group, indicating that PF could reduce liver lipid deposition (Figure 6E).

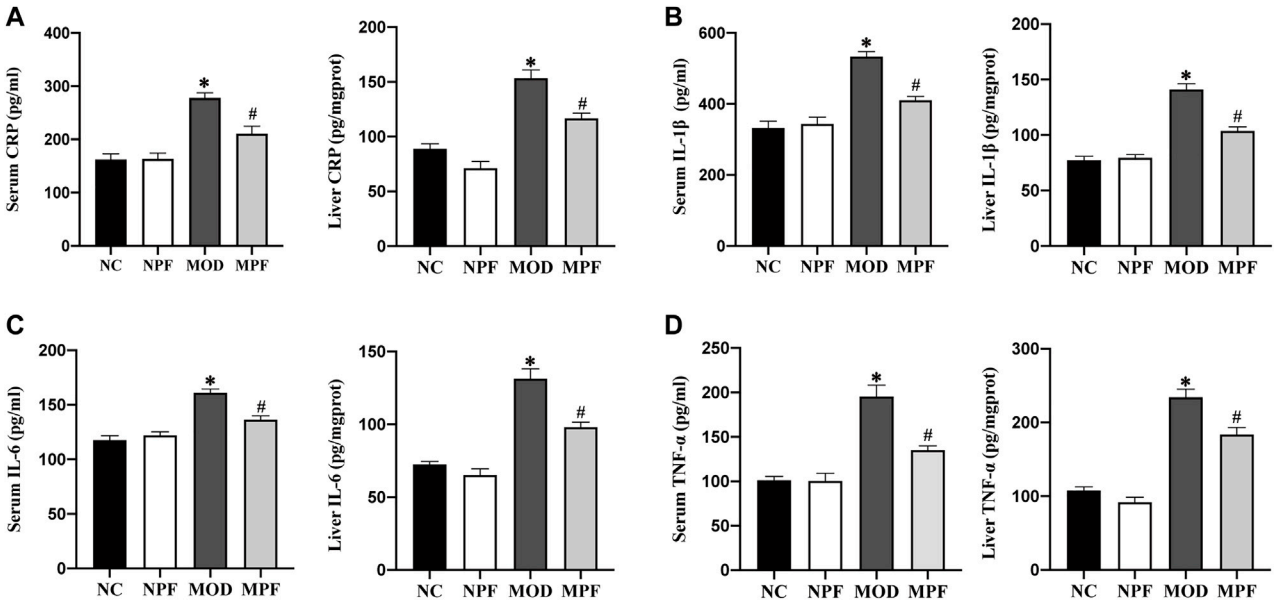

FIGURE 5
Effects of paeoniflorin (PF) on inflammatory cytokines in the serum and liver. Serum and liver levels of **(A)** CRP, **(B)** IL-1β, **(C)** IL-6, and **(D)** TNF-α. The serum and liver samples were obtained from the normal control group (NC), PF-treated control group (NPF), model group (MOD), and PF-treated model group (MPF). Data are presented as the mean ± S.E.M (n = 10). *p < 0.05 vs. NC and #p < 0.05 vs. MOD.

Effects of PF on lipids level in liver

As shown in Figure 7, in the MOD group, the liver levels of TC, TG, and LDL were markedly higher than those in the NC group, and the HDL level was markedly lower than those in the NC group (all $p < 0.05$). The liver TC, TG, and LDL levels were markedly decreased after PF treatment, and the liver HDL level was significantly increased (all $p < 0.05$). Among the above indicators, there were no differences between the NC and NPF groups.

Effects of PF on protein expression related to lipid metabolism in the liver

In Figure 8, LDLR protein expression in the MOD group was down-regulated remarkably compared to the NC group. After PF treatment, LDLR protein expression was significantly increased ($p < 0.05$). FAS and nuclear SREBP-1c protein expression in the MOD group was considerably higher than in the NC group. After treatment with PF, FAS and nuclear SREBP-1c protein expression was down-regulated rapidly ($p < 0.05$). There was no statistically significant difference between the NC and NPF groups.

Effects of PF on p-MYPT-1/p-AMPK protein expression in the liver

As shown in Figure 9, p-AMPK protein expression in the MOD group was down-regulated remarkably compared to the NC group. However, after treatment with PF, p-AMPK expression was significantly up-regulated ($p < 0.05$). Compared with the NC and NPF group, the MOD group rats had higher liver p-MYPT-1 protein expression ($p < 0.05$), and PF treatment decreased its expression in liver tissue ($p < 0.05$). There was no statistically significant difference between the NC and NPF groups.

Discussion

At present, hypercholesterolemia is mainly treated by lifestyle intervention and drugs. Therapeutic lifestyle interventions include diet control, increased exercise, smoking cessation, and alcohol restriction, etc. Drugs mainly include statins, intestinal cholesterol absorption inhibitors, bile acid chelators and other lipid-lowering drugs. Long term use of these drugs often has hepatotoxicity and gastrointestinal reactions. PF is the main active component of *Paeonia Lactiflora Pall* and has the effect of hepatic protection, anti-inflammation, anti-oxidation, and lipid metabolism. In our

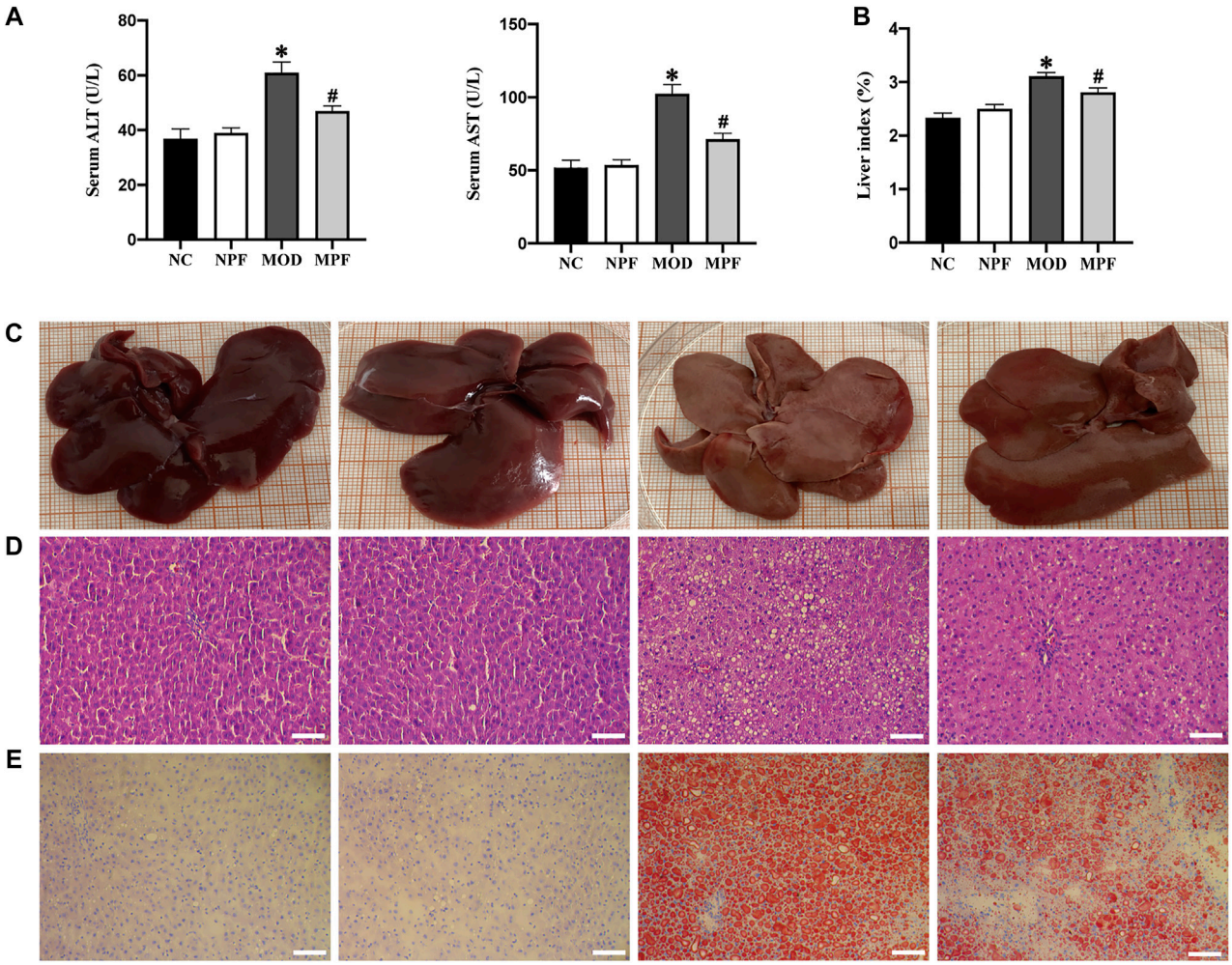

FIGURE 6
Effects of PF on liver function and histological changes in the liver. **(A)** Serum levels of ALT and AST activity. **(B)** Average liver index of rats in four groups. **(C)** Representative photos of rat liver in four groups. **(D)** Representative H and E staining histologic slices in four groups, (200×, scale bar = 100 μm). **(E)** Representative oil red O staining histologic slices in four groups, (200×, scale bar = 100 μm). The serum and liver samples were obtained from the normal control group (NC), PF-treated control group (NPF), model group (MOD), and PF-treated model group (MPF). Data are presented as the mean ± S.E.M (n = 10). *p < 0.05 vs. NC and #p < 0.05 vs. MOD.

previous study, we used HFD feeding for 14 weeks to establish NAFLD rat model and evaluate the insulin-sensitizing effect of PF and possible molecular mechanisms. However, the beneficial effects of PF on hypercholesterolemia-induced liver injury and the underlying molecular mechanisms remain unclear. In this study, we used the HCD for 4 weeks to establish the hypercholesterolemic model, and we explored the mechanism by which PF attenuated the development of hypercholesterolemia in rats. PF could inhibit ROCK, activate AMPK, and then inhibit the downstream SREBP-1c, FAS and LDLR to play the role of antioxidant, and anti-inflammatory, reducing lipid deposition and protecting the liver.

Because dietary intake of cholesterol is a critical factor in the etiopathogenesis of hypercholesterolemia, it is common for the HCD to induce hypercholesterolemia in rats (Cunha et al., 2021). It was shown that rats fed a HCD for 4 weeks could be used as an experimental animal model for hypercholesterolemia, and these rats showed a significant increase in blood cholesterol, especially LDL (Fidèle et al., 2017). This showed that we were successful in establishing the model for hypercholesterolemia in rats (AlSaad A. M. S. et al., 2020). HCD can increase the serum lipid level, while reducing the lipid level can alleviate hypercholesterolemia progression. We also detected the levels of other lipids in serum, including TC, TG, and HDL, and PF decreased serum TC, TG, LDL, and HDL in hypercholesterolemic rats. LDLR is widely expressed and is a key receptor for maintaining cholesterol homeostasis. It has been confirmed that the majority

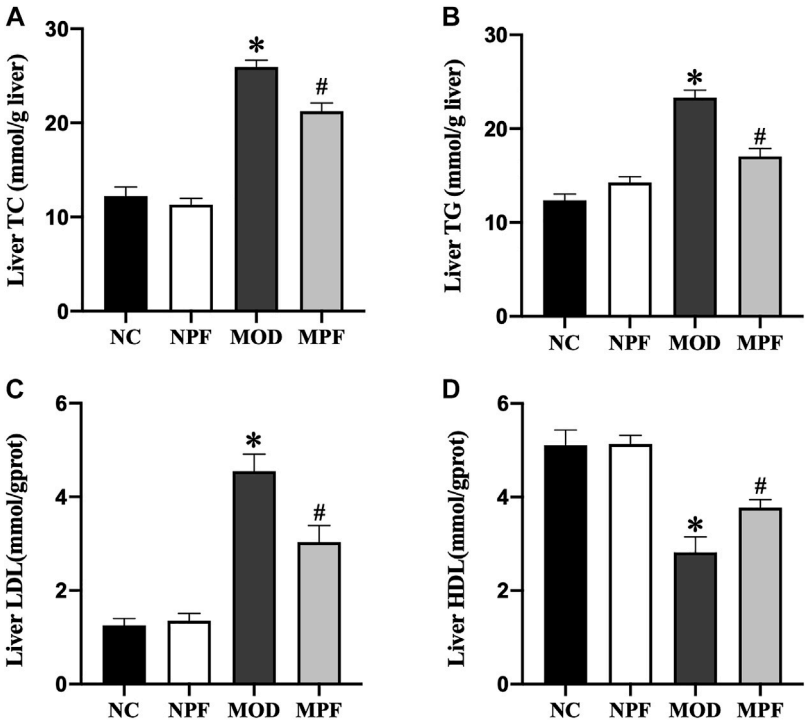

FIGURE 7
Effects of paeoniflorin (PF) on lipids in the liver. Hepatic levels of **(A)** TC, **(B)** TG, **(C)** LDL, and **(D)** HDL. The liver samples were obtained from the normal control group (NC), PF-treated control group (NPF), model group (MOD), and PF-treated model group (MPF). Data are presented as the mean ± S.E.M (n = 10). *$p < 0.05$ vs. NC and #$p < 0.05$ vs. MOD.

of blood LDL-C is recognized and eliminated by the endocytic cycle of LDLR in hepatocytes (Go and Mani, 2012; Yang et al., 2020). We found that PF could up-regulate the expression of LDLR, which may be one of the mechanisms of PF reducing serum cholesterol level. The specific mechanisms of PF to reduce blood lipids may be related to 3-hydroxy-3-methyl glutaryl coenzyme A reductase (HMG-CoA) and proliferator-activated receptor-alpha (PPAR-α). This is consistent with the results of Hu et al. (Hu et al., 2017).

Hypercholesterolemia can cause oxidative stress and inflammation. Excessive accumulation of cholesterol in the blood can cause significant ROS accumulation and affect the redox imbalance in tissues (Cammisotto et al., 2021). When the balance between the production of free radicals and endogenous antioxidants is destroyed, ROS is accelerated and leads to the oxidative stress response (AlSaad A. M. et al., 2020). A large amount of cholesterol or LDL accumulates in the blood and is deposited under the vascular endothelium, which is usually accompanied by vascular endothelial cell apoptosis and macrophage-dominated inflammation (Ma and Feng, 2016). Endothelial cell apoptosis and dysfunction induces a series of pro-inflammatory cytokines, which further aggravate the inflammatory reaction (Hou et al., 2019; Rudnicka et al., 2021). Macrophages phagocytose lipids are deposited under endothelial cells to form foam cells, which undergo the oxidative phosphorylation response. Massive lipid deposition in macrophages leads mitochondrial dysfunction and accelerates ROS production. The ROS converts LDL into a large amount of oxidized low-density lipoprotein (ox-LDL), and ox-LDL can cause inflammation and oxidative stress (Liao et al., 2021), which forms a vicious cycle. Thus, we tested the indexes related to oxidative stress and inflammation. The oxidative stress indexes showed that PF reduced the liver ROS content and the serum and liver MDA content and increased the serum and liver anti-oxidant indicators, including SOD, CAT, and GSH. For inflammatory indicators, PF decreased CRP, IL-1β, IL-6, and TNF- α in the serum and liver. This indicated that PF could reduce oxidative stress and the inflammatory response in hypercholesterolemic rats. These results are consistent with the study conducted by Xie et al. (Xie et al., 2018).

Systematic oxidative stress and the inflammatory response impair liver lipid metabolism, leading to liver lipid deposition in hypercholesterolemia (Stefan et al., 2019). We observed the hepatic pathological morphology using H&E staining and oil red O staining. We also determined the hepatic lipid content. The results showed that PF improved the liver structure, reduced inflammatory cell infiltration, and reduced lipid deposition in the liver. We also found that PF treatment reduced serum ALT and AST activity and the liver index. This suggests that PF can improve liver lipid deposition and protect the liver in hypercholesterolemic rats.

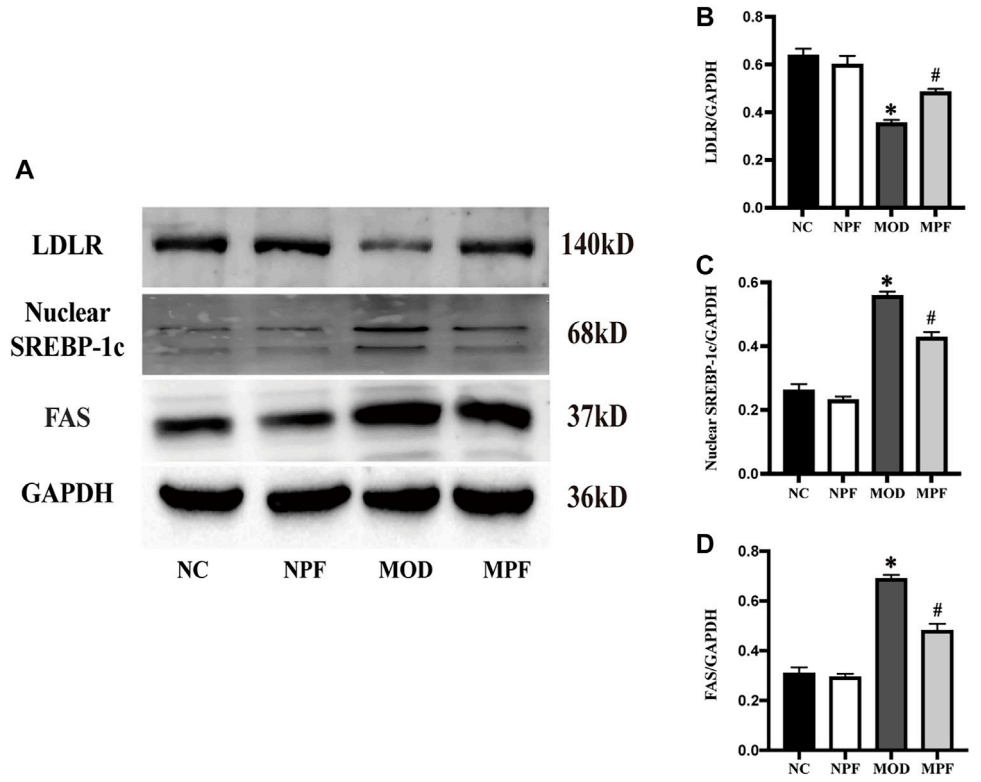

FIGURE 8
Effects of paeoniflorin (PF) on protein expression related to lipid metabolism in the liver. **(A)** Representative LDLR, nuclear SREBP-1c, and FAS expression brands. **(B–D)** Grey value of western blotting bands. The liver samples were obtained from the normal control group (NC), PF-treated control group (NPF), model group (MOD), and PF-treated model group (MPF). Data are presented as the mean ± S.E.M (n = 3). *$p < 0.05$ vs. NC, #$p < 0.05$ vs. MOD.

An important reason for hepatic lipid deposition is the increase of *in situ* lipid synthesis in the liver. SREBP-1c and FAS are important regulatory factors for *in situ* lipid synthesis in the liver. SREBP-1c is mainly expressed in the liver, and FAS is its key downstream pathway. Studies have shown that, in diet-induced obese mice, the effect of anti-hepatic steatosis is achieved by inhibiting SREBP-1c activity (Mun et al., 2019). The correlation between the inhibition of the SREBP-1c/FAS pathway and the reduction of liver lipid synthesis has been fully affirmed (Jiao et al., 2018; Fang et al., 2019). In this study, PF treatment significantly inhibited the expression of SREBP-1c and FAS, and finally reduced liver lipid deposition.

AMPK is the energy receptor of the body, and it plays a key role in regulating lipid metabolism (Chen et al., 2017). As a potential therapeutic target for metabolic diseases, AMPK is of great significance in treating NAFLD (Carling, 2017; Day et al., 2017). Activation of the AMPK pathway can inhibit the SREBP-1c and FAS expression, and reduce liver lipids synthesis. A recent study reported that ROCK is an upstream component of AMPK signaling, and the hepatic ROCK/AMPK signaling cascade is a crucial determinant of hepatic lipid synthesis (Sousa-Lima et al., 2021). Studies have shown that ROCK inhibition can improve hepatic steatosis and inhibit hepatic lipid synthesis (Huang et al., 2018; Sousa-Lima et al., 2021). ROCK inhibition can also activate AMPK and inhibit the downstream SREBP-1c and FAS, further reducing hepatic lipid deposition (Tang et al., 2017; Huang et al., 2018). Additionally, metformin, the most widely used anti-diabetes drug, can reduce liver lipid accumulation by inactivating ROCK (ÖzdemİR and Ark, 2021), which activates downstream AMPK signal transduction. Moreover, the ROCK signaling pathway regulates multiple biological functions throughout the body (Priviero et al., 2010) and is closely related to oxidative stress and inflammation. Our previous studies showed that inhibiting hepatic ROCK could improve oxidative stress and the inflammatory response in hypercholesterolemia (Ma et al., 2011a; Ma et al., 2011c). In this study, we used the p-MYPT-1 as a marker for ROCK activity (Innico et al., 2021), and we showed that p-MYPT-1 is highly expressed in the liver of hypercholesterolemic rats, which indicates that hepatic ROCK pathway expression was increased. After PF treatment, we found that p-MYPT-1 expression was significantly reduced, which also showed that PF could reduce hepatic oxidative stress and the inflammatory response, and these results are consistent with our previous research. Future studies should address the

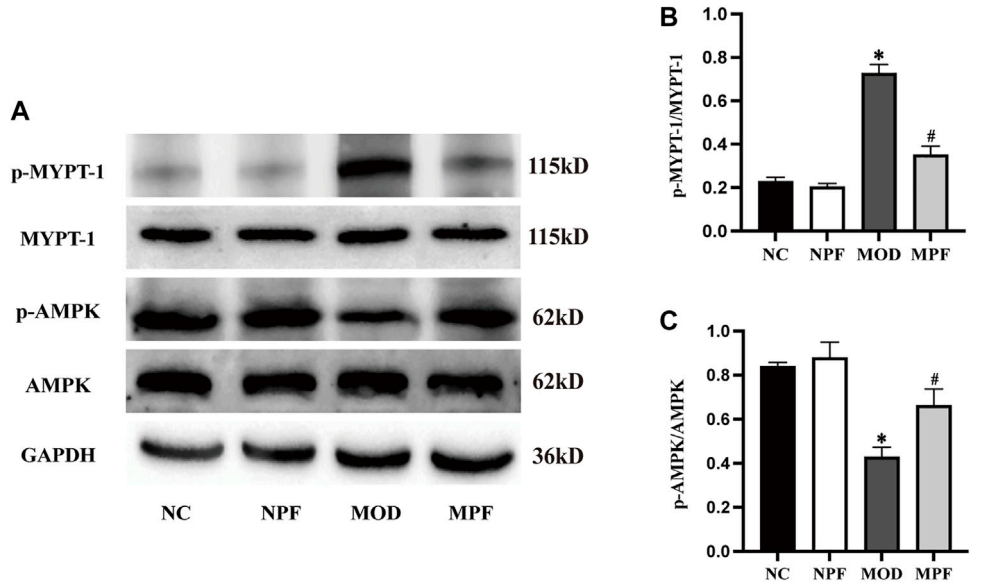

FIGURE 9
Effects of paeoniflorin (PF) on p-MYPT-1/p-AMPK protein expression in the liver. **(A)** Representative p-MYPT-1 and p-AMPK expression bands. **(B,C)** Grey value of western blotting bands. The liver samples were obtained from the normal control group (NC), PF-treated control group (NPF), model group (MOD), and PF-treated model group (MPF). Data are presented as the mean ± S.E.M (n = 3). *p < 0.05 vs. NC, #p < 0.05 vs. MOD.

regulation mechanism of PF on ROCK/AMPK signaling pathway and clarify the target of PF.

Conclusion

In this study, we found that PF exerted anti-inflammation and anti-oxidation, improved lipid deposition, and hepato-protective effects in hypercholesterolemic rats. The specific mechanism may be implemented through the ROCK/AMPK/SREBP-1c/FAS pathway. These findings suggest that PF may be a candidate drug for hypercholesterolemia, and further in-depth study of its mechanism and clinical applications are required.

Data Availability Statement

The raw data supporting the conclusion of this article will be made available by the authors, without undue reservation.

Ethics Statement

The animal study was reviewed and approved by the Ethics Committee for Animal Experiments at the Hebei University of Chinese Medicine.

Author contributions

TL: Conceptualization, Methodology, Data Curation, Writing original draft. NZ: Conceptualization, Formal analysis, Methodology, Data Curation. LK: Validation, Data Curation, Investigation. SC: Resources, Data Curation, Investigation. TZ: Validation, Formal analysis. GY: Validation, Formal analysis. DM: Conceptualization, Supervision, Project administration, Experimental guidance. JD: Conceptualization, Supervision, Project administration, Experimental guidance. ZM: Conceptualization, Supervision, Funding acquisition, Experimental guidance, Project administration. All authors read and approved the manuscript and agree to be accountable for all aspects of the research in ensuring that the accuracy or integrity of any part of the work is appropriately investigated and resolved.

Funding

This work was supported by the Natural Science Fund of Hebei Education Department (Nos. ZD2021080 and ZD2016091), the Construction Program of new research and development platform and institution, Hebei Province Innovation Ability Promotion Plan (NO. 20567624H), and the

Hebei Key Laboratory of Integrative Medicine on Liver-Kidney Patterns.

Conflict of Interest

The authors declare that the research was conducted in the absence of any commercial or financial relationships that could be construed as a potential conflict of interest.

Publisher's Note

References

Abbasi, E., Goodarzi, M. T., Tayebinia, H., Saidijam, M., and Khodadadi, I. (2021). Favorable effects of Anethum graveolens on liver oxidative stress and cholesterol 7 alpha-hydroxylase levels in non-alcoholic fatty liver disease (NAFLD) rat models. *Metabol. Open* 12, 100140. doi:10.1016/j.metop.2021.100140

AlSaad, A. M., Mohany, M., Almalki, M. S., Almutham, I., Alahmari, A. A., AlSulaiman, M., et al. (2020a). Baicalein neutralizes hypercholesterolemia-induced aggravation of oxidative injury in rats. *Int. J. Med. Sci.* 17 (9), 1156–1166. doi:10.7150/ijms.46108

AlSaad, A. M. S., Alasmari, F., Abuohashish, H. M., Mohany, M., Ahmed, M. M., and Al-Rejaie, S. S. (2020b). Renin angiotensin system blockage by losartan neutralize hypercholesterolemia-induced inflammatory and oxidative injuries. *Redox Rep.* 25 (1), 51–58. doi:10.1080/13510002.2020.1763714

Cammisotto, V., Nocella, C., Bartimoccia, S., Sanguigni, V., Francomano, D., Sciarretta, S., et al. (2021). The role of antioxidants supplementation in clinical practice: Focus on cardiovascular risk factors. *Antioxidants (Basel)* 10 (2), 146. doi:10.3390/antiox10020146

Carling, D. (2017). AMPK signalling in health and disease. *Curr. Opin. Cell Biol.* 45, 31–37. doi:10.1016/j.ceb.2017.01.005

Chen, Q., Wang, T., Li, J., Wang, S., Qiu, F., Yu, H., et al. (2017). Effects of natural products on fructose-induced nonalcoholic fatty liver disease (NAFLD). *Nutrients* 9 (2), E96. doi:10.3390/nu9020096

Csonka, C., Sárközy, M., Pipicz, M., Dux, L., and Csont, T. (2016). Modulation of hypercholesterolemia-induced oxidative/nitrative stress in the heart. *Oxid. Med. Cell. Longev.* 2016, 3863726. doi:10.1155/2016/3863726

Cunha, L. F., Ongaratto, M. A., Endres, M., and Barschak, A. G. (2021). Modelling hypercholesterolaemia in rats using high cholesterol diet. *Int. J. Exp. Pathol.* 102 (2), 74–79. doi:10.1111/iep.12387

Day, E. A., Ford, R. J., and Steinberg, G. R. (2017). AMPK as a therapeutic target for treating metabolic diseases. *Trends Endocrinol. Metab.* 28 (8), 545–560. doi:10.1016/j.tem.2017.05.004

Fang, K., Wu, F., Chen, G., Dong, H., Li, J., Zhao, Y., et al. (2019). Diosgenin ameliorates palmitic acid-induced lipid accumulation via AMPK/ACC/CPT-1A and SREBP-1c/FAS signaling pathways in LO2 cells. *BMC Complement. Altern. Med.* 19 (1), 255. doi:10.1186/s12906-019-2671-9

Fidèle, N., Joseph, B., Emmanuel, T., and Théophile, D. (2017). Hypolipidemic, antioxidant and anti-atherosclerogenic effect of aqueous extract leaves of Cassia. occidentalis Linn (Caesalpiniaceae) in diet-induced hypercholesterolemic rats. *BMC Complement. Altern. Med.* 17 (1), 76. doi:10.1186/s12906-017-1566-x

Go, G. W., and Mani, A. (2012). Low-density lipoprotein receptor (LDLR) family orchestrates cholesterol homeostasis. *Yale J. Biol. Med.* 85 (1), 19–28.

Hou, X., Yang, S., and Yin, J. (2019). Blocking the REDD1/TXNIP axis ameliorates LPS-induced vascular endothelial cell injury through repressing oxidative stress and apoptosis. *Am. J. Physiol. Cell Physiol.* 316 (1), C104–c110. doi:10.1152/ajpcell.00313.2018

Hu, H., Zhu, Q., Su, J., Wu, Y., Zhu, Y., Wang, Y., et al. (2017). Effects of an enriched extract of paeoniflorin, a monoterpene glycoside used in Chinese herbal medicine, on cholesterol metabolism in a hyperlipidemic rat model. *Med. Sci. Monit.* 23, 3412–3427. doi:10.12659/msm.905544

Huang, H., Lee, S. H., Sousa-Lima, I., Kim, S. S., Hwang, W. M., Dagon, Y., et al. (2018). Rho-kinase/AMPK axis regulates hepatic lipogenesis during overnutrition. *J. Clin. Invest.* 128 (12), 5335–5350. doi:10.1172/jci63562

Huang, R., Guo, F., Li, Y., Liang, Y., Li, G., Fu, P., et al. (2021). Activation of AMPK by triptolide alleviates nonalcoholic fatty liver disease by improving hepatic lipid metabolism, inflammation and fibrosis. *Phytomedicine.* 92, 153739. doi:10.1016/j.phymed.2021.153739

Incalza, M. A., D'Oria, R., Natalicchio, A., Perrini, S., Laviola, L., and Giorgino, F. (2018). Oxidative stress and reactive oxygen species in endothelial dysfunction associated with cardiovascular and metabolic diseases. *Vasc. Pharmacol.* 100, 1–19. doi:10.1016/j.vph.2017.05.005

Innico, G., Gobbi, L., Bertoldi, G., Rigato, M., Basso, A., Bonfante, L., et al. (2021). Oxidative stress, inflammation, and peritoneal dialysis: A molecular biology approach. *Artif. Organs* 45 (10), 1202–1207. doi:10.1111/aor.14001

Jiao, Y., Zhao, J., Zhang, Z., Li, M., Yu, X., Yang, Y., et al. (2018). SRY-box containing gene 4 promotes liver steatosis by upregulation of SREBP-1c. *Diabetes* 67 (11), 2227–2238. doi:10.2337/db18-0184

Li, K., Deng, Y., Deng, G., Chen, P., Wang, Y., Wu, H., et al. (2020). High cholesterol induces apoptosis and autophagy through the ROS-activated AKT/FOXO1 pathway in tendon-derived stem cells. *Stem Cell Res. Ther.* 11 (1), 131. doi:10.1186/s13287-020-01643-5

Li, X., Hu, X., Pan, T., Dong, L., Ding, L., Wang, Z., et al. (2021). Kanglexin, a new anthraquinone compound, attenuates lipid accumulation by activating the AMPK/SREBP-2/PCSK9/LDLR signalling pathway. *Biomed. Pharmacother.* 133, 110802. doi:10.1016/j.biopha.2020.110802

Liao, Y., Zhu, E., and Zhou, W. (2021). Ox-LDL aggravates the oxidative stress and inflammatory responses of THP-1 macrophages by reducing the inhibition effect of miR-491-5p on MMP-9. *Front. Cardiovasc. Med.* 8, 697236. doi:10.3389/fcvm.2021.697236

Ma, X., and Feng, Y. (2016). Hypercholesterolemia tunes hematopoietic stem/progenitor cells for inflammation and atherosclerosis. *Int. J. Mol. Sci.* 17 (7), E1162. doi:10.3390/ijms17071162

Ma, X., Zhang, W., Jiang, Y., Wen, J., Wei, S., and Zhao, Y. (2020). Paeoniflorin, a natural product with multiple targets in liver diseases-A mini review. *Front. Pharmacol.* 11, 531. doi:10.3389/fphar.2020.00531

Ma, Z., Chu, L., Liu, H., Wang, W., Li, J., Yao, W., et al. (2017). Beneficial effects of paeoniflorin on non-alcoholic fatty liver disease induced by high-fat diet in rats. *Sci. Rep.* 7, 44819. doi:10.1038/srep44819

Ma, Z., Zhang, J., Du, R., Ji, E., and Chu, L. (2011a). Rho kinase inhibition by fasudil has anti-inflammatory effects in hypercholesterolemic rats. *Biol. Pharm. Bull.* 34 (11), 1684–1689. doi:10.1248/bpb.34.1684

Ma, Z., Zhang, J., Ji, E., Cao, G., Li, G., and Chu, L. (2011b). Rho kinase inhibition by fasudil exerts antioxidant effects in hypercholesterolemic rats. *Clin. Exp. Pharmacol. Physiol.* 38 (10), 688–694. doi:10.1111/j.1440-1681.2011.05561.x

Ma, Z., Zhang, J., Ji, E., Cao, G., Li, G., and Chu, L. (2011c). Rho kinase inhibition by fasudil exerts antioxidant effects in hypercholesterolemic rats. *Clin. Exp. Pharmacol. Physiol.* 38 (10), 688–694. doi:10.1111/j.1440-1681.2011.05561.x

Matoba, K., Takeda, Y., Nagai, Y., Kanazawa, Y., Kawanami, D., Yokota, T., et al. (2020). ROCK inhibition may stop diabetic kidney disease. *Jma J.* 3 (3), 154–163. doi:10.31662/jmaj.2020-0014

Mohammadi, M., Abbasalipourkabir, R., and Ziamajidi, N. (2020). Fish oil and chicoric acid combination protects better against palmitate-induced lipid accumulation via regulating AMPK-mediated SREBP-1/FAS and PPARα/UCP2 pathways. *Arch. Physiol. Biochem.*, 1–9. doi:10.1080/13813455.2020.1789881

Mun, J., Kim, S., Yoon, H. G., You, Y., Kim, O. K., Choi, K. C., et al. (2019). Water extract of curcuma longa L. Ameliorates non-alcoholic fatty liver disease. *Nutrients* 11 (10), E2536. doi:10.3390/nu11102536

Özdemİr, A., and Ark, M. (2021). A novel ROCK inhibitor: Off-target effects of metformin. *Turk J. Biol.* 45 (1), 35–45. doi:10.3906/biy-2004-12

Priviero, F. B., Jin, L. M., Ying, Z., Teixeira, C. E., and Webb, R. C. (2010). Up-regulation of the RhoA/Rho-kinase signaling pathway in corpus cavernosum from endothelial nitric-oxide synthase (NOS), but not neuronal NOS, null mice. *J. Pharmacol. Exp. Ther.* 333 (1), 184–192. doi:10.1124/jpet.109.160606

Reyes-Gordillo, K., Shah, R., and Muriel, P. (2017). Oxidative stress and inflammation in hepatic diseases: Current and future therapy. *Oxid. Med. Cell. Longev.* 2017, 3140673. doi:10.1155/2017/3140673

Rudnicka, E., Suchta, K., Grymowicz, M., Calik-Ksepka, A., Smolarczyk, K., Duszewska, A. M., et al. (2021). Chronic low grade inflammation in pathogenesis of PCOS. *Int. J. Mol. Sci.* 22 (7), 3789. doi:10.3390/ijms22073789

Sousa-Lima, I., Kim, H. J., Jones, J., and Kim, Y. B. (2021). Rho-kinase as a therapeutic target for nonalcoholic fatty liver diseases. *Diabetes Metab. J.* 45 (5), 655–674. doi:10.4093/dmj.2021.0197

Stefan, N., Häring, H. U., and Cusi, K. (2019). Non-alcoholic fatty liver disease: Causes, diagnosis, cardiometabolic consequences, and treatment strategies. *Lancet. Diabetes Endocrinol.* 7 (4), 313–324. doi:10.1016/s2213-8587(18)30154-2

Tang, S., Wu, W., Tang, W., Ge, Z., Wang, H., Hong, T., et al. (2017). Suppression of Rho-kinase 1 is responsible for insulin regulation of the AMPK/SREBP-1c pathway in skeletal muscle cells exposed to palmitate. *Acta Diabetol.* 54 (7), 635–644. doi:10.1007/s00592-017-0976-z

Xiao, Q., Zhang, S., Yang, C., Du, R., Zhao, J., Li, J., et al. (2019). Ginsenoside Rg1 ameliorates palmitic acid-induced hepatic steatosis and inflammation in HepG2 cells via the AMPK/NF-κB pathway. *Int. J. Endocrinol.* 2019, 7514802. doi:10.1155/2019/7514802

Xie, C. H., Li, Z. J., Chen, L. J., Zhao, P., Zhang, J. J., Bai, S. W., et al. (2018). [The study of protective effect of paeoniflorin on lung injury in MRL/lpr mice]. *Sichuan Da Xue Xue Bao Yi Xue Ban.* 49 (3), 394–398.

Yang, H. X., Zhang, M., Long, S. Y., Tuo, Q. H., Tian, Y., Chen, J. X., et al. (2020). Cholesterol in LDL receptor recycling and degradation. *Clin. Chim. Acta.* 500, 81–86. doi:10.1016/j.cca.2019.09.022

Zhang, Q., Chao, T. C., Patil, V. S., Qin, Y., Tiwari, S. K., Chiou, J., et al. (2019). The long noncoding RNA ROCKI regulates inflammatory gene expression. *Embo J.* 38 (8), e100041. doi:10.15252/embj.2018100041

Zhang, Z., Dalan, R., Hu, Z., Wang, J. W., Chew, N. W., Poh, K. K., et al. (2022). Reactive oxygen species scavenging nanomedicine for the treatment of ischemic heart disease. *Adv. Mat.*, e2202169. doi:10.1002/adma.202202169

frontiers | Frontiers in Pharmacology

TYPE Original Research
PUBLISHED 02 September 2022
DOI 10.3389/fphar.2022.966759

OPEN ACCESS

EDITED BY
Tatsunori Miyata,
Cleveland Clinic, United States

REVIEWED BY
Yuanli Chen,
Hefei University of Technology, China
Jian Tu,
Guilin Medical University, China

*CORRESPONDENCE
Lijie Ma,
1077818878@qq.com

SPECIALTY SECTION
This article was submitted to Gastrointestinal and Hepatic Pharmacology, a section of the journal Frontiers in Pharmacology

RECEIVED 11 June 2022
ACCEPTED 29 July 2022
PUBLISHED 02 September 2022

CITATION
Hou X, Zhang Z, Ma Y, Jin R, Yi B, Yang D and Ma L (2022), Mechanism of hydroxysafflor yellow A on acute liver injury based on transcriptomics. *Front. Pharmacol.* 13:966759. doi: 10.3389/fphar.2022.966759

Mechanism of hydroxysafflor yellow A on acute liver injury based on transcriptomics

Xiangmei Hou, Ziying Zhang, Yuehong Ma, Rong Jin, Bing Yi, Dongdong Yang and Lijie Ma*

Inner Mongolia Key Laboratory of Molecular Biology, Inner Mongolia Medical University, Hohhot, China

Objective: To investigate how Hydroxysafflor yellow A (HSYA) effects acute liver injury (ALI) and what transcriptional regulatory mechanisms it may employ.

Methods: Rats were randomly divided into five groups (n = 10): Control, Model, HSYA-L, HSYA-M, and HSYA-H. In the control and model groups, rats were intraperitoneally injected with equivalent normal saline, while in the HSYA groups, they were also injected with different amounts of HSYA (10, 20, and 40 mg/kg/day) once daily for eight consecutive days. One hour following the last injection, the control group was injected into the abdominal cavity with 0.1 ml/100 g of peanut oil, and the other four groups got the same amount of a peanut oil solution containing 50% CCl_4. Liver indexes were detected in rats after dissection, and hematoxylin and eosin (HE) dyeing was utilized to determine HSYA's impact on the liver of model rats. In addition, with RNA-Sequencing (RNA-Seq) technology and quantitative real-time PCR (qRT-PCR), differentially expressed genes (DEGs) were discovered and validated. Furthermore, we detected the contents of anti-superoxide anion (anti-O_2^-) and hydrogen peroxide (H_2O_2), and verified three inflammatory genes (Icam1, Bcl2a1, and Ptgs2) in the NF-kB pathway by qRT-PCR.

Results: Relative to the control and HSYA groups, in the model group, we found 1111 DEGs that were up-/down-regulated, six of these genes were verified by qRT-PCR, including Tymp, Fabp7, Serpina3c, Gpnmb, Il1r1, and Creld2, indicated that these genes were obviously involved in the regulation of HSYA in ALI model. Membrane rafts, membrane microdomains, inflammatory response, regulation of cytokine production, monooxygenase activity, and iron ion binding were significantly enriched in GO analysis. KEGG analysis revealed that DEGs were primarily enriched for PPAR, retinol metabolism, NF-kB signaling pathways, etc. Last but not least, compared with the control group, the anti-O_2^- content was substantially decreased, the H_2O_2 content and inflammatory genes (Icam1, Bcl2a1, and Ptgs2) levels were considerably elevated in the model group. Compared with the model group, the anti-O_2^- content was substantially increased, the H_2O_2 content and inflammatory genes (Icam1, Bcl2a1, and Ptgs2) levels were substantially decreased in the HSYA group ($p < 0.05$).

Conclusion: HSYA could improve liver function, inhibit oxidative stress and inflammation, and improve the degree of liver tissue damage. The RNA-Seq

results further verified that HSYA has the typical characteristics of numerous targets and multiple pathway. Protecting the liver from damage by regulating the expression of Tymp, Fabp7, Serpina3c, Gpnmb, Il1r1, Creld2, and the PPAR, retinol metabolism, NF-kappa B signaling pathways.

KEYWORDS

acute liver injury, hydroxysafflor yellow A, RNA-sequencing, differentially expressed genes, targets

1 Introduction

Acute liver injury (ALI) is associated with a rapid reduction in liver enzymes (Tao et al., 2021), and it's mechanism involves a complicated interaction of hepatocyte degeneration, inflammatory reaction, reactive oxygen species (ROS), necrosis and apoptosis of hepatocytes (Yang et al., 2021). ALI is usually caused by viral infections (Marra et al., 2021), drugs or alcohol abuse (Oh and Park, 2015), and ingestion of toxic substances (Allard et al., 2019). Liver disease is a major health problem with a very poor prognosis, severe hepatic damage might result in liver failure or death (Åberg et al., 2018). Currently, there are no effective targeted drugs. Consequently, it is crucial to identify critical molecular targets for ALI prevention. Hydroxysafflor yellow A (HSYA), one of the most important active elements of safflower (Guo et al., 2019), is mainly used in clinical for coronary heart disease, cerebral ischemia-reperfusion, hyperlipidemia and other diseases (Han et al., 2016; Zou et al., 2018; Tan et al., 2020). It is reported that HSYA has the ability to neutralize oxygen free radicals, prevent lipid peroxidation and reduce inflammatory response (Li et al., 2017). Other studies have shown that HSYA has numerous biological roles, including anti-tumor, regulating glucose, lipid metabolism, anticoagulation, and antihypertensive (Ao et al., 2018). However, the mechanism related to the effect of HSYA on ALI is not clear. Our previous research showed that safflower and compound preparations with it had a very good mitigation effect on ALI (LV et al., 2018; Lu et al., 2021), we suspect that HSYA is one of the main protective components in safflower.

In recent years, RNA-Sequencing (RNA-Seq) has developed rapidly, and with it's advantages of high reproducibility, accuracy, and extensiveness (Jiang et al., 2015), it has gradually become a powerful tool for detecting genome-wide transcriptional patterns such as differentially expressed genes (DEGs), signaling pathways, novel transcripts, and disease biomarkers in complex tissues or cells (Tran et al., 2015; Zang et al., 2019). Rats were used to generate an ALI model caused by carbon tetrachloride (CCl_4) in this investigation, and the Illumina NovaSeq 6000 high-throughput sequencing technology was used to construct the corresponding transcriptome library. Then the differential expression analysis of genes and the functional annotation of GO and KEGG were carried out. We attempted to estimate the associated targets of HSYA on the protective impact of CCl_4-induced ALI rats and explore the associated mechanisms, providing a theoretical foundation for future investigation.

2 Materials and methods

2.1 Main instruments and reagents

Automatic chemistry analysis instrument (Beckman AU5800, BECKMAN COULTER, United States). HSYA (purity > 98%) was obtained from Chengdu Zhibiao Pure (Chengdu, China). The ALT, AST, ALP, SOD, MDA, Hydrogen peroxide, Inhibition and produce superoxide anion assay kits were from Nanjing Jiancheng (Nanjing, China). TNF-α, IL-6, and IL-1β assay kits were from Wuhan Gene Beauty (Wuhan, China). TRIzol reagent, FastKing RT Kit, SYBR Premix Ex Taq were purchased from Tiangen (Beijing, China). Other reagents possessed a higher degree of analytical purity.

2.2 Animals and treatment

SPF-grade Wistar rats (male, 180–220 g) were obtained from SPF Biotechnology Co., Ltd. (Beijing, China). The license number for Animal Production: SCXK (Beijing) 2019-0010. All animals were raised in the Laboratory Animal Center of Inner Mongolia Medical University (20°C ± 2°C, 12 h day/night cycle). Before beginning studies, animals were given adequate water and food for 5 days to adapt to the animal center's environment. The experiments were conducted according to the Animal Welfare Guidelines and approved by the Inner Mongolia Medical University's Animal Care and Use Committee (No. YKD202001020). These animals were arbitrarily separated into five categories (n = 10): Control, Model, HSYA-L, HSYA-M, and HSYA-H. The modeling method was as follows: in the control and model groups, rats were intraperitoneally injected with equivalent normal saline, and rats in HSYA groups were also injected with different amounts of HSYA (10, 20, and 40 mg/kg/day) once daily for eight consecutive days. One hour following the last injection, the control group was injected into the abdominal cavity with 0.1 ml/100 g of peanut oil. Meanwhile, the other four groups got the same amount of a peanut oil solution containing 50%

CCl_4. After 24 h, 150 mg/kg of sodium pentobarbital *via* intraperitoneally to euthanize the rats, and serum and liver tissues were collected for subsequent analysis.

2.3 Calculation of body mass, wet liver weight, and liver index

After collecting blood samples, rats were killed. The whole liver was immediately removed and put in ice-cold PBS, and then we wiped off the water on the liver surface with filter paper to calculate the liver index. Liver Index = Wet Liver Weight (g)/ Body Mass (g) × 100%.

2.4 Biochemical analysis

Using an automated biochemical analyzer and biochemical assay kits, ALT, AST, and ALP levels were determined.

2.5 Enzyme-linked immunosorbent assay

The right lobe tissues of rats in all groups were washed with normal cold saline, and 10% liver homogenate was prepared. The supernatant was taken by centrifugation (4°C, 12,000 r/min, and 15 min), and the SOD activity, MDA and inflammatory mediators (TNF-α, IL-1β, and IL-6) levels were measured as per directions for kits.

2.6 Liver histopathological examination

The right liver tissues of rats for each group were preserved in 10% buffered formalin. The tissues were dehydrated, wax-impregnated, fixed, sliced (4–5 m thick), with hematoxylin-eosin staining (HE), and viewed under a light microscope for histological liver alterations. The ratio between the necrotic area of tissue and the whole visual field was calculated using Image-Pro Plus 6.0 software.

2.7 Transcriptome sequencing

2.7.1 Total RNA extraction

Three liver samples were randomly selected from the control, model, and HSYA-M groups (Note: the HSYA group mentioned in the sequencing section only represented the HSYA-M). In each group, the liver's left region was removed. After extracting total RNA, Agilent 2100 bioanalyzer was used to accurately detect the concentration, total amount, and integrity of RNA.

2.7.2 Library preparation, quality inspection, and sequencing analyses

Oligo (dT) magnetic beads were used to enrich PolyA-tailed mRNA, which was subsequently fragmented. The first strand of cDNA was produced using fragmented mRNA and random oligonucleotide, whereas the second strand was generated by DNA polymerase I, RNase H, and dNTP. After adding purified cDNA to poly (A), Utilizing AMPure XP beads, a fragment of 300 bp was chosen for PCR amplification. PCR products were refined, and the final library was obtained. Moreover, using the Qubit 2.0 Fluorometer and Agilent 2100 Bioanalyzer, the filtered sequences were assessed. Finally, on the Illumina NovaSeq 6000 equipment, 150-bp partnered reads were used for the sequencing. These processes were operated by Beijing novogene Bioinformatics Technology Co., Ltd.

2.7.3 Gene quality control

To obtain the clean reads with high quality, the sequencing quality was assessed by fastp (version 0.19.7) software to remove the adaptor sequence, reads from N (N indicates that the data cannot be verified), which was >10% and poor quality reads which was >50% bases from raw reads. Using the HISAT2 program, the positional information of Reads in the reference genome was acquired.

2.7.4 Differential expression analysis

The quantitative study of gene expression was performed using the FeatureCount tool, and FPKM > 1 was used to define gene expression. The DEGs comparison across two groups was made using DESeq2 software, and DEGs with differential expression multiples ($|\log_2 FC| \geq 1$) and $p < 0.05$ were considered significantly DEGs. ClusterProfiler software was used to examine the enrichment of GO and KEGG. $p < 0.05$ was deemed statistical significance.

2.7.5 Real-time quantitative PCR analysis

For establishing the validity of RNA-Seq, DEGs were analyzed by qRT-PCR, GAPDH was used to standardize each sample. The kit's instructions were followed for total RNA extraction, inverse transcription, and qRT-PCR tests. Conditions for amplification were 95°C for 15 min, cycling at 95°C for 10 s, 60°C for 32 s, repeated 40 times. The $2^{-\triangle\triangle CT}$ method was used for quantification and analysis. Experiments were repeated three times. Sangon Biotech (Shanghai, China) synthesized the Primer combinations seen in Table 1.

2.8 Detection of anti-superoxide anion and hydrogen peroxide

To further determine the effects of HSYA against oxidative stress induced by CCl_4, we have determined the

TABLE 1 Primer sequences of DEGs to be measured.

Gene	Forward primer	Reverse primer
Tymp	CCCTGGAAGTGGAAGAAGCGTTG	CTGGTCTTGGGTTTCTGCCTGTC
Fabp7	TGTGATTCGGTTGGATGGAGACAAG	CATAACAGCGAACAGCAACGACATC
Serpina3c	GCTGTCCTCTGTGATGGCATACTG	TGTGAAGTCAGTGTTGATGGAAGCC
Gpnmb	AGATGCCAGAAGGAAGATGCCAAC	GGGTCAGAAGCCAGCTCCAAATC
Il1r1	CTGCCGAGGCTTGTGACATCTTC	CGACAGCAGAGGCACAATGAGAC
Creld2	AGAGGAACGAGACCCACAGCATC	GCCGCACACTCATCTACATCCAC
Icam1	TGTCGGTGCTCAGGTATCCATCC	TTCGCAAGAGGAAGAGCAGTTCAC
Bcl2a1	ATCCACTCCCTGGCTGAGAACTATC	AAAGCAACTCTCTGTAGCACTCTGG
Ptgs2	CACATTTGATTGACAGCCCACCAAC	AGTCATCAGCCACAGGAGGAAGG
GAPDH	TCACCCCATTTGATGTTAGCG	GCAAGTTCAACGGCACAGTCA

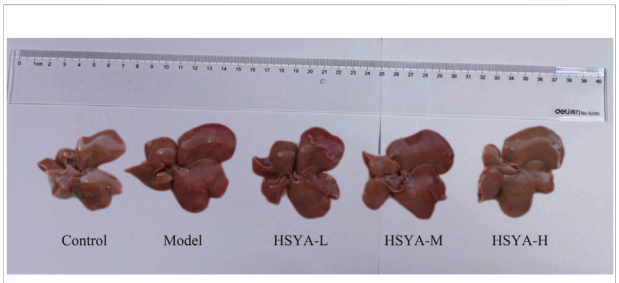

FIGURE 1
Morphology of liver tissues in each group.

contents of anti-superoxide anion (anti-O_2^-) and hydrogen peroxide (H_2O_2) in liver tissue of rats in each group, the specific operation was carried out according to the kits' instructions.

2.9 Statistical analysis

Using the GraphPad prism8 tool, statistical analyses were conducted, the tests were provided as means ± standard deviation ($\bar{x} \pm s$), the number of samples is represented by n. If the data satisfied the homogeneity tests of normality and variance, using One-way ANOVA, several groups were evaluated, while pairwise comparisons were conducted by the LSD test. If the data only conformed or did not conform to the normal distribution and/or did not satisfy the homogeneity test of variance, a rank-sum test was used to test rank count data. $p < 0.001$, $p < 0.01$, and $p < 0.05$ showed statistical validity.

3 Results

3.1 Effects of hydroxysafflor yellow A on liver morphology of CCl_4-induced acute liver injury in rats

As seen in Figure 1, in the control group, the hepatic of rats was bright red, and the membrane surface was smooth and soft. In contrast to the control group, in the model group, significantly greater liver volume was witnessed, the surface of capsule was rough, the texture was hard, and local rotten. Relative to the model group, the hepatic volume in HSYA groups decreased slightly smaller, the liver edge was slightly sharper, the surface was slightly rougher, the texture was slightly harder. The overall state was among the control and model groups.

3.2 Effects of hydroxysafflor yellow A on body mass, wet liver weight, and liver index

Weight loss and liver index increase might indicate liver damage (Li et al., 2019). As observed in Figure 2, relative to the control group, in the model group, the body mass of rats was dramatically decreased ($p < 0.05$). Relative to the model group, there was no significant change in the HSYA-L, but the body mass of rats was dramatically increased in the HSYA-M and HSYA-H groups ($p < 0.01$, $p < 0.05$). CCl_4 significantly increased rats' wet liver weight and liver index ($p < 0.001$). Relative to the model group, the wet liver weight and liver index of rats were greatly diminished in the HSYA-M and HSYA-H groups ($p < 0.01$, $p < 0.05$). The results showed that HSYA could effectively protect the liver.

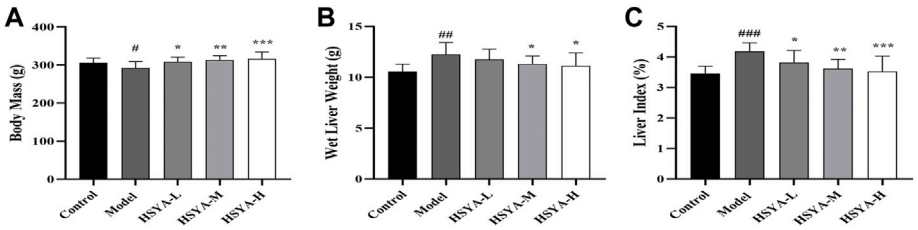

FIGURE 2
Effects of HSYA on Body Mass, Wet Liver Weight and Liver Index. **(A)** Body Mass; **(B)** Wet Liver weight; **(C)** Liver Index ($\bar{x} \pm s$, $n = 10$). $^{\#}p < 0.05$, $^{\#\#\#}p < 0.001$ vs. the control group; $^{*}p < 0.05$, $^{**}p < 0.01$ vs. the model group.

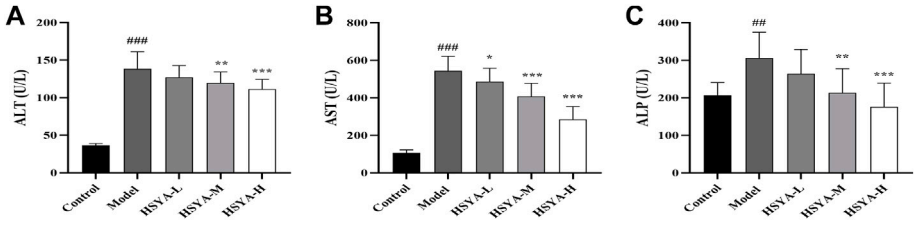

FIGURE 3
Effects of HSYA on Biochemical Indicators. **(A)** ALT; **(B)** AST; **(C)** ALP ($\bar{x} \pm s$, $n = 10$). $^{\#\#\#}p < 0.001$ vs. the control group; $^{*}p < 0.05$, $^{**}p < 0.01$, $^{***}p < 0.001$ vs. the model group.

3.3 Effects of hydroxysafflor yellow A on biochemical indicators

ALT, AST, and ALP are valuable biochemical indicators for examining early hepatotoxicity (Ali et al., 2021). As seen in Figure 3, relative to the control group, in the model group, the ALT, AST, and ALP activities were dramatically increased ($p < 0.001$, $p < 0.01$). In comparison with the model group, in the HSYA-M and HSYA-H groups, the ALT and ALP activities were considerably reduced ($p < 0.001$, $p < 0.01$), and the AST activity in all HSYA groups were also obviously decreased ($p < 0.001$, $p < 0.05$). The above revealed that HSYA could prevent ALI caused by CCl_4.

3.4 Effects of hydroxysafflor yellow A on oxidative indexes and expression levels of inflammatory factors

Oxidative stress and inflammation are strongly associated with the pathophysiology of ALI (Al-Dossari et al., 2020). To analyze HSYA's effects on CCl_4-induced hepatic lipid peroxidation and inflammatory response, we detected the SOD activity, MDA and inflammatory factors (TNF-α, IL-1β, and IL-6) expression levels. As seen in Figure 4, relative to the control group, the SOD activity in liver tissues was dramatically reduced, and the content of MDA and inflammatory factors levels were considerably elevated in the model group ($p < 0.001$). Relative to the model group, the SOD activity in liver tissues of all HSYA groups was dramatically increased, MDA and TNF-α levels in all HSYA groups were drastically reduced ($p < 0.001$, $p < 0.01$, and $p < 0.05$), IL-1β and IL-6 levels in HSYA-M and HSYA-H groups were also noticeably diminished ($p < 0.01$). These findings demonstrated that HSYA might decrease oxidative stress and inflammatory responses generated by CCl_4.

3.5 Effects of hydroxysafflor yellow A on the liver tissues pathology

As seen in Figure 5, the hepatic cords of rats in the control group were neatly arranged, the hepatic lobules and nucleus were visible without obvious inflammation, cell degeneration and necrosis (Figure 5A). In the model group, the hepatic cords were obviously disordered, the hepatic lobule structure mostly was destroyed, the surrounding liver tissues showed vacuolar degeneration, the major vein was surrounded by infiltrating inflammatory mediators, and apoptotic bodies were standard

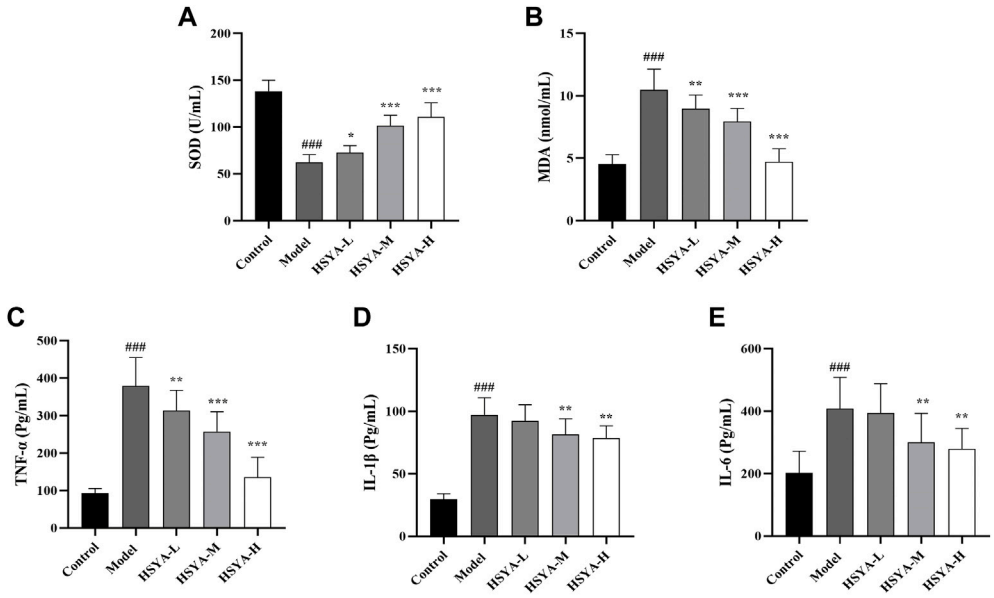

FIGURE 4
Effects of HSYA on oxidative indexes and expression levels of inflammatory factors. **(A)** SOD; **(B)** MDA; **(C)** TNF-α; **(D)** IL-1β; **(E)** IL-6 ($\bar{x} \pm s$, $n = 10$). $^{###}p < 0.001$ vs. the control group; $^{*}p < 0.05$, $^{**}p < 0.01$, $^{***}p < 0.001$ vs. the model group.

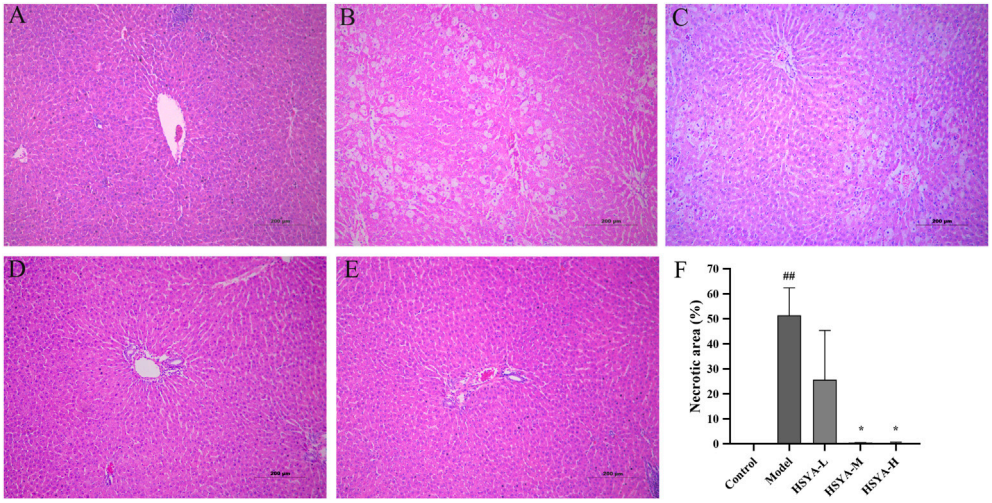

FIGURE 5
Effects of HSYA on the liver tissue pathology. **(A)** Control; **(B)** Model; **(C)** HSYA-L; **(D)** HSYA-M; **(E)** HSYA-H; **(F)** Hepatocyte necrosis quantified ($\bar{x} \pm s$, $n = 3$). $^{##}p < 0.01$ vs. the control group; $^{*}p < 0.05$ vs. the model group.

(Figure 5B). In the HSYA-L group, the hepatic cords of rats were disordered, the boundary of hepatic lobules was not clear, the liver cells showed obvious degeneration and necrosis, moderate diffuse vacuolar degeneration, and inflammatory infiltration was lighter than that in the model group (Figure 5C). In the HSYA-H group, the hepatic cords of rats were slightly disordered, it was easy to see the structure of liver lobules, the liver cells were accompanied by mild edema and steatosis, apoptotic bodies were occasionally seen around the central vein, the inflammatory infiltration was significantly reduced, and the pathological manifestations of liver tissues tended to be normal (Figure 5E). The

TABLE 2 RNA-seq data analysis.

Group	Clean_reads	Total_map (%)	Unique_map (%)	Q30 (%)	GC_pct (%)	Exon (%)	Intergenic (%)
Control	42515666	95.45	88.55	94.48	50.17	89.15	6.5
Model	42049237.33	95.58	89.27	94.52	50.56	88.49	7.32
HSYA	42794086	95.7	89.55	94.33	50.25	89.18	6.89

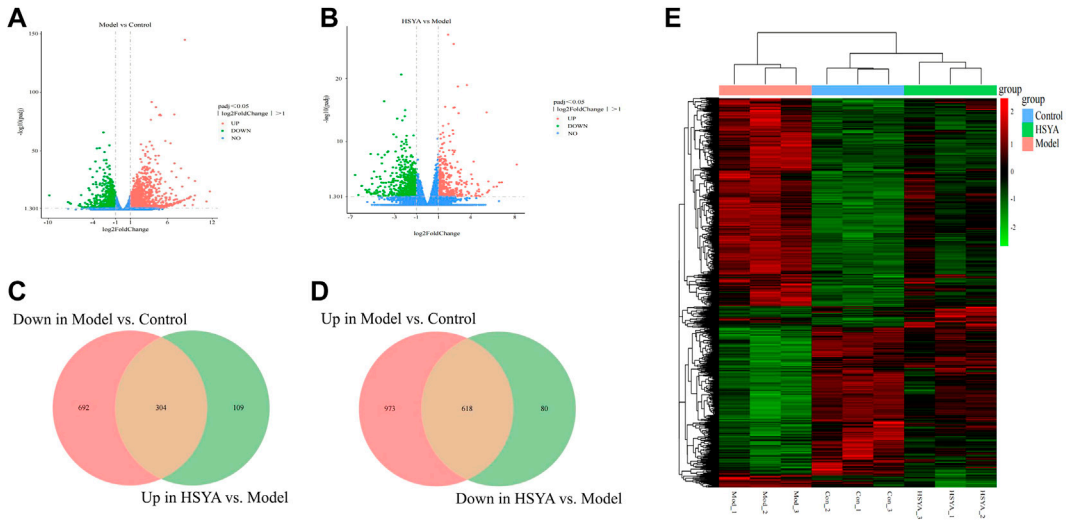

FIGURE 6
Quantitative analysis of DEGs. **(A,B)** Volcanic map of DEGs among groups; **(C,D)** Venn diagram of DEGs among groups; **(E)** Heat map among liver tissues.

pathological changes in the HSYA-M group were between the above two groups (Figure 5D). A quantitative analysis of necrotic areas in liver tissue revealed that there was no evidence of liver cell degeneration or necrosis around the central vein of the liver in the control group. Compared with the control group, the necrotic area of liver in the model group was significantly increased ($p < 0.01$). In addition, compared with the model group, except the HSYA-L group, the necrotic area of liver in the HSYA-M and HSYA-H groups were drastically reduced ($p < 0.05$) (Figure 5F).

3.6 RNA-sequencing data analysis

3.6.1 RNA-sequencing analysis

To elucidate the mechanism underlying how HSYA performed a protective role in ALI, three liver samples of rats were chosen at random from the control, model and HSYA-M groups (the following is represented by the HSYA group) to construct mRNA libraries. After the quality control of RNA-Seq was qualified, the sequencing data in the three groups were analyzed. As shown in Table 2, these data indicate that the sequencing data are reliable.

3.6.2 Quantitative analysis of differentially expressed genes

We detected the patterns of gene regulation in hepatic tissue from control, model, and HSYA (HSYA-M) groups by RNA-Seq. 1,591 DEGs were upregulated and 996 were downregulated between control and model groups, whereas 413 were upregulated and 698 were downregulated between HSYA and model groups (Figures 6A,B). To elucidate the improvement mechanism of HSYA on ALI, further DEGs screening has been carried out. According to the findings, 618 genes were elevated by CCl_4 and downregulated by HSYA. Meanwhile, 304 genes were downregulated by CCl_4 and elevated by HSYA (Figures 6C,D). We suspected these genes are potential genes for HSYA to prevent CCl_4-induced ALI. Cluster analysis revealed substantial differences between the three groups (Figure 6E).

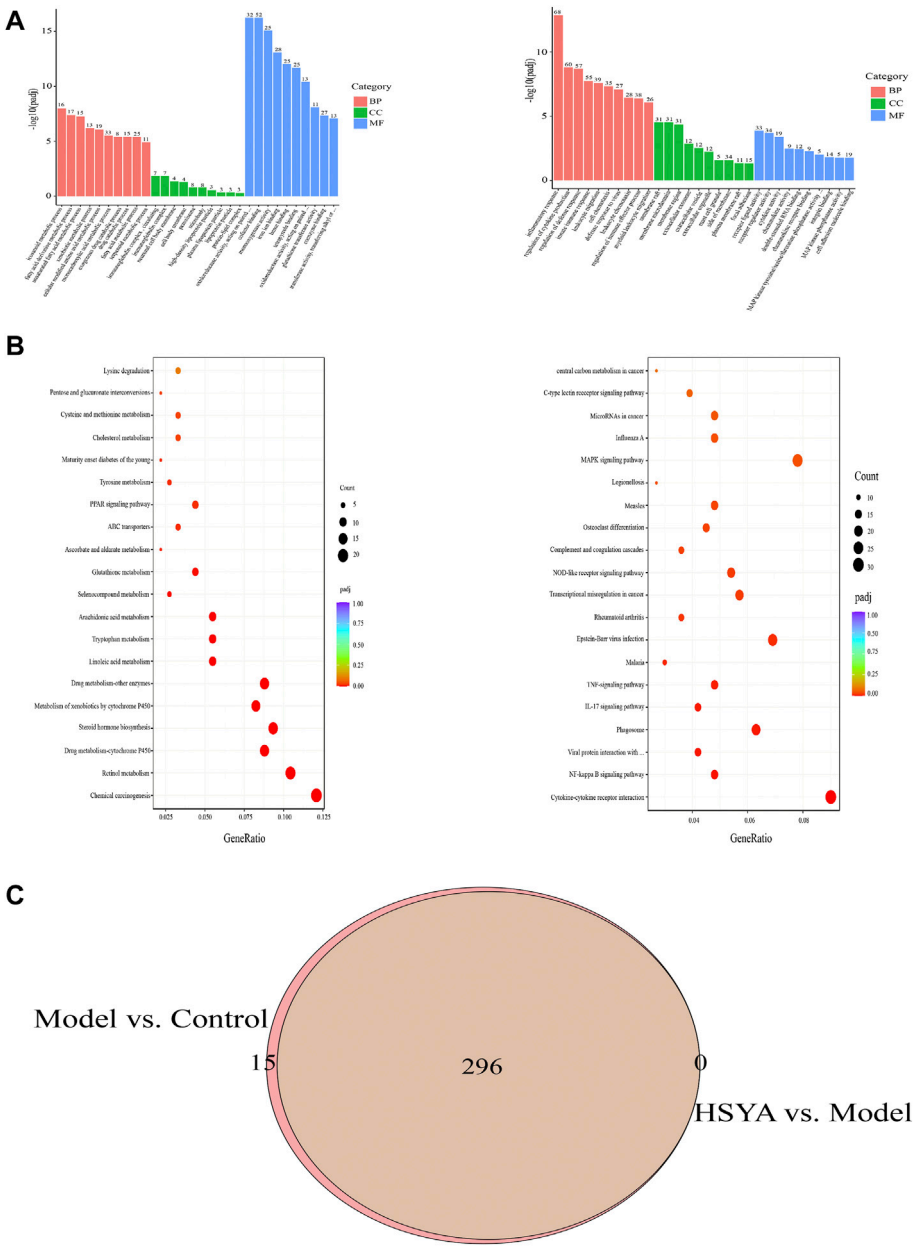

FIGURE 7
DEGs were analyzed by GO and KEGG. **(A)** Analysis of 304 upregulated DEGs and 618 downregulated DEGs by GO; **(B)** Analysis of 304 upregulated DEGs and 618 downregulated DEGs by KEGG; **(C)** 296 altered pathways by CCl4 treatment were attenuated by HSYA pretreatment.

3.6.3 Differentially expressed genes analyzed by GO and KEGG

After obtaining the DEGs of HSYA in the pretreatment of ALI, GO analysis was conducted on up- and down-regulated DEGs. The 30 most enhanced GO phrases were selected for analysis ($p < 0.05$). BP (Biological Process) analysis of the upregulated DEGs has mainly exhibited enrichment for icosanoid metabolic process, exogenous drug catabolic process, fatty acid derivative metabolic process and so on; the downregulated DEGs has mainly exhibited enrichment for inflammatory response, regulation of cytokine production, innate immune response, leukocyte migration and so on. The CC (Cellular Component) analysis revealed the upregulated DEGs were mostly found in the immunoglobulin complex,

TABLE 3 The top 10 up- and down-regulated DEGs in HSYA.

Gene ID	Gene name	Log_2FC	*p* adj
ENSRNOG00000032394	Tymp	1.896308884	1.23E-27
ENSRNOG00000000814	Fabp7	2.404946406	3.61E-26
ENSRNOG00000010410	Serpina3c	2.785841518	1.92E-19
ENSRNOG00000029993	Kynu	1.927743293	1.54E-13
ENSRNOG00000048874	Gckr	1.429194087	3.23E-13
ENSRNOG00000023116	Agmo	1.421670722	3.92E-12
ENSRNOG00000002878	Afm	1.210173494	6.98E-12
ENSRNOG00000001736	Bdh1	1.219810299	3.39E-11
ENSRNOG00000015438	Ces1f	1.527371	1.59E-10
ENSRNOG00000033010	Akr1c12	1.411245353	2.09E-10
ENSRNOG00000008816	Gpnmb	−2.20580116	7.25E-08
ENSRNOG00000014504	Il1r1	−1.367891194	4.61E-07
ENSRNOG00000004659	Creld2	−1.849881578	1.22E-06
ENSRNOG00000015078	Ifitm3	−1.146379749	3.04E-06
ENSRNOG00000026605	Ifi27l2b	−1.271733055	3.34E-06
ENSRNOG00000014117	Hmox1	−1.188417247	3.73E-06
ENSRNOG00000042499	Tmsb10	−1.300520436	5.21E-06
ENSRNOG00000049075	Fabp5	−1.077557324	6.01E-06
ENSRNOG00000007650	Cd63	−1.060319089	6.66E-06
ENSRNOG00000007089	Lgmn	−1.108294769	8.02E-06

neuronal cell body membrane and peroxisome; the downregulated DEGs were mostly found in the membrane raft, membrane microdomain, membrane region, etc. In terms of MF (Molecular Function), the upregulated DEGs were mostly concentrated on cofactor binding, monooxygenase activity, iron ion binding, etc; the downregulated DEGs mainly focus on receptor-ligand activity, double-stranded RNA binding, chemokine receptor binding, etc. (Figure 7A). Additionally, we did a KEGG analysis further to investigate the pathogenic mechanism of HSYA pretreatment ALI and to identify the pathways associated with the functions between Model vs. Control and HSYA vs. Model. The top 20 signaling pathways with the greatest enrichment were selected (Figure 7B). There were 296 shared pathways among the enriched pathways between Model vs. Control and HSYA vs. Model (Figure 7C). Among the intersecting paths, Retinol metabolism, PPAR, NF-kappa B, NOD-like receptor signaling pathways were observed; it is hypothesized that HSYA pretreatments may influence ALI with the above pathways.

3.6.4 qRT-PCR validation of differentially expressed genes

The genes involved in the regulation of ALI by HSYA were selected for qRT-PCR to estimate the mRNA expression levels. Screening genes according to the following principles: The *p* value should be much less than 0.05; genes ought to be highly expressed, that is, the FPKM value of each sample should be at least more than 20; $1.0 \leq |\log_2 FC| \leq 3.0$; the read count should be relatively high. Based on the above filters, a total of 91 upregulated and 28 downregulated DEGs were selected. The specifics of the top 10 DEGs that were upregulated or downregulated by HSYA administration are reported in Table 3. The first three upregulated DEGs and the first three downregulated DEGs were selected for qRT-PCR verification, the results are shown in Figure 8, compared with the control group, Tymp, Fabp7, and Serpina3c mRNA levels were diminished significantly in the model group ($p < 0.01$, $p < 0.05$), meanwhile, Gpnmb, Il1r1, and Creld2 mRNA levels elevated drastically ($p < 0.001$, $p < 0.01$, and $p < 0.05$). Tymp, Fabp7, and Serpina3c mRNA levels were considerably higher in the HSYA group than in the model group ($p < 0.001$, $p < 0.01$), Gpnmb, Il1r1, and Creld2 mRNA levels were declined substantially ($p < 0.01$, $p < 0.05$). qRT-PCR corroborated that the same pattern in the expression levels of DEGs that matched the RNA-seq data.

3.7 Effects of hydroxysafflor yellow A on the reactive oxygen species and inflammatory genes

As shown in Figure 9, two components of reactive oxygen species (ROS) were determined. The findings revealed that relative to the control group, the anti-O_2^- content was substantially decreased ($p < 0.01$), and the H_2O_2 content was considerably elevated in the model group ($p < 0.01$). Relative to the model group, the anti-O_2^- content was substantially increased ($p < 0.01$), and the content of H_2O_2 was substantially decreased in the HSYA group ($p < 0.001$) (Figure 9A). Moreover, we selected three inflammatory genes in the NF-kB signaling pathway to confirm the exact role of HSYA in CCl_4-induced ALI. The results showed that the gene expression levels of Icam1, Bcl2a1, and Ptgs2 in the model group were significantly higher than those of the control group ($p < 0.001$, $p < 0.01$). In the HSYA group, Bcl2a1 and Ptgs2 expression levels were significantly lower than that of the model group ($p < 0.001$, $p < 0.01$) (Figure 9B). Combined with the results in Section 3.4, it was further suggested that HSYA can protect the liver from damage by inhibiting inflammatory response and oxidative stress.

4 Discussion

HSYA is a water-soluble monomer component extracted from safflowers that promotes blood flow, removes blood clots, relaxes and activates tendons (Bai et al., 2020). CCl_4 model is one of the classical models for inducing ALI, which is often used to investigate hepatotoxicity and hepatic fibrosis, as well as the hepatoprotective functions of pharmaceuticals and natural substances (Zhao et al., 2020). The mechanism involves

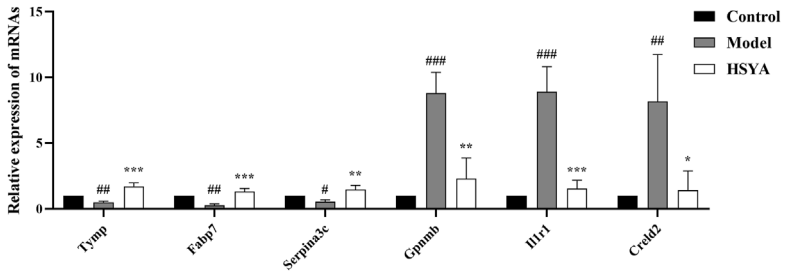

FIGURE 8
Three upregulated DEGs and three downregulated DEGs mRNA expression levels ($\bar{x} \pm s$, $n = 3$). $^{\#}p < 0.001$, $^{\#\#}p < 0.001$, $^{\#\#\#}p < 0.001$ vs. the control group; $^{*}p < 0.05$, $^{**}p < 0.01$, $^{***}p < 0.001$ vs. the model group.

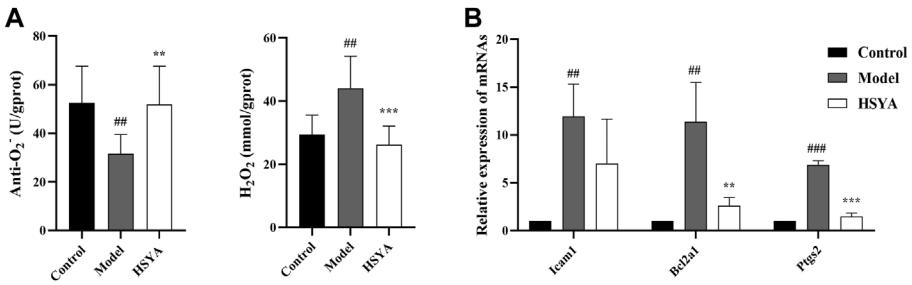

FIGURE 9
Effects of HSYA on the ROS and inflammatory genes. **(A)** The contents of Anti-O_2^- and H_2O_2; **(B)** The expression levels of inflammatory genes ($\bar{x} \pm s$, $n = 3$). $^{\#\#}p < 0.001$, $^{\#\#\#}p < 0.001$ vs. the control group; $^{**}p < 0.01$, $^{***}p < 0.001$ vs. the model group.

oxidative stress, lipid peroxidation of the liver membrane, inflammatory reaction, apoptosis, and necrosis of liver cells (Li et al., 2021a). Rats were used in this research to construct a CCl_4-induced ALI model, and the liver protective activity of HSYA was investigated. Using RNA-Seq to analyze the possible effects of HSYA on ALI, provides a reliable basis for further development of HSYA as a secure and reliable medication for liver damage avoidance and therapy.

In the metabolic process of the body, CCl_4 can generate CCL_3 and CCl_3O_2 free radicals through the cytochrome P450 enzymes, which may cause a structural collapse of liver cell membranes and enhance their permeability, and large amounts of intracellular enzymes, including ALT, AST, and ALP are released into the bloodstream, resulting in liver damage (Guo et al., 2016; Susilo et al., 2019). Consequently, the measurement of serum ALT, AST, and ALP activity is an essential criterion for assessing ALI (Xie et al., 2015).

Moreover, these ROS are capable of attacking fatty acids and causing peroxidation (Li et al., 2019). As the metabolic end-product of lipid peroxides, MDA can aggravate cell membrane damage by destroying the function, structure, and metabolism of biofilms (Lixin et al., 2019). SOD is the principal antioxidative enzyme, which can transform free radicals into water and molecular oxygen, thus reducing cell damage (Wu et al., 2017). Therefore, MDA and SOD are often considered sensitive oxidative stress indicators. Meanwhile, these free radicals can induce inflammatory, with the release of inflammatory factors, which accelerate the development of liver injuries (Li et al., 2020). In this study, it was discovered that HSYA considerably decreased the blood AST, ALT, and ALP levels of CCl_4-induced ALI in rats, alleviated the pathological alterations of liver tissue, decreased the MDA content, inflammatory factors (TNF-α, IL-1, and IL-6) levels, as well as increased the SOD activity. These findings imply that HSYA may effectively prevent rats with ALI caused by CCl_4.

The invention of RNA-seq technology facilitates the investigation of the molecular basis of illness. Thus, RNA-Seq was undertaken to study the DEGs and associated pathways after HSYA pretreatment that might help in the prevention and treatment of ALI by HSYA. We observed that HSYA pretreatment reversed most genes changed by CCl_4, such as Tymp, Fabp7, Serpina3c, Gpnmb, Il1r1, Creld2, etc. But, these genes have rarely been reported in ALI, so we performed qRT-PCR verification for them, and explored whether HSYA pretreatment exerts its functional role on ALI through these genes.

Tymp (thymidine phosphorylase) is a nucleoside metabolism enzyme induced by TNF-α, which is essential for angiogenesis, cell apoptosis and multiplication (Schwartz et al., 2010; Elamin et al., 2016). Earlier studies have shown that Tymp is overexpressed and associated with tumor growth in a variety of cancers (Marangoni et al., 2018; Ramadan et al., 2020; Gao et al., 2021; Poortahmasebi et al., 2022). But our research, compared to the control group, revealed that Tymp expression was considerably down-regulated in the model group, which could be reversed after HSYA intervention. The reason why the model group's Tymp expressions were lower, despite the fact that the TNF-α expressions were greater in the model group, remains unanswered. It's the first research to examine the Tymp expression in rats with ALI caused by CCl_4. Although the explanation of this surprising discovery is unclear, it heavily implies that the livers of rats with ALI may contain unique Tymp downregulation that are more efficient than TNF-α. Zhao et al. (2018) confirmed that Tymp could inhibit the purine, pyrimidine, and bile acid metabolism levels. We suspected that the Tymp expression levels in rats with ALI were inhibited by an increase in thymidine demand, but further fundamental research is required to investigate this possibility.

Fabp7 is a fatty acid-binding protein of the brain type. Recently, Zhang et al. (2013) reported that Fabp7 participates in the absorption and transport of fatty acids, as well as the control of other biological functions, like signal conduction, proliferation, and differentiation. Last but not least, it also performs a key function in oxidative stress resistance; lower Fabp could induce hepatocyte injury by encouraging the production of an abundance of ROS and initiating lipid peroxidation. Prior studies have shown that the Fabp expression decreased significantly after dexamethasone feeding, and the change in Fabp level occurred before the increase of hepatic and serum cholesterol levels, demonstrating that Fabp is an indicator of early hepatic damage (Rajaraman et al., 2007; Tu et al., 2021). Several observations indicate that some hepatoprotective medications, like clofibrate, diacerein, and icariin, can enhance the antioxidative capability of damaged liver cells by inducing Fabp expression, further reducing cell apoptosis and necrosis, and improve liver function (Rajaraman et al., 2007; Liu et al., 2014; Ibrahim et al., 2021). Consistent with the above reports, the present study showed that Fabp7 was down-regulated in the model group, and this process could be reversed after HSYA intervention, suggesting that HSYA has a substantial beneficial influence against CCl_4-induced ALI. Its mechanisms may include decreasing oxidative stress and improve Fabp7 expression.

In the rat, serpina3 was annotated as either serpina3k or serpina3c (Sánchez-Navarro et al., 2022). It is crucial for oxidative stress and inflammatory response, inflammatory response, tumor angiogenesis, apoptosis, proliferation, and migration (Yao et al., 2013; Jing et al., 2019; Ji et al., 2020; Qian et al., 2021). Some studies have shown that serpina3c participates in a series of pathophysiological processes: metabolic diseases, vascular diseases, optic nerve injury, etc. (Zheng et al., 2017; Choi et al., 2020; Qian et al., 2021). To our knowledge, until now, there has been no functional study on ALI-associated serpina3c. In the current experiment, serpina3c expression was dramatically decreased in the model group, whereas this decline was reversible with HSYA intervention. This finding suggested that HSYA may inhibit peroxidation and inflammation from protecting the liver from damage. Nevertheless, the precise mechanism may be explored deeper.

Glycoprotein nonmetastatic melanoma protein b (Gpnmb) contributes to osteoblast differentiation, inflammatory regulation, and tissue remodeling (Li et al., 2010; Abdelmagid et al., 2015; Nickl et al., 2021). Recently, some liver diseases have been associated with the expression of Gpnmb, such as ALI, cirrhosis, and alcohol-associated hepatitis (Onaga et al., 2003; Haralanova-Ilieva et al., 2005; Harris et al., 2022). Michalinos et al. (2020) found that Gpnmb was upregulated in the liver and kidneys following hepatic damage, but after treatment with hepatoprotective drugs, its expression was significantly decreased. Similar to the preceding outcomes, in this work, we observed that HSYA could drastically reduce the hepatic expression levels of Gpnmb in rats with CCl_4-induced ALI, suggesting that this gene may be a potential target for intervention in ALI.

The interleukin-1 receptor (IL-1R) mediates several physiologic activities of interleukin-1 (IL-1) to trigger a pro-inflammatory immunological system (Anzaghe et al., 2019; Li et al., 2021b). IL1R1 is overexpressed in some liver diseases, such as ALI, liver fibrosis, and liver cancer (Gehrke et al., 2018; Dang et al., 2020; Li et al., 2021c). The present study revealed that IL1R1 expression was considerably higher in the model group than in the control group, and obviously decreased after HSYA intervention, suggesting that this gene may be utilized as a diagnostic marker for ALI.

Creld2 is a ~50 kDa secretory glycoprotein (Oh-hashi et al., 2009). Some studies confirmed Creld2 is the crucial gene and a viable therapeutic target for hepatic steatosis and hepatocellular carcinoma (Liu et al., 2019; Kern et al., 2021). In the current research, compatible with the study of RNA-Seq, qRT-PCR suggested that HSYA can reduce Creld2 levels in rats with CCl_4-induced ALI. Although no studies have reported the correlation between Creld2 and ALI, Creld2 was discovered to be a new ER stress-inducible gene (Oh-hashi et al., 2009). ERS is closely related to ALI (Cai et al., 2022), so we suspected that this gene is closely related to ALI, and HSYA may inhibit ERS by regulating the expression of Creld2 to protect the liver from damage.

The above transcriptomics results analyzed the DEGs in the liver for CCl_4-induced under HSYA pretreatment. RNA-Seq and qRT-PCR studies yielded identical outcomes, supporting the validity of RNA-Seq data. We speculate that these genes may be the key genes for the diagnosis and prevention of ALI.

Meanwhile, our investigation revealed that HSYA might exhibit benefits for preventing ALI *via* numerous pathways, including those linked to inflammation and lipid metabolism. Pathways involved in inflammation include the TNF, NF-kappa B, NOD-like receptor signaling pathways, and pathways involved in lipid metabolism include retinol metabolism, and PPAR signaling pathway. It has been reported that retinol metabolism and PPAR signaling pathway are closely related to acute liver injury (Chen et al., 2019; Yan et al., 2022).

According to the transcriptome results, we further explored the exact possible mechanisms of HSYA on CCl_4-induced ALI. ROS are a group of highly reactive oxygen-containing substances, mainly including anti-O_2^-, hydroxyl radical (·OH), and hydrogen peroxide (H_2O_2) (Moloney and Cotter, 2018). Excessive ROS can induce oxidative stress in the liver and inhibit antioxidant stress defense pathways (Zhou et al., 2019). Some studies have confirmed that CCl_4 leads to necrosis and apoptosis of liver cells by increasing content of ROS, thus causing ALI (Xu et al., 2022). Therefore, reducing ROS contents is important for the prevention of CCl_4-induced ALI. In this study, we found that in the model group, the content of H_2O_2 was significantly increased and the level of anti-O_2^- was markedly decreased. However, after HSYA intervention, the phenomenon was able to be reversed. Meanwhile, the inflammatory response was researched. Inflammation plays an essential role in the process of ALI (Huang et al., 2017). Moreover, we selected three inflammatory genes in the NF-kB signaling pathway to confirm. The results showed that the gene expression levels of Icam1, Bcl2a1, and Ptgs2 in the model group were significantly higher than those of the control group. In the HSYA group, Icam1, Bcl2a1, and Ptgs2 expression levels were significantly lower than that of the model group. Combined with the above detected indicators, MDA, SOD and inflammatory factors (TNF-α, IL-1, and IL-6), it was further suggested that HSYA can protect the liver from damage by inhibiting inflammatory response and oxidative stress.

5 Conclusion

In a word, HSYA may prevent CCl_4-induced ALI through a number of mechanisms, as predicted from RNA-Seq analysis and experimentally confirmed. This research demonstrated that HSYA ameliorated hepatic pathological damage and function; the possible underlying molecular mechanism is that HSYA protects the liver from damage by decreasing oxidative stress, inflammatory response, regulating the Tymp, Fabp7, Serpina3c, Gpnmb, Il1r1, Creld2, and other genes expression levels as well as the retinol metabolism, PPAR, NF-kappa B, and NOD-like receptor signaling pathways. This work may help us comprehend the course of ALI and give a new proof that HSYA prevents ALI. However, more testing is required to confirm discovered genes and pathways.

Data availability statement

The original contributions presented in the study are included in the article/Supplementary Material, further inquiries can be directed to the corresponding author.

Ethics statement

The animal study was reviewed and approved by the Animal Care and Use Committee of Inner Mongolia Medical University (No. YKD202001020).

Author contributions

XH and LM: carried out the studies, and authored the paper. DY was involved in animal experiments. ZZ, YM, RJ, BY, DY, and LM provided suggestions for the study design of the article. Each author made contributions to the article.

Funding

This research was supported by the Natural Science Foundation of Inner Mongolia Autonomous Region (2020MS08040) and the National Natural Science Foundation of China (No. 81960759).

Conflict of interest

The authors declare that the research was conducted in the absence of any commercial or financial relationships that could be construed as a potential conflict of interest.

Publisher's note

References

Abdelmagid, S. M., Sondag, G. R., Moussa, F. M., Belcher, J. Y., Yu, B., Stinnett, H., et al. (2015). Mutation in osteoactivin promotes receptor activator of NFκB ligand (RANKL)-mediated osteoclast differentiation and survival but inhibits osteoclast function. *J. Biol. Chem.* 290 (33), 20128–20146. doi:10.1074/jbc.M114.624270

Åberg, F., Helenius-Hietala, J., Puukka, P., Färkkilä, M., and Jula, A. (2018). Interaction between alcohol consumption and metabolic syndrome in predicting severe liver disease in the general population. *Hepatol. Baltim. Md.)* 67 (6), 2141–2149. doi:10.1002/hep.29631

Al-Dossari, M. H., Fadda, L. M., Attia, H. A., Hasan, I. H., and Mahmoud, A. M. (2020). Curcumin and selenium prevent lipopolysaccharide/diclofenac-induced liver injury by suppressing inflammation and oxidative stress. *Biol. Trace Elem. Res.* 196 (1), 173–183. doi:10.1007/s12011-019-01910-4

Ali, H., Jahan, A., Samrana, S., Ali, A., Ali, S., Kabir, N., et al. (2021). Hepatoprotective potential of pomegranate in curbing the incidence of acute liver injury by alleviating oxidative stress and inflammatory response. *Front. Pharmacol.* 12, 694607. doi:10.3389/fphar.2021.694607

Allard, J., Le Guillou, D., Begriche, K., and Fromenty, B. (2019). Drug-induced liver injury in obesity and nonalcoholic fatty liver disease. *Adv. Pharmacol.* 85, 75–107. doi:10.1016/bs.apha.2019.01.003

Anzaghe, M., Resch, T., Schaser, E., Kronhart, S., Diez, C., Niles, M. A., et al. (2019). Organ-specific expression of IL-1 receptor results in severe liver injury in type I interferon receptor deficient mice. *Front. Immunol.* 10, 1009. doi:10.3389/fimmu.2019.01009

Ao, H., Feng, W., and Peng, C. (2018). Hydroxysafflor yellow A: A promising therapeutic agent for a broad spectrum of diseases. *Evidence-based complementary Altern. Med.* 2018, 8259280. doi:10.1155/2018/8259280

Bai, X., Wang, W. X., Fu, R. J., Yue, S. J., Gao, H., Chen, Y. Y., et al. (2020). Therapeutic potential of hydroxysafflor yellow A on cardio-cerebrovascular diseases. *Front. Pharmacol.* 11, 01265. doi:10.3389/fphar.2020.01265

Cai, J., Sun, Z., Zhang, L., and Xu, H. (2022). SERP1 reduces inchoate acute hepatic injury through regulation of endoplasmic reticulum stress via the GSK3β/β-catenin/TCF/LEF signaling pathway. *Mol. Med. Rep.* 25 (6), 193. doi:10.3892/mmr.2022.12709

Chen, R., Wang, Q., Zhao, L., Yang, S., Li, Z., Feng, Y., et al. (2019). Lomatogonium rotatum for treatment of acute liver injury in mice: A metabolomics study. *Metabolites* 9 (10), 227. doi:10.3390/metabo9100227

Choi, Y., Choi, H., Yoon, B. K., Lee, H., Seok, J. W., Kim, H. J., et al. (2020). Serpina3c regulates adipogenesis by modulating insulin growth factor 1 and integrin signaling. *iScience* 23 (3), 100961. doi:10.1016/j.isci.2020.100961

Dang, Y., Chen, J., Feng, W., Qiao, C., Han, W., Nie, Y., et al. (2020). Interleukin 1β-mediated HOXC10 overexpression promotes hepatocellular carcinoma metastasis by upregulating PDPK1 and VASP. *Theranostics* 10 (8), 3833–3848. doi:10.7150/thno.41712

Elamin, Y. Y., Rafee, S., Osman, N., O Byrne, K. J., and Gately, K. (2016). Thymidine phosphorylase in cancer; enemy or friend? *Cancer Microenviron.* 9 (1), 33–43. doi:10.1007/s12307-015-0173-y

Gao, Y., Zens, P., Su, M., Gemperli, C. A., Yang, H., Deng, H., et al. (2021). Chemotherapy-induced CDA expression renders resistant non-small cell lung cancer cells sensitive to 5'-deoxy-5-fluorocytidine (5'-DFCR). *J. Exp. Clin. Cancer Res.* 40 (1), 138. doi:10.1186/s13046-021-01938-2

Gehrke, N., Hövelmeyer, N., Waisman, A., Straub, B. K., Weinmann-Menke, J., Wörns, M. A., et al. (2018). Hepatocyte-specific deletion of IL1-RI attenuates liver injury by blocking IL-1 driven autoinflammation. *J. Hepatol.* 68 (5), 986–995. doi:10.1016/j.jhep.2018.01.008

Guo, S., Guo, T., Cheng, N., Liu, Q., Zhang, Y., Bai, L., et al. (2016). Hepatoprotective standardized EtOH-water extract from the seeds of *Fraxinus rhynchophylla* Hance. *J. Tradit. Complement. Med.* 7 (2), 158–164. doi:10.1016/j.jtcme.2016.05.001

Guo, X., Zheng, M., Pan, R., Zang, B., Gao, J., Ma, H., et al. (2019). Hydroxysafflor yellow A (HSYA) targets the platelet-activating factor (PAF) receptor and inhibits human bronchial smooth muscle activation induced by PAF. *Food Funct.* 10 (8), 4661–4673. doi:10.1039/c9fo00896a

Han, D., Wei, J., Zhang, R., Ma, W., Shen, C., Feng, Y., et al. (2016). Hydroxysafflor yellow A alleviates myocardial ischemia/reperfusion in hyperlipidemic animals through the suppression of TLR4 signaling. *Sci. Rep.* 6, 35319. doi:10.1038/srep35319

Haralanova-Ilieva, B., Ramadori, G., and Armbrust, T. (2005). Expression of osteoactivin in rat and human liver and isolated rat liver cells. *J. Hepatol.* 42 (4), 565–572. doi:10.1016/j.jhep.2004.12.021

Harris, P. S., Michel, C. R., Yun, Y., McGinnis, C. D., Assiri, M. A., Ahmadi, A. R., et al. (2022). Proteomic analysis of alcohol-associated hepatitis reveals glycoprotein NMB (GPNMB) as a novel hepatic and serum biomarker. *AlcoholFayettev. N.Y.)* 99, 35–48. doi:10.1016/j.alcohol.2021.11.005

Huang, Q. H., Xu, L. Q., Liu, Y. H., Wu, J. Z., Wu, X., Lai, X. P., et al. (2017). Polydatin protects rat liver against ethanol-induced injury: Involvement of CYP2E1/ROS/Nrf2 and TLR4/NF-κB p65 pathway. *Evidence-based complementary Altern. Med. eCAM* 2017, 7953850. doi:10.1155/2017/7953850

Ibrahim, M. A., Abdelzaher, W. Y., Ibrahim, Y. F., Ahmed, A. F., Welson, N. N., Al-Rashed, S., et al. (2021). Diacerein protects rats with liver ischemia/reperfusion damage: Down-regulation of TLR4/NFκ-B signaling pathway. *Biomed. Pharmacother. = Biomedecine Pharmacother.* 134, 111063. doi:10.1016/j.biopha.2020.111063

Ji, J. J., Qian, L. L., Zhu, Y., Wu, Y. P., Guo, J. Q., Ma, G. S., et al. (2020). Serpina3c protects against high-fat diet-induced pancreatic dysfunction through the JNK-related pathway. *Cell. Signal.* 75, 109745. doi:10.1016/j.cellsig.2020.109745

Jiang, Z., Zhou, X., Li, R., Michal, J. J., Zhang, S., Dodson, M. V., et al. (2015). Whole transcriptome analysis with sequencing: methods, challenges and potential solutions. *Cell. Mol. Life Sci.* 72 (18), 3425–3439. doi:10.1007/s00018-015-1934-y

Jing, Y., Yang, D., Fu, Y., Wang, W., Yang, G., Yuan, F., et al. (2019). Neuroprotective effects of Serpina3k in traumatic brain injury. *Front. Neurol.* 10, 1215. doi:10.3389/fneur.2019.01215

Kern, P., Balzer, N. R., Blank, N., Cygon, C., Wunderling, K., Bender, F., et al. (2021). Creld2 function during unfolded protein response is essential for liver metabolism homeostasis. *FASEB J. official Publ. Fed. Am. Soc. Exp. Biol.* 35 (10), e21939. doi:10.1096/fj.202002713RR

Li, B., Castano, A. P., Hudson, T. E., Nowlin, B. T., Lin, S. L., Bonventre, J. V., et al. (2010). The melanoma-associated transmembrane glycoprotein Gpnmb controls trafficking of cellular debris for degradation and is essential for tissue repair. *FASEB J. official Publ. Fed. Am. Soc. Exp. Biol.* 24 (12), 4767–4781. doi:10.1096/fj.10-154757

Li, D., Song, Y., Wang, Y., Guo, Y., Zhang, Z., Yang, G., et al. (2020). *Nos2* deficiency enhances carbon tetrachloride-induced liver injury in aged mice. *Iran. J. Basic Med. Sci.* 23 (5), 600–605. doi:10.22038/ijbms.2020.39528.9380

Li, D., Wang, Z., Zhang, C., and Xu, C. (2021). IL-1R1 deficiency impairs liver regeneration after 2/3 partial hepatectomy in aged mice. *Turkish J. Biol. = Turk biyoloji dergisi* 45 (2), 225–234. doi:10.3906/biy-2010-51

Li, N., Liu, F. J., Li, D. D., Sun, C. X., Li, J., Qu, M. H., et al. (2019). Hepatopoietin cn (HPPCn) generates protective effects on acute liver injury. *Front. Pharmacol.* 10, 646. doi:10.3389/fphar.2019.00646

Li, T., Su, G., and Zhao, Y. (2021). Anti-hepatic fibrosis effects of AD-2 affecting the Raf-MEK signaling pathway and inflammatory factors in thioacetamide-induced liver injury. *J. Food Sci.* 86 (6), 2753–2765. doi:10.1111/1750-3841.15731

Li, X., Liu, X., Zhang, Y., Cheng, C., Fan, J., Zhou, J., et al. (2021). Hepatoprotective effect of apolipoprotein A4 against carbon tetrachloride induced acute liver injury through mediating hepatic antioxidant and inflammation response in mice. *Biochem. Biophys. Res. Commun.* 534, 659–665. doi:10.1016/j.bbrc.2020.11.024

Li, Y., Shi, Y., Sun, Y., Liu, L., Bai, X., Wang, D., et al. (2017). Restorative effects of hydroxysafflor yellow A on hepatic function in an experimental regression model of hepatic fibrosis induced by carbon tetrachloride. *Mol. Med. Rep.* 15 (1), 47–56. doi:10.3892/mmr.2016.5965

Liu, G. M., Zeng, H. D., Zhang, C. Y., and Xu, J. W. (2019). Key genes associated with diabetes mellitus and hepatocellular carcinoma. *Pathol. Res. Pract.* 215 (11), 152510. doi:10.1016/j.prp.2019.152510

Liu, P., Jin, X., Lv, H., Li, J., Xu, W., Qian, H. H., et al. (2014). Icaritin ameliorates carbon tetrachloride-induced acute liver injury mainly because of the antioxidative function through estrogen-like effects. *Vitro Cell. Dev. Biol. Anim.* 50 (10), 899–908. doi:10.1007/s11626-014-9792-8

Lixin, X., Erli, G., Songping, H., Yonggen, Z., Wang, J., and Lijun, Y. (2019). Yi guan jian, a traditional Chinese herbal medicine, alleviates carbon tetrachloride-induced liver injury. *Evidence-based complementary Altern. Med.* 2019, 9824728. doi:10.1155/2019/9824728

Lu, R. L., Jin, R., Zhang, Z. Y., Gong, Y. P., and Ma, L. J. (2021). Honghua qinggan shisanwei pill alleviates acute liver injury in rats by inhibiting JNK/c-Jun signaling pathway. *Pharmacol. Clin. Chin. Materia Medica* 37 (03), 21–26. doi:10.13412/j.cnki.zyyl.2021.03.005

Lv, X. M., Lu, R. L., and Ma, L. J. (2018). Protective effect of Honghua (Safflower, Flos Carthami) on acute liver injury induced by carbon tetrachloride in rats and mechanism study. *J. Beijing Univ. Traditional Chin. Med.* 41 (11), 943–949.

Marangoni, E., Laurent, C., Coussy, F., El-Botty, R., Château-Joubert, S., Servely, J. L., et al. (2018). Capecitabine efficacy is correlated with TYMP and RB1 expression in PDX established from triple-negative breast cancers. *Clin. Cancer Res.* 24 (11), 2605–2615. doi:10.1158/1078-0432.CCR-17-3490

Marra, F., Smolders, E. J., El-Sherif, O., Boyle, A., Davidson, K., Sommerville, A. J., et al. (2021). Recommendations for dosing of repurposed COVID-19 medications in patients with renal and hepatic impairment. *Drugs R. D.* 21 (1), 9–27. doi:10.1007/s40268-020-00333-0

Michalinos, A., Tsaroucha, A. K., Lambropoulou, M., Schizas, D., Valsami, G., Kostomitsopoulos, N., et al. (2020). Glycoprotein non-metastatic melanoma B expression after hepatic ischemia reperfusion and the effect of silibinin. *Transl. Gastroenterol. Hepatol.* 5, 7. doi:10.21037/tgh.2019.11.01

Moloney, J. N., and Cotter, T. G. (2018). ROS signalling in the biology of cancer. *Semin. Cell Dev. Biol.* 80, 50–64. doi:10.1016/j.semcdb.2017.05.023

Nickl, B., Qadri, F., and Bader, M. (2021). Anti-inflammatory role of Gpnmb in adipose tissue of mice. *Sci. Rep.* 11 (1), 19614. doi:10.1038/s41598-021-99090-6

Oh, I. S., and Park, S. H. (2015). Immune-mediated liver injury in hepatitis B virus infection. *Immune Netw.* 15 (4), 191–198. doi:10.4110/in.2015.15.4.191

Oh-hashi, K., Koga, H., Ikeda, S., Shimada, K., Hirata, Y., and Kiuchi, K. (2009). CRELD2 is a novel endoplasmic reticulum stress-inducible gene. *Biochem. Biophys. Res. Commun.* 387 (3), 504–510. doi:10.1016/j.bbrc.2009.07.047

Onaga, M., Ido, A., Hasuike, S., Uto, H., Moriuchi, A., Nagata, K., et al. (2003). Osteoactivin expressed during cirrhosis development in rats fed a choline-deficient, L-amino acid-defined diet, accelerates motility of hepatoma cells. *J. Hepatol.* 39 (5), 779–785. doi:10.1016/s0168-8278(03)00361-1

Poortahmasebi, V., Nejati, A., Abazari, M. F., Nasiri Toosi, M., Ghaziasadi, A., Mohammadzadeh, N., et al. (2022). Identifying potential new gene expression-based biomarkers in the peripheral blood mononuclear cells of hepatitis B-related hepatocellular carcinoma. *Can. J. Gastroenterol. Hepatol.* 2022, 9541600. doi:10.1155/2022/9541600

Qian, L. L., Ji, J. J., Guo, J. Q., Wu, Y. P., Ma, G. S., and Yao, Y. Y. (2021). Protective role of serpina3c as a novel thrombin inhibitor against atherosclerosis in mice. *Clin. Sci.* 135 (3), 447–463. (London, England : 1979). doi:10.1042/CS20201235

Rajaraman, G., Wang, G. Q., Yan, J., Jiang, P., Gong, Y., and Burczynski, F. J. (2007). Role of cytosolic liver fatty acid binding protein in hepatocellular oxidative stress: effect of dexamethasone and clofibrate treatment. *Mol. Cell. Biochem.* 295 (1-2), 27–34. doi:10.1007/s11010-006-9268-6

Ramadan, R. A., Moghazy, T. F., Hafez, R., Morsi, H., Samir, M., and Shamesya, M. (2020). Significance of expression of pyrimidine metabolizing genes in colon cancer. *Arab. J. Gastroenterol.* 21 (3), 189–193. doi:10.1016/j.ajg.2020.07.006

Sánchez-Navarro, A., Murillo-de-Ozores, A. R., Pérez-Villalva, R., Linares, N., Carbajal-Contreras, H., Flores, M. E., et al. (2022). Transient response of serpinA3 during cellular stress. *FASEB J. official Publ. Fed. Am. Soc. Exp. Biol.* 36 (3), e22190. doi:10.1096/fj.202101912R

Schwartz, P. A., Vetticatt, M. J., and Schramm, V. L. (2010). Transition state analysis of thymidine hydrolysis by human thymidine phosphorylase. *J. Am. Chem. Soc.* 132 (38), 13425–13433. doi:10.1021/ja105041j

Susilo, R., Winarni, D., Husen, S. A., Hayaza, S., Punnapayak, H., Wahyuningsih, S., et al. (2019). Hepatoprotective effect of crude polysaccharides extracted from *Ganoderma lucidum* against carbon tetrachloride-induced liver injury in mice. *Vet. World* 12 (12), 1987–1991. doi:10.14202/vetworld.2019.1987-1991

Tan, L., Wang, Y., Jiang, Y., Wang, R., Zu, J., and Tan, R. (2020). Hydroxysafflor yellow A together with blood-brain barrier regulator lexiscan for cerebral ischemia reperfusion injury treatment. *ACS omega* 5 (30), 19151–19164. doi:10.1021/acsomega.0c02502

Tao, X. M., Li, D., Zhang, C., Wen, G. H., Wu, C., Xu, Y. Y., et al. (2021). Salvianolic acid B protects against acute and chronic liver injury by inhibiting Smad2C/L phosphorylation. *Exp. Ther. Med.* 21 (4), 341. doi:10.3892/etm.2021.9772

Tran, N. T., Gao, Z. X., Zhao, H. H., Yi, S. K., Chen, B. X., Zhao, Y. H., et al. (2015). Transcriptome analysis and microsatellite discovery in the blunt snout bream (*Megalobrama amblycephala*) after challenge with Aeromonas hydrophila. *Fish. Shellfish Immunol.* 45 (1), 72–82. doi:10.1016/j.fsi.2015.01.034

Tu, C., Xu, Z., Tian, L., Yu, Z., Wang, T., Guo, Z., et al. (2021). Multi-omics integration to reveal the mechanism of hepatotoxicity induced by dictamnine. *Front. Cell Dev. Biol.* 9, 700120. doi:10.3389/fcell.2021.700120

Wu, T., Li, J., Li, Y., and Song, H. (2017). Antioxidant and hepatoprotective effect of swertiamarin on carbon tetrachloride-induced hepatotoxicity via the Nrf2/HO-1 pathway. *Cell. Physiol. biochem.* 41 (6), 2242–2254. doi:10.1159/000475639

Xie, J., Liu, J., Chen, T. M., Lan, Q., Zhang, Q. Y., Liu, B., et al. (2015). Dihydromyricetin alleviates carbon tetrachloride-induced acute liver injury via JNK-dependent mechanism in mice. *World J. Gastroenterol.* 21 (18), 5473–5481. doi:10.3748/wjg.v21.i18.5473

Xu, Q., Deng, Y., Ming, J., Luo, Z., Chen, X., Chen, T., et al. (2022). Methyl 6-O-cinnamoyl-α-d-glucopyranoside ameliorates acute liver injury by inhibiting oxidative stress through the activation of Nrf2 signaling pathway. *Front. Pharmacol.* 13, 873938. doi:10.3389/fphar.2022.873938

Yan, R., Wang, K., Wang, Q., Jiang, H., Lu, Y., Chen, X., et al. (2022). Probiotic Lactobacillus casei Shirota prevents acute liver injury by reshaping the gut microbiota to alleviate excessive inflammation and metabolic disorders. *Microb. Biotechnol.* 15 (1), 247–261. doi:10.1111/1751-7915.13750

Yang, Z., Zhang, J., Wang, Y., Lu, J., and Sun, Q. (2021). Caveolin-1 deficiency protects mice against carbon tetrachloride-induced acute liver injury through regulating polarization of hepatic macrophages. *Front. Immunol.* 12, 713808. doi:10.3389/fimmu.2021.713808

Yao, Y., Li, L., Huang, X., Gu, X., Xu, Z., Zhang, Y., et al. (2013). SERPINA3K induces apoptosis in human colorectal cancer cells via activating the Fas/FasL/caspase-8 signaling pathway. *FEBS J.* 280 (14), 3244–3255. doi:10.1111/febs.12303

Zang, L., Shimada, Y., Nakayama, H., Kim, Y., Chu, D. C., Juneja, L. R., et al. (2019). RNA-seq based transcriptome analysis of the anti-obesity effect of green tea extract using zebrafish obesity models. *Mol. (Basel, Switz.* 24 (18), 3256. doi:10.3390/molecules24183256

Zhang, Y., Jiang, Z., Su, Y., Chen, M., Li, F., Liu, L., et al. (2013). Gene expression profiling reveals potential key pathways involved in pyrazinamide-mediated hepatotoxicity in Wistar rats. *J. Appl. Toxicol.* 33 (8), 807–819. doi:10.1002/jat.2736

Zhao, D. S., Jiang, L. L., Wang, L. L., Wu, Z. T., Li, Z. Q., Shi, W., et al. (2018). Integrated metabolomics and proteomics approach to identify metabolic abnormalities in rats with Dioscorea bulbifera rhizome-induced hepatotoxicity. *Chem. Res. Toxicol.* 31 (9), 843–851. doi:10.1021/acs.chemrestox.8b00066

Zhao, Q., Tang, P., Zhang, T., Huang, J. F., Xiao, X. R., Zhu, W. F., et al. (2020). Celastrol ameliorates acute liver injury through modulation of PPARα. *Biochem. Pharmacol.* 178, 114058. doi:10.1016/j.bcp.2020.114058

Zheng, X., Cui, H., Yin, Y., Zhang, Y., Zong, R., Bao, X., et al. (2017). SERPINA3K ameliorates the corneal oxidative injury induced by 4-hydroxynonenal. *Invest. Ophthalmol. Vis. Sci.* 58 (7), 2874–2883. doi:10.1167/iovs.17-21544

Zhou, W. B., Zhang, X. X., Cai, Y., Sun, W., and Li, H. (2019). Osthole prevents tamoxifen-induced liver injury in mice. *Acta Pharmacol. Sin.* 40 (5), 608–619. doi:10.1038/s41401-018-0171-y

Zou, J., Wang, N., Liu, M., Bai, Y., Wang, H., Liu, K., et al. (2018). Nucleolin mediated pro-angiogenic role of Hydroxysafflor Yellow A in ischaemic cardiac dysfunction: Post-transcriptional regulation of VEGF-A and MMP-9. *J. Cell. Mol. Med.* 22 (5), 2692–2705. doi:10.1111/jcmm.13552

frontiers | Frontiers in Pharmacology

TYPE Original Research
PUBLISHED 08 September 2022
DOI 10.3389/fphar.2022.951906

OPEN ACCESS

EDITED BY
Tatsunori Miyata,
Cleveland Clinic, United States

REVIEWED BY
Yan Zhang,
Fourth Military Medical University, China, University of Florence, Italy
Daniele Bani,
University of Florence, Italy
Kavita Jadhav,
AstraZeneca, United States
Ping Yao,
Huazhong University of Science and Technology, China

*CORRESPONDENCE
Shengli Cao,
shenglicao66@126.com
Changju Zhu,
fccpanj@zzu.edu.cn

†These authors have contributed equally to this work

SPECIALTY SECTION
This article was submitted to Gastrointestinal and Hepatic Pharmacology, a section of the journal Frontiers in Pharmacology

RECEIVED 24 May 2022
ACCEPTED 08 August 2022
PUBLISHED 08 September 2022

CITATION
Chen S, Yu Q, Song Y, Cui Z, Li M, Mei C, Cui H, Cao S and Zhu C (2022), Inhibition of macrophage migration inhibitory factor (MIF) suppresses apoptosis signal-regulating kinase 1 to protect against liver ischemia/reperfusion injury.
Front. Pharmacol. 13:951906.
doi: 10.3389/fphar.2022.951906

Inhibition of macrophage migration inhibitory factor (MIF) suppresses apoptosis signal-regulating kinase 1 to protect against liver ischemia/reperfusion injury

Sanyang Chen[1,2,3†], Qiwen Yu[3,4†], Yaodong Song[1,2], Zongchao Cui[1,2], Mengke Li[1,2], Chaopeng Mei[1,2], Huning Cui[1,2], Shengli Cao[3,4*] and Changju Zhu[1,2*]

[1]Department of Emergency Surgery, First Affiliated Hospital of Zhengzhou University, Zhengzhou, Henan, China, [2]Henan Medical Key Laboratory of Emergency and Trauma Research, Zhengzhou, China, [3]Henan Key Laboratory of Digestive Organ Transplantation, Zhengzhou, Henan, China, [4]Department of Hepatobiliary and Pancreatic Surgery, First Affiliated Hospital of Zhengzhou University, Zhengzhou, Henan, China

Background: Hepatic ischemia–reperfusion (I/R) injury is a major complication leading to surgical failures in liver resection, transplantation, and hemorrhagic shock. The role of cytokine macrophage migration inhibitory factor (MIF) in hepatic I/R injury is unclear.

Methods: We examined changes of MIF expression in mice after hepatic I/R surgery and hepatocytes challenged with hypoxia–reoxygenation (H/R) insult. Subsequently, MIF global knock-out mice and mice with adeno-associated-virus (AAV)-delivered MIF overexpression were subjected to hepatic I/R injury. Hepatic histology, the inflammatory response, apoptosis and oxidative stress were monitored to assess liver damage. The molecular mechanisms of MIF function were explored *in vivo* and *in vitro*.

Results: MIF was significantly upregulated in the serum whereas decreased in liver tissues of mice after hepatic I/R injury. MIF knock-out effectively attenuated I/R -induced liver inflammation, apoptosis and oxidative stress *in vivo* and *in vitro*, whereas MIF overexpression significantly aggravated liver injury. *Via* RNA-seq analysis, we found a significant decreased trend of MAPK pathway in MIF knock-out mice subjected hepatic I/R surgery. Using the apoptosis signal-regulating kinase 1 (ASK1) inhibitor NQDI-1 we determined that, mechanistically, the protective effect of MIF deficiency on hepatic I/R injury was dependent on the suppressing of the ASK1-JNK/P38 signaling pathway. Moreover, we found MIF inhibitor ISO-1 alleviate hepatic I/R injury in mice.

Conclusion: Our results confirm that MIF deficiency suppresses the ASK1-JNK/P38 pathway and protects the liver from I/R -induced injury. Our findings

suggest MIF as a novel biomarker and therapeutic target for the diagnosis and treatment of hepatic I/R injury.

KEYWORDS

MIF deficiency protects from hepatic I/R injury hepatic ischemia-reperfusion injury, macrophage migration inhibitory factor, apoptosis signal-regulating kinase 1, inflammation, apoptosis, oxidative stress

Introduction

Hepatic ischemia–reperfusion (I/R) injury is associated with high morbidity and mortality in patients following liver trauma, liver resection or transplantation, and can cause hemorrhagic shock (Chen et al., 2021). Liver I/R injury accounts for up to 10% of early transplantation failures in liver transplantation, although surgical and allograft preservation techniques have been greatly improved (Kong et al., 2021). Unfortunately, despite its profound clinical importance, there are no effective treatments available for liver I/R injury, and clinical therapy is mainly limited to the prevention and control of risk factors (Guo et al., 2020; Guan et al., 2021). Therefore, thorough understanding of the underlying mechanisms and effective intervention measures to limit I/R-induced liver damage are urgently needed.

The mechanisms of hepatic I/R injury are highly complex and have been the focus of investigation for decades. Numerous previous studies show that inflammation, highly reactive oxygen species (ROS), nitrogen monoxide (NO) and cell death are the most critical factors associated with pathophysiology of hepatic I/R injury (Yuan et al., 2021; Zhang et al., 2021). During the ischemic period, the impeded blood supply results in an imbalance between metabolic supplements and demands, and causes eNOS failure. In the reperfusion phase, reoxygenation of the ischemic liver can stimulate the generation of excessive ROS through activated nicotinamide adenine dinucleotide phosphate oxidases. Meanwhile, the excess NO reacts with ROS to generate peroxynitrite (ONOO-), resulting in endothelial dysfunction and aggravating liver damage (Ferrer-Sueta and Radi, 2009; Zhang et al., 2022). Additionally, reperfusion causes the infiltration of neutrophils, macrophages and other inflammatory cells to the ischemic liver. The intense oxidative stress and inflammatory response can directly result in severe or even irreversible apoptosis, tissue injury, and organ dysfunction (Zhou et al., 2021a; Sahu et al., 2021). Therefore, determining strategies to suppress inflammation, oxidative stress and apoptosis could effectively ameliorate I/R-induced liver injury and contribute to the identification of novel pharmacological interventions to improve patient prognosis.

MIF was first discovered in 1966 as a pro-inflammatory cytokine that retains macrophages at sites of inflammation by preventing their random migration (Schindler et al., 2021). MIF is widely expressed in many cell types including lymphocytes, macrophages and non-immune cells such as hepatocytes, endothelial, epithelial, and tumor cells (de Azevedo et al., 2020). It is released from pre-formed storage pools when stimulated by inflammation. In addition to promoting inflammatory response, MIF displays various biological activities such as pro-apoptotic (Zhao et al., 2020), pro-oxidative-stress (Yang et al., 2020) and pro-angiogenic functions (Xu et al., 2008). Moreover, MIF has been reported to activate JNK and P38 in several disease, which play key roles during hepatic I/R injury. However, the function of MIF in hepatic I/R injury remains unknown.

The present study delineated that MIF plays an important role in hepatic I/R injury by aggravating inflammation, apoptosis, and oxidative stress *in vitro* and *in vivo*. Further molecular experiments showed that MIF deficiency could inhibit apoptosis signal-regulating kinase 1 (ASK1) activation and downstream JNK and p38 signaling during hepatic I/R injury. Our findings suggest MIF as a novel biomarker and therapeutic target for the diagnosis and treatment of hepatic I/R injury.

Materials and methods

Animals

Male C57 BL/6 mice and MIF knock out (KO) mice (C57 BL/6 background as previously described) (Zhu et al., 2020) aged 8–10 weeks (25 ± 2 g) were housed in a specific pathogen-free (SPF) facility under a controlled environment with 12-h light/dark photocycle (temperature, 23 ± 2°C). Food and water were available *ad libitum* throughout the study period. Animals received human care in adherence with the "Guide for the Care and Use of Laboratory Animals" prepared by the National Academy of Sciences and published by the National Institutes of Health (NIH; publication 86–23 revised in 1985). All animal procedures were approved by the Ethics Committee of The First Affiliated Hospital of Zhengzhou University. For studies in MIF overexpression in liver, we transduced adeno-associated virus (AAV) 8 system carrying GFP scramble (as a negative control) or MIF (designed and synthesized by Hanbio, Shanghai, China) into mice at a dose of 1×10^{12} vg (200 μl per mice) through tail-vein injection.

Murine model of I/R injury

Partial (70%) liver warm ischemia mouse model was established as previously described (Chen et al., 2021).

Briefly, mice were first anesthetized by pentobarbital sodium (60 mg/kg; Sigma) and subjected to midline laparotomy. A microvascular clip was used to clamp the left and middle portal vein and hepatic artery branches to interrupt the blood supply of the liver. After 1 h of ischemia, the clamp was removed for reperfusion. After 6 h reperfusion, the animals were sacrificed to collect liver and serum samples for further analysis. The residual blood was discharged by portal vein injection of normal saline. Part of the liver tissue was stored in liquid nitrogen and then transferred to the refrigerator at −80°C. Another part of liver tissue was preserved in 10% formalin for pathological examination. As a sham control group, mice underwent the same surgical procedure but without vasculature clamping. To inhibit MIF and ASK1 in mice, specific ASK1 inhibitor NQDI-1 (Sigma; 10 mg/kg, dissolution by DMSO and dilute with PBS to 1.25 mg/ml, 200 μl per mice) and MIF inhibitor ISO-1 (MedChemExpress LLC; 3.5 mg/kg, dissolution by DMSO and dilute with PBS to 0.44 mg/ml, 200 μl per mice) were intraperitoneally injected 2 h before the ischemic surgery. The same volume of DMSO (diluted to 0.1% by PBS) was used as control (Xu et al., 2020; Liu et al., 2021).

Serum aminotransferase activities

Serum concentrations of alanine aminotransferase (ALT), aspartate aminotransferase (AST) and lactate dehydrogenase (LDH) were detected using the ADVIA 2400 Chemistry System (Siemens, Tarrytown, NY, United States) according to the manufacturer's protocols.

Liver hematoxylin and eosin and immunohistochemical staining

H&E staining was used to assess the necrosis of the liver. Paraffin-embedded sections of mouse liver tissues were sectioned to 4 μm slides. After deparaffinization and rehydration, the histomorphology analysis was carried out using H&E staining. For IHC staining, liver samples were dehydrated, paraffin embedded and sectioned to 4 μm slides. After incubating with primary antibodies of CD68 (GB11067, Servicebio, 1:50 dilution), Ly6g (GB11229, Servicebio, 1: 50 dilution), and BAX (GB11007-1, Servicebio, 1:50 dilution) at 4°C overnight, the slides were washed and incubated with appropriate secondary antibodies conjugated with HRP were added for 1 h at room temperature. A 3,3′-diaminobenzidine (DAB) (ZLI-9032, Zhongshan Biotech, Beijing, China) was used to observed the sections followed by hematoxylin counterstaining. Images were visualized using a light microscope (Olympus, Tokyo, Japan).

TdT-mediated dUTP nick-end labeling (TUNEL) staining

TUNEL staining was carried out to detect apoptosis in liver tissues according to the manufacturer's protocol (Roche, 11684817910) as described previously (Pan et al., 2021).

Enzyme-linked immunosorbent assay

The liver tissue sample was homogenized with homogenizer. ELISA was performed to detect the oxidative stress related factors malondialdehyde (MDA), superoxide dismutase (SOD), Glutathione (GSH) (ab118970, Abcam, Cambridge, United Kingdom) using commercial kits (MDA, ab118970, Abcam, Cambridge, United Kingdom; SOD, CSB-E08556m, CUSABIO, Wuhan, China; GSH, CSB-E13068m, CUSABIO, Wuhan, China) following the manufacturer's instructions.

RNA-seq analysis

Total RNA was isolated using mirVana miRNA Isolation Kit (Ambion) followingthe manufacturer's protocol. RNA integrity was evaluated using the Agilent 2,100 Bioanalyzer (Agilent Technologies, Santa Clara, CA, United States). The libraries were constructed using TruSeq Stranded mRNA LTSample Prep Kit (Illumina, San Diego, CA, United States) according to the manufacturer's instructions. Then these libraries were sequenced on the Illumina sequencing platform (HiSeqTM 2,500 or Illumina HiSeq X Ten) and 125/150 bp paired-end reads were generated. FPKM value of each gene was calculated using cufflinks, and the read counts of each genewere obtained by htseq-count. DEGs were identified using the DESeq (2012) R package functions estimateSizeFactors and nbinomTest.

Cell lines culture and treatment

The mouse AML12 hepatic cell line was purchased from the Cell Bank of the Chinese Academy of Sciences. The cells were cultured in Dulbecco's modified Eagle's medium (DMEM) supplemented with 10% fetal bovine serum, and 1% penicillin-streptomycin. For the hypoxia-reoxygenation (H/R) model, cells were challenged with sugar-free, serum-free DMEM under hypoxia conditions (1% O2, 5% CO2, and 94% N2) in a modular incubator chamber (Biospherix, Lacona, NY, United States). After hypoxia for 6 h, the hepatocytes were returned to normal air conditions (95% air, 5% CO2) and medium incubating 6 h for reoxygenation. The full-length homo MIF cDNA was cloned into pHAGE-3×flag plasmids to express Flag-tagged MIF, Flag-tagged recombinant proteins.

Several siRNA sequences for MIF were designed, and the knockdown sequences were constructed into the pLKO.1 vector. The primers used in this study are listed in Supplementary Table S3.

Reactive oxygen species measurement

ROS production in mouse liver tissues were detected by DHE staining as previously described (Li et al., 2021). Dihydroethidium (DHE) can freely enter cells through living cells and be oxidized by ROS in cells to form oxyethidium; Ethidium oxide can be incorporated into chromosomal DNA to produce red fluorescence. In brief, fresh frozen liver sections (8 μm) were immediately incubated with 5 μM dihydroethidium (Invitrogen) at 37°C for 15 min. After the incubation, and then visualized by using a fluorescence microscope (Olympus DX51). Excitation and emission wavelength (DAPI ultraviolet excitation wavelength 330–380nm, emission wavelength 420nm, blue light; FITC excitation wavelength 465–495nm, emission wavelength 515–555 nm, green light; Cy3 excitation wavelength 510–560, emission wavelength 590 nm, red light).

Quantitative real-time polymerase chain reaction

The mRNA expression in liver tissues and cell samples were detected using qRT-PCR as described previously (Chen et al., 2021). TRIzol reagent (Invitrogen) was used to extract total RNA. cDNA was reverse transcribed by using the HiScript® III RT SuperMix for qPCR (+gDNA wiper) (Cat# R312, Vazme, Nanjing, China) and qRT-PCR was performed with ChamQTM SYBR qPCR Master Mix (Cat# Q311-02, Vazme, Nanjing, China). The mRNA levels were normalized against *ß*-actin expression. Primer sequences of the target genes are listed in Supplementary Table S1.

Western blot

The protein levels in liver tissues and cell samples were detected using Western blot analysis as previously reported (Guo et al., 2020). Briefly, RIPA lysis buffer (65 mM Tris-HCl pH 7.5, 150 mM NaCl, 1 mM EDTA, 1% Nonidet P-40, 0.5% sodium deoxycholate and 0.1% SDS) with Protease and Phosphatase Inhibitor Cocktail (04693132001; Roche) was used to extract total proteins. Protein concentrations were detected using the BCA Protein Assay Kit (23225; Thermo Fisher Scientific) and were separated by SDS-PAGE, transferred to a nitrocellulose PVDF membrane. After incubation with primary and secondary antibodies, the blots were performed with enhanced chemiluminescence (ECL) reagents (170–5,061; Bio-Rad, Hercules, CA, United States) and captured by the ChemiDoc XRS + System (Bio-Rad). All the antibodies used in the western blot are listed in Supplementary Table S2.

Statistical analysis

All data in the study was analyzed with SPSS (version 21.0, IBM, Armonk, NY, United States) and expressed as the mean ± SD. A two-tailed Student's t test was used for comparisons between two groups and one-way analysis of variance (ANOVA) was used for comparisons between multiple groups. $p < 0.05$ was considered statistically significant.

Results

MIF expression is significantly increased in serum of mice subjected to hepatic I/R injury

To analyze the correlation between MIF and liver I/R injury, we assessed the expression of MIF after reperfusion in our mouse and cell model. Using ELISA, we found that MIF levels in mice serum and culture medium of AML12 hepatocytes was markedly increased after I/R or H/R treatment (Figures 1A,B). We further evaluated MIF protein expression in liver tissues after I/R injury and AML12 hepatocytes challenged by H/R using western blotting. Interestingly, we found that MIF protein expression was significantly downregulated *in vivo* and *in vitro* (Figures 1C,D). We speculate that MIF is released into the serum or medium after the hepatocytes are stimulated by I/R or H/R. Taken together, these data suggest that MIF participates in the regulation of hepatic I/R injury.

MIF exacerbates liver damage after hepatic I/R injury

We next investigated whether MIF mediates hepatic I/R injury using MIF KO mice and mice injected with AAV8 to deliver MIF expression. MIF deletion or overexpression in the liver was confirmed by western blot analyses (Figures 2A,B). Notably, MIF deletion significantly reduced the elevated serum levels of ALT and AST in mice subjected to liver I/R injury compared with levels in WT control mice (Figure 2C). Compared with the WT controls, considerably fewer necrosis was found in the liver sections of MIF-KO mice after hepatic I/R injury as assessed by hematoxylin and eosin staining (Figure 2D). We further confirmed the role of MIF overexpression in liver I/R injury. In contrast to MIF-KO mice, AAV-MIF mice exhibited the opposite phenotype. Mice with MIF overexpression showed

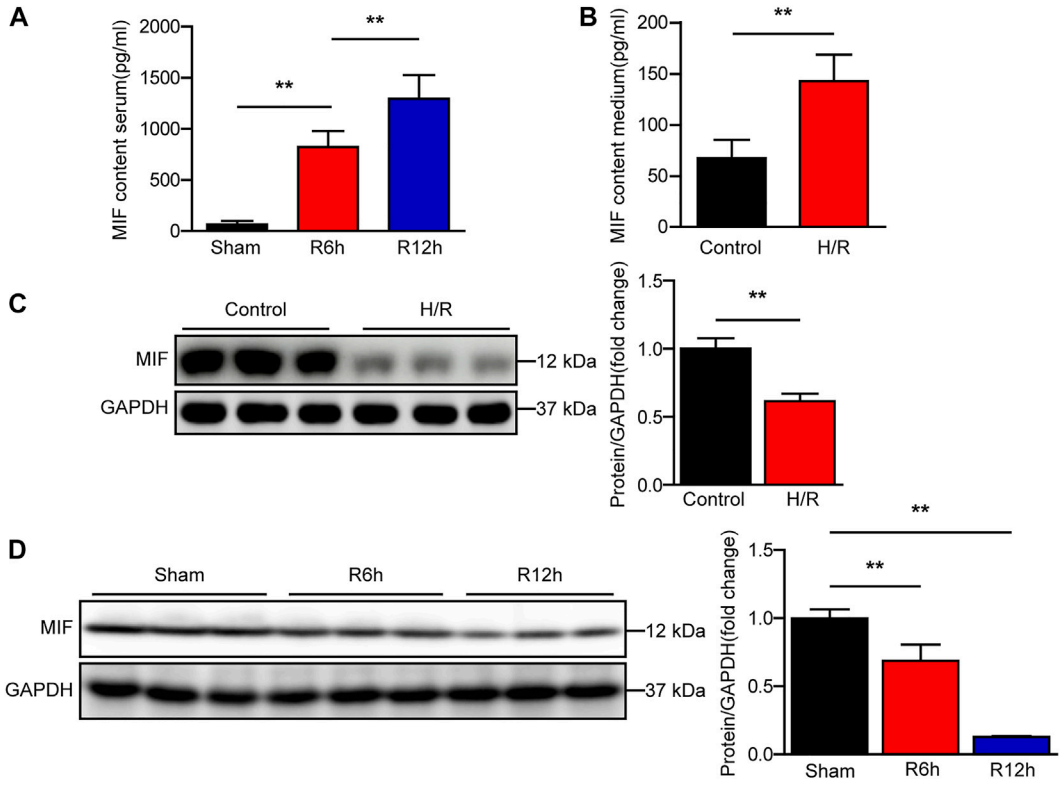

FIGURE 1
MIF expression is significantly increased in serum of mice subjected to hepatic I/R injury. **(A)** ELISA detection of MIF level in serum of mice at 6 and 12 h after hepatic IR surgery (n = 6 per group). **(B)** ELISA detection of MIF level in medium of hepatocytes subjected to H/R treatment (n = 3 per group). **(C)** MIF protein expression in cultured hepatocytes challenged by H/R treatment. GAPDH served as the loading control. Representative of three independent experiments. **(D)** MIF protein expression in the liver of mice at 6 and 12 h after hepatic IR surgery (n = 6 per group). GAPDH served as the loading control. All data are presented as the mean ± SD. Levels of statistical significance are indicated as $^{**}p < 0.01$. For statistical analysis, one-way ANOVA with Bonferroni's posthoc analysis or Tamhane's T2 posthoc analysis and two-tailed Student's t test were used.

increased levels of AST and ALT in serum and more necrosis in liver tissues compared with AAV-GFP control mice after hepatic I/R injury (Figures 2E,F). These results suggest that MIF deficiency protects against hepatic I/R injury.

MIF promotes inflammatory response during hepatic I/R injury

During hepatic I/R injury, the inflammatory response plays a pivotal role throughout the ischemia and reperfusion phases and inhibition of inflammation can effectively alleviate liver I/R injury (Zhang et al., 2019). As a proinflammatory cytokine, we tested the role of MIF in the inflammatory response in hepatic I/R injury. As shown in Figure 3A, MIF deficiency significantly reduced gene expression of inflammatory factors such as tumor necrosis factor a (TNFα), interleukin 6 (IL6), interleukin 1b (IL1β), and monocyte chemoattractant protein-1 (MCP-1) in the liver of mice subjected to I/R injury compared with the WT controls. Moreover, after liver I/R surgery, immunohistochemistry staining revealed that the number of inflammatory immune cells ($CD68^+$ monocyte-macrophages and Ly6g + neutrophils) in the liver of MIF-KO mice was significantly decreased compared with those of their counterparts (Figure 3B). In contrast, AAV-MIF mice showed significantly higher expression of inflammatory cytokines and more inflammatory-cell infiltration in the liver of mice challenged by I/R (measured by qRT-PCR and IHC staining) compared with AAV-GFP mice (Figures 3C,D). These experiments suggest that MIF is an essential factor controlling the inflammatory response during liver I/R injury.

MIF regulates apoptosis in hepatic I/R injury

Cellular apoptosis is directly involved in liver damage during hepatic I/R injury (Zheng et al., 2020). In our study, IHC and TUNEL staining revealed that the number of apoptotic cells significantly increased in WT mice after hepatic I/R injury, while

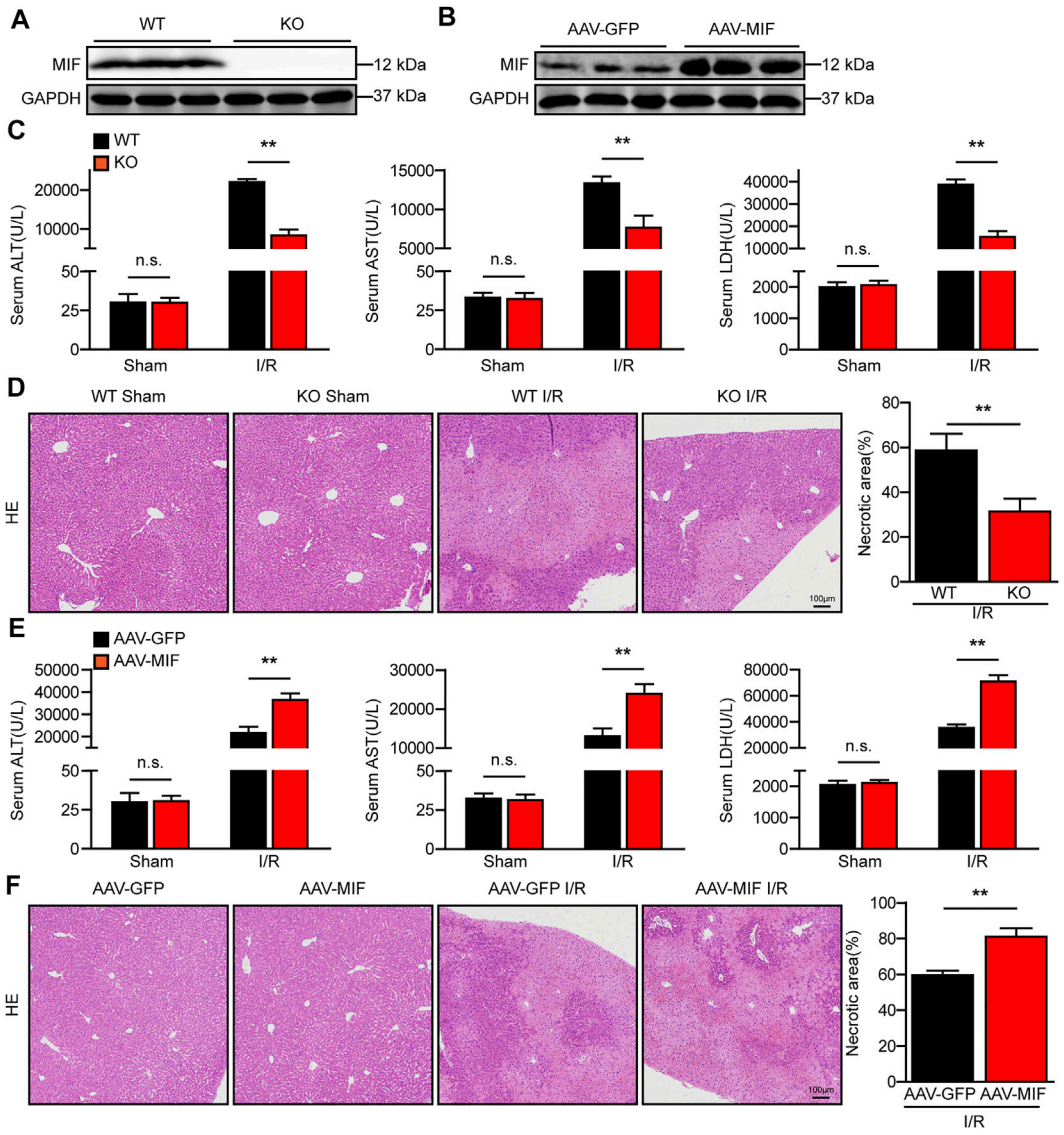

FIGURE 2
MIF deficiency alleviates liver damage after hepatic I/R injury. **(A)** MIF protein expression in the liver of WT and MIF-KO mice. GAPDH served as the loading control (n = 3 per group). **(B)** MIF protein expression in the liver of mice injected with AAV-GFP or AAV-MIF. GAPDH served as the loading control (n = 3 per group). **(C)** Serum ALT/AST/LDH activities in WT and MIF-KO mice after hepatic IR surgery (n = 6/group). **(D)** Representative histological HE-stained images and statistics showing necrotic areas in liver tissue from WT and MIF-KO mice after hepatic IR surgery (n = 6/group). Scale bar, 100 μm. **(E)** Serum ALT/AST/LDH activities in the serum of AAV-GFP or AAV-MIF mice after hepatic IR injury (n = 6/group). **(F)** Representative histological HE-stained images and statistics showing necrotic areas in the liver of AAV-GFP or AAV-MIF mice after hepatic IR injury (n = 6/group). Scale bar, 100 μm. All data are presented as the mean ± SD. Levels of statistical significance are indicated as**$p < 0.01$ and n. s = not significant. For statistical analysis, one-way ANOVA with Bonferroni's post hoc analysis or Tamhane's T2 post hoc analysis and two-tailed Student t test were used.

MIF deletion significantly suppressed hepatocyte apoptosis in liver tissues (Figure 4A). Furthermore, the expression of c-caspase 3 and the ratio between the pro-apoptotic protein Bax and the anti-apoptotic protein Bcl-2 were also dramatically reduced in the MIF-KO mice subjected to I/R injury (Figure 4B). In contrast, MIF overexpression aggravated apoptosis during hepatic I/R injury compared with the control mice, as demonstrated by induction of Bax and TUNEL-positive nuclei, a higher BAX/Bcl-2 ratio, and upregulation levels of c-caspase 3 (Figures 4C,D). Collectively, these data suggest that MIF deficiency suppresses liver apoptosis during hepatic I/R injury.

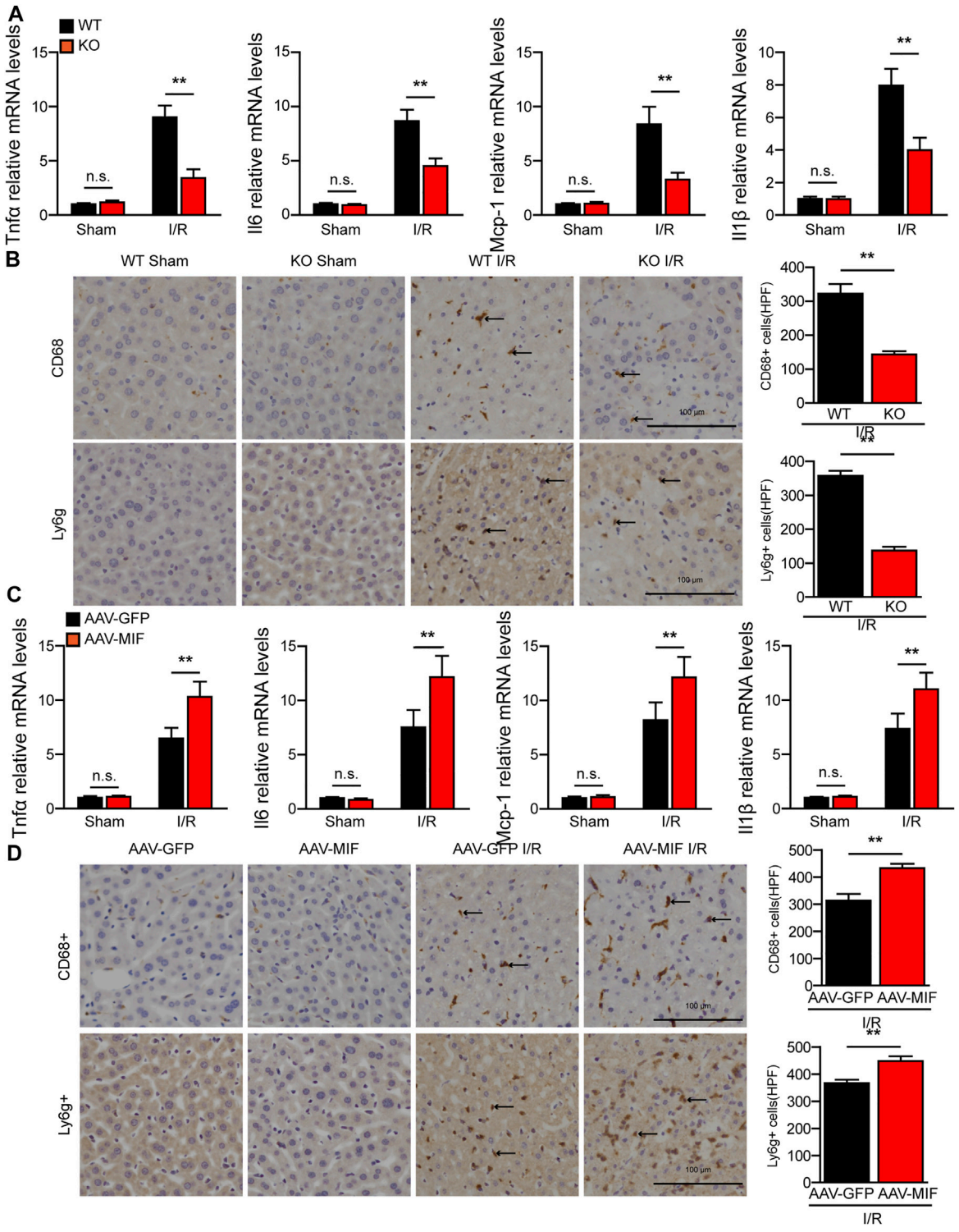

FIGURE 3
MIF promotes inflammatory response during hepatic I/R injury. **(A)** mRNA levels of proinflammatory factors (*Tnfα*, *Il6*, *IL1β*, and *Mcp-1*) in the liver of WT and *MIF*-KO mice after hepatic I/R surgery (n = 4/group). **(B)** Representative CD68 and Ly6g IHC staining in the liver lobes of WT and *MIF*-KO mice after hepatic I/R surgery (n = 4/group). Scale bar, 100 μm. Marked by black arrow. **(C)** mRNA levels of proinflammatory factors (*Tnfα*, *Il6*, *IL1β*, and *Mcp-1*) in the liver of AAV-GFP or AAV-MIF mice after hepatic I/R injury (n = 4/group). **(D)** Representative CD68 and Ly6g IHC staining in the liver of AAV-GFP or AAV-MIF mice after hepatic I/R injury (n = 4/group). Scale bar, 100 μm. Marked by black arrow. All data are presented as the mean ± SD. Levels of statistical significance are indicated as**$p < 0.01$ and n. s = not significant. For statistical analysis, one-way ANOVA with Bonferroni's post hoc analysis or Tamhane's T2 post hoc analysis and two-tailed Student t test were used.

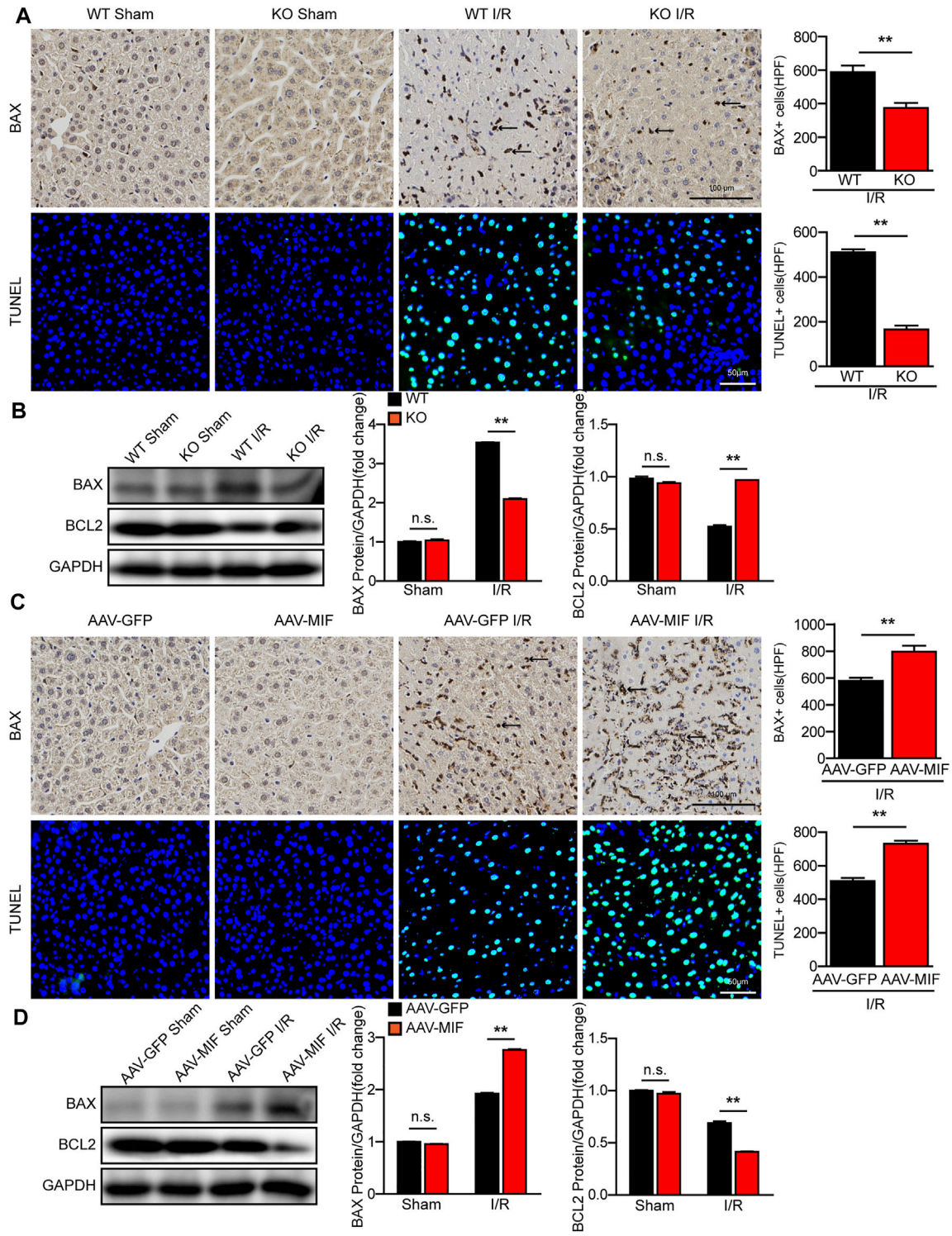

FIGURE 4
MIF deletion suppresses apoptosis in hepatic I/R injury. **(A)** IHC staining of BAX and TUNEL staining in liver sections from WT and MIF-KO mice after hepatic I/R surgery (n = 4/group). Scale bar, 100 μm of IHC staining and 50 μm of TUNEL staining respectively. Marked by black arrow. **(B)** Western blot analysis of apoptosis-related molecules (BAX, BCL2 and C-Caspase-3) protein levels in the liver of WT and MIF-KO mice at 6 h after hepatic I/R surgery. GAPDH served as a loading control (n = 3/group). **(C)** IHC staining of BAX and TUNEL staining in liver sections from AAV-GFP or AAV-MIF mice after hepatic I/R injury (n = 4/group). Scale bar, 100 μm of IHC staining and 50 μm of TUNEL staining respectively. Marked by black arrow. **(D)** Western blot analysis of apoptosis-related molecules (BAX, BCL2 and C-Caspase-3) protein levels in the liver of AAV-GFP or AAV-MIF mice after hepatic I/R injury. GAPDH served as a loading control (n = 3/group). All data are shown as the mean ± SD. Levels of statistical significance are indicated as $^{**}p < 0.01$. For statistical analysis, one-way ANOVA with Bonferroni's post hoc analysis or Tamhane's T2 post hoc analysis and two-tailed Student t test were used.

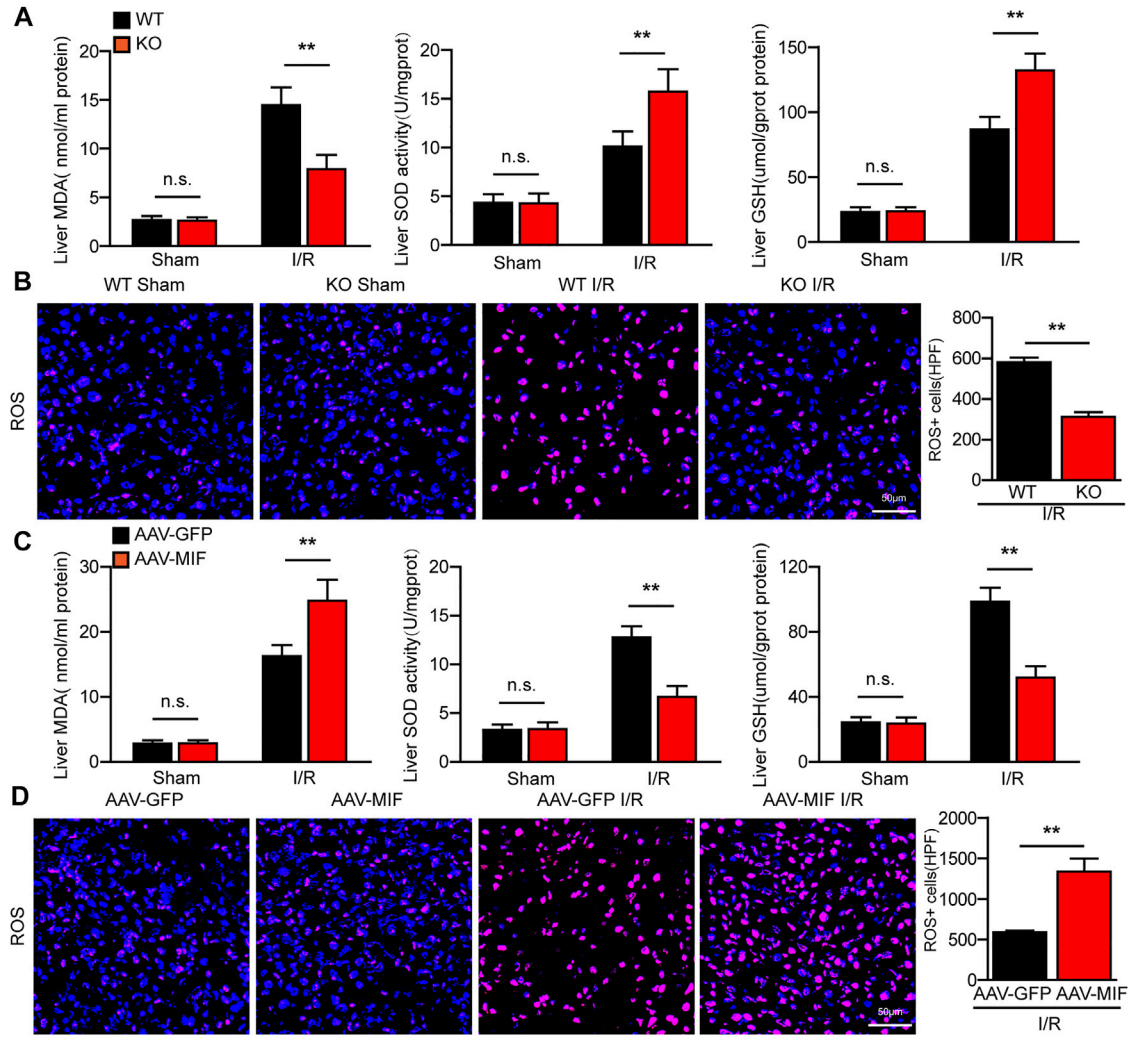

FIGURE 5
MIF ablation inhibits oxidative stress in hepatic I/R injury. **(A)** ELISA detection of MDA, SOD and GSH level in serum of WT and MIF-KO mice after hepatic I/R surgery (n = 6 per group). **(B)** DHE staining in liver sections from WT and MIF-KO mice after hepatic I/R surgery (n = 4/group). Scale bar, 50 μm. **(C)** ELISA detection of MDA, SOD and GSH level in serum of AAV-GFP or AAV-MIF mice after hepatic I/R surgery (n = 6 per group). **(D)** DHE staining in liver sections from AAV-GFP or AAV-MIF mice after hepatic I/R surgery (n = 4/group). Scale bar, 50 μm. All data are shown as the mean ± SD. Levels of statistical significance are indicated as $^{**}p < 0.01$. For statistical analysis, one-way ANOVA with Bonferroni's post hoc analysis or Tamhane's T2 post hoc analysis and two-tailed Student t test were used.

MIF aggravates oxidative stress in hepatic I/R injury

During hepatic I/R injury, the accumulation of ROS promotes several cellular processes that aggravate liver damage, including metabolism disequilibrium, apoptosis, and inflammation (Bi et al., 2019). Interestingly, we found that the level of oxidative related factor MDA was significantly reduced, whereas the anti-oxidative factors SOD and GSH were markedly increased in the liver of MIF-KO mice subjected to hepatic I/R surgery compared with those in WT control mice (Figure 5A). Meanwhile, DHE staining showed that ROS production was highly suppressed by MIF deficiency after I/R injury (Figure 5B). However, AAV-mediated MIF overexpression exacerbates oxidative stress in the livers of mice after hepatic I/R injury compared with the AAV-GFP control mice, as demonstrated by higher levels of MDA and ROS and lower levels of SOD and GSH in liver (Figures 5C,D). These findings indicate that MIF ablation inhibits oxidative stress in hepatic I/R injury.

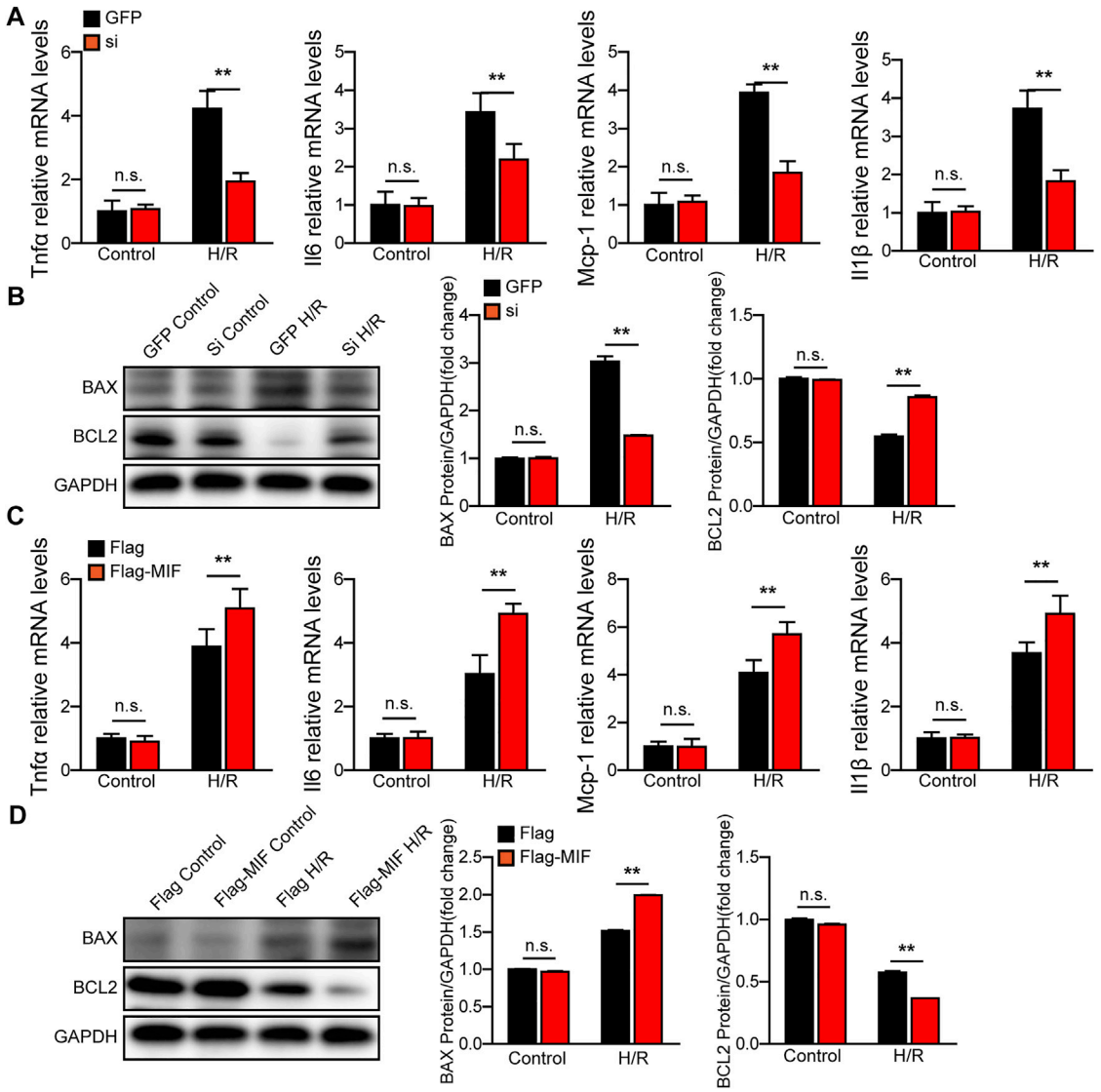

FIGURE 6
MIF knock-down protects hepatocytes from H/R injury. **(A)** The mRNA levels of proinflammatory factors (*Tnfα*, *Il6*, *IL1β*, and *Mcp-1*) in cultured MIF knockdown hepatocytes challenged by H/R treatment. Representative of three independent experiments. **(B)** Western blot analysis of the protein expression levels of Caspase3, Bax, and Bcl2 in cultured MIF knockdown hepatocytes challenged by H/R treatment. GAPDH served as the loading control. Representative of three independent experiments. **(C)** The mRNA levels of proinflammatory factors (*Tnfα*, *Il6*, *IL1β*, and *Mcp-1*) in cultured MIF overexpressed hepatocytes challenged by H/R treatment. Representative of three independent experiments. **(D)** Western blot analysis of the protein expression levels of Caspase3, Bax, and Bcl2 in cultured MIF overexpressed hepatocytes challenged by H/R treatment. GAPDH served as the loading control. Representative of three independent experiments. All data are shown as the mean ± SD. Levels of statistical significance are indicated as $^{**}p < 0.01$. For statistical analysis, one-way ANOVA with Bonferroni's post hoc analysis or Tamhane's T2 post hoc analysis were used.

MIF knock-down protects hepatocytes from H/R injury

We further evaluated the function of MIF in AML12 hepatocytes challenged by H/R stimulation. We used MIF siRNA and MIF expression plasmids to establish MIF-knockdown or MIF-overexpressing hepatocytes, respectively. Compared with the control group, MIF knockdown markedly inhibited hepatocyte inflammation, apoptosis and oxidative stress after H/R challenge, as determined by RT-PCR detecting inflammatory cytokines (TNFα, IL6, IL1β and MCP-1) (Figure 6A), ELISA detecting oxidative stress factors (MDA, SOD and GSH) (Supplementary Figure S6A), and western blot detecting c-caspase3, BAX, and Bcl-2 (Figure 6B). However, hepatocytes transfected with Flag-MIF exhibited exacerbated inflammation, apoptosis and oxidative

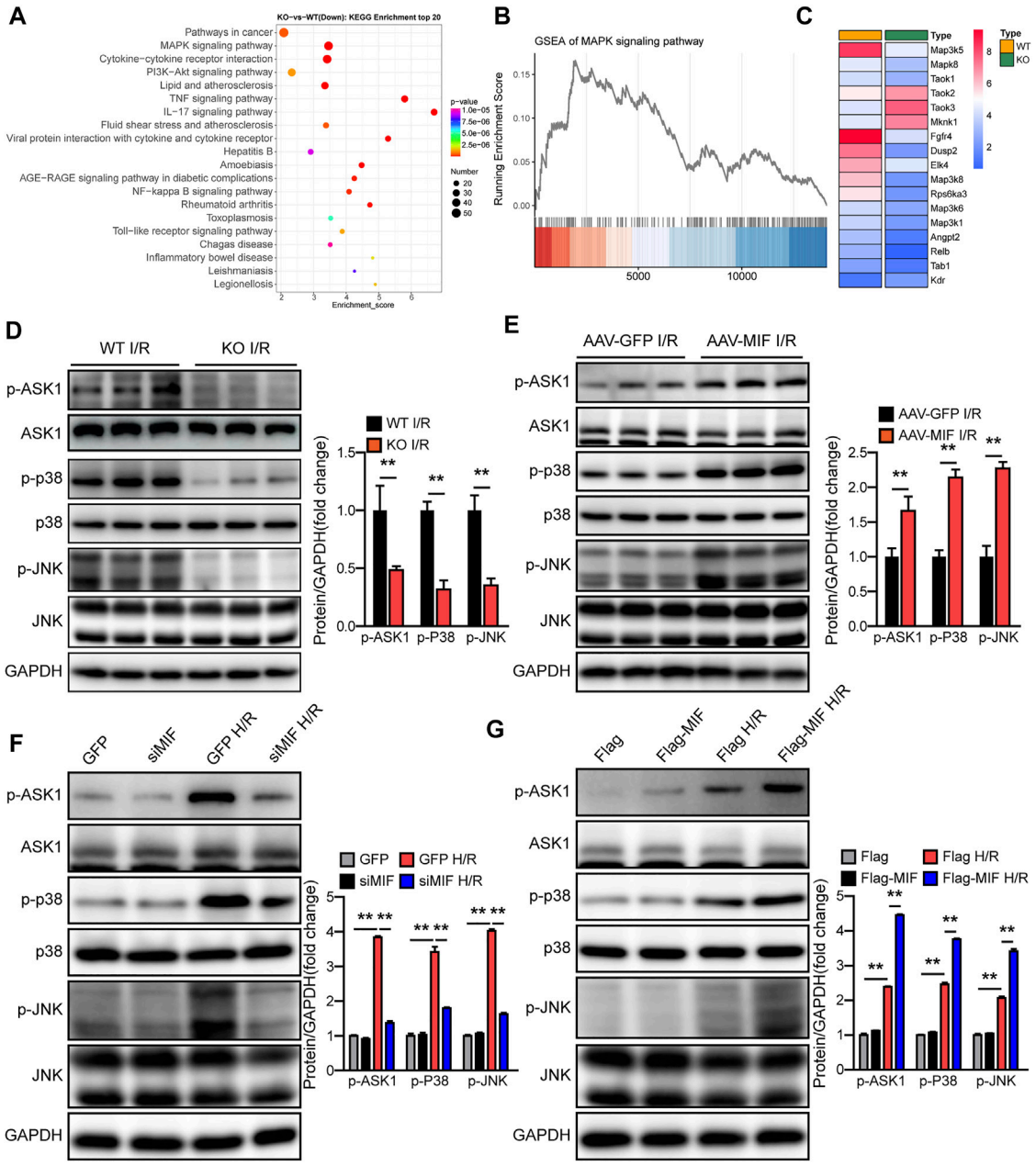

FIGURE 7
MIF activates the ASK1-JNK/p38 signaling during hepatic I/R injury. **(A)** KEGG pathway enrichment analysis of the major biological pathways contributing to MIF function. **(B)** GSEA-enriched analysis of MAPK pathways. **(C)** Heatmap showing expression of genes involved in MAPK pathways. **(D)** Protein levels of the total and phosphorylated protein expression levels of ASK1, P38, and JNK in the liver of MIF-KO and WT mice after hepatic I/R operation. GAPDH served as the loading control (n = 3 per group). **(E)** Protein levels of the total and phosphorylated protein expression levels of ASK1, P38, and JNK in the liver of AAV-GFP and AAV-MIF mice after hepatic I/R operation mice. GAPDH served as the loading control (n = 3 per group). **(F)** Protein levels of the total and phosphorylated protein expression levels of ASK1, P38, and JNK in GFP and siMIF hepatocytes that were challenged by H/R insult. GAPDH served as the loading control. Representative of three independent experiments. **(G)** Protein levels of the total and phosphorylated protein expression levels of ASK1, P38, and JNK in Flag and Flag-MIF hepatocytes that were challenged by H/R insult. GAPDH served as the loading control. Representative of three independent experiments. All data are presented as the mean ± SD. Levels of statistical significance are indicated as$^{**}p < 0.01$. For statistical analysis, two-tailed Student t test were used.

stress after H/R stimulation compared with those in Flag Controls (Figures 6C,D and Supplementary Figure S6B). These findings suggest that MIF knock protects against H/R-induced injury in hepatocytes.

MIF activates the ASK1-JNK/p38 signaling during hepatic I/R injury

To understand the underlying mechanisms responsible for the positive effect of MIF on liver I/R injury, we performed RNA sequencing (RNA-Seq) with I/R-challenged liver samples of WT and MIF-KO mice. Principal component analysis (PCA) defined the primary determinants of differences between liver samples of WT and MIF-KO mice (PC1, 38.1%; PC2, 17.7%). All samples were clearly separated into their respective groups (Supplementary Figure S7). Kyoto Encyclopedia of Genes and Genomes (KEGG) pathway enrichment analysis showed that the MAPK signaling pathway was one of the most significantly down regulated enriched pathways contributing to MIF-mediated hepatic I/R injury (Figure 7A). Gene Set Enrichment Analysis (GSEA) analysis indicated that MAPK pathway was down regulated in MIF-KO mice during hepatic I/R injury (Figure 7B). Heat map analysis showed that ASK1 (MAP3K5) was also significantly down regulated in MIF-KO mice during hepatic I/R injury (Figure 7C). We further confirmed the influence of MIF on MAPK signaling by loss- and gain-of-function of MIF *in vivo* and *in vitro*. In line with the results from RNA-seq, MIF deficiency suppressed ASK1, JNK and p38 phosphorylation post hepatic I/R injury and hepatocyte challenged by H/R treatment (Figures 7D,F), while MIF overexpression significantly promoted the ASK1, JNK and p38 phosphorylation compared to control group (Figures 7E,G). Together, these results suggest that MIF activates the ASK1-JNK/P38 signaling during hepatic I/R injury.

The protective effect of MIF deficiency in hepatic I/R injury depends on the suppression of ASK1

To ascertain the critical role of ASK1-JNK/P38 pathway in MIF-mediated hepatic I/R injury, we used a specific ASK1 inhibitor (NQDI-1) to perform an intraperitoneal injection in AAV-MIF mice prior to I/R injury. Compared with I/R group, NQDI-1 largely abolished the MIF overexpression-induced enhancement of liver injury, as demonstrated by reduced serum aminotransferase activity (ALT, AST, LDH) and decreased liver necrosis, inflammation, apoptosis, and oxidative stress in mice challenged by hepatic I/R injury (Figures 8A,B). Thus, it can be deduced that the protective effect of MIF deficiency in hepatic I/R injury depends on the suppression of ASK1.

Pharmacological inhibition of MIF attenuated I/R responsive liver injury

Finally, we used a specific inhibitor of MIF (ISO-1) to explore its therapeutic effect on hepatic I/R injury. As shown in Figure 9A, ISO-1 treated mice exhibited lower ALT and AST activities than those of DMSO treated mice after liver I/R surgery. Furthermore, histological analysis of the livers also demonstrated reduced necrotic area in ISO-1 treated mice compared with that of DMSO treated mice (Figure 9B). These results suggest that pharmacological inhibition of MIF attenuated I/R responsive liver injury and MIF could therefore serve as a potential therapeutic strategy for treating hepatic injury.

Discussion

Hepatic I/R injury leads to irreversible liver damage, but the mechanism has not been fully resolved. MIF is abundantly expressed in various tissues and regulates multiple biological processes (Osipyan et al., 2021). MIF has been reported to be a key mediator in alcohol-induced liver injury by promoting inflammation (Marin et al., 2017). Paradoxically, other study reported that MIF improve myocardial infarction by suppressing oxidative stress and apoptosis (Liu et al., 2020). We speculate that this may be because MIF plays different roles in different diseases and organs. To date, the role and molecular mechanism of MIF in hepatic I/R injury remain unclear. In the present study, we revealed that MIF act as novel biomarker and therapeutic target for the diagnosis and treatment of hepatic I/R injury. During liver I/R injury, MIF was released from the liver into the serum. Functional experiments demonstrated that MIF deficiency significantly diminished I/R- or H/R-induced inflammation, apoptosis, and oxidative stress in both cultured hepatocytes and mice. Moreover, we suggest that these beneficial effects of MIF deletion on hepatic I/R injury are largely dependent on the suppression of the ASK1-JNK/P38 pathway (Figure 9C).

MIF can not only promote the activation of T cells and macrophages, but also promote the chemical attraction to immune cells, promote the production of inflammatory cytokines and stress molecules, and resist the immunosuppressive effect of glucocorticoids. Therefore, MIF is involved in the pathogenesis of many autoimmune and inflammatory diseases, including rheumatoid arthritis (RA), liver injury, and pancreatitis. Moreover, it has been reported that MIF acts in an autocrine and paracrine manner by binding to receptors CD74/CD44, CXCR2, CXCR4 and CXCR7, thereby activating downstream MAPK, AMPK and Akt signals to mediate pro-inflammatory responses (Kong YZ, et al. Int J Mol Sci. 2022 April 28; 23 (9): 4908; Farr L, et al. Front Immunol. 2020 June 23; 11:1273.). In the process of liver I/R injury, we speculate that MIF from macrophages and hepatocytes aggravates liver injury by promoting the production of inflammatory chemokines and promoting inflammatory response by activating MAPK signaling pathway.

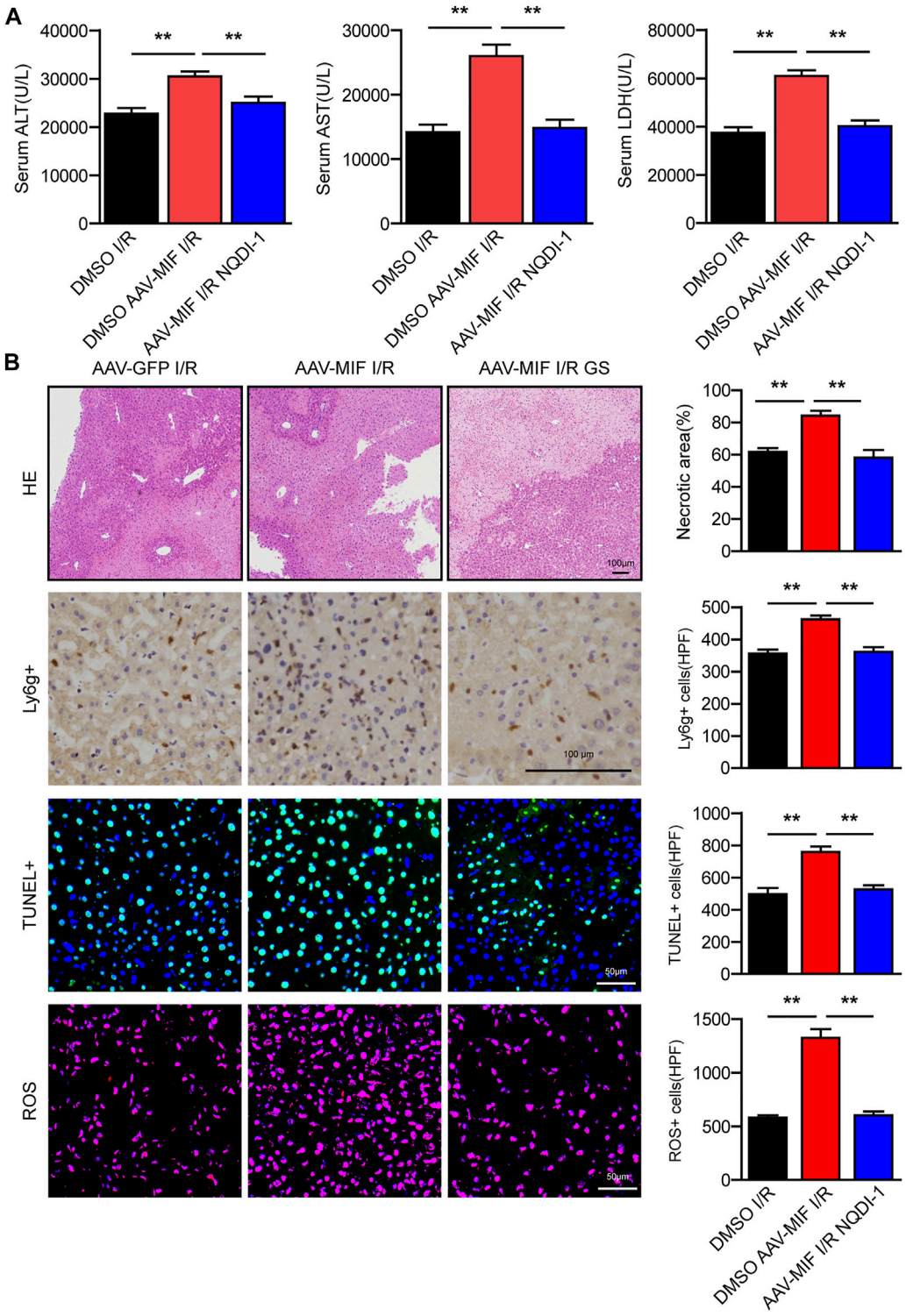

FIGURE 8
The protective effect of MIF deficiency in hepatic I/R injury depends on the suppression of ASK1. **(A)** Serum ALT/AST/LDH activities in mice after hepatic I/R surgery (n = 6/group). **(B)** Representative histological HE-stained images, Ly6g positive IHC stained images, TUNEL stained images, DHE stained images and statistical analysis in liver tissue of mice after hepatic I/R surgery (n = 4–6/group). Scale bar, 100 μm. All data are presented as the mean ± SD. Levels of statistical significance are indicated as**$p < 0.01$. For statistical analysis, one-way ANOVA with Bonferroni's post hoc analysis or Tamhane's T2 post hoc analysis.

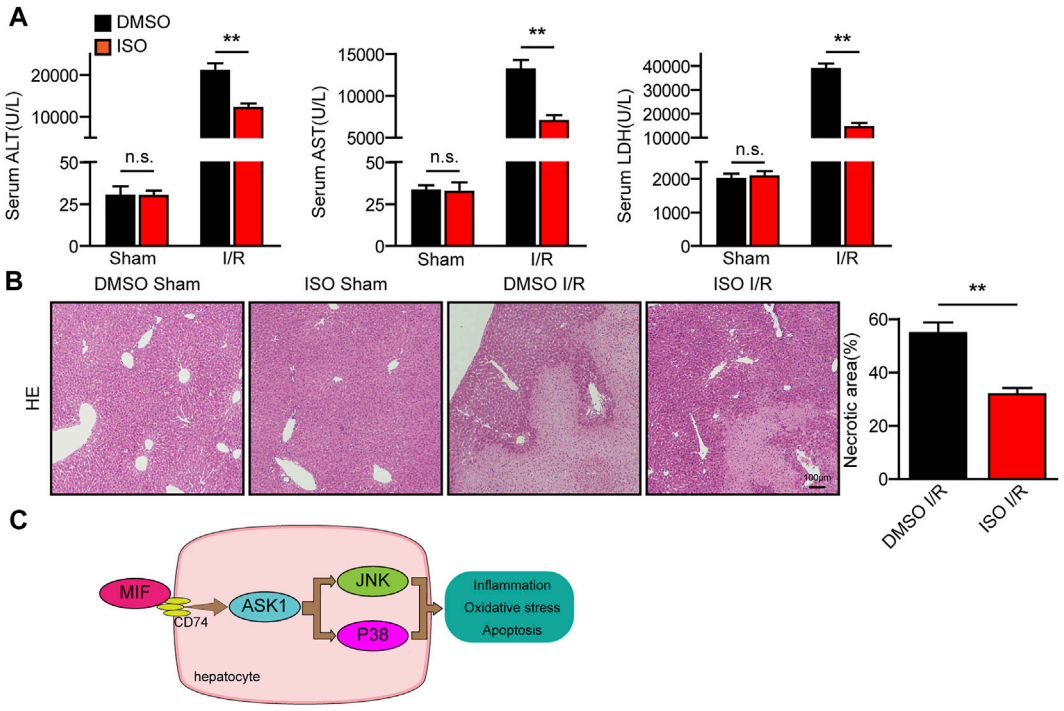

FIGURE 9
Pharmacological inhibition of MIF attenuated the I/R responsive liver injury. **(A)** Serum ALT/AST/LDH activities in mice after hepatic I/R surgery (n = 6/group). **(B)** Representative histological HE-stained images and statistics showing necrotic areas in liver tissue of mice after hepatic I/R surgery (n = 6/group). Scale bar, 100 μm. **(C)** Mechanism of MIF regulating liver I/R injury. All data are presented as the mean ± SD. Levels of statistical significance are indicated as$^{**}p < 0.01$. For statistical analysis, one-way ANOVA with Bonferroni's post hoc analysis or Tamhane's T2 post hoc analysis.

Extensive research has shown that inhibition of the inflammatory response may be an effective strategy to ameliorate hepatic I/R injury (Yan et al., 2019). During hepatic I/R injury, macrophages and neutrophils are recruited to the ischemic liver, contributing to ROS production and hepatocellular apoptosis (Abu-Amara et al., 2010). MIF can not only promote the activation of T cells and macrophages, but also promote the chemical attraction to immune cells, promote the production of inflammatory cytokines and stress molecules, and resist the immunosuppressive effect of glucocorticoids. Moreover, it has been reported that MIF acts in an autocrine and paracrine manner by binding to receptors CD74/CD44, CXCR2, CXCR4 and CXCR7, thereby activating downstream MAPK, AMPK and Akt signals to mediate pro-inflammatory responses (Farr et al., 2020; Kong et al., 2022). As a pro-inflammatory cytokine, the association between MIF and the inflammatory response has been reported in different studies and is the subject of some controversy. It seems that MIF might either positively or negatively regulate the inflammatory response. In our previous study using a mouse model of severe acute pancreatitis, we found that deletion of MIF reduced inflammation (Zhu et al., 2020). However, other research suggests that MIF serves as a defense mechanism, decreasing hepatic inflammatory cells and pro-inflammatory cytokines in nonalcoholic steatohepatitis (Heinrichs et al., 2014). In the present study, we found that MIF deteriorated the inflammatory response during hepatic I/R injury *in vivo* and *in vitro*. We speculate that MIF from macrophages and hepatocytes aggravates liver injury by promoting the production of inflammatory chemokines and promoting inflammatory response by activating MAPK signaling pathway.

During hepatic I/R injury, anoxia followed by reperfusion results in massive ROS production, inducing activation of inflammatory cells and cell death (Li et al., 2015). MIF has been shown to promote apoptosis and oxidative stress in many diseases (Yang et al., 2020; Wang et al., 2021). Studies have indicated that MIF deficiency improve hepatic function by suppressing oxidative stress and inflammation in thioacetamide-induced liver Injury in mice (Vukićević et al., 2021). Moreover, MIF inhibition significantly decreases the production of nitric oxide synthase (iNOS) as well as ROS in LPS-stimulated microglia cells (Zhang et al., 2016). However, it has also been reported that MIF deletion abolished the protective effects of ischemic preconditioning in myocardial I/R injury through aggravating myocyte apoptosis, ROS production, inflammatory-cell infiltration (Ruze et al., 2019). In the present study, our *in vivo*

and *in vitro* results also showed that MIF exacerbated the apoptosis and oxidative stress in hepatic I/R injury.

MAPK signaling has been recognized as the major molecular event contributing to hepatic I/R injury (Imarisio et al., 2017; Wang et al., 2017). During the hepatic I/R process, damage-associated molecular patterns (DAMPs) and ROS stimulation of hepatocytes can activate JNK and p38 signals that result in cellular inflammation and apoptosis (Yang et al., 2019; Zhou et al., 2021b). Importantly, MIF has been reported to function in regulating MAPK signaling. Previous studies have demonstrated that MIF promotes MAPK signaling through activation or inhibition of JNK phosphorylation, depending on the cell type and underlying stimulation context (Lue et al., 2011). In addition, MIF inhibitor ISO-1 was reported to protect severe acute pancreatitis by suppressing phosphorylated P38 and nuclear factor-κB (NF-κB) signaling (Wang et al., 2020). In the present study, we found MAPK signaling was significantly activated during hepatic I/R injury. Further *in vivo* and *in vitro* experiments showed that MIF promoted the activation of JNK and P38 pathway. However, how MIF fine-tunes the inhibition of MARK signaling remains unknown. ASK1 acts as a key mediator of JNK/P38 activation, mediating cellular death and inflammatory responses in a cell- and stimulus-dependent manner (Ogier et al., 2020; Obsilova et al., 2021). More importantly, we found that the protective effect of MIF deficiency in hepatic I/R injury depends on the suppression of ASK1.

Conclusion

In summary, the present study demonstrates that MIF deficiency protects from liver I/R injury via suppression of the inflammatory response, apoptosis, and oxidative stress. Moreover, the protective effect of MIF deficiency in hepatic I/R injury depends on the activation of ASK1-JNK/P38 signaling. These findings provide experimental evidence that may support MIF as a potential therapeutic target for strategies against hepatic I/R injury.

Data availability statement

The datasets presented in this study can be found in online repositories. The names of the repository/repositories and accession number(s) can be found in the Supplementary Material. The raw data of gene sequencing can be viewed at https://www.ncbi.nlm.nih.gov/geo/query/acc.cgi?acc=GSE212508 with number GSE212508.

Ethics statement

The animal study was reviewed and approved by The All experimental procedures were reviewed and approved by the Animal Research Ethics Committee of the First Affiliated Hospital of Zhengzhou University (2022-KY-0026-002).

Author contributions

SaC and QY designed and performed the experiments, analyzed and interpreted the data, and wrote the manuscript. YS and ZC participated in performing the experiments. ML assisted in data analysis and material support. CM and HC revised the paper, ShC provided financial support and experimental guidance, CZ designed the study and revised the manuscript. All authors have read and agreed to the published version of the manuscript.

Funding

This work was supported by the General funded projects of China Postdoctoral Science Foundation (2021M700129) and the Key scientific research projects of colleges and universities in Henan Province (22A320054), Regional joint project of National Natural Science Foundation of China (U2004122).

Acknowledgments

We thank Helen Roberton, from Liwen Bianji (Edanz) (www.liwenbianji.cn), for editing the English text of a draft of this manuscript.

Conflict of interest

The authors declare that the research was conducted in the absence of any commercial or financial relationships that could be construed as a potential conflict of interest.

Publisher's note

Supplementary material

The Supplementary Material for this article can be found online at: https://www.frontiersin.org/articles/10.3389/fphar.2022.951906/full#supplementary-material

References

Abu-Amara, M., Yang, S., Tapuria, N., Fuller, B., Davidson, B., and Seifalian, A. (2010). Liver ischemia/reperfusion injury: Processes in inflammatory networks--a review. *Liver Transpl.* 16, 1016–1032. doi:10.1002/lt.22117

Bi, J., Zhang, J., Ren, Y., Du, Z., Li, Q., Wang, Y., et al. (2019). Irisin alleviates liver ischemia-reperfusion injury by inhibiting excessive mitochondrial fission, promoting mitochondrial biogenesis and decreasing oxidative stress. *Redox Biol.* 20, 296–306. doi:10.1016/j.redox.2018.10.019

Chen, S., Zhang, H., Li, J., Shi, J., Tang, H., Zhang, Y., et al. (2021). Tripartite motif-containing 27 attenuates liver ischemia/reperfusion injury by suppressing transforming growth factor β-activated kinase 1 (TAK1) by TAK1 binding protein 2/3 degradation. *Hepatology* 73, 738–758. doi:10.1002/hep.31295

de Azevedo, R., Shoshan, E., Whang, S., Markel, G., Jaiswal, A., Liu, A., et al. (2020). MIF inhibition as a strategy for overcoming resistance to immune checkpoint blockade therapy in melanoma. *Oncoimmunology* 9, 1846915. doi:10.1080/2162402X.2020.1846915

Farr, L., Ghosh, S., and Moonah, S. (2020). Role of MIF cytokine/CD74 receptor pathway in protecting against injury and promoting repair. *Front. Immunol.* 11, 1273. doi:10.3389/fimmu.2020.01273

Ferrer-Sueta, G., and Radi, R. (2009). Chemical biology of peroxynitrite: Kinetics, diffusion, and radicals. *ACS Chem. Biol.* 4, 161–177. doi:10.1021/cb800279q

Guan, Y., Yao, W., Yi, K., Zheng, C., Lv, S., Tao, Y., et al. (2021). Nanotheranostics for the management of hepatic ischemia-reperfusion injury. *Small (Weinheim der Bergstrasse, Ger.* 17, e2007727. doi:10.1002/smll.202007727

Guo, W., Fang, H., Cao, S., Chen, S., Li, J., Shi, J., et al. (2020). Six-transmembrane epithelial antigen of the prostate 3 deficiency in hepatocytes protects the liver against ischemia-reperfusion injury by suppressing transforming growth factor-β-activated kinase 1. *Hepatology* 71, 1037–1054. doi:10.1002/hep.30882

Heinrichs, D., Berres, M., Coeuru, M., Knauel, M., Nellen, A., Fischer, P., et al. (2014). Protective role of macrophage migration inhibitory factor in nonalcoholic steatohepatitis. *FASEB J.* 28, 5136–5147. doi:10.1096/fj.14-256776

Imarisio, C., Alchera, E., Bangalore Revanna, C., Valente, G., Follenzi, A., Trisolini, E., et al. (2017). Oxidative and ER stress-dependent ASK1 activation in steatotic hepatocytes and Kupffer cells sensitizes mice fatty liver to ischemia/reperfusion injury. *Free Radic. Biol. Med.* 112, 141–148. doi:10.1016/j.freeradbiomed.2017.07.020

Kong, W., Li, W., Bai, C., Dong, Y., Wu, Y., and An, W. (2021). Augmenter of liver regeneration-mediated mitophagy protects against hepatic ischemia/reperfusion injury. *Am. J. Transpl.* 22, 130–143. doi:10.1111/ajt.16757

Kong, Y., Chen, Q., and Lan, H. (2022). Macrophage migration inhibitory factor (MIF) as a stress molecule in renal inflammation. *Int. J. Mol. Sci.* 23, 4908. doi:10.3390/ijms23094908

Li, J., Li, R., Lv, G., and Liu, H. (2015). The mechanisms and strategies to protect from hepatic ischemia-reperfusion injury. *Eur. Rev. Med. Pharmacol. Sci.* 19, 2036–2047.

Li, S., Zhu, Z., Xue, M., Pan, X., Tong, G., Yi, X., et al. (2021). The protective effects of fibroblast growth factor 10 against hepatic ischemia-reperfusion injury in mice. *Redox Biol.* 40, 101859. doi:10.1016/j.redox.2021.101859

Liu, X., Li, X., Zhu, W., Zhang, Y., Hong, Y., Liang, X., et al. (2020). Exosomes from mesenchymal stem cells overexpressing MIF enhance myocardial repair. *J. Cell. Physiol.* 235, 8010–8022. doi:10.1002/jcp.29456

Liu, Y., Liu, Y., Wang, Q., Song, Y., Chen, S., Cheng, B., et al. (2021). MIF inhibitor ISO-1 alleviates severe acute pancreatitis-associated acute kidney injury by suppressing the NLRP3 inflammasome signaling pathway. *Int. Immunopharmacol.* 96, 107555. doi:10.1016/j.intimp.2021.107555

Lue, H., Dewor, M., Leng, L., Bucala, R., and Bernhagen, J. (2011). Activation of the JNK signalling pathway by macrophage migration inhibitory factor (MIF) and dependence on CXCR4 and CD74. *Cell. Signal.* 23, 135–144. doi:10.1016/j.cellsig.2010.08.013

Marin, V., Poulsen, K., Odena, G., McMullen, M., Altamirano, J., Sancho-Bru, P., et al. (2017). Hepatocyte-derived macrophage migration inhibitory factor mediates alcohol-induced liver injury in mice and patients. *J. Hepatol.* 67, 1018–1025. doi:10.1016/j.jhep.2017.06.014

Obsilova, V., Honzejkova, K., and Obsil, T. (2021). Structural insights support targeting ASK1 kinase for therapeutic interventions. *Int. J. Mol. Sci.* 22, 13395. doi:10.3390/ijms222413395

Ogier, J., Nayagam, B., and Lockhart, P. (2020). ASK1 inhibition: A therapeutic strategy with multi-system benefits. *J. Mol. Med.* 98, 335–348. doi:10.1007/s00109-020-01878-y

Osipyan, A., Chen, D., and Dekker, F. (2021). Epigenetic regulation in macrophage migration inhibitory factor (MIF)-mediated signaling in cancer and inflammation. *Drug Discov. Today* 26, 1728–1734. doi:10.1016/j.drudis.2021.03.012

Pan, J., Chen, S., Guo, W., Cao, S., Shi, X., Zhang, J., et al. (2021). Alpinetin protects against hepatic ischemia/reperfusion injury in mice by inhibiting the NF-κB/MAPK signaling pathways. *Int. Immunopharmacol.* 95, 107527. doi:10.1016/j.intimp.2021.107527

Ruze, A., Chen, B., Liu, F., Chen, X., Gai, M., Li, X., et al. (2019)., 133. London, England, 665–680. Macrophage migration inhibitory factor plays an essential role in ischemic preconditioning-mediated cardioprotection *Clin. Sci.* doi:10.1042/CS20181013

Sahu, A., Jeon, J., Lee, M., Yang, H., and Tae, G. (2021). Nanozyme impregnated mesenchymal stem cells for hepatic ischemia-reperfusion injury alleviation. *ACS Appl. Mat. Interfaces* 13, 25649–25662. doi:10.1021/acsami.1c03027

Schindler, L., Smyth, L., Bernhagen, J., Hampton, M., and Dickerhof, N. (2021). Macrophage migration inhibitory factor (MIF) enhances hypochlorous acid production in phagocytic neutrophils. *Redox Biol.* 41, 101946. doi:10.1016/j.redox.2021.101946

Vukićević, D., Rovčanin, B., Gopčević, K., Stanković, S., Vučević, D., Jorgačević, B., et al. (2021). The role of MIF in hepatic function, oxidative stress, and inflammation in thioacetamide-induced liver injury in mice: Protective effects of betaine. *Curr. Med. Chem.* 28, 3249–3268. doi:10.2174/0929867327666201104151025

Wang, B., Zhao, K., Hu, W., Ding, Y., and Wang, W. (2020). Protective mechanism of MIF inhibitor ISO-1 on intrahepatic bile duct cells in rats with severe acute pancreatitis. *Dig. Dis. Sci.* 66, 3415–3426. doi:10.1007/s10620-020-06674-9

Wang, X., Mao, W., Fang, C., Tian, S., Zhu, X., Yang, L., et al. (2017). Dusp14 protects against hepatic ischaemia-reperfusion injury via Tak1 suppression. *J. Hepatology* 68, 118–129. doi:10.1016/j.jhep.2017.08.032

Wang, Y., Hu, Y., Wang, H., Liu, N., Luo, L., Zhao, C., et al. (2021). Deficiency of MIF accentuates overloaded compression-induced nucleus pulposus cell oxidative damage via depressing mitophagy. *Oxid. Med. Cell. Longev.* 2021, 6192498. doi:10.1155/2021/6192498

Xu, X., Wang, B., Ye, C., Yao, C., Lin, Y., Huang, X., et al. (2008). Overexpression of macrophage migration inhibitory factor induces angiogenesis in human breast cancer. *Cancer Lett.* 261, 147–157. doi:10.1016/j.canlet.2007.11.028

Xu, X., Zhang, Z., Lu, Y., Sun, Q., Liu, Y., Liu, Q., et al. (2020). ARRB1 ameliorates liver ischaemia/reperfusion injury via antagonizing TRAF6-mediated Lysine 6-linked polyubiquitination of ASK1 in hepatocytes. *J. Cell. Mol. Med.* 24, 7814–7828. doi:10.1111/jcmm.15412

Yan, Z., Huang, Y., Wang, X., Wang, H., Ren, F., Tian, R., et al. (2019). Integrated omics reveals tollip as an regulator and therapeutic target for hepatic ischemia-reperfusion injury in mice. *Hepatology* 70, 1750–1769. doi:10.1002/hep.30705

Yang, D., Shu, T., Zhao, H., Sun, Y., Xu, W., and Tu, G. (2020). Knockdown of macrophage migration inhibitory factor (MIF), a novel target to protect neurons from parthanatos induced by simulated post-spinal cord injury oxidative stress. *Biochem. Biophys. Res. Commun.* 523, 719–725. doi:10.1016/j.bbrc.2019.12.115

Yang, L., Wang, W., Wang, X., Zhao, J., Xiao, L., Gui, W., et al. (2019). Creg in hepatocytes ameliorates liver ischemia/reperfusion injury in a TAK1-dependent manner in mice. *Hepatology* 69, 294–313. doi:10.1002/hep.30203

Yuan, Z., Ye, L., Feng, X., Zhou, T., Zhou, Y., Zhu, S., et al. (2021). YAP-dependent induction of CD47-enriched extracellular vesicles inhibits dendritic cell activation and ameliorates hepatic ischemia-reperfusion injury. *Oxid. Med. Cell. Longev.* 2021, 6617345. doi:10.1155/2021/6617345

Zhang, T., Guo, J., Gu, J., Chen, K., Li, H., and Wang, J. (2019). Protective role of mTOR in liver ischemia/reperfusion injury: Involvement of inflammation and autophagy. *Oxid. Med. Cell. Longev.* 2019, 7861290. doi:10.1155/2019/7861290

Zhang, X., Hu, J., Becker, K., Engle, J., Ni, D., Cai, W., et al. (2021). Antioxidant and C5a-blocking strategy for hepatic ischemia-reperfusion injury repair. *J. Nanobiotechnology* 19, 107. doi:10.1186/s12951-021-00858-9

Zhang, Y., Gu, R., Jia, J., Hou, T., Zheng, L., and Zhen, X. (2016). Inhibition of macrophage migration inhibitory factor (MIF) tautomerase activity suppresses

microglia-mediated inflammatory responses. *Clin. Exp. Pharmacol. Physiol.* 43, 1134–1144. doi:10.1111/1440-1681.12647

Zhang, Y., Liu, X., Yang, M., Yang, S., and Hong, F. (2022). New progress in understanding roles of nitric oxide during hepatic ischemia-reperfusion injury. *World J. Hepatol.* 14, 504–515. doi:10.4254/wjh.v14.i3.504

Zhao, Y., Wei, X., Li, W., Shan, C., Song, J., and Zhang, M. (2020). Inhibition of macrophage migration inhibitory factor protects against inflammation through a toll-like receptor-related pathway after diffuse axonal injury in rats. *Biomed. Res. Int.* 2020, 5946205. doi:10.1155/2020/5946205

Zheng, J., Chen, L., Lu, T., Zhang, Y., Sui, X., Li, Y., et al. (2020). MSCs ameliorate hepatocellular apoptosis mediated by PINK1-dependent mitophagy in liver ischemia/reperfusion injury through AMPKα activation. *Cell. Death Dis.* 11, 256. doi:10.1038/s41419-020-2424-1

Zhou, J., Guo, L., Ma, T., Qiu, T., Wang, S., Tian, S., et al. (2021). *N-Acetylgalactosaminyltransferase-4 protects against hepatic ischaemia/reperfusion injury via blocking ASK1 N-terminal dimerization*. Baltimore, Md: Hepatology.

Zhou, J., Hu, M., He, M., Wang, X., Sun, D., Huang, Y., et al. (2021). *TNIP3 is a novel activator of Hippo-YAP signaling protecting against hepatic ischemia/reperfusion injury*. Baltimore, Md: Hepatology.

Zhu, C., Liu, Y., Song, Y., Wang, Q., Liu, Y., Yang, S., et al. (2020). Deletion of macrophage migration inhibitory factor ameliorates inflammation in mice model severe acute pancreatitis. *Biomed. Pharmacother. = Biomedecine Pharmacother.* 125, 109919. doi:10.1016/j.biopha.2020.109919

frontiers | Frontiers in Pharmacology

TYPE Original Research
PUBLISHED 15 September 2022
DOI 10.3389/fphar.2022.972397

OPEN ACCESS

EDITED BY
Lei Zhang,
Anhui Medical University, China

REVIEWED BY
Ming Xiang,
Huazhong University of Science and Technology, China
Qiong Huang,
Xiangya Hospital, Central South University, China

*CORRESPONDENCE
Ting-Ting Liu,
liutingting@ahmu.edu.cn

†These authors have contributed equally to this work

SPECIALTY SECTION
This article was submitted to Gastrointestinal and Hepatic Pharmacology, a section of the journal Frontiers in Pharmacology

RECEIVED 18 June 2022
ACCEPTED 15 August 2022
PUBLISHED 15 September 2022

CITATION
Jin C, Gao B-B, Zhou W-J, Zhao B-J, Fang X, Yang C-L, Wang X-H, Xia Q and Liu T-T (2022), Hydroxychloroquine attenuates autoimmune hepatitis by suppressing the interaction of GRK2 with PI3K in T lymphocytes. *Front. Pharmacol.* 13:972397. doi: 10.3389/fphar.2022.972397

Hydroxychloroquine attenuates autoimmune hepatitis by suppressing the interaction of GRK2 with PI3K in T lymphocytes

Chao Jin[1,2†], Bei-Bei Gao[3†], Wen-Jing Zhou[1,2], Bao-Jing Zhao[4], Xing Fang[5], Chun-Lan Yang[2], Xiao-Hua Wang[2], Quan Xia[2] and Ting-Ting Liu[2*]

[1]School of Pharmacy, Anhui Medical University, Hefei, China, [2]Department of Pharmacy, The First Affiliated Hospital of Anhui Medical University, The Grade 3 Pharmaceutical Chemistry Laboratory of State Administration of Traditional Chinese Medicine, Hefei, China, [3]Department of Pharmacy, The Second Hospital of Anhui Medical University, Hefei, China, [4]Department of Obstetrics and Gynecology, The First Affiliated Hospital of Anhui Medical University, Hefei, China, [5]Department of Pharmacy, The Second People's Hospital of Hefei, Hefei Hospital Affiliated to Anhui Medical University, Hefei, China

Hydroxychloroquine (HCQ) is derivative of the heterocyclic aromatic compound quinoline, which has been used for the treatment of autoimmune diseases. The central purpose of this study was to investigate therapeutic effects and inflammatory immunological molecular mechanism of HCQ in experimental autoimmune hepatitis (AIH). Treatment with HCQ ameliorated hepatic pathologic damage, inflammatory infiltration, while promoted regulatory T cell (T_{reg}) and down-regulated $CD8^+$T cell differentiation in AIH mice induced by S-100 antigen. *In vitro*, HCQ also suppressed pro-inflammatory cytokine (IFN-γ, TNF-α, and IL-12) secretion, promoted anti-inflammatory cytokine (TGF-β_1) secretion. HCQ mainly impaired T cell lipid metabolism but not glycolysis to promote T_{reg} differentiation and function. Mechanistically, HCQ down-regulated GRK2 membrane translocation in T cells, inhibited GRK2-PI3K interaction to reduce the PI3K recruiting to the membrane, followed by suppressing the phosphorylation of PI3K-AKT-mTOR signal. Pretreating T cells with paroxetine, a GRK2 inhibitor, disturbed HCQ effect to T cells. HCQ also reversed the activation of the PI3K-AKT axis by 740 Y-P (PI3K agonist). Meanwhile, HCQ inhibited the PI3K-AKT-mTOR, JAK2-STAT3-SOCS3 and increased the AMPK signals in the liver and T cells of AIH mice. In conclusion, HCQ exhibited specific and potent therapeutic effects on AIH and attendant liver injury, which was attributed to HCQ acted on GRK2 translocation, inhibited metabolism-related PI3K-AKT and inflammation-related JAK2-STAT3 signal in T lymphocytes, thereby modulating lipid metabolism of T cell function to regulate T_{reg} differentiation and function.

KEYWORDS

hydroxychloroquine, autoimmune hepatitis, regulatory T cells, glycolipid metabolism, G protein-coupled receptor kinase 2, PI3K-AKT axis

Introduction

Autoimmune hepatitis (AIH) is a severe inflammatory liver disease, characterized by lymphocytic infiltration and immune cells imbalance, which induce the destruction of liver parenchyma and the elevated levels of transaminase (Yang et al., 2018). The current standard therapy of AIH is glucocorticoid alone or combinating with azathioprine, which would usually produce severe adverse effects (Christen, 2019). It is necessary to develop specific and safer therapeutic agents. Hydroxychloroquine (HCQ) is derivative of the heterocyclic aromatic compound quinoline, which has been used as antimalarial agent for a long time. Currently, it is an excellent candidate for the treatment of autoimmune diseases, such as systemic lupus erythematosus (SLE) and rheumatoid arthritis (RA) (Martinez et al., 2020). It was reported that the liver injury of COVID-19 patients could be alleviated with the treatment of HCQ (Sima et al., 2021). Other study found that HCQ probably have inhibitory effects on immune cellular infiltration and activation underlying joint inflammation (Ben-Zvi et al., 2012; Rainsford et al., 2015).

Defective immunoregulation in AIH might result from T_{regs} number and function reducing (Zhu et al., 2021). It was reported that HCQ rebalances Th17/T_{reg}-mediated immunity and ameliorates SLE (An et al., 2017). Whether HCQ play a therapeutic role by regulating T_{reg} function in AIH has been attracted. Cell glucolipid metabolism is one of the key factors affecting T_{reg} differentiation (Matias et al., 2021). PI3K-AKT-mTOR pathway is reported to involve in immune cells metabolism (Xiang et al., 2016). mTOR inhibition could induce AMP-activated protein kinase (AMPK) activity and lipid oxidation in T_{regs}, which promoted T_{reg} differentiation (Pompura and Dominguez-Villar, 2018).

G protein-coupled receptor kinases 2 (GRK2) is a key participant to modulate phosphorylation-dependent G protein coupled receptors (GPCRs) desensitization, endocytosis, intracellular trafficking and re-sensitization as well as the subsequent intracellular signaling cascades. Recent data indicated that GRK2 could interact with non-GPCR substrates such as PI3K, AKT, MEK and so on (Ribas et al., 2007), which involved in inflammatory, cardiovascular disease, and tumor treatment (Cheng et al., 2021). The composition of the C-terminal domain of approximately 230 amino acids allows GRK2 to combine with PI3K, AKT, PIP2, $G_{\beta\gamma}$ and so on (Han et al., 2016). In RA, inhibiting the expression of GRK2 in membrane and increasing its expression in cytoplasm improved the abnormal proliferation of fibroblast like synovial cells. In addition, inhibition of GRK2 expression in rat spleen T cells can regulate T cell function to alleviate RA (Wang et al., 2017a; Wang et al., 2018). In the fibroblast-like synoviocytes of RA patients, the interaction of GRK2 with PI3Kγ promoted PI3K to recruit to the membrane, which contributed to the signal transduction (Wang et al., 2020). Other study showed that GRK2 also play a crucial role in function and differentiation of T_{regs} due to the interaction of GRK2 with PI3K-AKT pathway (Han et al., 2020).

Based on these observations, we hypothesize that HCQ ameliorates AIH by suppressing the inflammatory T-cell activity and promoting T_{reg} differentiation. To explore this, we detected the role of HCQ in AIH therapy and mechanism *in vivo* and *in vitro*. The results suggested that HCQ attenuated inflammation by regulating T cells lipid metabolism and T_{reg} differentiation, which was attributed to promoting the interaction of GRK2 with PI3K in the cytoplasm of T lymphocyte and inhibiting PI3K-AKT axis.

Materials and methods

Experimental autoimmune hepatitis model and treatment

Six-week-old male C57BL/6 mice were provided by Laboratory animal center of Anhui Medical University. All animal experimental procedures were approved by the Laboratory Animal Ethics Committee of Anhui Medical University (No. LLSC20190534). Mice were randomly divided into six groups (n = 6 per group) including control, AIH model, AIH+HCQ 10 mg/kg, AIH+HCQ 20 mg/kg, AIH+Prednisone (PRE) 8 mg/kg (positive control), AIH+HCQ 20 mg/kg+ PRE 8 mg/kg (drug combination) and control+HCQ 20 mg/kg (biosafety of HCQ). Hepatic syngeneic liver antigen (S-100) preparation: under non-sterile culture conditions, the livers of four female C57BL/6 mice were removed and cut into pieces on the surface of ice, then grinded on glass slides. After PBS washing, the protein in the liver cells was fully released and supernatant fluid was collected by ultracentrifugation. The experimental group was administered by intraperitoneal injection S-100 after fully emulsified on 1st day and 7th day with 0.5 ml of 0.5–2.0 g/L and an equal volume of complete freund's adjuvant (CFA) (Beyotime, China). On the 14th day of modeling, the drug was administered by gavage for 2 weeks until all mice were sacrificed. The control mice were orally administered with normal saline.

Histopathology and immunohistochemistry staining

Liver tissues were fixed in 4% paraformaldehyde for more than 24 h. Then the fixed liver tissues were stained for hematoxylin and eosin (H&E). Sections were incubated overnight at 4°C with CD3 and F4/80 primary antibodies (Proteintech, China) and incubated with biotin-labeled secondary antibody for 30 min after washing with phosphate-buffered saline. Slices were stained with chromogen diaminobenzidine and hematoxylin, dehydrated, and then treated with xylene.

ALT/AST/MDA/SOD assay

The levels of alanine aminotransferase (ALT), aspartate aminotransferase (AST), malondialdehyde (MDA) and superoxide dismutase (SOD) in the serum of mice were assessed using Kit (#C009-1-1, #C010-1-1, #A003-1 and #A001-1, Nanjing Jiancheng Bioengineering Institute, China) according to manufacturer's instructions.

Cell culture and drug treatment

Spleen T lymphocytes were collected from the spleen of mice and activated with concanavalin A (ConA, 0.1 μM) and incubated with HCQ using doses in our concentration screening tests (100, 50, and 25 μM) for 24 h. Bone marrow derived dendritic cells (BMDCs) were collected from the tibia and femur of AIH mice. DCs were cultured with cytokines GM-CSF (20 ng/ml) and IL-4 (10 ng/ml) (Liu et al., 2015). All cells were cultured in RPMI 1640 medium (#BC-M-017, Biochannel, China) with 10% fetal bovine serum (FBS; Biological Industries, Israel) and maintained at 37°C in an incubator with 5% CO_2 (Liu et al., 2014; Fang et al., 2020).

FCM analysis

Immune cells were analyzed by FCM. Briefly, the cells underwent staining with fluorochrome-antibodies (Multi Sciences Lianke Bio, China) targeting cell antigens at 4°C for 60 min. Tissue abrasive fluid and T cell suspension were stained with the FITC-CD4, PE-CD25, APC-Foxp3 to identify T_{regs} and APC-CD3, FITC-CD4, PE-CD8 to identify $CD4^+$ or $CD8^+$T cells. The expressions of Foxp3 were observed in $CD4^+CD25^+$ cell gate, and the expressions of CD4 and CD8 were observed in $CD3^+$ cell gate. BMDCs were stained with FITC-CD11c, APC-CD86 and PE-MHC-II (Liu et al., 2015), the expressions of MHC-II and CD86 were calculated in $CD11c^+$ cell gate. The gate was chosen by the compare between negative cells (without fluorescent dye) and single fluorescent dye or mixed fluorescent dye cells. Furthermore, mitochondrial membrane potential (MMP) of cells was evaluated using JC-1 molecular probes and analyzed by flow cytometry. In cells with a high MMP ($\Delta\Psi m$ >80–100 mV), JC-1 forms aggregates that emit red-orange fluorescence (wavelength, 590 nm), whereas in cells with low mitochondrial potential ($\Delta\Psi m$ <80–100 mV), JC-1 forms monomers that emit green fluorescence (wavelength, 525–530 nm). The high MMP exerted high ratio of JC-1 Red/JC-1 Green. T lymphocytes were stained with JC-1 and tested in FITC and PE channels. The gate was chosen by the clustering of cells.

Membrane and cytoplasm protein extraction

Membrane and cytoplasm protein of T lymphocytes was extracted by membrane and cytosol protein extraction kit (#P0033, Beyotime, China). T lymphocytes were lysed with membrane protein extraction reagent A and centrifuged at 700 g for 10 min at 4°C. The supernatant was centrifuged at 14,000 g for 30 min at 4°C. The supernatant was cytoplasm protein and the precipitate was the membrane proteins, which was resuspended in membrane protein extraction reagent B.

Western blot analysis

The total proteins of liver tissues and spleen T lymphocytes were extracted by RIPA (#P0013C, Beyotime, China) with phosphatase inhibitor and PMSF (#P0012S, Beyotime, China). Immunoblotting was performed as previously described (Xiang et al., 2022). Primary antibodies were listed in Supplementary Table S1. Secondary antibodies were as follows: HRP-conjugated affinipure goat anti-rabbit IgG (H+L) (#SA00001-2, Proteintech, China) and HRP-conjugated affinipure goat anti-rabbit IgG (H+L) (#SA00001-1, Proteintech, China). The protein samples were visualized using the ECL-chemiluminescent kit (#WBKLS0100, Millipore, United States) and analysed by ImageJ software.

Quantitative real-time-PCR

Specifically, total RNA was extracted from liver tissues and spleen T lymphocytes by TRIzol reagent (#257401, Invitrogen, United States). RNA was reverse transcribed in to cDNA by reverse transcription system kit (#R222-01, Vazyme, China). The mRNA levels were measured by qPCR using SYBR Green qPCR Master Mix (#Q111-02/03, Vazyme, China) according to the manufacturer protocol. The primers were listed in Supplementary Table S2. Gene expression was normalized to expression of β-actin.

Enzyme-linked immunosorbent assay, free fatty acid secretion and glucose uptake assay

Levels of transforming growth factor-β_1 (TGF-β_1), interferon-γ (IFN-γ), interleukin-12 (IL-12), and tumor necrosis factor-α (TNF-α) in cell culture supernatant and serum were assessed with the ELISA assay (Proteintech, China). Free fatty acid was examined with the free fatty acid assay kit (#A042-1-1, Nanjing Jiancheng Bioengineering

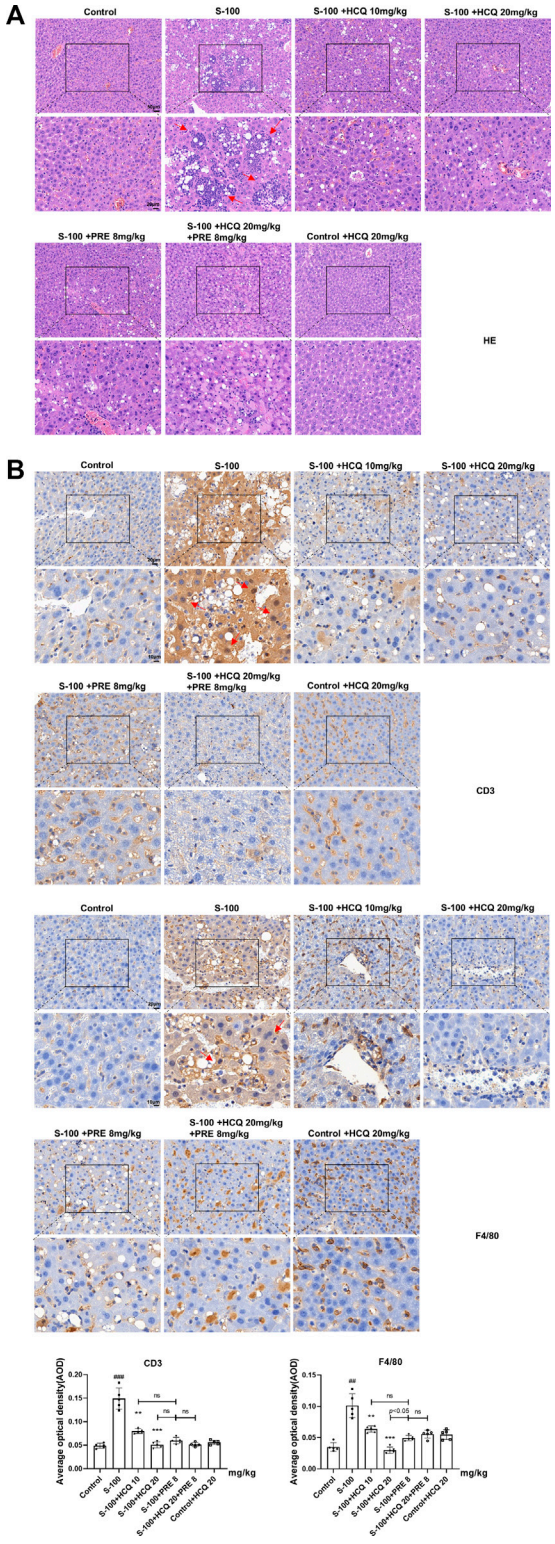

FIGURE 1
HCQ protected hepatic architecture and inhibited the infiltration of inflammatory cells in AIH mice. **(A)** Representative images of H&E (arrows represent inflammatory infiltrations, (*Continued*)

FIGURE 1
original magnification: ×200, scale bar of initial images: 50 μm; scale bar of enlarged images: 20 μm). **(B)** Representative immunohistochemical images of CD3 or F4/80 staining (arrows represent CD3 or F4/80 expression, original magnification: ×400, scale bar of initial images: 20 μm; scale bar of enlarged images: 10 μm). Data expressed as mean ± SD (n = 5). $^{\#}p < 0.05$, $^{\#\#}p < 0.01$, $^{\#\#\#}p < 0.001$ relative to controls; $^{*}p < 0.05$, $^{**}p < 0.01$, $^{***}p < 0.001$ relative to S-100-induced AIH mice; ns, not significant.

Institute, China), glucose uptake was examined by the glucose oxidase-peroxidase method with test kit (#361510, Rongsheng, China).

Cell counting Kit-8 assay

The proliferation of T cell was assessed using CCK-8 kit (#GK10001, GLPBIO, China). After stimulation, the reagent was added into the culture medium, and the mixture was maintained in an incubator comprising 5% CO_2 + 95% air at 37°C for 2°h. The absorbance at 450 nm was detected utilizing a Microplate Reader.

Co-immunoprecipitation

To examine the association between GRK2 and PI3K or AKT in spleen T lymphocytes under different conditions, total cell lysates were immunoprecipitated using anti-GRK2 antibody and analyzed by western blot with an anti-GRK2, anti-PI3K or anti-AKT. Briefly, the preparation of lysate is as described above for western blots, and then pre-cleared using IgG. The total protein (1,000 μg of each lysate sample) was incubated with GRK2 antibody (4 μl) on a rotating shaker at 4°C overnight, the Protein A/G was added with agarose and then the small ball (20 μl) was added to each tube and placed in the rotating shaker at 4°C for 2 h. Then the tube was washed three times with cracking buffer. Resin-bound immune complexes were boiled for 5 min after protein loading buffer was added. Finally, repeating steps as Western blot.

Statistical analyses

All data were statistically analyzed using GraphPad Prism 8.0. The data were normally distributed and expressed by the mean ± standard deviation (SD). Multiple comparisons were carried out by one-way (ANOVA). Comparisons between two groups were performed using independent-sample t-tests. All experiments were performed at least three times, $p < 0.05$ was considered statistically significant.

Results

Hydroxychloroquine ameliorated hepatic pathologic damage and inflammatory infiltration of autoimmune hepatitis mice

In S-100-treated AIH mice, oral administration of 10 or 20 mg/kg HCQ, which referred to the report (Zheng et al., 2021), for 2°weeks markedly diminished the extent of AIH with the loss of liver architecture, congestion, lymphocytic infiltration and large area necrosis (arrows represent inflammatory infiltrations) (Figure 1A). We focused on inflammatory cell related markers, such as mature macrophages cell marker F4/80 and lymphocyte marker CD3 to investigate the alleviating effect of HCQ on the inflammatory infiltration of AIH. The results showed that the expression of CD3 and F4/80 significantly increased in the liver of AIH, which was slipped to basal levels by HCQ treatment (Figure 1B). The liver index and spleen index decreased in HCQ treatment compared with AIH group to a certain extent (Figure 2A). Serum levels of ALT and AST were decreased after HCQ treatment (Figure 2B). HCQ memorably attenuated hepatic oxidative stress with lower MDA and higher SOD compared with S-100 treatment (Figure 2C). Furthermore, the decrease of anti-inflammatory factor, TGF-β_1 and the increase of proinflammatory factor, IFN-γ, TNF-α and IL-12 in serum caused by S-100 could be reversed by HCQ (Figure 2D). These effects were better or comparable to those of PRE, which was used in clinical settings against AIH. In addition, there was synergistic effect in treating AIH by combination of HCQ and PRE. Furthermore, HCQ treatment did not alter levels of ALT, AST, or inflammatory factors in healthy mice (Figures 1, 2). The results demonstrated that HCQ exerted liver-protective and anti-inflammatory effects on S-100-induced AIH and appeared to have no serious adverse effects.

Hydroxychloroquine regulated T cells function and T_{reg} differentiation in autoimmune hepatitis

Numerous immune cells regulate the development of hepatic inflammation (Koyama and Brenner, 2017). We quantitatively determined the proportions of various immune cells of multiple organs in AIH. The results showed that, after S-100 administration, T_{regs} reduced in the spleen and liver, $CD8^+$T cells differentiated in the spleen, and bone marrow derived dendritic cells (BMDCs) matured. HCQ reversed the effect of S-100 (Figures 3A–C), but had little effect on other subtypes of immune cells in the liver and spleen of AIH mice (Date not shown). Here, we also noted that HCQ increased the fork head box protein 3 (Foxp3) mRNA expressions in the liver of AIH mice, which facilitated T_{regs} immune tolerance. The serine protease granzyme B (GzmB), markers of $CD8^+$T cell-induced cytotoxicity, was reduced by HCQ in the liver of AIH mice. HCQ showed a potential immunosuppressive effect on DC-$CD8^+$T cell communication by upregulating the negative regulatory molecules CTLA-4 and PD-1 in the liver. The effect of HCQ to other costimulatory molecules were indistinctive (Figure 3D).

In vitro, HCQ significantly suppressed spleen T-lymphocyte proliferation in a dose dependent manner (Figure 4A). It also decreased the pro-inflammatory cytokines, and increased the anti-inflammatory cytokines production in the supernatant of T cells (Figure 4B). These effects were comparable to those of MTX, which is used to inhibit T cells proliferation and function. Of note, *in vitro*, HCQ strongly increased T_{regs} and slightly retarded $CD8^+$T cells differentiation (Figure 4C). HCQ represented similar effects on Foxp3 and GzmB mRNA expressions *in vitro* compared to *in vivo* experiment (Figure 4D). The apparent modulation involving T_{regs} of HCQ might be important to maintain immune homeostasis during progression of AIH.

Impaired lipid metabolism in hydroxychloroquine-modulated T lymphocyte

Manipulating the metabolism of immune cells may alter immune homeostasis (Fox et al., 2005). Induced T_{regs} differentiate from conventional naïve $CD4^+$T cells under a variety of conditions that range from inflammatory environments, in the presence of particular cytokines, mainly TGF-β_1, to suboptimal glycolysis and/or fatty acid oxidation signals (Murphy et al., 1990). Previous reports indicated that HCQ exerted substantial metabolic regulation effects including lipid and insulin metabolism (Hu et al., 2017). Thus, HCQ might ameliorate AIH partly by suppressing T cells metabolism, which promoted T_{reg} development. Our results showed that HCQ inhibited NEFA secretion of T cells, but had little effect on T cell glucose uptake (Figures 5A,B). In the presence of HCQ, glucose transporter (GLUT)-1, the predominant glucose transporter in T cells, were lower compared to that of activated cells without treatment (Figure 5C). We found that HCQ treatment resulted in a significant reduction in MMP of T cells (Figure 5D). We also tested the marker genes of glycolysis and lipid metabolism [lipid synthesis and fatty acid oxidation (FAO)]. The result showed that there was no

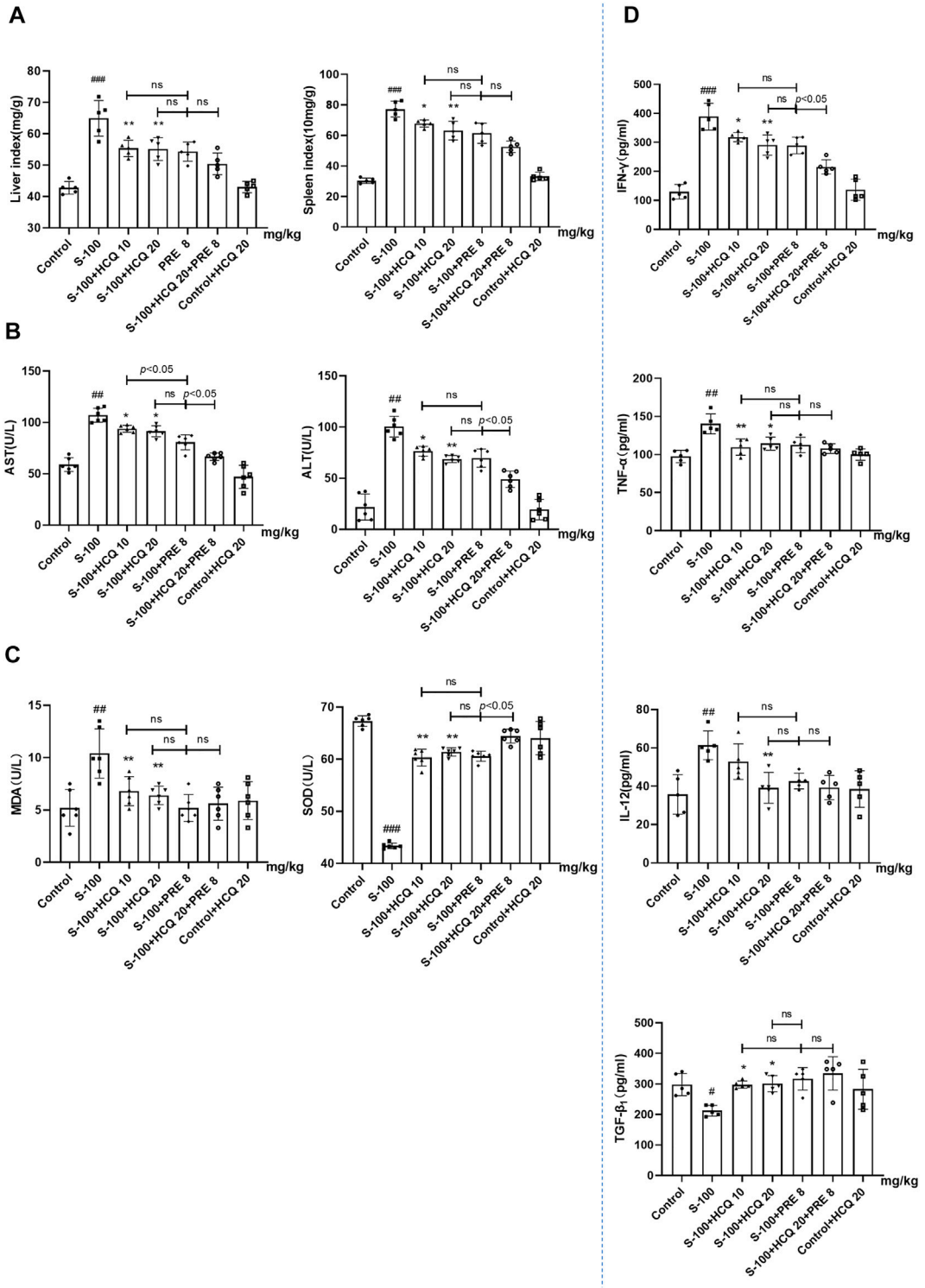

FIGURE 2
HCQ ameliorated hepatic pathologic damage and inflammatory infiltration of AIH mice. **(A)** Liver index [liver wet weight (mg)/mouse body weight (g) ×100%] and spleen index [spleen wet weight (10 mg)/mouse body weight (g) × 100%]. **(B)** Levels of ALT and AST in serum. **(C)** Levels of MDA and SOD in serum. **(D)** Serum inflammatory cytokine concentrations. Data expressed as mean ± SD (n = 5 or 6). $^{\#}p < 0.05$, $^{\#\#}p < 0.01$, $^{\#\#\#}p < 0.001$ relative to controls; $^{*}p < 0.05$, $^{**}p < 0.01$, $^{***}p < 0.001$ relative to S-100-induced AIH mice; ns, not significant.

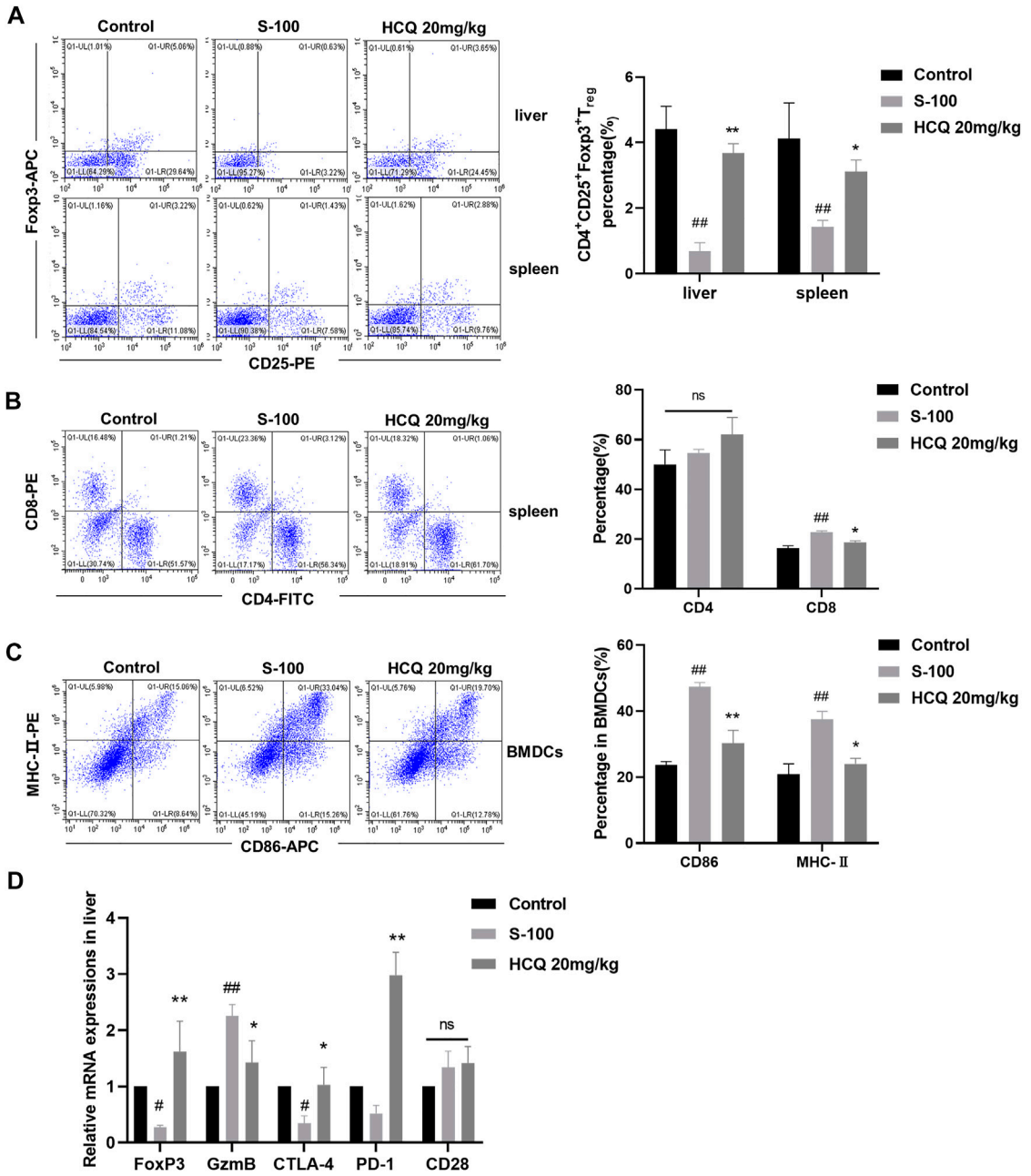

FIGURE 3
HCQ regulated immune cells differentiation in S-100-induced AIH. **(A)** The percentage of T_{regs} in the liver and spleen ($n = 3$). **(B)** The percentage of $CD4^+$T cells and $CD8^+$T cells in the liver ($n = 3$). **(C)** The MHC-II and CD86 expression on $CD11c^+$ BMDCs ($n = 3$). **(D)** Expression of Foxp3, GzmB, CTLA-4, PD-1, CD28 mRNA in the liver ($n = 5$). Data expressed as mean ± SD. $^{\#}p < 0.05$, $^{\#\#}p < 0.01$ relative to controls; $^{*}p < 0.05$, $^{**}p < 0.01$ relative to S-100-induced AIH mice.

significant effect of HCQ to glycolysis in T cells, however, HCQ substantially downregulated mRNAs encoding lipid utilization components in T cells (*Srebp2* and *Acaca*), upregulated the fatty acid oxidation related genes expression (*SirT1*, *SirT2*, and *SirT3*), which might promote T_{reg} differentiation (Figure 5C). Given that mitochondria were central to the metabolism of lipid (Seenappa et al., 2016), we speculated that suppression of fuel metabolism and promotion of FAO might contribute importantly to the mechanism of T_{reg} development induced by HCQ.

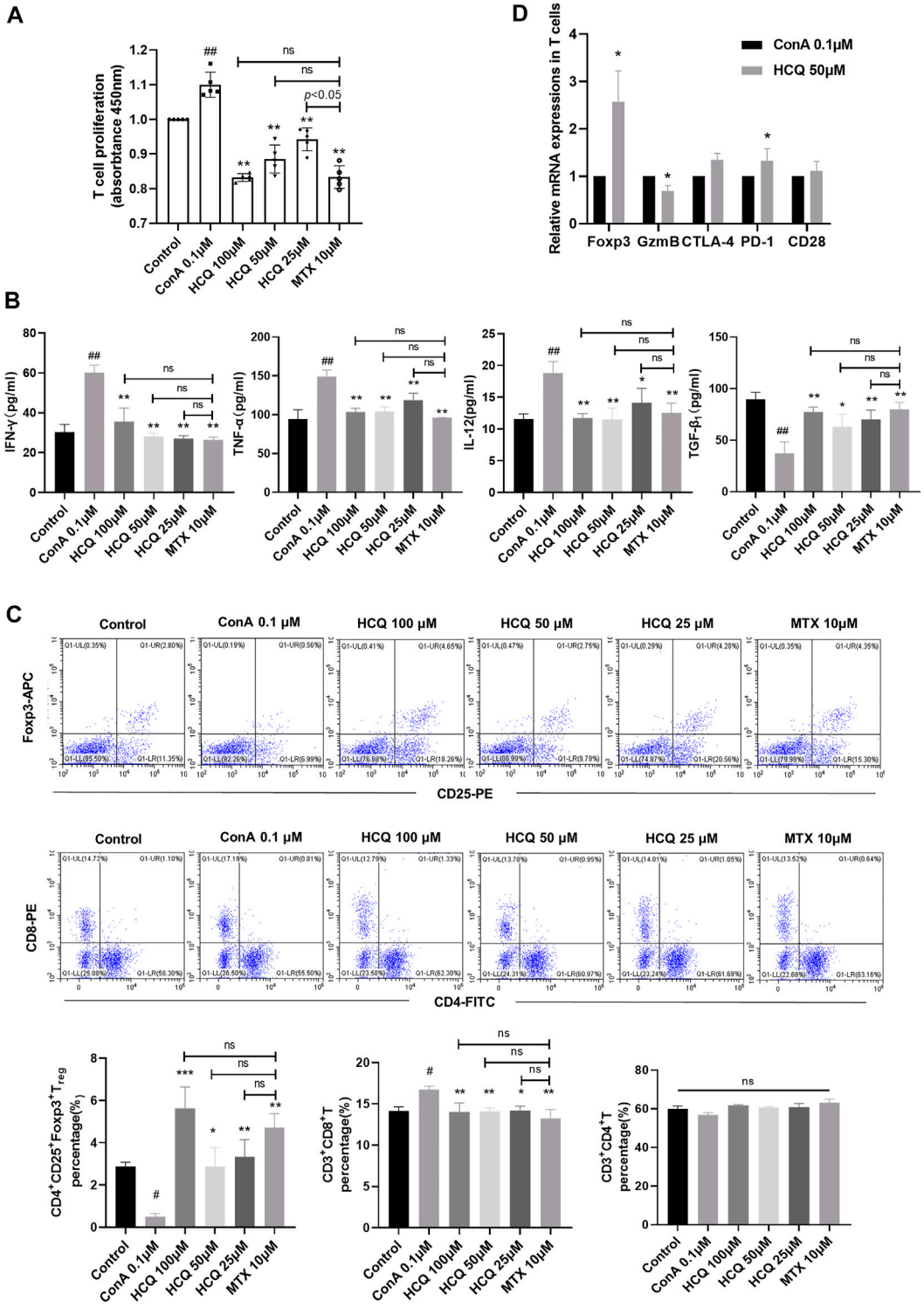

FIGURE 4
HCQ regulated T cell function and differentiation *in vitro*. **(A)** Proliferation of T cells (n = 5). **(B)** Inflammatory cytokine concentrations in T cell culture supernatant (n = 5). **(C)** The percentage of T_{regs}, $CD4^+$T cells, $CD8^+$T cells in T lymphocytes (n = 3). **(D)** Expression of Foxp3, GzmB, CTLA-4, PD-1, CD28 mRNA in T lymphocytes (n = 5). Data expressed as mean ± SD. $^{\#}p < 0.05$, $^{\#\#}p < 0.01$ relative to controls; $^{*}p < 0.05$, $^{**}p < 0.01$, $^{***}p < 0.001$ relative to ConA group; ns, not significant.

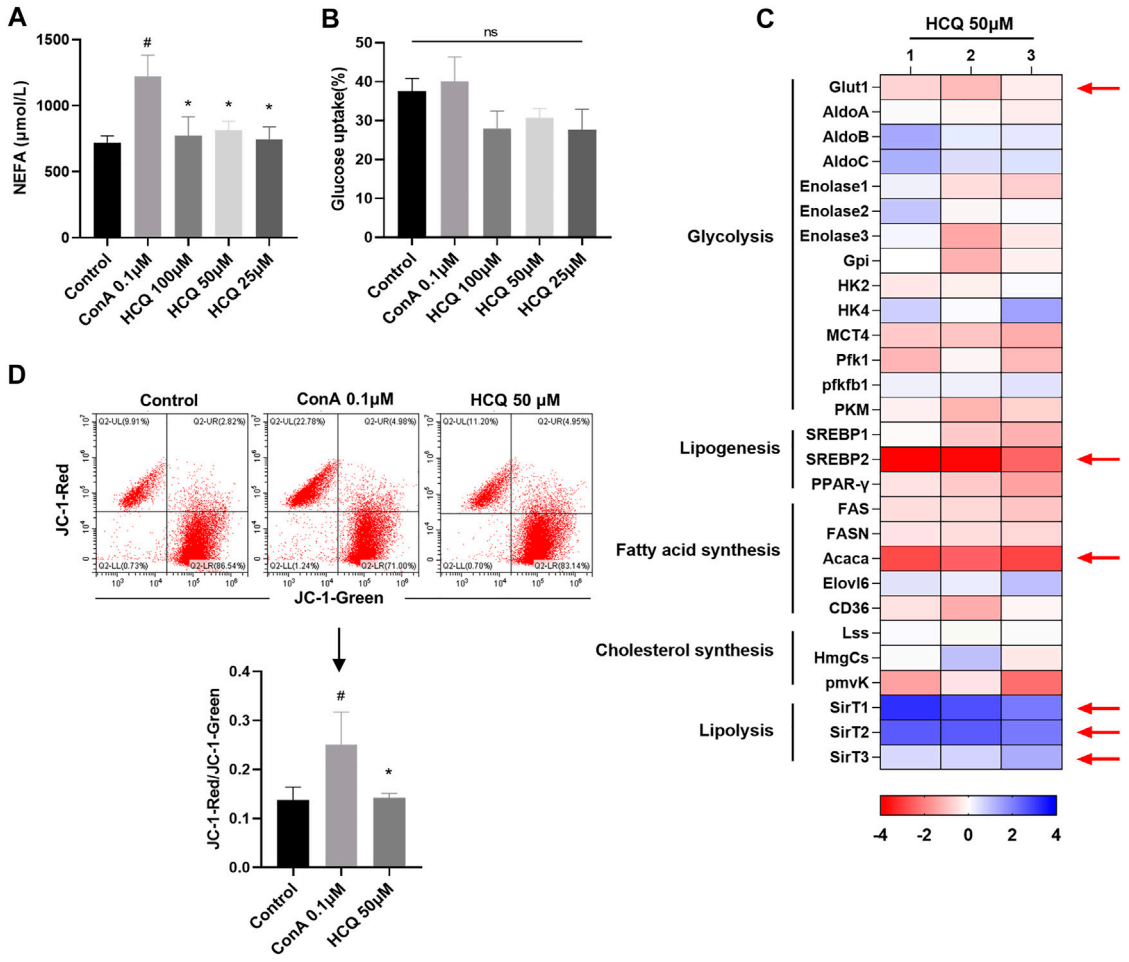

FIGURE 5
Lipid metabolism in T cells was controlled by HCQ. **(A)** Appearance of NEFA (n = 5). **(B)** Glucose uptake (n = 5). **(C)** Marker genes of glycolysis and lipid metabolism, mRNA levels in model controls were set to 1, the heat map represented the $\log_2$ value of the relative mRNA expression levels (see color scale), 1, 2, and 3 represent three parallel experiments. **(D)** MMP of T cells (n = 3). Data expressed as mean ± SD. $^{\#}p < 0.05$, $^{\#\#}p < 0.01$ relative to controls; $^{*}p < 0.05$ relative to ConA.

Hydroxychloroquine acted on G protein-coupled receptor kinases 2 translocation and reduced the membrane recruitment of PI3K in spleen T lymphocytes

The network pharmacology studies showed that multi-targets mechanism associated with HCQ treatment in SLE and RA. The related 3,316 proteins' network data showed that ErbB, HIF-1, NF-κB, FoxO, chemokines, MAPK, JAK-STAT, PI3K-AKT pathways participate in the multi-targets mechanism of HCQ in RA (Lyu et al., 2020; Xie et al., 2021). The efficacy of HCQ against SLE is mainly associated with the targets of cyclin dependent kinase 2 (CDK2), estrogen receptor alpha (ESR1) and CDK1, which regulate PI3K/AKT/GSK3β as well as IFN signaling pathway (Xie et al., 2020). Another study showed that C-C chemokine receptor type 4 (CCR4), a GPCR modulated by GRK2, might an immunomodulatory target of HCQ (Beck et al., 2020). Our studies detected the protein expression of GRK2/PI3K-AKT signal in blood lymphocytes of RA patients and normal people, the results showed that the protein expression of GRK2, p-PI3K and p-AKT were increased in RA patients. The above indicators were reversed after treating by HCQ. In addition, the expression of GzmB was decreased, while the expression of Foxp3 was increased after HCQ treatment in the blood lymphocyte of RA patients (Data not shown). Based on above results and given that the GRK2/PI3K-AKT pathway contributes to the regulation of immune cell metabolism (Yang et al., 2020), we speculated that inhibiting the over activated PI3K-AKT pathway in immune cells might be effective methods for the treatment of RA and other autoimmune diseases such as AIH.

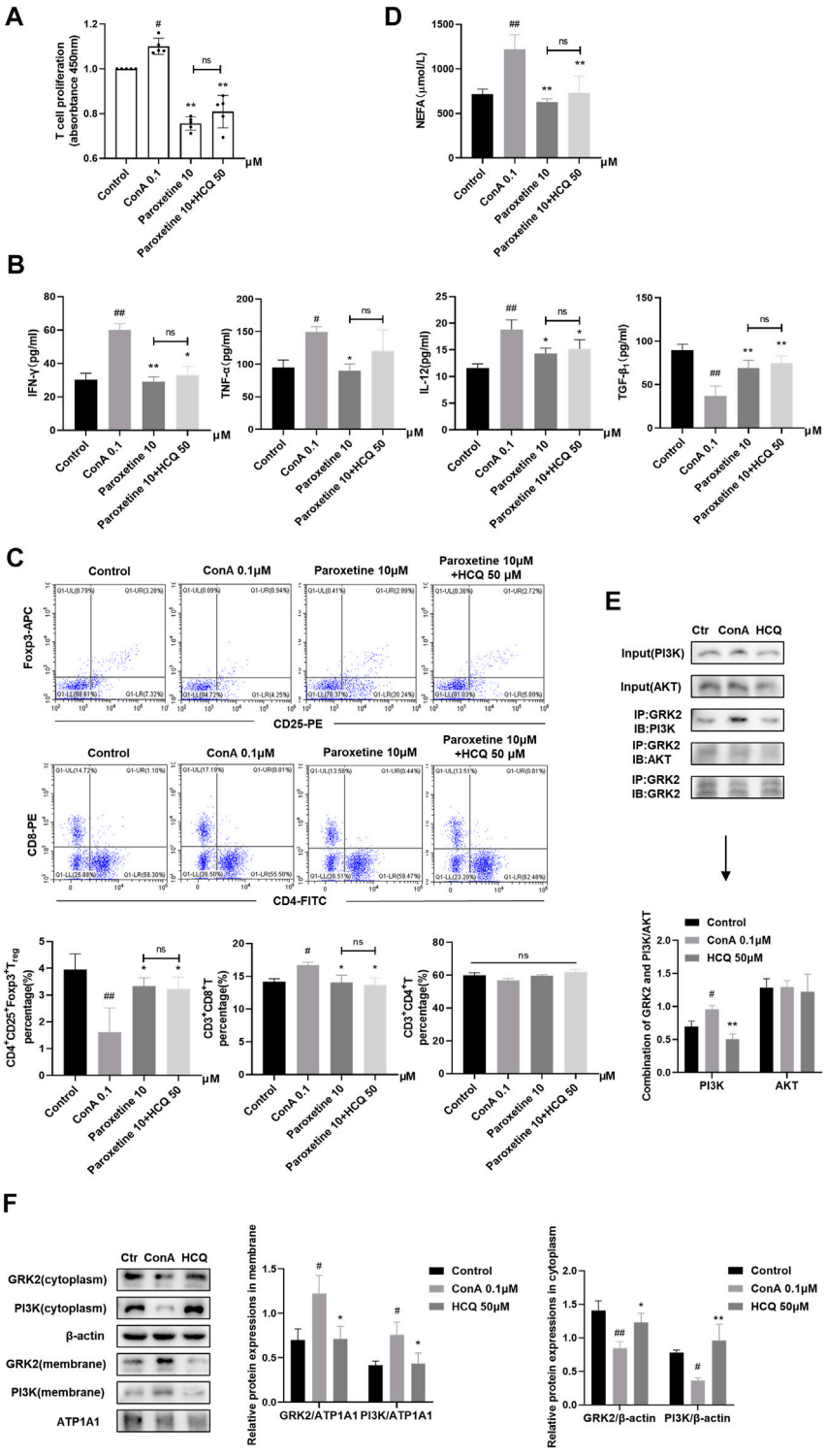

FIGURE 6
HCQ acted on GRK2 translocation and reduced the membrane recruitment of PI3K in spleen T lymphocytes **(A)** Proliferation of T cells after inhibiting GRK2 (n = 5). **(B)** Inflammatory cytokine concentrations in T cell culture supernatant after inhibiting GRK2 (n = 5). **(C)** The percentage of T_{regs}, $CD4^+$T cells, $CD8^+$T cells in T lymphocytes after inhibiting GRK2 (n = 3). **(D)** Appearance of NEFA after inhibiting GRK2 (n = 5). **(E)** The combination of GRK2 and PI3K or AKT (n = 3). **(F)** Membrane and cytoplasm protein expression of GRK2 and PI3K (n = 3). Data expressed as mean ± SD. $^{\#}p < 0.05$, $^{\#\#}p < 0.01$ relative to controls; $^{*}p < 0.05$, $^{**}p < 0.01$ relative to ConA group; ns, not significant.

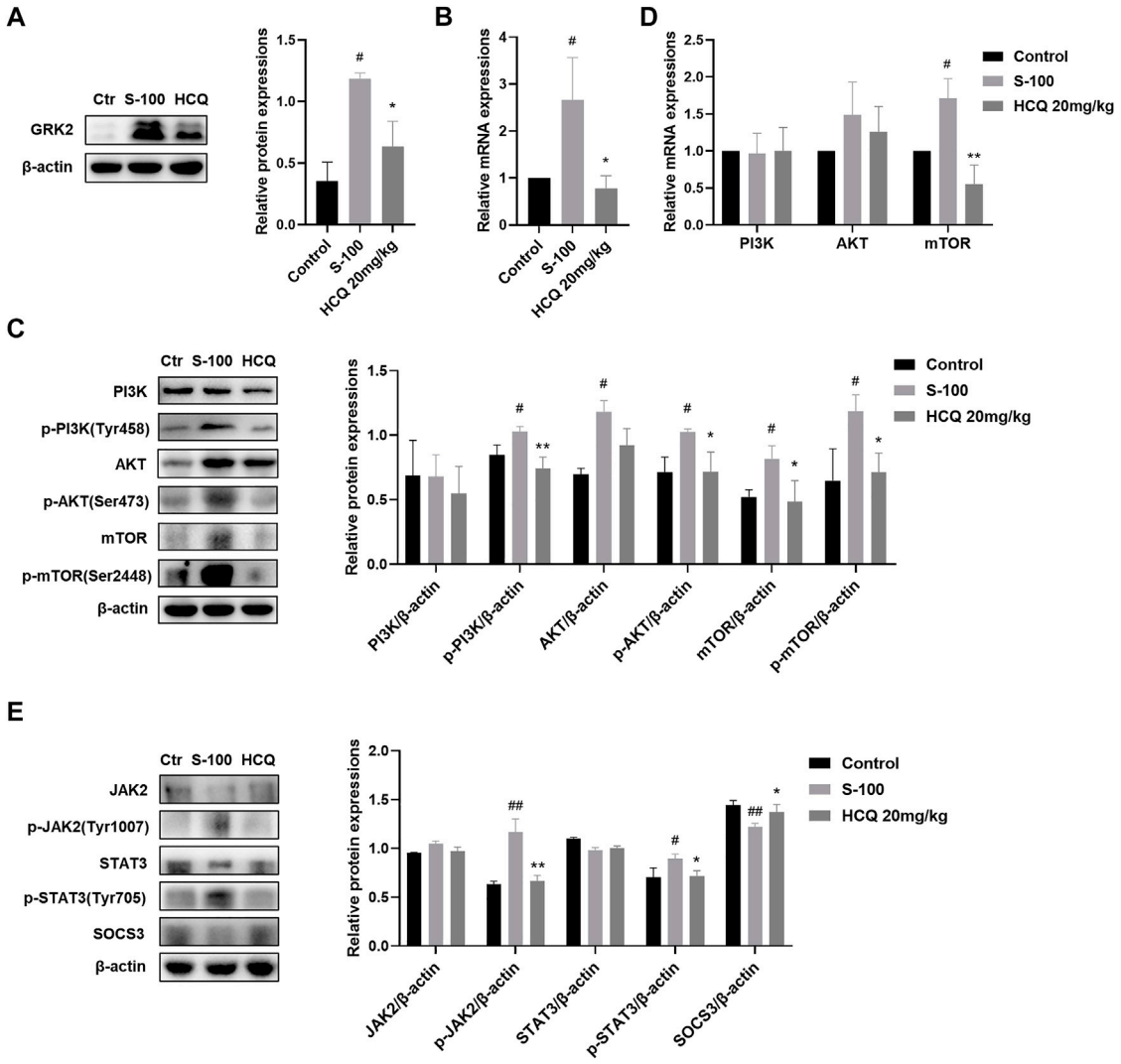

FIGURE 7
HCQ suppressed GRK2/PI3K-AKT-mTOR and JAK2-STAT3-SOCS3 pathways in the liver. **(A)** Total levels of GRK2 proteins in liver (n = 3). **(B)** Transcript levels of GRK2 in the liver (n = 5). **(C)** Total and phosphorylated levels of PI3K, AKT, and mTOR in the liver (n = 3). **(D)** Transcript levels of PI3K, AKT, and mTOR in the liver (n = 5). **(E)** Total and phosphorylated levels of JAK2, STAT3, and total levels of SOCS3 proteins in the liver (n = 3). Data expressed as mean ± SD. $^{\#}p < 0.05$, $^{\#\#}p < 0.01$ relative to controls; $^{*}p < 0.05$, $^{**}p < 0.01$ relative to S-100-induced AIH mice.

We pre-treated ConA induced T cells with paroxetine (GRK2 inhibitor), which retarded the proliferation, proinflammatory factor (IFN-γ, TNF-α, and IL-12) secretion, and NEFA secretion, meanwhile, promoted T_{reg} differentiation and anti-inflammatory factor (TGF-β_1) secretion. Adding HCQ did not enhance the effect of paroxetine, which suggested that the main target of HCQ might have been blocked (Figures 6A–D). Previous studies showed that the interaction of GRK2 with PI3Kγ promoted PI3K to recruit to the membrane to contribute to the signal transduction. Therefore, we detected the combination of GRK2 and PI3K by CO-IP and the membrane and cytoplasmic expression of GRK2 and PI3K by WB respectively after HCQ treatment. The results found that GRK2 and PI3K co-expression increased by ConA stimulation, and HCQ down-regulated GRK2 and PI3K interaction (Figure 6E). In addition, HCQ down-regulated GRK2 and PI3K translocation, inhibited the expression of GRK2 and PI3K in the cell membrane and increased their expression in the cytoplasm of spleen T lymphocytes (Figure 6F). Based on above results, we proposed that HCQ acted on GRK2, inhibited the interaction of GRK2-PI3K and their translocation, which reduced the recruitment of PI3K to the membrane, inhibited downstream signal transduction to disturb the function of activated T cells.

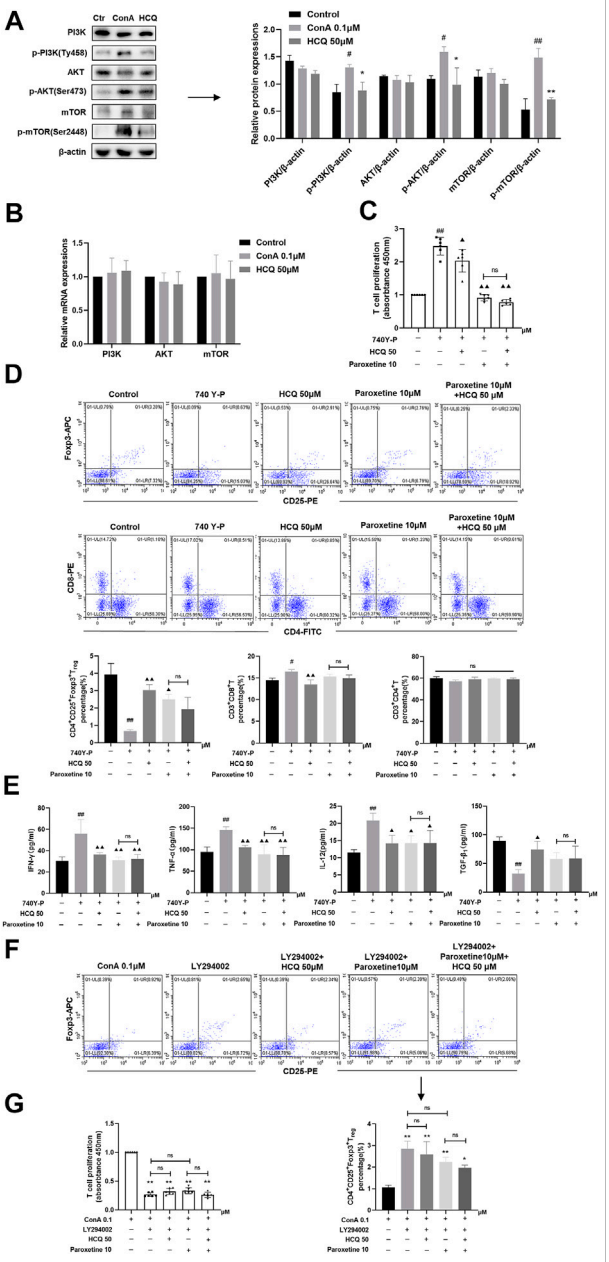

FIGURE 8
HCQ modulated T cell function and T_{reg} differentiation via the PI3K-AKT-mTOR pathway. **(A)** Total and phosphorylated levels of PI3K, AKT, and mTOR proteins of T lymphocytes (n = 3). **(B)** Transcript levels of PI3K, AKT, and mTOR in T lymphocytes (n = 5). **(C)** Proliferation of T cells (n = 6). **(D)** The percentage of T_{regs}, $CD4^+$T cells, $CD8^+$T cells in T lymphocytes (n = 3). **(E)** Inflammatory cytokine concentrations in T cell culture supernatant (n = 5). T lymphocytes isolated from C57BL/6 J mice were incubated with 740 Y-P or 740 Y-P+HCQ. **(F)** The percentage of T_{regs} in T lymphocytes (n = 3). **(G)** Proliferation of T cells (n = 6). T lymphocytes isolated from C57BL/6 J mice were incubated with LY294002, LY294002+HCQ. Data expressed as mean ± SD. $^{\#}p < 0.05$, $^{\#\#}p < 0.01$ relative to controls; $^{*}p < 0.05$, $^{**}p < 0.01$ relative to ConA group; $^{\blacktriangle}p < 0.05$, $^{\blacktriangle\blacktriangle}p < 0.01$ relative to 740Y-P; ns, not significant.

Hydroxychloroquine decreased the activation of metabolism-related PI3K-AKT-mTOR and inflammation-related JAK2-STAT3-SOCS3 pathways in the T cells and liver tissue of AIH mice

The PI3K-AKT pathway contributes to the regulation of immune cell metabolism (Yang et al., 2020), and JAK2-STAT3 pathway is widely considered to be involved in inflammation related diseases. In addition, it has been reported that HCQ may be involved in the regulation of these two pathways (Lyu et al., 2020; Li et al., 2022). Our results showed that HCQ treatment inhibited the protein and mRNA expression of GRK2 (Figures 7A,B) and reversed the activated PI3K-AKT-mTOR pathway induced by S-100 in the liver (Figure 7C). HCQ also suppressed phosphorylation of JAK2, STAT3, and increased SOCS3, the negative regulatory factor, in the liver of AIH mice (Figure 7D).

In T lymphocytes, HCQ suppressed phosphorylation of PI3K (Tyr458), AKT (Ser473) and mTOR (Ser2448), without affecting their mRNA and total protein expressions (Figures 8A,B). Following the PI3K agonist (740 Y-P, 20 μg/ml, 12 h)-mediated activation of PI3K, T cells exhibited proliferation, with enhanced levels of T_{regs}, elevated secretion of IFN-γ, TNF-α and IL-12, and lowered expression TGF-β_1. HCQ, on the other hand, eliminated the impact induced by 740Y-P (Figures 8C–E). In addition, PI3K inhibitors (LY294002, 10 μM, 12 h) inhibited T cell proliferation and promote T_{reg} differentiation compared with ConA group, adding HCQ did not enhance the effect of LY294002 (Figures 8F,G). GRK2 inhibitor also appeared to inhibit pathway activation in the present of 740 Y-P. And the effect of GRK2 inhibitor was weak after LY294002 treatment in T cells. The results suggested that HCQ effect on PI3K-AKT signal might be mediated by GRK2 (Figures 8C–G).

AMPK is a highly conserved serine/threonine protein kinase, which was the inhibition of mTOR in the lipid oxidation of T_{regs} (Michalek et al., 2011). Our results showed that HCQ significantly increased the expression of p-AMPK compared with ConA pretreatment T lymphocyte, which indicated there was the cross-talk of GRK2/PI3K-AKT and AMPK for HCQ effect in AIH (Figure 9A). We also examined the protein expressions of JAK2-STAT3-SOCS3 pathway in ConA-treated spleen T lymphocytes. The results showed that HCQ suppressed the phosphorylation of JAK2 (Tyr1007), STAT3 (Tyr705), without affecting their total protein expressions, and increased the expressions of SOCS3 (Figure 9B), which appears to indicate the mechanism of anti-inflammatory effect of HCQ. HCQ might have a potential inhibition to signals cross-talk and modulation for immunologic homeostasis in AIH. The multi-targets mechanism of HCQ in the treatment of AIH was shown in Figure 10.

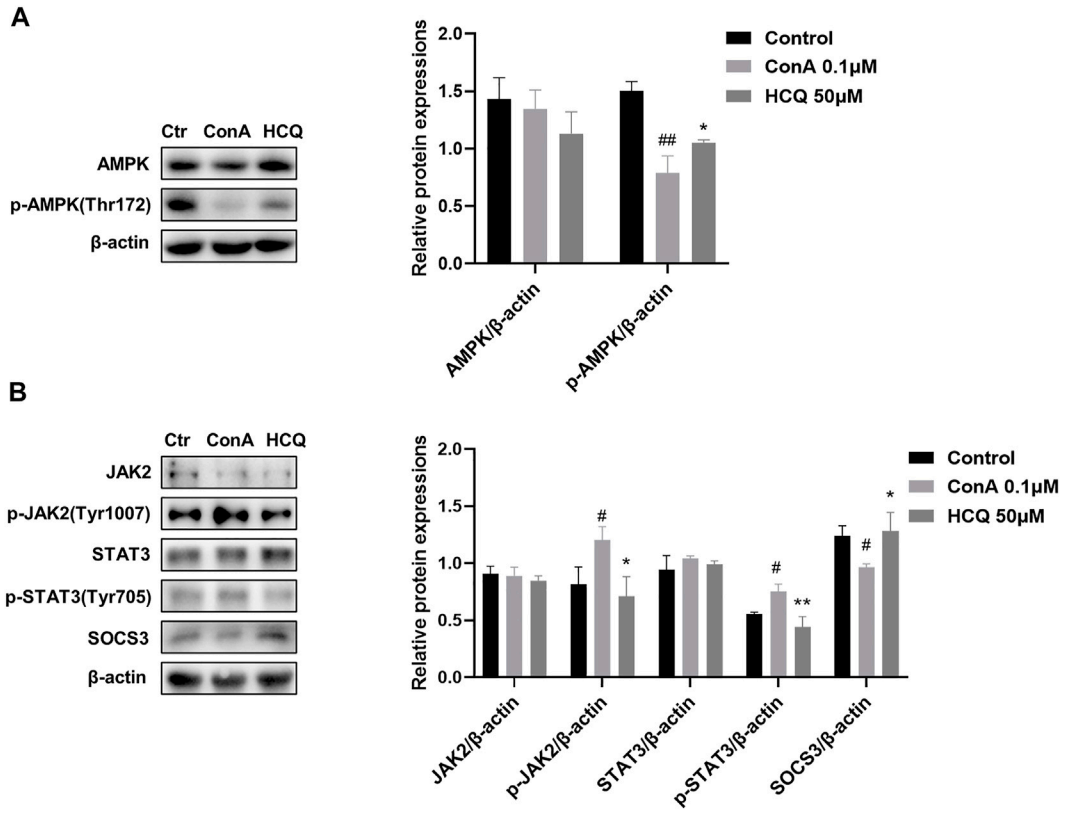

FIGURE 9
HCQ suppressed the activation of JAK2-STAT3-SOCS3 and promoted the phosphorylation of AMPK in T lymphocytes. **(A)** Total and phosphorylated levels of JAK2, STAT3, and total levels of SOCS3 proteins of T lymphocytes (n = 3). **(B)** Total and phosphorylated levels of AMPK of T lymphocytes (n = 3). Data expressed as mean ± SD. $^{\#}p < 0.05$, $^{\#\#}p < 0.01$ relative to controls; $^{*}p < 0.05$, $^{**}p < 0.01$ relative to ConA group.

Discussion

AIH is an autoimmune liver disease, which progress to cirrhosis and liver failure with untreating (Fan et al., 2019). Although the pathogenesis of AIH is not fully understood, it is generally recognized that immunoregulatory networks plays a crucial role (Liberal et al., 2015; Zhu et al., 2021). In a healthy population, circulating autoreactive T cells are suppressed by peripheral tolerance mechanisms to limit autoimmune tissue damage, among which T_{reg}-exerted immune suppression plays a key role. Patients with AIH display a reduced T_{reg} frequency or function compared to healthy subjects (Ferri et al., 2010; Sakaguchi et al., 2010; Liberal et al., 2017; Zhu et al., 2021). In addition, several cytokines are implicated in the pathogenesis of ConA-induced hepatitis, of which TNF-α, IFN-γ, TGF-β are the most important (Sass et al., 2002; Wang et al., 2017b; Zhang et al., 2020). HCQ, as an antimalarial agent, has been used for the treatment of immunological diseases: RA and SLE(3). Recently, HCQ exhibited the probable protective effect in liver injury among the COVID-19 patients (Sima, 2021). It was reported that HCQ restored the Th17/T_{reg} balance in MRL/lpr (mouse model that develops SLE) mice, which resulted in a significant decrease in the expression of IL-17 in Th17 cells and a considerable increase in Foxp3 and TGF-β levels (An et al., 2017).

Based on that observation, we established a model of chronic AIH induced by S-100 combined with CFA, which relatively resembled human AIH. Meanwhile, *in vitro*, we tested the effect of HCQ in ConA activated murine spleen T-lymphocyte. The results showed that HCQ ameliorated hepatic pathologic damage and inflammatory infiltration. Besides, HCQ promoted T_{reg} differentiation and the mRNA expression of Foxp3, and retarded $CD8^{+}$T cells differentiation both *in vivo* and *in vitro*. The critical role of HCQ was the inhibition of the metabolism-related GRK2/PI3K-AKT pathway and the inflammation-related JAK2-STAT3 pathway in T cells. The sequence appears to be: ① HCQ acted on GRK2, inhibited the translocation of GRK2, decreased the interaction between GRK2 and PI3K, and reduced the recruitment of PI3K to the membrane ② the blockade of the PI3K-AKT pathway by HCQ accompanied with the inhibition of the inflammation-related JAK2-STAT3 pathway in T cells ③ the diminished lipid metabolism of T cells impaired its function, followed by increasing T_{reg} differentiation,

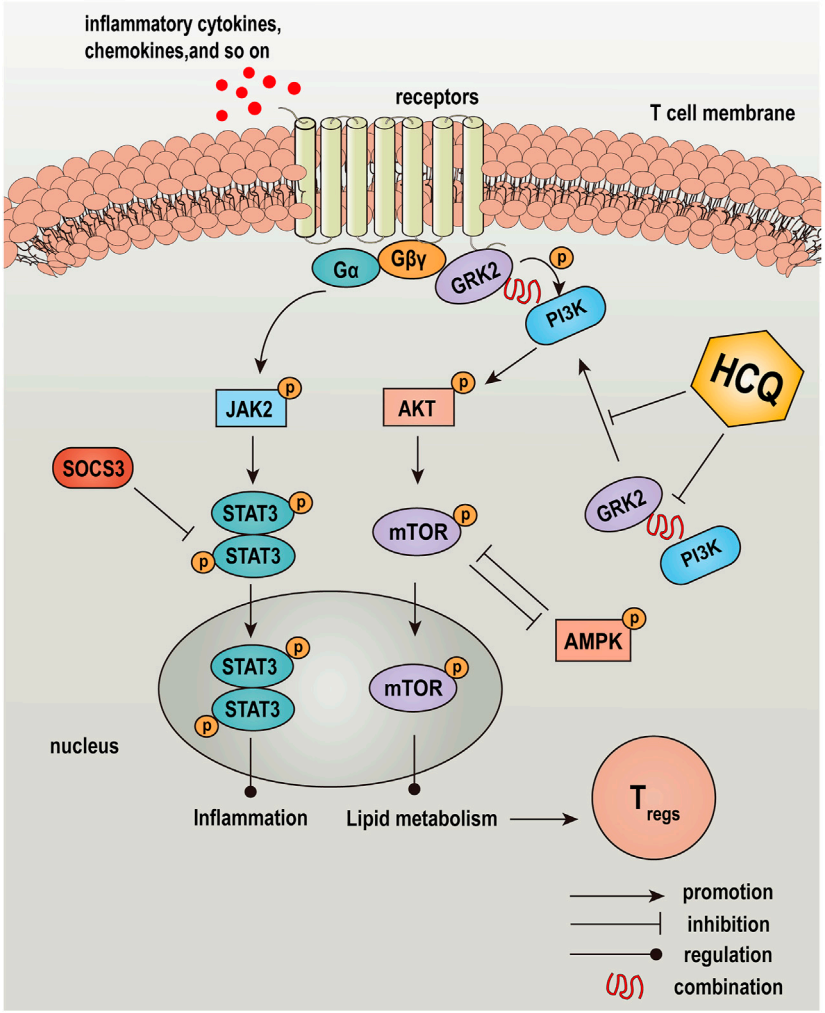

FIGURE 10
Graphical abstract: a schematic diagram depicted the effect and mechanism of HCQ in the treatment of AIH. HCQ targeted GRK2-PI3K interaction and translocation to modulated lipid metabolism of T lymphocyte, which mediated T cells differentiation and function, and reversed inflammation injury in the liver of AIH.

disrupting $CD8^+$T cell responses, upregulating co-inhibition signal and anti-inflammatory cytokine TGF-β_1 expression, and decreasing proinflammatory cytokines released from T cells; and ④ consequently, HCQ inhibited inflammatory cell infiltration and immune responses against liver tissue, and thus diminished autoimmune liver injury (Figure 8C).

Activation of immune cells is associated with a dramatic increase in metabolism. Glucose and lipid metabolism is related to differentiation of T_{reg} (Cluxton et al., 2019; Shan et al., 2020). Besides, it has also been reported that glucose and lipid metabolism is also related to other immune cells, such as $CD4^+$T, $CD8^+$T, DC, natural killer T (NKT) cells (Palmer et al., 2016; Giovanelli et al., 2019). Our results showed that HCQ treatment decreased NEFA secretion while increased fatty acid oxidation in T lymphocytes, but HCQ had little effect on T cell glucose uptake and glycolysis. Suppressed lipid metabolism predominantly rather than glycolysis of T cell may contribute to immunosuppressive effects of HCQ in AIH. PI3K-AKT-mTOR has been proved to be a classical pathway linking the activation of the insulin receptor to regulate glucose metabolism, which was also shown to be responsible for the accumulation of intracellular lipids by regulating fatty acid synthesis (Chen et al., 2019; Sun et al., 2022). In addition, the activation of PI3K-AKT-mTOR is accompanied with the inhibition of differentiation and function of T_{reg} (Gao et al., 2020). mTOR is the downstream protein of PI3K-AKT, inhibition of mTOR favors naive $CD4^+$T-cell conversion to iT_{regs}, and mTOR knockout or treatment with the mTOR-specific inhibitor, rapamycin, favors T_{reg}

development (Battaglia et al., 2005; Kopf et al., 2007; Delgoffe et al., 2009; Pompura and Dominguez-Villar, 2018). AMPK and mTOR reciprocally regulate each other, which favors FAO and T_{reg} development (Hardie et al., 2006; Hardie, 2011). Our results showed that HCQ may inhibited NEFA secretion, fatty acid synthesis gene expression and promoted FAO through PI3K-AKT-mTOR and AMPK signals. In addition, JAK-STAT is an important pathway mediating most actions of inflammatory cytokines (Xin et al., 2020). HCQ might affect the modulation loop involving interactions of these three signals to maintain immune homeostasis during the progression of AIH. The multi-targets of immune cells and signals affected by HCQ optimized the treatment of HCQ in AIH.

Accumulating data indicate that GRK2 is overexpressed in RA and cardiac dysfunction to play a critical role in ameliorating inflammatory (Penela et al., 2008; Woodall et al., 2016). Previous study proposed that inhibiting the expression of GRK2 in the membrane and increasing its expression in cytoplasm improved the abnormal proliferation of fibroblast like synovial cells in RA(15). In addition, inhibition of GRK2 expression in rat spleen T cells can regulate T cell function to alleviate RA(16). GRK2 specifically recognize and phosphorylate agonist-activated GPCRs, and it also interact with non-GPCRs such as PI3K, AKT (Ribas et al., 2007). The interaction of PI3Kγ with GRK2 mediated PI3K recruitment to the membrane after agonist stimulation. In addition, the inhibition of GRK2-$G_{\beta\gamma}$ complex membrane translocation in the fibroblast-like synoviocytes might reduce the membrane expression and activation of PI3K, which mediated the inhibition of AKT activity (Wang et al., 2020). AKT had also been reported to associate with GRK2 directly through the GRK2 C-terminus. GRK2 might inhibit agonist-dependent AKT phosphorylation, although the exact mechanisms were not well established (Ribas et al., 2007). The inhibition of GRK2 rescued AKT activity to promote T_{reg} differentiation in mice with diabetic cardiomyopathy (Han et al., 2020). There was also reported that GRK2 knock down prevented AKT activation in cardiac myocytes but the interaction between GRK2 and AKT was not clear (Penela et al., 2010; Pathania et al., 2019). In addition, increasing PI3K produced polyphosphoinositides that interacted with protein kinases, leading to activation of the kinase AKT (Saltiel, 2021). HCQ has been reported to inhibit PI3K-AKT pathway in renal interstitial fibrosis (Li et al., 2022). Therefore, we tested whether HCQ inhibited the PI3K-AKT pathway by regulating the interaction between GRK2 and PI3K or AKT in T cells of AIH. Our results found that GRK2 and PI3K were co expressed in T lymphocytes. HCQ down-regulated GRK2-PI3K interaction to reduce the complex translocation, and suppressed the phosphorylation of PI3K, AKT, and mTOR. The direct interaction of GRK2 with AKT was undefined. After blocking GRK2, the effect of HCQ was diminished.

In conclusion, HCQ exhibits specific and potent therapeutic effects on AIH and attendant liver injury. The critical role appears to be: HCQ acted on GRK2 translocation mediated PI3K-AKT-mTOR signal inhibition in spleen T lymphocyte, thereby modulating lipid metabolism in T lymphocytes and promoting T_{reg} activity. And HCQ might block the cross-talk of JAK2-STAT3-SOCS3, PI3K-AKT-mTOR and AMPK signals.

Data availability statement

Data supporting the results of this study can be obtained from the corresponding author upon reasonable request.

Ethics statement

The animal study was reviewed and approved by the Laboratory Animal Ethics Committee of Anhui Medical University.

Author contributions

T-TL participated in the study design, experimental validation, analyzed the data, material support, coordination, drafted the manuscript, and supervision of the study. CJ designed the experimental validation, performed experiments, analyzed the data, and drafted the manuscript. B-BG performed experiments and analyzed the data. W-JZ, B-JZ, XF, C-LY, and X-HW carried out parts of the experiments. QX gave technical guidance. All authors read and approved the final manuscript.

Funding

This work was supported by the National Natural Science Foundation of China (No. 81903622), the Nature Science Foundation of Anhui Province of China (No. 1908085QH378), the Echelon Talents and Academic Leaders Training Object Funding of First Affiliated Hospital of Anhui Medical University (No. 1290) and the Natural Science Foundation of Hefei, Anhui Province (No. 2021012).

Acknowledgments

We acknowledge the Center for Scientific Research of the First Affiliated Hospital of Anhui Medical University and the Center for Scientific Research of Anhui Medical University for providing some laboratory instruments in this study.

Conflict of interest

The authors declare that the research was conducted in the absence of any commercial or financial relationships that could be construed as a potential conflict of interest.

The handling editor LZ declared a shared parent affiliation with the authors at the time of review.

Publisher's note

All claims expressed in this article are solely those of the authors and do not necessarily represent those of their affiliated organizations, or those of the publisher, the editors and the reviewers. Any product that may be evaluated in this article, or claim that may be made by its manufacturer, is not guaranteed or endorsed by the publisher.

Supplementary material

The Supplementary Material for this article can be found online at: https://www.frontiersin.org/articles/10.3389/fphar.2022.972397/full#supplementary-material

References

An, N., Chen, Y., Wang, C., Yang, C., Wu, Z. H., Xue, J., et al. (2017). Chloroquine autophagic inhibition rebalances Th17/treg-mediated immunity and ameliorates systemic lupus erythematosus. *Cell. Physiol. biochem.* 44 (1), 412–422. doi:10.1159/000484955

Battaglia, M., Stabilini, A., and Roncarolo, M. G. (2005). Rapamycin selectively expands CD4+CD25+FoxP3+ regulatory T cells. *Blood* 105 (12), 4743–4748. doi:10.1182/blood-2004-10-3932

Beck, T. C., Beck, K. R., Holloway, C. B., Hemings, R. A., Jr., Dix, T. A., and Norris, R. A. (2020). The C-C chemokine receptor type 4 is an immunomodulatory target of hydroxychloroquine. *Front. Pharmacol.* 11, 1253. doi:10.3389/fphar.2020.01253

Ben-Zvi, I., Kivity, S., Langevitz, P., and Shoenfeld, Y. (2012). Hydroxychloroquine: From malaria to autoimmunity. *Clin. Rev. Allergy Immunol.* 42 (2), 145–153. doi:10.1007/s12016-010-8243-x

Chen, Q., Tang, L., Xin, G., Li, S., Ma, L., Xu, Y., et al. (2019). Oxidative stress mediated by lipid metabolism contributes to high glucose-induced senescence in retinal pigment epithelium. *Free Radic. Biol. Med.* 130, 48–58. doi:10.1016/j.freeradbiomed.2018.10.419

Cheng, J., Lucas, P. C., and McAllister-Lucas, L. M. (2021). Canonical and non-canonical roles of GRK2 in lymphocytes. *Cells* 10 (2), 307. doi:10.3390/cells10020307

Christen, U. (2019). Animal models of autoimmune hepatitis. *Biochim. Biophys. Acta. Mol. Basis Dis.* 1865 (5), 970–981. doi:10.1016/j.bbadis.2018.05.017

Cluxton, D., Petrasca, A., Moran, B., and Fletcher, J. M. (2019). Differential regulation of human Treg and Th17 cells by fatty acid synthesis and glycolysis. *Front. Immunol.* 10, 115. doi:10.3389/fimmu.2019.00115

Delgoffe, G. M., Kole, T. P., Zheng, Y., Zarek, P. E., Matthews, K. L., Xiao, B., et al. (2009). The mTOR kinase differentially regulates effector and regulatory T cell lineage commitment. *Immunity* 30 (6), 832–844. doi:10.1016/j.immuni.2009.04.014

Fan, X., Men, R., Wang, H., Shen, M., Wang, T., Ye, T., et al. (2019). Methylprednisolone decreases mitochondria-mediated apoptosis and autophagy dysfunction in hepatocytes of experimental autoimmune hepatitis model via the akt/mTOR signaling. *Front. Pharmacol.* 10, 1189. doi:10.3389/fphar.2019.01189

Fang, X., Tan, T., Gao, B., Zhao, Y., Liu, T., and Xia, Q. (2020). Germacrone regulates HBXIP-mediated cell cycle, apoptosis and promotes the formation of autophagosomes to inhibit the proliferation of gastric cancer cells. *Front. Oncol.* 10, 537322. doi:10.3389/fonc.2020.537322

Ferri, S., Longhi, M. S., De Molo, C., Lalanne, C., Muratori, P., Granito, A., et al. (2010). A multifaceted imbalance of T cells with regulatory function characterizes type 1 autoimmune hepatitis. *Hepatology* 52 (3), 999–1007. doi:10.1002/hep.23792

Fox, C. J., Hammerman, P. S., and Thompson, C. B. (2005). Fuel feeds function: Energy metabolism and the T-cell response. *Nat. Rev. Immunol.* 5 (11), 844–852. doi:10.1038/nri1710

Gao, L., Dong, Y., Lin, R., Meng, Y., Wu, F., and Jia, L. (2020). The imbalance of Treg/Th17 cells induced by perinatal bisphenol A exposure is associated with activation of the PI3K/Akt/mTOR signaling pathway in male offspring mice. *Food Chem. Toxicol.* 137, 111177. doi:10.1016/j.fct.2020.111177

Giovanelli, P., Sandoval, T. A., and Cubillos-Ruiz, J. R. (2019). Dendritic cell metabolism and function in tumors. *Trends Immunol.* 40 (8), 699–718. doi:10.1016/j.it.2019.06.004

Han, C. C., Ma, Y., Li, Y., Wang, Y., and Wei, W. (2016). Regulatory effects of GRK2 on GPCRs and non-GPCRs and possible use as a drug target (Review). *Int. J. Mol. Med.* 38 (4), 987–994. doi:10.3892/ijmm.2016.2720

Han, Y., Lai, J., Tao, J., Tai, Y., Zhou, W., Guo, P., et al. (2020). Sustaining circulating regulatory T cell subset contributes to the therapeutic effect of paroxetine on mice with diabetic cardiomyopathy. *Circ. J.* 84 (9), 1587–1598. doi:10.1253/circj.CJ-19-1182

Hardie, D. G. (2011). AMP-Activated protein kinase: An energy sensor that regulates all aspects of cell function. *Genes. Dev.* 25 (18), 1895–1908. doi:10.1101/gad.17420111

Hardie, D. G., Hawley, S. A., and Scott, J. W. (2006). AMP-activated protein kinase--development of the energy sensor concept. *J. Physiol.* 574 (1), 7–15. doi:10.1113/jphysiol.2006.108944

Hu, C., Lu, L., Wan, J. P., and Wen, C. (2017). The pharmacological mechanisms and therapeutic activities of hydroxychloroquine in rheumatic and related diseases. *Curr. Med. Chem.* 24 (20), 2241–2249. doi:10.2174/0929867324666170316115938

Kopf, H., de la Rosa, G. M., Howard, O. M., and Chen, X. (2007). Rapamycin inhibits differentiation of Th17 cells and promotes generation of FoxP3+ T regulatory cells. *Int. Immunopharmacol.* 7 (13), 1819–1824. doi:10.1016/j.intimp.2007.08.027

Koyama, Y., and Brenner, D. A. (2017). Liver inflammation and fibrosis. *J. Clin. Invest.* 127 (1), 55–64. doi:10.1172/JCI88881

Li, D., Yu, K., Feng, F., Zhang, Y., Bai, F., Zhang, Y., et al. (2022). Hydroxychloroquine alleviates renal interstitial fibrosis by inhibiting the PI3K/Akt signaling pathway. *Biochem. Biophys. Res. Commun.* 610, 154–161. doi:10.1016/j.bbrc.2022.04.058

Liberal, R., Grant, C. R., Longhi, M. S., Mieli-Vergani, G., and Vergani, D. (2015). Regulatory T cells: Mechanisms of suppression and impairment in autoimmune liver disease. *IUBMB Life* 67 (2), 88–97. doi:10.1002/iub.1349

Liberal, R., Grant, C. R., Yuksel, M., Graham, J., Kalbasi, A., Ma, Y., et al. (2017). Regulatory T-cell conditioning endows activated effector T cells with suppressor function in autoimmune hepatitis/autoimmune sclerosing cholangitis. *Hepatology* 66 (5), 1570–1584. doi:10.1002/hep.29307

Liu, T., Cao, H., Ji, Y., Pei, Y., Yu, Z., Quan, Y., et al. (2015). Interaction of dendritic cells and T lymphocytes for the therapeutic effect of Dangguiliuhuang decoction to autoimmune diabetes. *Sci. Rep.* 5, 13982. doi:10.1038/srep13982

Liu, T. T., Ding, T. L., Ma, Y., and Wei, W. (2014). Selective α1B- and α1D-adrenoceptor antagonists suppress noradrenaline-induced activation, proliferation and ECM secretion of rat hepatic stellate cells *in vitro*. *Acta Pharmacol. Sin.* 35 (11), 1385–1392. doi:10.1038/aps.2014.84

Lyu, X., Zeng, L., Zhang, H., Ke, Y., Liu, X., Zhao, N., et al. (2020). Hydroxychloroquine suppresses lung tumorigenesis via inducing FoxO3a nuclear translocation through STAT3 inactivation. *Life Sci.* 246, 117366. doi:10.1016/j.lfs.2020.117366

Martinez, G. P., Zabaleta, M. E., Di Giulio, C., Charris, J. E., and Mijares, M. R. (2020). The role of chloroquine and hydroxychloroquine in immune regulation and diseases. *Curr. Pharm. Des.* 26 (35), 4467–4485. doi:10.2174/1381612826666200707132920

Matias, M. I., Yong, C. S., Foroushani, A., Goldsmith, C., Mongellaz, C., Sezgin, E., et al. (2021). Regulatory T cell differentiation is controlled by αKG-induced

alterations in mitochondrial metabolism and lipid homeostasis. *Cell Rep.* 37 (5), 109911. doi:10.1016/j.celrep.2021.109911

Michalek, R. D., Gerriets, V. A., Jacobs, S. R., Macintyre, A. N., MacIver, N. J., Mason, E. F., et al. (2011). Cutting edge: Distinct glycolytic and lipid oxidative metabolic programs are essential for effector and regulatory CD4+ T cell subsets. *J. Immunol.* 186 (6), 3299–3303. doi:10.4049/jimmunol.1003613

Murphy, K. M., Heimberger, A. B., and Loh, D. Y. (1990). Induction by antigen of intrathymic apoptosis of CD4+CD8+TCRlo thymocytes *in vivo*. *Science* 250 (4988), 1720–1723. doi:10.1126/science.2125367

Palmer, C. S., Hussain, T., Duette, G., Weller, T. J., Ostrowski, M., Sada-Ovalle, I., et al. (2016). Regulators of glucose metabolism in CD4(+) and CD8(+) T cells. *Int. Rev. Immunol.* 35 (6), 477–488. doi:10.3109/08830185.2015.1082178

Pathania, A. S., Ren, X., Mahdi, M. Y., Shackleford, G. M., and Erdreich-Epstein, A. (2019). GRK2 promotes growth of medulloblastoma cells and protects them from chemotherapy-induced apoptosis. *Sci. Rep.* 9 (1), 13902. doi:10.1038/s41598-019-50157-5

Penela, P., Murga, C., Ribas, C., Lafarga, V., and Mayor, F., Jr (2010). The complex G protein-coupled receptor kinase 2 (GRK2) interactome unveils new physiopathological targets. *Br. J. Pharmacol.* 160 (4), 821–832. doi:10.1111/j.1476-5381.2010.00727.x

Penela, P., Murga, C., Ribas, C., Salcedo, A., Jurado-Pueyo, M., Rivas, V., et al. (2008). G protein-coupled receptor kinase 2 (GRK2) in migration and inflammation. *Arch. Physiol. Biochem.* 114 (3), 195–200. doi:10.1080/13813450802181039

Pompura, S. L., and Dominguez-Villar, M. (2018). The PI3K/AKT signaling pathway in regulatory T-cell development, stability, and function. *J. Leukoc. Biol.* 103, 1065–1076. doi:10.1002/JLB.2MIR0817-349R

Rainsford, K. D., Parke, A. L., Clifford-Rashotte, M., and Kean, W. F. (2015). Therapy and pharmacological properties of hydroxychloroquine and chloroquine in treatment of systemic lupus erythematosus, rheumatoid arthritis and related diseases. *Inflammopharmacology* 23 (5), 231–269. doi:10.1007/s10787-015-0239-y

Ribas, C., Penela, P., Murga, C., Salcedo, A., Garcia-Hoz, C., Jurado-Pueyo, M., et al. (2007). The G protein-coupled receptor kinase (GRK) interactome: Role of GRKs in GPCR regulation and signaling. *Biochim. Biophys. Acta* 1768 (4), 913–922. doi:10.1016/j.bbamem.2006.09.019

Sakaguchi, S., Miyara, M., Costantino, C. M., and Hafler, D. A. (2010). FOXP3+ regulatory T cells in the human immune system. *Nat. Rev. Immunol.* 10 (7), 490–500. doi:10.1038/nri2785

Saltiel, A. R. (2021). Insulin signaling in health and disease. *J. Clin. Invest.* 131 (1), 142241. doi:10.1172/JCI142241

Sass, G., Heinlein, S., Agli, A., Bang, R., Schumann, J., and Tiegs, G. (2002). Cytokine expression in three mouse models of experimental hepatitis. *Cytokine* 19 (3), 115–120. doi:10.1006/cyto.2002.1948

Seenappa, V., Das, B., Joshi, M. B., and Satyamoorthy, K. (2016). Context dependent regulation of human phosphoenolpyruvate carboxykinase isoforms by DNA promoter methylation and RNA stability. *J. Cell. Biochem.* 117 (11), 2506–2520. doi:10.1002/jcb.25543

Shan, J., Jin, H., and Xu, Y. (2020). T cell metabolism: A new perspective on Th17/treg cell imbalance in systemic lupus erythematosus. *Front. Immunol.* 11, 1027. doi:10.3389/fimmu.2020.01027

Sima, A. R. (2021). Hydroxychloroquine's probable protective effect in liver injury among the COVID-19 patients. *Middle East J. Dig. Dis.* 13 (1), 80–81. doi:10.34172/mejdd.2021.209

Sun, J. P., Shi, L., Wang, F., Qin, J., and Ke, B. (2022). Modified linggui zhugan decoction ameliorates glycolipid metabolism and inflammation via PI3K-Akt/mTOR-S6K1/AMPK-PGC-1 alpha signaling pathways in obese type 2 diabetic rats. *Chin. J. Integr. Med.* 28 (1), 52–59. doi:10.1007/s11655-020-3285-2

Wang, D. D., Jiang, M. Y., Wang, W., Zhou, W. J., Zhang, Y. W., Yang, M., et al. (2020). Paeoniflorin-6'-O-benzene sulfonate down-regulates CXCR4-Gβγ-PI3K/AKT mediated migration in fibroblast-like synoviocytes of rheumatoid arthritis by inhibiting GRK2 translocation. *Biochem. Biophys. Res. Commun.* 526 (3), 805–812. doi:10.1016/j.bbrc.2020.03.164

Wang, L., Zhang, W., Ge, C. H., Yin, R. H., Xiao, Y., Zhan, Y. Q., et al. (2017). Toll-like receptor 5 signaling restrains T-cell/natural killer T-cell activation and protects against concanavalin A-induced hepatic injury. *Hepatology* 65 (6), 2059–2073. doi:10.1002/hep.29140

Wang, Q., Wang, L., Wu, L., Zhang, M., Hu, S., Wang, R., et al. (2017). Paroxetine alleviates T lymphocyte activation and infiltration to joints of collagen-induced arthritis. *Sci. Rep.* 7, 45364. doi:10.1038/srep45364

Wang, Y., Han, C. C., Cui, D., Luo, T. T., Li, Y., Zhang, Y., et al. (2018). Immunomodulatory effects of CP-25 on splenic T cells of rats with adjuvant arthritis. *Inflammation* 41 (3), 1049–1063. doi:10.1007/s10753-018-0757-z

Woodall, M. C., Woodall, B. P., Gao, E., Yuan, A., and Koch, W. J. (2016). Cardiac fibroblast GRK2 deletion enhances contractility and remodeling following ischemia/reperfusion injury. *Circ. Res.* 119 (10), 1116–1127. doi:10.1161/CIRCRESAHA.116.309538

Xiang, M., Liu, T., Tan, W., Ren, H., Li, H., Liu, J., et al. (2016). Effects of kinsenoside, a potential immunosuppressive drug for autoimmune hepatitis, on dendritic cells/CD8(+) T cells communication in mice. *Hepatology* 64 (6), 2135–2150. doi:10.1002/hep.28825

Xiang, M., Liu, T., Tian, C., Ma, K., Gou, J., Huang, R., et al. (2022). Kinsenoside attenuates liver fibro-inflammation by suppressing dendritic cells via the PI3K-AKT-FoxO1 pathway. *Pharmacol. Res.* 177, 106092. doi:10.1016/j.phrs.2022.106092

Xie, B., Geng, Q., Xu, J., Lu, H., Luo, H., Hu, Y., et al. (2020). The multi-targets mechanism of hydroxychloroquine in the treatment of systemic lupus erythematosus based on network pharmacology. *Lupus* 29 (13), 1704–1711. doi:10.1177/0961203320952541

Xie, B., Lu, H., Xu, J., Luo, H., Hu, Y., Chen, Y., et al. (2021). Targets of hydroxychloroquine in the treatment of rheumatoid arthritis. A network pharmacology study. *Jt. Bone Spine* 88 (2), 105099. doi:10.1016/j.jbspin.2020.105099

Xin, P., Xu, X., Deng, C., Liu, S., Wang, Y., Zhou, X., et al. (2020). The role of JAK/STAT signaling pathway and its inhibitors in diseases. *Int. Immunopharmacol.* 80, 106210. doi:10.1016/j.intimp.2020.106210

Yang, H., Cao, Q., Xiong, X., Zhao, P., Shen, D., Zhang, Y., et al. (2020). Fluoxetine regulates glucose and lipid metabolism via the PI3KAKT signaling pathway in diabetic rats. *Mol. Med. Rep.* 22 (4), 3073–3080. doi:10.3892/mmr.2020.11416

Yang, Y., Zhang, P., Wang, Y., Wei, S., Zhang, L., Wang, J., et al. (2018). Hepatoprotective effect of san-cao granule on con A-induced liver injury in mice and mechanisms of action exploration. *Front. Pharmacol.* 9, 624. doi:10.3389/fphar.2018.00624

Zhang, M., Li, Q., Zhou, C., Zhao, Y., Li, R., and Zhang, Y. (2020). Demethyleneberberine attenuates concanavalin A-induced autoimmune hepatitis in mice through inhibition of NF-κB and MAPK signaling. *Int. Immunopharmacol.* 80, 106137. doi:10.1016/j.intimp.2019.106137

Zheng, H., Zhang, Y., He, J., Yang, Z., Zhang, R., Li, L., et al. (2021). Hydroxychloroquine inhibits macrophage activation and attenuates renal fibrosis after ischemia-reperfusion injury. *Front. Immunol.* 12, 645100. doi:10.3389/fimmu.2021.645100

Zhu, H., Liu, Z., An, J., Zhang, M., Qiu, Y., and Zou, M. H. (2021). Activation of AMPKα1 is essential for regulatory T cell function and autoimmune liver disease prevention. *Cell. Mol. Immunol.* 18 (12), 2609–2617. doi:10.1038/s41423-021-00790-w

frontiers | Frontiers in Pharmacology

TYPE Review
PUBLISHED 01 November 2022
DOI 10.3389/fphar.2022.972320

OPEN ACCESS

EDITED BY
Baoming Wu,
Anhui Medical University, China

REVIEWED BY
Xiaogang Xiang,
Shanghai Jiao Tong University, China
Prasanna K. Santhekadur,
JSS Academy of Higher Education and Research, India

*CORRESPONDENCE
Sharifa T. Love-Rutledge,
sharifa.love-rutledge@uah.edu

SPECIALTY SECTION
This article was submitted to Gastrointestinal and Hepatic Pharmacology, a section of the journal Frontiers in Pharmacology

RECEIVED 18 June 2022
ACCEPTED 12 October 2022
PUBLISHED 01 November 2022

CITATION
Wimalarathne MM, Wilkerson-Vidal QC, Hunt EC and Love-Rutledge ST (2022), The case for FAT10 as a novel target in fatty liver diseases.
Front. Pharmacol. 13:972320.
doi: 10.3389/fphar.2022.972320

The case for FAT10 as a novel target in fatty liver diseases

Madushika M. Wimalarathne, Quiana C. Wilkerson-Vidal, Emily C. Hunt and Sharifa T. Love-Rutledge*

Department of Chemistry, The University of Alabama in Huntsville, Huntsville, AL, United States

Human leukocyte antigen F locus adjacent transcript 10 (FAT10) is a ubiquitin-like protein that targets proteins for degradation. TNFα and IFNγ upregulate FAT10, which increases susceptibility to inflammation-driven diseases like nonalcoholic fatty liver disease (NAFLD), non-alcoholic steatohepatitis (NASH), and hepatocellular carcinoma (HCC). It is well established that inflammation contributes to fatty liver disease, but how inflammation contributes to upregulation and what genes are involved is still poorly understood. New evidence shows that FAT10 plays a role in mitophagy, autophagy, insulin signaling, insulin resistance, and inflammation which may be directly associated with fatty liver disease development. This review will summarize the current literature regarding FAT10 role in developing liver diseases and potential therapeutic targets for nonalcoholic/alcoholic fatty liver disease and hepatocellular carcinoma.

KEYWORDS

FAT10, fatty liver, non-alcoholic fatty liver, fibrosis, cancer

1 Introduction

1.1 The structure and function of F locus adjacent transcript 10

Human leukocyte antigen F locus adjacent transcript 10 (FAT10) is a ubiquitin-like protein that is encoded in the major histocompatibility complex (MHC). FAT10 was first discovered in 1996 (Fan, et al., 1996) and located on chromosome six in humans, chromosome 17 in mice, and chromosome 20 in rats (ncbi.nlm.nih.gov). FAT10 is an 18-kDa protein with 165 amino acids, two tandem ubiquitin-like domains, and belongs to the ubiquitin family of proteins (UBL) (uniport.org). The binding domains are 85 amino acids in length, consist of four sheets and three helixes each, and are connected by a flexible linker to form the FAT10 molecule (rscb.org). The FAT10 amino acid sequence is conserved in most mammals except for the C and N terminals (Aichem et al., 2018) The C and N terminals of FAT10 are highly variable even among mammalian species, including *Mus musculus, Rattus norvegicus, Myotis myotis, Mustela erminea, Talpa occidentalis, Gorilla gorilla, Molossus molossus, Mirounga leonina, Hylobates moloch, Nomascus leucogenys* (Figure 1). The clustal omega comparison shows that 60%–70% identity match even among mammalians suggesting FAT10 is rapidly evolving despite being present only in mammals. These

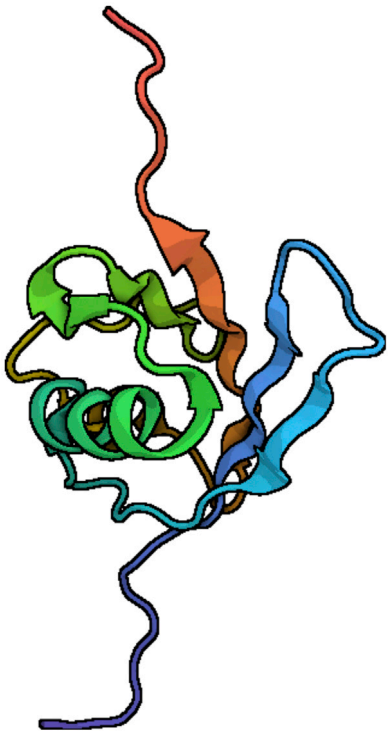

FIGURE 1
Ribbon diagrams of the FAT10 model structure. N-and C-terminal domains of FAT10 show the typical b-grasp fold. The central α-helix (turquoise) is made with β-sheets (Aichem et al., 2018). The diagrams were generated with the Pymol program, using the Research Collaboratory for Structural Bioinformatics (RCSB) Protein Data Bank entry. PDB ID 6GF2.

evolutionary changes of FAT10 attenuate binding properties and functional characteristics of FAT10 proteins.

FAT10 acts as a modifier to target proteins for degradation. FAT10 is expressed in specific tissues, such as the lymph nodes, kidney, liver, pancreas, and gastrointestinal tract, in response to proinflammatory stimuli. FAT10 is active in several types of cells, including dendritic cells, T cells and B cells (Fan, et al., 1996; Bates et al., 1997) due to cytokine induction of cells (Mah et al., 2020). FAT10 has also been associated with inflammation and the immune response, as part of the MHC, where it plays a role in antigen presentation (Ebstein et al., 2012). It is well known that the inflammatory cytokines tumor necrosis factor α (TNF-α), a presumptive tumor promoter, and interferon-γ (IFN-γ) upregulate FAT10 (S. Lukasiak et al., 2008). Furthermore, FAT10 has been shown to interact with the tumor suppressor protein p53 in a mutually inhibitory manner (Zhang et al., 2006; Choi et al., 2014; Zhang and Fu, 2021). Hence, FAT10 has been found to be highly upregulated in cancers of the liver, colon, uterus, and ovaries (Lee et al., 2003; Lukasiak et al., 2008). FAT10 is an important target for research and therapeutics for cancer and inflammation implicating a potential role of FAT10 on inflammation induced tumorigenesis.

FAT10 overexpression is associated with the regulation of several inflammation driving pathways in cancer development, such as the AKT pathway, the Wnt pathway, and the NF-κB (Liu et al., 2014; Yuan et al., 2014; Luo et al., 2018; Zou et al., 2021). In fact, the NF-κB pathway may link inflammation with the development of cancer, making FAT10 important in the mechanism of inflammation-induced tumorigenesis. FAT10 also directly interacts with other downstream targets, such as p53 and β-catenin (Li et al., 2011; Choi et al., 2014; Yuan et al., 2014). Furthermore, FAT10 has been shown to negatively influence DNA damage repair (Chen et al., 2018). The regulatory role of FAT10 in these pathways makes it important in the progression of cancer.

However, FAT10 is also known to have roles in the development of other diseases, such as kidney disease (Ross et al., 2006) inflammatory bowel disease (Kawamoto et al., 2019) and diabetes (Baschal et al., 2011; Brozzi et al., 2016). The role of FAT10 in the development of inflammation is critical to its role in these diseases and may also contribute to its role in the development of liver diseases. Additionally, FAT10 has been shown to have a role in regulating autophagy and insulin signaling, which may contribute to its role in the development of inflammation and insulin resistance.

2 F locus adjacent transcript 10 and liver inflammation

FAT10 expression is known to be increased related to inflammation. FAT10 is presented in the primary insulin dependent diabetes mellitus susceptibility locus (Iddm37) near the major histocompatibility complex II (MHC II) (Fan, et al., 1996) where single-nucleotide polymorphisms in MHC II genes have been linked to an increased risk of drug-induced liver damage (Willemin et al., 2013). The transcript analysis in nonalcoholic fatty liver disease (NAFLD) patients showed that upregulation of proinflammatory cytokines IL-32 and FAT10 levels suggests a possible connection between FAT10 and inflammation responses in liver diseases (Dali-Youcef et al., 2019).

As a result of liver damage and lipid accumulation in the liver, inflammatory cells release cytokines. The significant increase of cytokines, triglycerides and cholesterol adds to the oxidative stress developed in hepatocytes (Yang et al., 2008). The increased mitochondrial damage and ROS production in the liver are associated with fibrogenesis and inflammatory function (Middleton and Vergis, 2021). Hepatic liver inflammation is commonly induced by liver disease by triggering hepatic tissue damage, progressing from NAFLD to severe fibrogenesis and hepatocellular carcinoma (HCC) (Begriche et al., 2013; Buzzetti et al., 2016).

2.1 Fat10ylation to major histocompatibility complex class presentation and increased inflammation

Protein homeostasis regulation is a developing topic of research in cancer biology and inflammatory diseases (Calamini and Morimoto, 2012; Cheng et al., 2018). The MHC class I antigen presentation pathway plays a critical role in alerting the immune system (Ebstein et al., 2012). FAT10 serves as a signal for proteasome-dependent degradation and impacts MHC class I presentation. As an example, N-terminal fusion of the human cytomegalovirus (HCMV)-derived pp65 antigen with FAT10 accelerates the proteasomal degradation of pp65 and results in improved presentation in HLA-A2 cells (Ebstein et al., 2012).

All nucleated cells have MHC class I molecules on their cell surfaces, which contain peptide fragments originating from intracellular proteins. In this pathway, covalently attached ubiquitin (Ub) typically marks a substrate protein for degradation by the 26 S proteasome. Furthermore, production of $CD8^+$ T cell antigenic peptides mainly depends on the degradation of target proteins by the ubiquitin-proteasome system (UPS) (Lecker et al., 2006). It has been shown that ubiquitylation can facilitate MHC class I antigen presentation (Townsend et al., 1988; Ebstein et al., 2012). In the case of FAT10, substrate protein increases peptide supply for MHC class I-restricted antigen presentation leading to distinctive MHC class I antigen presentation causing changes in inflammation and tumorigenesis (Ebstein et al., 2012). So, we suggest FAT10 modification facilitates MHC class I antigen presentation which may associate with liver inflammation.

A small ubiquitin-like modifier member or SUMO covalently binds to a family of proteins with lysine residues in specific target proteins in a process called SUMOylation. The post-translational protein modification by SUMO is an essential cellular process, involved in protein localization and activation (Seeler and Dejean, 2017). Several isoforms of SUMO have been identified, including SUMO1, SUMO2/3, and SUMO4 (Baczyk et al., 2017; Aichem et al., 2019).

SUMOylation is closely related to the development of liver diseases, including HCC, viral hepatitis, NAFLD, cirrhosis, and primary biliary cirrhosis (PBC) (Zhang et al., 2021).

Alcohol inducible enzyme Cytochrome P450 (CYP2E1) catalyzes reactive oxygen species produced by alcohol (Koop, 2006). The SUMOylation of the pre-oxidant CYP2E1 increases the protein stability and function, resulting in fibrogenesis and inflammation in alcoholic hepatitis patients (Lu and Cederbaum, 2008). The inhibition of SUMOylation in obese mice promotes inflammation by activating the NF-κB pathway, causing liver inflammation (Kim et al., 2015; Zeng et al., 2020). FAT10 binds to SUMO E1-activating enzyme AOS1/UBA2 and competes with SUMO for thioester formation, which reduces the SUMOylation process (Aichem et al., 2019). Furthermore, reduced SUMOylation substantially increases pro-inflammatory immune responses and develops alcoholic steatohepatitis (Decque et al., 2015). So, we suggest that downregulation of SUMO protein activation by FAT10 can induce liver inflammation.

FAT10 and Ubiquitin proteins have different binding specificities which can also affect the rate of proteasomal degradation (Hipp et al., 2005). The two domains of FAT10 are structurally independent and joined by a flexible linker, providing a structural basis for discovering that the two FAT10 ubiquitin domains can dock to different reader domains and thus link two FAT10 binding complexes at the proteasome. For example, this happens with RPN10 and long isoform of NEDD8-ultimate buster 1 (NUB1L) (Groettrup et al., 2008), (Liu et al., 1999). NUB1L is an interferon-induced protein which can bind with NEDD8 and FAT10 and increases FAT10 degradation by around eightfold (Schmidtke et al., 2009). NUB1L has stronger binding affinity toward FAT10 compared to NEDD8 which eventually attenuates the neddylation (covalently conjugating NEDD8 to specific protein), where the neddylation is involved with pathology of NAFLD and NASH (Sen et al., 2015; Yao et al., 2020).

2.2 F locus adjacent transcript 10 mediated Mallory Denk Body formation

Mallory Denk Body formation is another example of the impact FAT10-mediated proteasomal degradation processes have in alcoholic hepatitis (AH), alcoholic steatohepatitis (ASH), NASH and HCC (Liu, et al., 2014, Jia et al., 2020). Mallory Denk Bodies (MDBs) are aggresomes formed of undigested ubiquitinated short-lived proteins that have collected due to reducing the 26 S proteasome's degradation rate. Hepatocyte ballooning and lobular inflammation are required to meet the criteria for MDB formation. 26 S proteasome chymotrypsin activity, measured by the Western blot method in FAT10 KO mice, showed a diminished rate of liver proteolysis compared to wild-type mice, which is associated with MDB formation and balloon degeneration (Oliva et al., 2010). Additionally, betaine prevents FAT10 overexpression in mice fed 3,5-Diethoxycarbonyl-1,4-dihydrocollidine (DCC), preventing MDB formation (French et al., 2012). Consistent with the above data, FAT10 expression increases by 4.5-fold in AH livers compared to NASH and control livers with elevated Mallory Denk Body formation (Jia et al., 2020).

According to Liu H. et al. (2014) an epigenetic mechanism plays a role in MDB formation. SAMe and betaine are methyl donors that prevent the demethylation of histones in the DDC-induced MDB mouse model. The MDB formation is associated with the downregulation of the ufm1 conjugation system (Ufmylation) and FAT10-conjugation system (FAT10ylation) pathways (Jia et al., 2020). As evidenced, MDB formation is

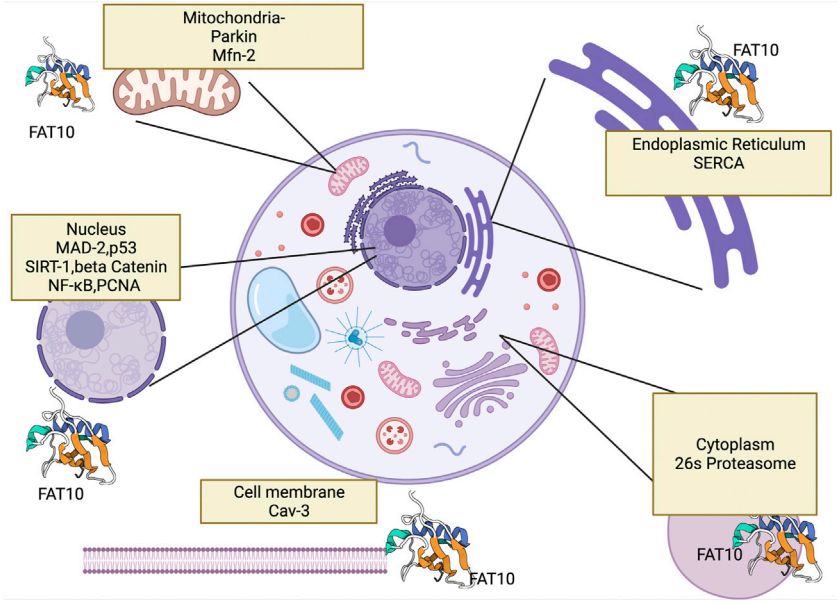

FIGURE 2
This figure shows FAT10's interaction with cell organelles and with genes that FAT10 binds. Here we show FAT10 interactions with nucleus (Ramos et al., 2021), (Li et al., 2011) mitochondria (Roverato et al., 2021), cytoplasm (Jia et al., 2020), endoplasm reticulum (Buchsbaum et al., 2012) and cell membrane which may contribute to liver disease development. The figure created by Biorender.com (Accessed on 22nd of March 2021).

associated with liver inflammation and FAT10 induces MDB formation in AH, ASH, and NASH and HCC patients.

2.3 F locus adjacent transcript 10 mediated mitochondrial dysfunction induces liver inflammation

The mitochondrion is double-membrane organelle with self-replicating ability. It produces energy through the Krebs cycle, oxidizing fatty acids, and numerous metabolites. For decades, mitochondrial dysfunctions have negatively affected people's health (Khan et al., 2015). The morphology and replication of mitochondria are mainly regulated by fusion and fission processes (Ni et al., 2015; Zilocchi et al., 2018). Mitochondrial defects are well recognized within human tissue and disease models of alcoholic liver diseases, NAFLD and HCC. Common mitochondrial defects can lead to mitochondrial reactive oxygen species (mtROS) production (Gao et al., 2004) and impaired oxidative phosphorylation, altering hepatocyte cell metabolism, ROS signaling, cell apoptosis, and inflammatory signaling. The mitochondria has several targets of FAT10ylation that affect mitophagy as well as numerous signaling pathways (Figure 2) which have led to changes in inflammation and development of liver diseases (Ren et al., 2011). Increased lipogenesis and elevated free fatty acid (FFA) uptake in hepatocytes are characteristics of the pathogenesis of NAFLD (Petrosillo et al., 2007). Lipotoxicity induces mitochondrial dysfunction, excessive oxidative stress, ER stress, inflammation, and profibrogenic response, predisposing the liver to high-risk conditions. The patients with NASH showed signs of enlarged and swollen hepatocellular mitochondria with a loss of cristae (Middleton and Vergis, 2021), suggesting a close relationship between mitochondrial dysfunction on liver diseases.

Mitofusion or aligning and binding of two mitochondria together to form a larger mitochondrion plays a role in embryonic development, coordination between mitochondria (Chen et al., 2003) and exchange of genetic content between mitochondria. Emerging evidence suggests that mitochondrial fusion responds to chemical and other stresses (Meyer et al., 2017). Upregulated mitochondrial fusion protects against mitochondrial depolarization and promotes cell autophagy in HCC cell lines. The most prominent proteins related to this process are Mitofusion 1 (MFN-1) and Mitofusion 2 (MFN-2), located outside the mitochondrial membrane (Youle and van der Bliek, 2012). MFN-1 and MFN-2 proteins are closely related and play a role in the last steps of mitofusion (Hales and Fuller, 1997). When MFN-2 is responsible for outer membrane fusion, Opa1 protein mediates the fusion of inner membranes (Song et al., 2009; Ge et al., 2018). Mitofission, on the other hand, segregates damaged and malfunctioning mitochondria allowing for degradation *via* the mitophagy process (Middleton and

Vergis, 2021). There is no evidence that FAT10 effects the mitofission process.

According to Lehmann et al. (2016) eighty-seven ubiquitin-protein system components, including ubiquitination machinery (E1, E2, and E3 ligases), are localized and interact with 127 mitochondrial matrix proteins in the mitochondria in yeast and humans. Half of these proteins are exclusively located within the mitochondria's inner matrix, suggesting a strong connection between ubiquitin proteins with mitochondrial regulations. Parkin-dependent fat10lyation of Mitofusion2 was observed in Hek293 cells suggesting that FAT10 proteins present in the outer mitochondrial membrane (OMM) bind to OMM proteins (Roverato et al., 2021). FAT10 mediates the degradation of MFN-2 in neuronal cells, which affects the mitofusion process (Roverato et al., 2021) MFN-2 KO and MFN-1 KO led to severe mitochondrial fragmentation (Papanicolaou et al., 2012; Dong et al., 2016). However, the role of FAT10 in mitochondrial fusion and fission is still to be discovered.

Altered fission and fusion have been observed in tumor cells due to membrane permeability and polarization changes. MFN-1 and MFN-2 activity in the mitochondrial membrane changes with tumor progression and target autophagy, and decreased MFN-2 expression was observed in tumor cells (Boland et al., 2013; Chávez et al., 2017). So, we suggest that FAT10 overexpression may also be associated with reduced MFN-2 levels since FAT10 overexpression can lead to proteasomal degradation of MFN-2.

Mitophagy or selective degradation of mitochondria is another mitochondrial process regulating mitochondrial dynamics. Mitophagy is known for playing a role in paternal mitochondrial degradation (Ma et al., 2020), neurogenerative diseases (Roverato et al., 2021), erythropoiesis (van Vuren et al., 2021) and tissue injuries (Ke, 2020). Impaired mitophagy has been critically linked with the pathogenesis of inflammatory diseases like fatty liver disease and HCC (Ke, 2020; Wu et al., 2020). It was unknown how FAT10 interferes with the mitophagy process until very recently. This connection negatively affects Parkin by changing the structure of the N terminus of the protein, leading to autoFAT10lytion followed by degradation of Parkin (Roverato et al., 2021).

The stress-responsive mitochondrial sirtuin SIRT4 plays a role in the mitochondrial function of NAFLD patients (Tarantino et al., 2014). SIRT4 interacts with GTPase optic atrophy 1 (L-OPA1) to promote mitochondrial fusion, inhibiting mitophagy and increasing ROS production (Lang et al., 2017). Furthermore, TNF-α and IFN-γ induce FAT10 expression, leading to reactive oxygen species (ROS) accumulation and impaired mitophagy (Mah et al., 2020). In summary, FAT10ylation of mitochondrial proteins leads to rapid proteasomal degradation, which eventually alters mitochondrial dynamics like mitofusion and mitophagy leading to fatty liver disease development.

2.4 F locus adjacent transcript 10 association with insulin resistance

Decreased insulin sensitivity or insulin resistance is a hepatic component of metabolic syndrome, leading to increased blood glucose, triglyceride, and cholesterol levels. Studies have shown that reduced insulin clearance is associated with increased lipid accumulation in the liver (Seppälä-Lindroos et al., 2002; Utzschneider and Kahn, 2006). Liver insulin resistance is linked to steatosis (Bril et al., 2014), type 2 diabetes (Lukic et al., 2014), NAFLD (Paschos and Paletas, 2009), hepatocellular carcinoma, and cardiovascular disease (Bril et al., 2014).

FAT10 KO mice show increased insulin sensitivity, elevated lipolysis, and insulin-stimulated AKT phosphorylation compared to control rats (Canaan et al., 2014). FAT10 KO mice had upregulated gene and protein expression of fatty acid oxidation in skeletal muscle, and increased lipolysis in adipocytes (Canaan et al., 2014). According to Ge et al. (2018) FAT10 may downregulate insulin receptor substrate 2 (IRS2), decreasing insulin sensitivity in the liver. They hypothesize that the overexpression of FAT10 inhibits the activity of insulin receptor substrates 1 and 2, which leads to the downregulation of PI3K1 expression and causes insulin resistance in mice. The Attie Lab Diabetes database shows relative mRNA expression of FAT10 in the liver of four groups of BTBR mice (4-week-old normal group, 4-week-old obese group, 10-week-old normal group, and 10-week-old obese group, five mice in each group) where ob/ob mice showed increased FAT10 expression compared to lean mice (Kolishovski et al., 2019). BTBR ob/ob mice exhibit insulin resistance and elevated triglyceride levels, suggesting that FAT10 may be associated with metabolic disorders and increased liver inflammation.

These data suggest that FAT10 may play a role in insulin resistance, and the FAT10 pathway may be a practical therapeutic approach to metabolic disorders. However, the relative contribution of FAT10 to insulin resistance is not well established.

3 F locus adjacent transcript 10 and liver diseases

Alcoholic liver disease (ALD) and NAFLD have similar pathological characteristics, from simple steatosis to liver cirrhosis, making it difficult to differentiate between them. During the development of fatty liver, increased lipid accumulation and decreased mitochondrial oxidation, liver injury ballooning, changes in lipid composition, and increased ROS production are observed (Ipsen et al., 2018). The fatty accumulation in the liver occurs to a greater degree in NAFLD than in ALD (Toshikuni et al., 2014). On the

contrary, inflammation is more pronounced in ALD than in NAFLD (Toshikuni et al., 2014). In addition, venous or perivenular fibrosis, phlebosclerosis, and lymphocytic phlebitis are more common in ALD than in NAFLD (Toshikuni et al., 2014).

FAT10 is known to be associated with the development of liver diseases. The progression of liver disease is described as a "multiple-hit" process (Tilg and Moschen, 2010). After the first hit of insulin resistance, subsequent hits include inflammation, oxidative stress, apoptosis, and fibrogenesis. The development of liver disease may be exacerbated by lifestyle factors, such as alcohol consumption. With each hit, liver disease progresses from fatty liver development to liver disease, steatohepatitis, fibrosis, and hepatocellular carcinoma (HCC). In this section, we will discuss the association of FAT10 with the progression of liver disease. We will follow the progression of liver disease from NAFLD and ALD, NASH and ASH, fibrosis, and finally HCC, discussing how FAT10 is associated with each stage in the development of the disease.

3.1 F locus adjacent transcript 10 and alcoholic and nonalcoholic fatty liver diseases

Alcoholic fatty liver pateints showed increased FAT10 expression in the liver along with Mallory Denk body formation (Section 2.3). Alcoholic mediated SUMOylation enhances alcoholic liver disease development *via* upregulating CYP2E1, suggesting FAT10 plays a critical role in alcoholic liver disease development (Section 2.1).

As recently identified, FAT10 plays a role in energy and nutrient sensing, bile acid metabolism, and insulin signaling by modulating pathways like PI3K/AKT/mTOR (Canaan et al., 2014), cAMP-dependent signaling, as well as NF-κB–dependent gene expression (Leng et al., 2014). Some studies have demonstrated that during the development of NAFLD, autophagy is inhibited by the PI3K/AKT signaling pathway *via* both short-term and long-term regulation mechanisms (Mao et al., 2016). AKT is phosphorylated by PI3K and becomes activated, and phospho-AKT can bind and regulate many downstream effectors such as BCL-2 family proteins which play a protective role against NAFLD development (Matsuda et al., 2013). p53, a recognized tumor suppressor protein, acts as a master regulator with pleiotropic effects on metabolism, and is involved in cell apoptosis during NAFLD by regulating the balance between BCL-2 and BAX (Panasiuk et al., 2006). FAT10 has negative effects on p53; downregulating p53 may have a negative downstream effect on BCL-2, leading to increased liver cell death, which suggests possible intervention of FAT10 on NAFLD development.

Another study suggests that FAT10 decreases autophagy through modulating SIRT1 degradation, which increases steatosis, hepatocellular injury, and inflammation in NAFLD. Increased SIRT1 levels in the liver reduce NAFLD development by increasing Nrf2 and HO-1 expression in primary hepatic stellate cells, which are regulated by SIRT1-mediated pathway (Wan et al., 2021). SIRT1 also deacetylates PGC-1α and increases autophagy (Wan et al., 2021) both of which are possibly downregulated by FAT10 overexpression with NAFLD development.

Additionally, NAFLD activity scores (NAS) positively correlate with FAT10 expression, suggesting that FAT10 may contribute to hepatic steatosis and inflammation (Dali-Youcef et al., 2019). Mordes et al. (2005), first mentioned that LEW.1WR1 rats developed fatty liver infiltration. Further research by the group identified increased FAT10 expression in the pancreatic lymph nodes due to a missing short interspersed nuclear element near the promoter region of the gene (Canaan et al., 2014). Recent studies of the livers LEW.1WR1 rats have shown increased glucose intolerance and significant upregulation of FAT10 expression in the livers of the rats (Wilkerson-Vidal et al., 2021). Despite these findings, little is understood about how FAT10 specifically affects the lipid metabolism of the liver.

3.2 F locus adjacent transcript 10, steatohepatitis, and fibrosis

ASH patients have higher FAT10 expression in the liver compared to NASH patients, suggesting FAT10 has an association with liver disease progressions (Jia et al., 2020). Patients also showed increased FAT10 expression which correlate with CXCL9 and CXCL10, supporting solid crosstalk between FAT10 and these proinflammatory cytokines in NASH pathophysiology (Dali-Youcef et al., 2019). Immune cell recruitment is essential to develop NASH from simple steatosis. The chemokine receptor 4 (CXCR4) and 7 (CXCR7) are G-protein-coupled receptors, both significantly upregulated in FAT10-overexpressed NASH liver tissues (Liu et al., 2014). FAT10 was found to activate NF-κB, which in turn upregulates CXCR4/7 in NeHepLxHT and HCT116 cells (Gao et al., 2014). The CXCR4 promotes the recruitment of $CD4^+$ T cells in NASH. Furthermore NF-κB-CXCR4/7 pathway induces inflammation by forming Mallory Denk Bodies (MDB) in NASH patients (Wang et al., 2021). Another study with NASH patients shows increased proinflammatory chemokines levels, namely CXCL9, CXCL10, IL-32 in the blood (Dali-Youcef et al., 2019). These findings correlate FAT10 expression plays a role in NASH development. NASH has similar histological features to alcoholic hepatitis (ASH), such as increased lipid accumulation, which may progress to fibrosis, cirrhosis, and ultimately HCC.

In vitro experiments have confirmed that FAT10 expression gradually increases in liver fibrosis, cirrhosis, and HCC, suggesting that FAT10 may play a role in fibrosis development (Zhang et al., 2021). Fibrosis is the result of chronic inflammatory reactions, and FAT10 increases inflammation by increasing TNF-α/IFN-γ and NF-κB and

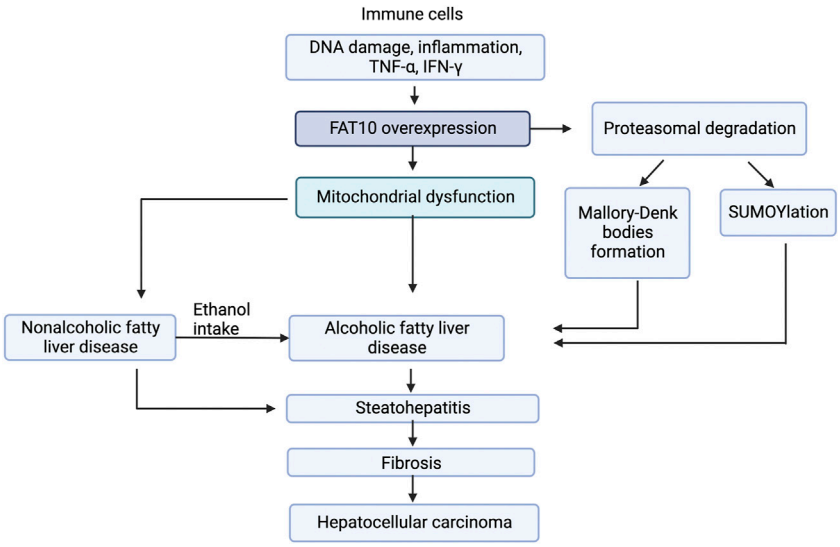

FIGURE 3
Model for FAT10 effect on liver diseases. The figure shows that FAT10 effects fatty liver diseases *via* altering insulin resistance, mitochondrial function, and inflammation responses. Insulin resistance and mitochondrial dysfunction are closely related to inflammation suggesting potential significance of FAT10 in fatty liver disease development.

STAT3 pathways, all of which were up regulated in fibrosis patients (Jia et al., 2020). Furthermore, NF-κB modulates liver fibrogenesis by regulating hepatocyte injury, inflammatory signals, and fibrogenic responses (Luedde and Schwabe, 2011). Inhibition of NF-κB in Kupffer cells decreases liver fibrosis while activation of NF-κB in hepatocytes and Kupffer cells leads to liver fibrosis. Fibrosis occurs due to chronic liver injury, increased liver inflammation and activated macrophages and myofibroblasts secreting TGFβ and other agonists, which help to release collagens in the liver (Lee and Friedman, 2011). Hepatitis B and C virus infection, alcoholic steatohepatitis, non-alcoholic hepatic steatohepatitis, nonalcoholic fatty liver disease, and hemochromatosis can progress to liver fibrosis with the formation of a fibrous scars in the liver (Phillips et al., 2004; Bataller and Brenner, 2005).

Mitochondrial dysfunction is also observed with fibrosis, and it is known that mitochondria dysfunction contributes to the development and progression of fibrosis. Fibrosis development connects with the innate immune response, and ongoing liver injury leads to activation of inflammation-dependent and independent mechanisms, including secretion of cytokines (Pellicoro et al., 2014) and mitochondrial ROS production from dying hepatocytes (Zhang and Fu, 2021). Mitochondria do not fully function in fibrogenic tissues but actively participate in fibrogenesis. Most importantly, NASH patients with advanced stage fibrosis show increased levels of circulating mtDNA. The mtDNA from hepatocytes release into the bloodstream promoting inflammation through binding to endosomal TLR9 of liver Kupffer cells (Garcia-Martinez et al., 2016). These findings suggest that mitochondrial dysfunction plays a role in fibrosis development in the liver.

Defective mitophagy, such as that resulting from PINK1 deficiency, leads to the accumulation of dysfunctional mitochondria (McLelland et al., 2018). An impairment of mitophagy potentially participates in hepatic fibrosis (Gunton et al., 2003; Mao et al., 2016). The changes in mitophagy increases mitochondrial dysfunction leading to depletion of mtDNA in NASH patients with fibrosis (Schröder et al., 2016). Despite these findings, little is understood about how FAT10 is involved in fibrosis development, but we believe that FAT10 may be a potential therapeutic target in treating patients with NASH-induced liver fibrosis.

3.3 F locus adjacent transcript 10 and hepatocellular carcinoma

Hepatocellular carcinoma is one of the most common organ tumors in the world. HCC is a severe complication of chronic liver diseases, especially advanced liver fibrosis and/or cirrhosis. In carcinoma patients and rodents with liver carcinoma, FAT10 is overexpressed in liver (Lee and Friedman, 2011; Liu et al., 2018). Changes of methylation of the promoter region in the FAT10 gene or binding of key tumorigenic promoters increase the FAT10 expression (Liu et al., 2018).

FAT10 has a strong connection with the inflammatory signaling pathway which eventually leads to HCC development (Liu H et al., 2014). According to (Ren et al., 2011), TNF-α activates the NF-κB pathway, which causes FAT10 gene expression in cells leading to tumorgenesis.

FAT10 also promotes HCC by binding to β-catenin and preventing its degradation, which in turn prevents the degradation of HOXB9. It should be noted that HOXB9 plays a role in tumor metastasis and is regulated *via* the Wnt/β-catenin/TCF4 pathway (Yuan et al., 2014). Notably, cDNA microarray analysis showed that loss of FAT10 inhibits HOXB9 expression in liver carcinoma cells, suggesting FAT10 affects HCC tumor metastasis by regulating HOXB9 (Yuan et al., 2014).

FAT10 is also associated with tumorigenesis *via* its interactions with DNA replication proteins and tumor suppressor proteins. FAT10 has been shown to interact with the damage repair protein proliferating cell nuclear antigen (PCNA). FAT10 and PCNA expression is high in hepatocellular carcinoma tissues; however, the FAT10 expression is reduced in regenerated liver tissues, while PCNA expression is elevated, thus suggesting that the association between FAT10 and PCNA expression is only exhibited in tumor tissues. FAT10 binds with PCNA, leading to proteasomal degradation of PCNA in the nucleus and cytoplasm (Chen et al., 2018), leading to increased tumor cell invasion. FAT10 also interacts with mitotic arrest-deficient 2 (MAD2) and induces tumor malignancy. Abrogation of the FAT10–MAD2 interaction reduces the tumor progression (Theng et al., 2014).

Increased FAT10 inhibits the transcriptional activity of the tumor suppressor p53, a protein that hastens FAT10 protein breakdown. p53 double-negative regulation promotes tumor development in the solid tumor model (Rivlin et al., 2011), suggesting FAT10 has pro-oncogenic function in promoting carcinoma (Aichem and Groettrup, 2016; Dai et al., 2016).

4 Conclusion

These data strongly suggest FAT10 can be used as a prognostic marker for fatty liver diseases and that it is a potential therapeutic target. FAT10 plays a role in prosurvival pathways by altering apoptotic pathways. FAT10 is upregulated in NAFLD, ASH, NASH, and HCC patients (Figure 3). FAT10 may exert its influence in a tissue-specific and cell signaling-specific manner modulating *via* anti-inflammatory mediators, mitochondrial functions, SUMOylation, and MDB formation. The most prominent pathways affected by FAT10 include inflammation, insulin signaling, cell proliferation, mitochondrial protein degradation, and proteasomal degradation.

Research into how FAT10 affects diabetes mellitus and NAFLD could further demonstrate FAT10's pleiotropic effects in metabolic disorders, but our knowledge of FAT10 and liver diseases is still limited. FAT10 is a biomarker for certain cancers, but it may also serve as a harbinger for the early detection of liver diseases.

Author contributions

MW: Formal Analysis, Investigation, Writing, Visualization; QW-V: Formal Analysis, Investigation, Writing, Visualization; EH: Formal Analysis, Writing. MW: First Author. QV-W and EH: Coauthors. SL-R: Supervised edited and organized this work.

Funding

The submission of this work was partially funded by a American Association of University Women Research Publication Grant in Engineering, Medicine, and Science through the PRIDE-FTG program and Research Publication Grant in Engineering Medicine and Science.

Conflict of interest

The authors declare that the research was conducted in the absence of any commercial or financial relationships that could be construed as a potential conflict of interest.

Publisher's note

References

Aichem, A., Anders, S., Catone, N., RoBler, P., Stotz, S., Berg, A., et al. (2018). The structure of the ubiquitin-like modifier FAT10 reveals an alternative targeting mechanism for proteasomal degradation. *Nat. Commun.* 9 (1), 3321. doi:10.1038/s41467-018-05776-3

Aichem, A., and Groettrup, M. (2016). The ubiquitin-like modifier FAT10 in cancer development. *Int. J. Biochem. Cell Biol.* 79, 451–461. doi:10.1016/J.BIOCEL.2016.07.001

Aichem, A., Sailer, C., Ryu, S., Catone, N., Stankovic-Valentin, N., Schmidtke, G., et al. (2019). The ubiquitin-like modifier FAT10 interferes with SUMO activation. *Nat. Commun.* 10 (1), 4452. doi:10.1038/S41467-019-12430-Z

Baczyk, D., Boyle, T. A., Siebert, J. C., Jasinski, J. M., Grabek, K. R., Baschal, E. E., et al. (2017). 'SUMO-4: A novel functional candidate in the human placental protein SUMOylation machinery', PLoS ONE Replication and further characterization of a type 1 diabetes-associated locus at the telomeric end of the

major histocompatibility complex. *J. Diabetes* 123 (53), 10238–10247. doi:10.1111/J.1753-0407.2011.00131.X

Baschal, E. E., Sarkar, A., Boyle, T. A., Siebert, J. C., Jasinski, J. M., Grabek, K. R., et al. (2011). Replication and further characterization of a Type 1 diabetes-associated locus at the telomeric end of the major histocompatibility complex. *J. Diabetes* 3 (3), 238–247. doi:10.1111/j.1753-0407.2011.00131.x

Bataller, R., and Brenner, D. A. (2005). Liver fibrosis. *J. Clin. Invest.* 115 (2), 209–218. doi:10.1172/JCI24282

Bates, E. E. M., Ravel, O., Dieu, M. C., Ho, S., Guret, C., Bridon, J. M., et al. (1997). Identification and analysis of a novel member of the ubiquitin family expressed in dendritic cells and mature B cells. *Eur. J. Immunol.* 27 (10), 2471–2477. doi:10.1002/EJI.1830271002

Begriche, K., Massart, J., Robin, M. A., Bonnet, F., and Fromenty, B. (2013). Mitochondrial adaptations and dysfunctions in nonalcoholic fatty liver disease. *Hepatology* 58 (4), 1497–1507. doi:10.1002/HEP.26226

Boland, M. L., Chourasia, A. H., and Macleod, K. F. (2013). Mitochondrial dysfunction in cancer. *Front. Oncol.* 3, 292. doi:10.3389/FONC.2013.00292

Bril, F., Lomonaco, R., Orsak, B., Ortiz-Lopez, C., Webb, A., Tio, F., et al. (2014). Relationship between disease severity, hyperinsulinemia, and impaired insulin clearance in patients with nonalcoholic steatohepatitis. *Hepatology* 59 (6), 2178–2187. doi:10.1002/HEP.26988

Brozzi, F., Gerlo, S., Grieco, F. A., Juusola, M., Balhuizen, A., Lievens, S., et al. (2016). Ubiquitin D regulates ire1α/c-jun N-terminal kinase (JNK) protein-dependent apoptosis in pancreatic beta cells. *J. Biol. Chem.* 291 (23), 12040–12056. doi:10.1074/JBC.M115.704619

Buchsbaum, S., Bercovich, B., Ziv, T., and Ciechanover, A. (2012). Modification of the inflammatory mediator LRRFIP2 by the ubiquitin-like protein FAT10 inhibits its activity during cellular response to LPS. *Biochem. Biophys. Res. Commun.* 428 (1), 11–16. doi:10.1016/J.BBRC.2012.09.110

Buzzetti, E., Pinzani, M., and Tsochatzis, E. A. (2016). The multiple-hit pathogenesis of non-alcoholic fatty liver disease (NAFLD) *Metabolism.* 65 (8), 1038–1048. doi:10.1016/j.metabol.2015.12.012

Calamini, B., and Morimoto, R. I. (2012). Protein homeostasis as a therapeutic target for diseases of protein conformation. *Curr. Top. Med. Chem.* 12 (22), 2623–2640. doi:10.2174/1568026611212220014

Canaan, A., DeFuria, J., Perelman, E., Schultz, V., Seay, M., Tuck, D., et al. (2014). Extended lifespan and reduced adiposity in mice lacking the FAT10 gene. *Proc. Natl. Acad. Sci. U. S. A.* 111 (14), 5313–5318. doi:10.1073/PNAS.1323426111

Chávez, E., Lozano-Rosas, M. G., Dominguez-Lopez, M., Velasco-Loyden, G., Rodriguez-Aguilera, J. R., Jose-Nunez, C., et al. (2017). Functional, metabolic, and dynamic mitochondrial changes in the rat cirrhosis-hepatocellular carcinoma model and the protective effect of IFC-305. *J. Pharmacol. Exp. Ther.* 361 (2), 292–302. doi:10.1124/jpet.116.239301

Chen, H., Detmer, S. A., Ewald, A. J., Griffin, E. E., Fraser, S. E., and Chan, D. C. (2003). Mitofusins Mfn1 and Mfn2 coordinately regulate mitochondrial fusion and are essential for embryonic development. *J. Cell Biol.* 160 (2), 189–200. doi:10.1083/JCB.200211046

Chen, Z., Zhang, W., Yun, Z., Zhang, X., Gong, F., Wang, Y., et al. (2018). Ubiquitin-like protein FAT10 regulates DNA damage repair via modification of proliferating cell nuclear antigen. *Mol. Med. Rep.* 17 (6), 7487–7496. doi:10.3892/MMR.2018.8843

Cheng, J., North, B. J., Zhang, T., Dai, X., Tao, K., Guo, J., et al. (2018). The emerging roles of protein homeostasis-governing pathways in Alzheimer's disease. *Aging Cell* 17 (5), e12801. doi:10.1111/ACEL.12801

Choi, Y., Kim, J. K., and Yoo, J. Y. (2014). NFκB and STAT3 synergistically activate the expression of FAT10, a gene counteracting the tumor suppressor p53. *Mol. Oncol.* 8 (3), 642–655. doi:10.1016/j.molonc.2014.01.007

Dai, B., Zhang, Y., Zhang, P., Pan, C., Xu, C., Wan, W., et al. (2016). Upregulation of p-Smad2 contributes to FAT10-induced oncogenic activities in glioma. *Tumour Biol.* 37 (7), 8621–8631. doi:10.1007/s13277-015-4739-6

Dali-Youcef, N., Vix, M., Costantino, F., El-Saghire, H., Lhermitte, B., Callari, C., et al. (2019). Interleukin-32 contributes to human nonalcoholic fatty liver disease and insulin resistance. *Hepatol. Commun.* 3 (9), 1205–1220. doi:10.1002/HEP4.1396

Decque, A., Joffre, O., Magalhaes, J. G., Cossec, J. C., Blecher-Gonen, R., Lapaquette, P., et al. (2015). Sumoylation coordinates the repression of inflammatory and anti-viral gene-expression programs during innate sensing. *Nat. Immunol.* 1717 (22), 140–149. doi:10.1038/ni.3342

Dong, D., Jiang, W., Lei, J., Chen, L., Liu, X., Ge, J., et al. (2016). Ubiquitin-like protein FAT10 promotes bladder cancer progression by stabilizing survivin. *Oncotarget* 7 (49), 81463–81473. doi:10.18632/ONCOTARGET.12976

Ebstein, F., Lehmann, A., and Kloetzel, P. M. (2012). The FAT10- and ubiquitin-dependent degradation machineries exhibit common and distinct requirements for MHC class I antigen presentation. *Cell. Mol. Life Sci.* 69 (14), 2443–2454. doi:10.1007/s00018-012-0933-5

Fan, W., Cai, W., Parimoo, S., Lennon, G., and Weissman, S. M. (1996). Identification of seven new human MHC class I region genes around the HLA-F locus. *Immunogenetics* 44 (2), 97–103. doi:10.1007/BF02660056

French, S. W., French, B. A., Oliva, J., Li, J., Bardag-Gorce, F., Tillman, B., et al. (2012). Fat10 knock out mice livers fail to develop mallory-denk bodies in the ddc mouse model. *Exp. Mol. Pathol.* 93 (3), 309–314. doi:10.1016/J.YEXMP.2012.09.002

Gao, D., Wei, C., Chen, L., Huang, J., Yang, S., and Diehl, A. M. (2004). Oxidative DNA damage and DNA repair enzyme expression are inversely related in murine models of fatty liver disease. *Am. J. Physiol. Gastrointest. Liver Physiol.* 287 (5), G1070–G1077. doi:10.1152/AJPGI.00228.2004

Gao, Y., Theng, S. S., Zhuo, J., Teo, W. B., Ren, J., and Lee, C. G. L. (2014). FAT10, an ubiquitin-like protein, confers malignant properties in non-tumorigenic and tumorigenic cells. *Carcinogenesis* 35 (4), 923–934. doi:10.1093/CARCIN/BGT407

Garcia-Martinez, I., Santoro, N., Chen, Y., Hoque, R., Ouyang, X., Caprio, S., et al. (2016). Hepatocyte mitochondrial DNA drives nonalcoholic steatohepatitis by activation of TLR9. *J. Clin. Invest.* 126 (3), 859–864. doi:10.1172/JCI83885

Ge, Q., Zhang, S., Chen, L., Tang, M., Liu, L., Kang, M., et al. (2018). Mulberry leaf regulates differentially expressed genes in diabetic mice liver based on RNA-seq analysis. *Front. Physiology* 9, 1051. doi:10.3389/FPHYS.2018.01051/BIBTEX

Groettrup, M., Pelzer, C., Schmidtke, G., and Hofmann, K. (2008). Activating the ubiquitin family: UBA6 challenges the field. *Trends biochem. Sci.* 33 (5), 230–237. doi:10.1016/J.TIBS.2008.01.005

Gunton, J. E., Delhanty, P. J. D., Takahashi, S. I., and Baxter, R. C. (2003). Metformin rapidly increases insulin receptor activation in human liver and signals preferentially through insulin-receptor substrate-2. *J. Clin. Endocrinol. Metab.* 88 (3), 1323–1332. doi:10.1210/jc.2002-021394

Hales, K. G., and Fuller, M. T. (1997). Developmentally regulated mitochondrial fusion mediated by a conserved, novel, predicted GTPase. *Cell* 90 (1), 121–129. doi:10.1016/S0092-8674(00)80319-0

Hipp, M. S., Kalveram, B., Raasi, S., Groettrup, M., and Schmidtke, G. (2005). FAT10, a ubiquitin-independent signal for proteasomal degradation. *Mol. Cell. Biol.* 25 (9), 3483–3491. doi:10.1128/MCB.25.9.3483-3491.2005

Ipsen, D. H., Lykkesfeldt, J., and Tveden-Nyborg, P. (2018). Molecular mechanisms of hepatic lipid accumulation in non-alcoholic fatty liver disease. *Cell. Mol. Life Sci.* 75 (18), 3313–3327. doi:10.1007/S00018-018-2860-6

Jia, Y., Ji, P., and French, S. W. (2020). The role of FAT10 in alcoholic hepatitis pathogenesis. *Biomedicines* 8 (7), E189. doi:10.3390/BIOMEDICINES8070189

Kawamoto, A., Nagata, S., Anzai, S., Takahashi, J., Kawai, M., Hama, M., et al. (2019). Ubiquitin D is upregulated by synergy of notch signalling and TNF-α in the inflamed intestinal epithelia of IBD patients. *J. Crohns Colitis* 13 (4), 495–509. doi:10.1093/ECCO-JCC/JJY180

Ke, P. Y. (2020). Mitophagy in the pathogenesis of liver diseases. *Cells* 9 (4), E831. doi:10.3390/CELLS9040831

Khan, N. A., Govindaraj, P., Meena, A. K., and Thangaraj, K. (2015). Mitochondrial disorders: Challenges in diagnosis & treatment. *Indian J. Med. Res.* 141, 13–26. doi:10.4103/0971-5916.154489

Kim, D., Xiao, Z., Kwon, S., Sun, X., Ryerson, D., Tkac, D., et al. (2015). A dysregulated acetyl/SUMO switch of FXR promotes hepatic inflammation in obesity. *EMBO J.* 34 (2), 184–199. doi:10.15252/EMBJ.201489527

Kolishovski, G., Lamoureux, A., Hale, P., Richardson, J. E., Recla, J. M., Adesanya, O., et al. (2019). The JAX Synteny Browser for mouse-human comparative genomics. *Mamm. Genome* 30 (11–12), 353–361. doi:10.1007/S00335-019-09821-4

Koop, D. R. (2006). Alcohol metabolism's damaging effects on the cell: A focus on reactive oxygen generation by the enzyme Cytochrome P450 2E1. *Alcohol Res. Health.* 29 (4), 274–280.

Lang, A., Anand, R., Altinoluk-Hambuchen, S., Ezzahoini, H., Stefanski, A., Iram, A., et al. (2017). SIRT4 interacts with OPA1 and regulates mitochondrial quality control and mitophagy. *Aging (Albany NY)* 9 (10), 2163–2189. doi:10.18632/AGING.101307

Lecker, S. H., Goldberg, A. L., and Mitch, W. E. (2006). Protein degradation by the ubiquitin–proteasome pathway in normal and disease states. *J. Am. Soc. Nephrol.* 17 (7), 1807–1819. doi:10.1681/ASN.2006010083

Lee, C. G. L., Ren, J., Cheong, I. S. Y., Ban, K. H. K., Ooi, L. L. P. J., Yong Tan, S., et al. (2003). Expression of the FAT10 gene is highly upregulated in hepatocellular carcinoma and other gastrointestinal and gynecological cancers. *Oncogene* 22 (17), 2592–2603. doi:10.1038/SJ.ONC.1206337

Lee, U. E., and Friedman, S. L. (2011). Mechanisms of hepatic fibrogenesis *Best. Pract. Res. Clin. Gastroenterol.* 25 (2), 195–206. doi:10.1016/J.BPG.2011.02.005

Lehmann, G., Ziv, T., Braten, O., Admon, A., Udasin, R. G., and Ciechanover, A. (2016). Ubiquitination of specific mitochondrial matrix proteins. *Biochem. Biophys. Res. Commun.* 475 (1), 13–18. doi:10.1016/J.BBRC.2016.04.150

Leng, L., Xu, C., Wei, C., Zhang, J., Liu, B., Ma, J., et al. (2014). A proteomics strategy for the identification of FAT10-modified sites by mass spectrometry. *J. Proteome Res.* 13 (1), 268–276. doi:10.1021/PR400395K

Li, T., Santockyte, R., Yu, S., Shen, R. F., Tekle, E., Lee, C. G. L., et al. (2011). FAT10 modifies p53 and upregulates its transcriptional activity. *Arch. Biochem. Biophys.* 509 (2), 164–169. doi:10.1016/J.ABB.2011.02.017

Liu, H., Gong, M., French, B. A., Li, J., Tillman, B., and French, S. W. (2014). Mallory-Denk body (MDB) formation modulates ufmylation expression epigenetically in alcoholic hepatitis (AH) and non alcoholic steatohepatitis (NASH). *Exp. Mol. Pathol.* 97 (3), 477–483. doi:10.1016/J.YEXMP.2014.10.001

Liu, L., Dong, Z., Liang, J., Cao, C., Sun, J., Ding, Y., et al. (2014). As an independent prognostic factor, FAT10 promotes Hepatitis B virus-related hepatocellular carcinoma progression via Akt/GSK3β pathway. *Oncogene* 33 (7), 909–920. doi:10.1038/onc.2013.236

Liu, S., Jin, Y., Zhang, D., Wang, J., Wang, G., and Lee, C. G. L. (2018). Investigating the promoter of FAT10 gene in HCC patients. *Genes* 9 (7), E319. doi:10.3390/GENES9070319

Liu, Y. C., Pan, J., Zhang, C., Fan, W., CollingeM.Bender, J. R., et al. (1999). A MHC-encoded ubiquitin-like protein (FAT10) binds noncovalently to the spindle assembly checkpoint protein MAD2. *Proc. Natl. Acad. Sci. U. S. A.* 96 (8), 4313–4318. doi:10.1073/PNAS.96.8.4313

Lu, Y., and Cederbaum, A. I. (2008). CYP2E1 and oxidative liver injury by alcohol. *Free Radic. Biol. Med.* 44 (5), 723–738. doi:10.1016/J.FREERADBIOMED.2007.11.004

Luedde, T., and Schwabe, R. F. (2011). NF-κB in the liver--linking injury, fibrosis and hepatocellular carcinoma *Nat. Rev. Gastroenterol. Hepatol.* 8 (2), 108–118. doi:10.1038/NRGASTRO.2010.213

Lukasiak, S., Schiller, C., Oehlschlaeger, P., Schmidtke, G., Krause, P., Legler, D. F., et al. (2008). Proinflammatory cytokines cause FAT10 upregulation in cancers of liver and colon. *Oncogene* 27 (46), 6068–6074. doi:10.1038/ONC.2008.201

Lukic, L., Lalic, N. M., Rajkovic, N., Jotic, A., Lalic, K., Milicic, T., et al. (2014). Hypertension in obese type 2 diabetes patients is associated with increases in insulin resistance and IL-6 cytokine levels: Potential targets for an efficient preventive intervention. *Int. J. Environ. Res. Public Health* 11 (4), 3586–3598. doi:10.3390/IJERPH110403586

Luo, C., Xiong, H., Chen, L., Liu, X., Zou, S., Guan, J., et al. (2018). GRP78 Promotes Hepatocellular Carcinoma proliferation by increasing FAT10 expression through the NF-κB pathway. *Exp. Cell Res.* 365 (1), 1–11. doi:10.1016/j.yexcr.2018.02.007

Ma, X., McKeen, T., Zhang, J., and Ding, W. X. (2020). Role and mechanisms of mitophagy in liver diseases. *Cells* 9 (4), E837. doi:10.3390/CELLS9040837

Mah, M. M., Roverato, N., and Groettrup, M. (2020). Regulation of interferon induction by the ubiquitin-like modifier FAT10. *Biomolecules* 10 (6), 951. doi:10.3390/BIOM10060951

Mao, Y., Yu, F., Wang, J., Guo, C., and Fan, X. (2016). Autophagy: A new target for nonalcoholic fatty liver disease therapy. *Hepat. Med.* 8, 27–37. doi:10.2147/HMER.S98120

Matsuda, S., Kobayashi, M., and Kitagishi, Y. (2013). Roles for PI3K/AKT/PTEN pathway in cell signaling of nonalcoholic fatty liver disease. *ISRN Endocrinol.* 2013, 472432. doi:10.1155/2013/472432

McLelland, G. L., Goiran, T., Yi, W., Dorval, G., Chen, C. X., Lauinger, N. D., et al. (2018). Mfn2 ubiquitination by PINK1/parkin gates the p97-dependent release of ER from mitochondria to drive mitophagy. *eLife* 7, e32866. doi:10.7554/ELIFE.32866

Meyer, J. N., Leuthner, T. C., and Luz, A. L. (2017). Mitochondrial fusion, fission, and mitochondrial toxicity *Toxicology* 391, 42–53. doi:10.1016/J.TOX.2017.07.019

Middleton, P., and Vergis, N. (2021). Mitochondrial dysfunction and liver disease: Role, relevance, and potential for therapeutic modulation. *Ther. Adv. Gastroenterol.* 14, 17562848211031394. doi:10.1177/17562848211031394

Mordes, J. P., Guberski, D. L., Leif, J. H., Woda, B. A., Flanagan, J. F., Greiner, D. L., et al. (2005). LEW.1WR1 rats develop autoimmune diabetes spontaneously and in response to environmental perturbation. *Diabetes* 54 (9), 2727–2733. doi:10.2337/DIABETES.54.9.2727

Ni, H. M., Williams, J. A., and Ding, W. X. (2015). Mitochondrial dynamics and mitochondrial quality control. *Redox Biol.* 4, 6–13. doi:10.1016/J.REDOX.2014.11.006

Oliva, J., Bardag-Gorce, F., French, B. A., Li, J., and French, S. W. (2010). Independent phenotype of binuclear hepatocytes and cellular localization of UbD. *Exp. Mol. Pathol.* 89 (1), 103–108. doi:10.1016/j.yexmp.2010.06.006

Panasiuk, A., Dzieciol, J., Panasiuk, B., and Prokopowicz, D. (2006). Expression of p53, Bax and Bcl-2 proteins in hepatocytes in non-alcoholic fatty liver disease. *World J. Gastroenterol.* 12 (38), 6198–6202. doi:10.3748/WJG.V12.I38.6198

Papanicolaou, K. N., Ngoh, G. A., Dabkowski, E. R., O'Connell, K. A., Ribeiro, R. F., Stanley, W. C., et al. (2012). Cardiomyocyte deletion of mitofusin-1 leads to mitochondrial fragmentation and improves tolerance to ROS-induced mitochondrial dysfunction and cell death. *Am. J. Physiol. Heart Circ. Physiol.* 302 (1), H167–H179. doi:10.1152/AJPHEART.00833.2011

Paschos, P., and Paletas, K. (2009). Non alcoholic fatty liver disease and metabolic syndrome. *Hippokratia* 13 (1), 9–19. doi:10.31032/ijbpas/2021/10.1.1009

Pellicoro, A., Ramachandran, P., Iredale, J. P., and Fallowfield, J. A. (2014). Liver fibrosis and repair: Immune regulation of wound healing in a solid organ. *Nat. Rev. Immunol.* 1414 (33), 181–194. doi:10.1038/nri3623

Petrosillo, G., Portincasa, P., Grattagliano, I., Casanova, G., Matera, M., Ruggiero, F. M., et al. (2007). Mitochondrial dysfunction in rat with nonalcoholic fatty liver Involvement of complex I, reactive oxygen species and cardiolipin. *Biochim. Biophys. Acta* 1767 (10), 1260–1267. doi:10.1016/J.BBABIO.2007.07.011

Phillips, R. J., Burdick, M. D., Hong, K., Lutz, M. A., Murray, L. A., Xue, Y. Y., et al. (2004). Circulating fibrocytes traffic to the lungs in response to CXCL12 and mediate fibrosis. *J. Clin. Invest.* 114 (3), 438–446. doi:10.1172/JCI20997

Ramos, V. de M., Kowaltowski, A. J., and Kakimoto, P. A. (2021). Autophagy in hepatic steatosis: A structured review. *Front. Cell Dev. Biol.* 9. doi:10.3389/fcell.2021.657389

Ren, J., Wang, Y., Gao, Y., Mehta, S. B. K., and Lee, C. G. L. (2011). FAT10 mediates the effect of TNF-α in inducing chromosomal instability. *J. Cell Sci.* 124 (21), 3665–3675. doi:10.1242/jcs.087403

Rivlin, N., Brosh, R., Oren, M., and Rotter, V. (2011). Mutations in the p53 tumor suppressor gene: Important milestones at the various steps of tumorigenesis. *Genes Cancer* 2 (4), 466–474. doi:10.1177/1947601911408889

Ross, M. J., Wosnitzer, M. S., Ross, M. D., Granelli, B., Gusella, G. L., Husain, M., et al. (2006). Role of ubiquitin-like protein FAT10 in epithelial apoptosis in renal disease. *J. Am. Soc. Nephrol.* 17 (4), 996–1004. doi:10.1681/ASN.2005070692

Roverato, N. D., Sailer, C., Catone, N., Aichem, A., Stengel, F., and Groettrup, M. (2021). Parkin is an E3 ligase for the ubiquitin-like modifier FAT10, which inhibits Parkin activation and mitophagy *Cell Rep.* 34, 108857. doi:10.1016/j.celrep.2021.108857

Schmidtke, G., Kalveram, B., and Groettrup, M. (2009). Degradation of FAT10 by the 26S proteasome is independent of ubiquitylation but relies on NUB1L. *FEBS Lett.* 583 (3), 591–594. doi:10.1016/J.FEBSLET.2009.01.006

Schröder, T., Kucharczyk, D., Bar, F., Pagel, R., Derer, S., Jendrek, S. T., et al. (2016). Mitochondrial gene polymorphisms alter hepatic cellular energy metabolism and aggravate diet-induced non-alcoholic steatohepatitis. *Mol. Metab.* 5 (4), 283–295. doi:10.1016/j.molmet.2016.01.010

Seeler, J. S., and Dejean, A. (2017). SUMO and the robustness of cancer. *Nat. Rev. Cancer* 17 (3), 184–197. doi:10.1038/NRC.2016.143

Sen, S., Langiewicz, M., Jumaa, H., and Webster, N. J. G. (2015). Deletion of serine/arginine-rich splicing factor 3 in hepatocytes predisposes to hepatocellular carcinoma in mice *Hepatology* 61 (1), 171–183. doi:10.1002/HEP.27380

Seppälä-Lindroos, A., Vehkavaara, S., Hakkinen, A. M., Goto, T., Westerbacka, J., Sovijarvi, A., et al. (2002). Fat accumulation in the liver is associated with defects in insulin suppression of glucose production and serum free fatty acids independent of obesity in normal men. *J. Clin. Endocrinol. Metab.* 87 (7), 3023–3028. doi:10.1210/JCEM.87.7.8638

Song, Z., Ghochani, M., McCaffery, J. M., Frey, T. G., and Chan, D. C. (2009). Mitofusins and OPA1 mediate sequential steps in mitochondrial membrane fusion. *Mol. Biol. Cell* 20 (15), 3525–3532. doi:10.1091/MBC.E09-03-0252

Tarantino, G., Carmine, F., Franco, S., Fabrizio, P., Franco, C., Domenico, C., et al. (2014). Circulating levels of sirtuin 4, a potential marker of oxidative metabolism, related to coronary artery disease in obese patients suffering from nafld, with normal or slightly increased liver enzymes. *Oxidative Med. Cell. Longev.* 2014. doi:10.1155/2014/920676

Theng, S. S., Wei, W., Way-champ, M., and Caroline, G. l. (2014). Disruption of FAT10-MAD2 binding inhibits tumor progression. *Proc. Natl. Acad. Sci. U. S. A.* 111 (49), E5282–E5291. doi:10.1073/PNAS.1403383111/SUPPL_FILE/PNAS.201403383SI.PDF

Tilg, H., and Moschen, A. R. (2010). Evolution of inflammation in nonalcoholic fatty liver disease: The multiple parallel hits hypothesis. *Hepatology* 52 (5), 1836–1846. doi:10.1002/HEP.24001

Toshikuni, N., Tsutsumi, M., and Arisawa, T. (2014). Clinical differences between alcoholic liver disease and nonalcoholic fatty liver disease. *World J. Gastroenterol.* 20 (26), 8393–8406. doi:10.3748/WJG.V20.I26.8393

Townsend, A., Bastin, J., Gould, K., Brownlee, G., Andrew, M., Coupar, B., et al. (1988). Defective presentation to class I-restricted cytotoxic T lymphocytes in vaccinia-infected cells is overcome by enhanced degradation of antigen. *J. Exp. Med.* 168 (4), 1211–1224. doi:10.1084/JEM.168.4.1211

Utzschneider, K. M., and Kahn, S. E. (2006). Review: The role of insulin resistance in nonalcoholic fatty liver disease. *J. Clin. Endocrinol. Metab.* 91 (12), 4753–4761. doi:10.1210/JC.2006-0587

van Vuren, A. J., van Beers, E. J., and van Wijk, R. (2021). A proposed concept for defective mitophagy leading to late stage ineffective erythropoiesis in pyruvate kinase deficiency. *Front. Physiol.* 11, 1854. doi:10.3389/fphys.2020.609103

Wan, R., Yuan, P., Guo, L., Shao, J., Liu, X., Lai, W., et al. (2021). Ubiquitin-like protein FAT10 suppresses SIRT1-mediated autophagy to protect against ischemic myocardial injury. *J. Mol. Cell. Cardiol.* 153, 1–13. doi:10.1016/J.YJMCC.2020.11.007

Wang, S., Gao, S., Li, Y., Qian, X., Luan, J., and Lv, X. (2021). Emerging importance of chemokine receptor CXCR4 and its ligand in liver disease. *Front. Cell Dev. Biol.* 9, 2053. doi:10.3389/fcell.2021.716842

Wilkerson-Vidal, Q. C., Collins, G. L., Fowler, E., Wimalarathne, M. M., Mercado, L. D., Gibson, H., et al. (2021). Young adult LEW.1WR1 rats develop dysregulated islet function and impaired liver insulin responses. *J. Endocr. Soc.* 5 (1), A444–A445. doi:10.1210/JENDSO/BVAB048.909

Willemin, G., Roger, C., Bauduret, A., and Minehira, K. (2013). Major histocompatibility class II pathway is not required for the development of nonalcoholic fatty liver disease in mice. *Int. J. Endocrinol.* 2013, 972962. doi:10.1155/2013/972962

Wu, H., Wang, T., Liu, Y., Li, X., Xu, S., Wu, C., et al. (2020). Mitophagy promotes sorafenib resistance through hypoxia-inducible ATAD3A dependent Axis. *J. Exp. Clin. Cancer Res.* 39 (1), 274. doi:10.1186/s13046-020-01768-8

Yang, R. L., Shi, Y. H., Hao, G., and Li, W. (2008). Increasing oxidative stress with progressive hyperlipidemia in human: Relation between malondialdehyde and atherogenic index. *J. Clin. Biochem. Nutr.* 43 (3), 154–158. doi:10.3164/jcbn.2008044

Yao, J., Liang, X., Liu, Y., and Zheng, M. (2020). Neddylation: A versatile pathway takes on chronic liver diseases. *Front. Med.* 7, 586881. doi:10.3389/FMED.2020.586881

Youle, R. J., and van der Bliek, A. M. (2012). Mitochondrial fission, fusion, and stress. *Science* 337 (6098), 1062–1065. doi:10.1126/SCIENCE.1219855

Yuan, R., Wang, K., Hu, J., Yan, C., Li, M., Yu, X., et al. (2014). Ubiquitin-like protein FAT10 promotes the invasion and metastasis of hepatocellular carcinoma by modifying β-catenin degradation. *Cancer Res.* 74 (18), 5287–5300. doi:10.1158/0008-5472.CAN-14-0284

Zeng, M., Liu, W., Hu, Y., and Fu, N. (2020). Sumoylation in liver disease. *Clin. Chim. Acta.* 510, 347–353. doi:10.1016/J.CCA.2020.07.044

Zhang, D. W., Jeang, K.-T., and Lee, C. G. L. (2006). p53 negatively regulates the expression of FAT10, a gene upregulated in various cancers. *Oncogene* 25 (16), 2318–2327. doi:10.1038/sj.onc.1209220

Zhang, H., and Fu, L. (2021). The role of ALDH2 in tumorigenesis and tumor progression: Targeting ALDH2 as a potential cancer treatment. *Acta Pharm. Sin. B* 11 (6), 1400–1411. doi:10.1016/J.APSB.2021.02.008

Zhang, Y., Zuo, Z., Liu, B., Yang, P., Wu, J., Han, L., et al. (2021). FAT10 promotes hepatocellular carcinoma (HCC) carcinogenesis by mediating P53 degradation and acts as a prognostic indicator of HCC. *J. Gastrointest. Oncol.* 12 (4), 1823–1837. doi:10.21037/JGO-21-374

Zilocchi, M., Finzi, G., Lualdi, M., Sessa, F., Fasano, M., and Alberio, T. (2018). Mitochondrial alterations in Parkinson's disease human samples and cellular models. *Neurochem. Int.* 118, 61–72. doi:10.1016/J.NEUINT.2018.04.013

Zou, Y., Du, Y., Cheng, C., Deng, X., Shi, Z., Lu, X., et al. (2021). FAT10 promotes the progression of bladder cancer by upregulating HK2 through the EGFR/AKT pathway. *Exp. Cell Res.* 398 (1), 112401. doi:10.1016/J.YEXCR.2020.112401

Frontiers in Pharmacology

Explores the interactions between chemicals and living beings

The most cited journal in its field, which advances access to pharmacological discoveries to prevent and treat human disease.

Discover the latest Research Topics

See more →

Frontiers

Avenue du Tribunal-Fédéral 34
1005 Lausanne, Switzerland
frontiersin.org

Contact us

+41 (0)21 510 17 00
frontiersin.org/about/contact